QUANTIFYING HEALTH IMPACTS OF TRAFFIC-RELATED FINE PARTICULATE AIR POLLUTION AT THE URBAN PROJECT SCALE

Chidsanuphong Chart-asa

A dissertation submitted to the faculty of the University of North Carolina at Chapel Hill in partial fulfillment of the requirements for the degree of Doctor of Philosophy in the Department of Environmental Sciences and Engineering.

Chapel Hill
2013

Approved by:

Jacqueline MacDonald-Gibson

Jason West

Marc Serre

Rob Pinder

H. Christopher Frey

Kenneth Sexton

ABSTRACT

Chidsanuphong Chart-asa: Quantifying Health Impacts of
Traffic-Related Fine Particulate Air Pollution at the Urban Project Scale
(Under the direction of Jacqueline MacDonald Gibson)

Public health practitioners in the United States are increasingly advocating the use of formal health impact assessments (HIAs) to inform local decision-makers of adverse health consequences of local urban and transportation planning decisions. Yet only 5 of 70 transportation-related HIAs conducted in the United States between 1999 and 2013 quantified health impacts of the decisions under consideration. Furthermore, none of these quantitative HIAs accounted for variability and uncertainty; rather, each provided a single, deterministic estimate of health risks. This research aims to expand the evidence and tools available for quantitative HIAs of traffic-related fine particulate matter air pollution (denoted as PM2.5) at the urban project scale. The research objectives are to (1) develop and empirically validate an improved approach for characterizing variability and uncertainty in local population exposure to near-roadway PM2.5 under alternative future traffic scenarios, (2) determine the extent to which including variability and uncertainty in an HIA affects HIA results, and (3) develop a simplified method for quantifying traffic-related PM2.5 health impacts that can include variability and uncertainty but also ease the quantitative burden for HIA practitioners. The methods in this research are demonstrated using a case study roadway corridor in Chapel Hill, North Carolina, where a future extension to the University of North Carolina campus is predicted to increase local traffic volumes. Key findings of this research include that (1) air quality model prediction

error appears to have a greater effect on estimated near-roadway seasonal daily average PM2.5 concentrations than hourly meteorological variability, (2) the current deterministic HIA approach may under-estimate health impacts, and (3) a simplified parametric approach for HIA may estimate transportation-related health impacts sufficiently for conservative, screening-level analysis, saving the time and costs of more complex modeling for situations in which the screening analysis shows risks may exceed a pre-determined threshold of acceptability.

To my Mom, Dad, Aunt, Brothers, and Phra Mahanaruepol Sayacharoen
This dissertation would not have been possible without your support.

ACKNOWLEDGEMENTS

I would like to express my deepest gratitude to my advisor, Dr. Jacqueline MacDonald Gibson, for her guidance, support, patience, and generosity throughout my Ph.D. study. I am very thankful to all members of my committee: Drs. Jason West, Marc Serre, Rob Pinder, H. Christopher Frey, and Kenneth Sexton for their valuable suggestions and comments. Additionally, I am indebted to Dr. Kenneth Sexton for his considerable assistance with roadside measurements.

I would like to thank the Royal Thai government, Mae Fah Luang University, and the University of North Carolina at Chapel Hill for affording me this educational and life-changing opportunity. I also gratefully acknowledge Jack Whaley and the faculty and staff at the Department of Environmental Sciences and Engineering, Gillings School of Global Public Health for their kind assistance with my Ph.D. program, especially concerning tuition remission aid.

I would like to acknowledge Kumar Neppalli and Robert Myers at the Traffic Engineering Division, Town of Chapel Hill, for providing the data sets needed for this research.

My gratitude is also due to all colleagues and friends from Gillings School of Global Public Health and elsewhere for their friendship and assistance during my stay in the United States.

Last but not least, I would like to thank my family and relatives for their love, care, support, encouragement, understanding, and companionship that have helped me reach this point in my life.

PREFACE

The dissertation is organized in a nontraditional format in that it includes three manuscripts to be submitted for publication. Chapter 1 presents an introduction, a case study, and a description of objectives of the dissertation. Chapters 2, 3, and 4 present three manuscripts as stand alone sections and thus have some redundancies with earlier chapters. Chapter 5 presents conclusions and suggestions for future research.

TABLE OF CONTENTS

LIST OF TABLES xiii

LIST OF FIGURES xv

LIST OF ABBREVIATIONS xviii

LIST OF SYMBOLS xx

CHAPTER 1 Introduction 1

References 8

CHAPTER 2 Traffic Impacts on Fine Particulate Matter Air Pollution at the Urban Project Scale: A Quantitative Assessment 11

Introduction 11

Materials and Methods 14

Modeling Approach 16

Model Validation Approach 22

Data Cleaning 26

Results 27

Vehicle Emission Rates 27

Model Performance Evaluation 31

Estimated PM2.5 Exposure under Current and Future Scenarios 32

Discussion 35

Conclusions 38

References 39

CHAPTER 3 Health Impact Assessment of Traffic-Related Air Pollution at the Urban Project Scale: Influence of Variability and Uncertainty 43

Introduction 43

Case Study Site 47

Method for Quantifying Health Impacts 50

Overview of Modeling Framework 50

PM2.5 Exposure Concentration 52

Concentration-Response Functions 54

Baseline Incidence Rates of Adverse Health Effects 56

Method for Testing Effects of Variability and Uncertainty on Predicted Health Impacts 58

Method for Comparing Health Impacts under Alternative Scenarios 58

Results and Discussion 61

Effect of Including Variability and Uncertainty 61

Population Health Risks at the Case Study Site 67

Sensitivity and Uncertainty Analysis 75

Conclusions 76

References 79

CHAPTER 4 Simplified Approach for Quantifying Health Impacts of Traffic-Related Air Pollution at the Urban Project Scale 82

Introduction 82

Modeling Method 85

Conceptual Approach 85

Reduced-Form Model Rationale 86

Linked MOVES-CAL3QHCR Modeling 88

Fitting of Reduced-Form Model 89

Incorporation of Health Impacts 95

Reduced-Form Model Validation Approach 97

Results and Discussion 97

Simplified Equations for Quantifying Near-Road Traffic-Related PM2.5 Pollution and Related Health Impacts....97

Sensitivity Analysis 104

Model Validation 112

Conclusions....118

References....119

CHAPTER 5 Conclusions....123

APPENDIX A Supplemental Materials for MOVES Modeling of Emission Rates of Traffic-Related PM2.5....126

APPENDIX B Supplemental Materials for CAL3QHCR Modeling of Traffic-Related PM2.5 Concentrations at 160 Cencus Block Centroids Analyzed....136

APPENDIX C Supplemental Materials for CAL3QHCR Modeling of Traffic-Related PM2.5 Concentrations at Perpendicular Distances from the Middle of the Edges of Hypothetical Roadway....156

APPENDIX D Supplemental Materials for Modeling of Health Burdens Attributable to Short-term Exposure to Traffic-Related PM2.5 at 160 Cencus Block Centroids Analyzed....168

APPENDIX E Distribution of the Centroid Distances from the Edges of Study Corridor Among 160 Census Blocks Analyzed....173

APPENDIX F Population Demographic Characteristics within 160 Census Blocks Analyzed....174

APPENDIX G Cumulative Distribution of Predicted Seasonal Average of 24-Hour Traffic-Related PM2.5 Concentration within 160 Census Blocks Analyzed....175

APPENDIX H Cumulative Distribution of Predicted Seasonal Average of Cardiovascular Mortality Attributable to Short-term Exposure to Traffic-Related PM2.5 within 160 Census Blocks Analyzed....178

APPENDIX I Cumulative Distribution of Predicted Seasonal Average of Respiratory Mortality Attributable to Short-term Exposure to Traffic-Related PM2.5 within 160 Census Blocks Analyzed....181

APPENDIX J Cumulative Distribution of Predicted Seasonal Average of Cardiovascular Hospital Admissions (Unscheduled) Attributable to Short-term Exposure to Traffic-Related PM2.5 within 160 Census Blocks Analyzed 184

APPENDIX K Cumulative Distribution of Predicted Seasonal Average of Respiratory Hospital Admissions (Unscheduled) Attributable to Short-term Exposure to Traffic-Related PM2.5 within 160 Census Blocks Analyzed 187

LIST OF TABLES

Table 2.1 Measured and predicted PM2.5 concentrations (μg/m^3) 26

Table 2.2 Traffic and meteorological data used in CAL3QHCR modeling 27

Table 3.1 Previous quantitative transportation-related HIAs in the United States 46

Table 3.2 Highest traffic volume and population size under three scenarios considered 50

Table 3.3 Mean concentration-response coefficient (95% CI) used in this study 57

Table 3.4 Annual mortality rates by race, gender, and age group for Orange County 59

Table 3.5 Annual emergency department visits rates for North Carolina State 60

Table 3.6 Sources of uncertainty and variability included in the five simulations 60

Table 3.7 Averages of seasonal mean values of $PM_{exposure}$ for the 12 selected census blocks; seasonal mean values of β; and seasonal incidence fractions used to adjust y^0 for cardiovascular and respiratory mortality and unscheduled hospital admissions in five simulations including different uncertainty and variability sources shown in Table 3.6 62

Table 3.8 Ratios of averages of seasonal mean values of $PM_{exposure}$ for the 12 selected census blocks; seasonal mean values of β; and seasonal incidence fractions used to adjust y^0 in simulations 1b, 2, 3, and 4 to those in simulation 1a 63

Table 3.9 Aggregate effects of including variability and/or uncertainty in simulations 1b, 2, 3, and 4 65

Table 3.10 Comparison of HIA results by development scenario 68

Table 4.1 Season-specific means and standard deviation used in the disease burden assessment 96

Table 4.2 2009 power-law curve parameters for the 24-hour traffic-related PM2.5 concentrations (μg/m^3) and corresponding attributable fractions (AF) of cardiovascular (CVD) and respiratory (RD) diseases events (per million) as a function of a perpendicular distance from the middle of road edge (feet) 102

Table 4.3 2025 power-law curve parameters for the 24-hour traffic-related PM2.5 concentrations ($\mu g/m^3$) and corresponding attributable fractions (*AF*) of cardiovascular (CVD) and respiratory (RD) diseases events (per million) as a function of a perpendicular distance from the middle of road edge (feet).....103

LIST OF FIGURES

Figure 2.1 The study corridor runs from the intersection of Martin Luther King Jr. Boulevard and Whitfield Road to the intersection of South Columbia Street and Mt. Carmel Church Road, Chapel Hill, NC....15

Figure 2.2 Flowchart showing the nine steps of our modeling framework....18

Figure 2.3 Seasonal temperature profiles from 6 a.m. to 7 p.m., according to the meteorological data used in the CAL3QHCR modeling....20

Figure 2.4 Seasonal wind roses from 6 a.m. to 7 p.m., according to the meteorological data used in the CAL3QHCR modeling....21

Figure 2.5 Diagram of sampling points along the study corridor....24

Figure 2.6 Example of 2009 link-specific emission rate fractions (%) at 35 mph average speed, 0% grade, and 90°F by fuel types, age groups, and vehicle types....29

Figure 2.7 Examples of 2009 link-specific emission rate (g/veh-mile) changes by average speeds, grades, and temperatures....30

Figure 2.8 Factor-of-two plots of concentration differences (μg/m3) observed during roadside measurements and predicted byCAL3QHCR (dated 13196 and dated 04244)....32

Figure 2.9 PM2.5 concentrations attributable to roadway emissions from the study corridor, as predicted by the combined MOVES-CAL3QHCR approach ($\mu g/m^3$) by season for the year 2009....33

Figure 2.10 PM2.5 concentrations attributable to roadway emissions, as predicted by the combined MOVES-CAL3QHCR approach ($\mu g/m^3$) by season for the year 2025, assuming the Carolina North Campus is built....34

Box 3.1 Sources of variability and uncertainty in estimating health effects of PM2.5 from traffic....47

Figure 3.1 (A) The study corridor between the intersection of Martin Luther King, Jr., Blvd. and Whitfield Rd and the intersection of South Columbia St. and Mt. Carmel Church Rd., Chapel Hill, NC, and the census blocks located within 500 meters from the study corridor. (B) The road segment and census blocks for simulations to demonstrate differences in health burden estimates when including the variability and the uncertainty into the modeling approach....49

Figure 3.2 Overview of framework for incorporating variability and uncertainty into assessment of the health impacts of traffic-related PM2.5....52

Figure 3.3 Sums of mean estimates of health burdens for the 12 selected census blocks over a year (annual excess cases) using five simulation approaches accounting for different uncertainty and variability sources shown in Table 3.6 67

Figure 3.4 The spatial distributions and the total excess cases of adverse health effects of traffic-related PM2.5 in each season in the 2009 scenario 69

Figure 3.5 The spatial distributions and the total excess cases of adverse health effects of traffic-related PM2.5 in each season in the 2025 scenario without the Carolina North development 70

Figure 3.6 The spatial distributions and the total excess cases of adverse health effects of traffic-related PM2.5 in each season in the 2025 scenario with the Carolina North development 71

Figure 3.7 Comparisons of total annual excess cases of adverse health effects of traffic-related PM2.5 from the Carolina North campus by the year 2025 with and without cleaner vehicle technologies and fuels 72

Figure 3.8 Age distribution of traffic-related health impacts in the 2009 scenario 74

Figure 3.9 Sensitivity of predicted CVD deaths attributable to traffic-related PM2.5 to changing random variables in the model to extreme values representing the upper and lower ends of the 95% confidence intervals 76

Figure 4.1 Illustration of hypothetical roadway and receptors at eight perpendicular distances from the middle of the roadway edges (10, 25, 50, 100, 200, 300, 400, and 500 feet) 90

Figure 4.2 Flow chart showing ten steps for estimating parameters *A* and *B* for traffic-related PM2.5 94

Figure 4.3 2009 horizontal profiles of 24-hour traffic-related PM2.5 concentrations ($\mu g/m^3$) and corresponding attributable fractions (per million) simulated by assigning both traffic way the base traffic condition 99

Figure 4.4 2025 horizontal profiles of 24-hour traffic-related PM2.5 concentrations ($\mu g/m^3$) and corresponding attributable fractions (per million) simulated by assigning both traffic way the base traffic condition 100

Figure 4.5 2009 and 2025 average percentage contributions of the 24-hour traffic-related PM2.5 concentrations and corresponding attributable fractions by fuel types, age groups, and vehicle types 101

Figure 4.6 Average percentage changes in near-road traffic-related PM2.5 pollution and related health impacts when changing traffic volumes on the hypothetical roadway from 1600 veh/hr each way to 800, 2400, and 3200 veh/hr each way 105

Figure 4.7 2009 and 2025 Average percentage changes in near-road traffic-related PM2.5 pollution and related health impacts when adjusting traffic activity on each way of the hypothetical roadway from cruise to queue and acceleration 108

Figure 4.8 2009 and 2025 average percentage changes in near-road traffic-related PM2.5 pollution and related health impacts when altering the average traffic speed on each way of the hypothetical roadway from 35 mph to 25 and 45 mph 109

Figure 4.9 2009 and 2025 average percentage changes in near-road traffic-related PM2.5 pollution and related health impacts on the uphill-roadside receptors when changing road grade on each way of the hypothetical roadway from 0% to ± 10% (both traffic ways were assigned the same road grades, but one with positive values and another with negative values) 110

Figure 4.10 2009 and 2025 average percentage changes in near-road traffic-related PM2.5 pollution and related health impacts on the downhill-roadside receptors when changing road grade on each way of the hypothetical roadway from 0% to ±10% (both traffic ways were assigned the same road grades, but one with positive values and another with negative values) 111

Figure 4.11 Comparisons between the 24-hour traffic-related PM2.5 concentrations ($\mu g/m^3$) from the simplified equations and the full MOVES-CAL3QHCR modeling in 2009 and 2025 with Carolina North scenarios 116

Figure 4.12 Comparisons between the attributable fractions (AF) of cardiovascular (CVD) mortality (per million) from the simplified equations and the full MOVES-CAL3QHCR modeling in 2009 and 2025 with Carolina North scenarios 117

LIST OF ABBREVIATIONS

B F	Black or African American female
B M	Black or African American male
CDC WONDER	Centers for Disease Control and Prevention Wide-ranging Online Data for Epidemiologic Research
CVD	Cardiovascular diseases
EPA	U.S. Environmental Protection Agency
GIS	Geographic Information Systems
HIA	Health impact assessment
ICD	International Classification of Diseases
ISA	Integrated science assessment
MOVES	Motor Vehicle Emission Simulator
NC DETECT	North Carolina Disease Event Tracking and Epidemiologic Collection Tool
NZTA	New Zealand Transport Agency
O F	Other races female
O M	Other races male
PM10	Coarse particle/ particulate matter
PM2.5	Fine particle/ particulate matter
RD	Respiratory diseases
RIA	Regulatory impact analysis
SMAQMD	Sacramento Metropolitan Air Quality Management District
TIA	Transportation impact analysis
TRM	Triangle Regional Travel Demand Model

UNC	The University of North Carolina
VSP	Vehicle specific powers
W F	White female
W M	White male
WHO	World Health Organization

LIST OF SYMBOLS

y^0	Number of baseline case of adverse health event in census block, cases
$y^0_{i,j,k,l,m,n}$	Number of baseline case of adverse health event n attributable to traffic-related PM2.5 in season m in census block i for age group j, gender k, and race l, cases
$\Delta y_{i,j,k,l,m,n}$	Number of cases of adverse health event n attributable to traffic-related PM2.5 in season m in census block i for age group j, gender k, and race l, cases
$AF_{i,j,k,l,m,n}$	Fraction and number of cases of adverse health event n attributable to traffic-related PM2.5 in season m in census block i for age group j, gender k, and race l, unitless
$C_{(x,0)}$	Ground-level concentration of a pollutant at any perpendicular distance x from a road segment, μg/m^3
$PM_{exposure_{i,m}}$	Average of 24-hour PM2.5 concentration in census block i during season m, μg/m^3
$PM_{model_{i,m}}$	Model-predicted seasonal average of 24-hour PM2.5 concentration in census block i during season m, μg/m^3
$PM_{exposure}$	Average of 24-hour PM2.5 concentration in census block, μg/m^3
$RR_{i,m,n}$	Relative risk of health outcome n during season m in census block i, unitless
p_i	A substitution term of y_i/σ_{y_i} (i = 1,2)
y_i	Positions in the cross-wind direction of the ends of the line source, m or ft
$\beta_{m,n}$	Concentration-response coefficient describing the effects of PM on health outcome n during season m, m^3/μg
σ_y	Contaminant diffusivity in the cross-wind directions, m or ft
σ_z	Contaminant diffusivity in the vertical directions, m or ft
Δy	Number of cases of adverse health event attributable to traffic-related PM2.5 in census block, cases

Δy	Number of cases of adverse health event, cases
AF	Fraction and number of cases of adverse health, unitless
$C(x)$	Seasonal average 24-hr traffic-related PM2.5 concentrations at an exposure point at distance *x* from the roadway, μg/m^3
H	Roadway height, m or ft
$P(p_1 < Z < p_2)$	Probability distribution function for a standard normal random variable, unitless
UF	Model uncertainty factor, unitless
Z	Standard normal random variable, unitless
q	Total mass of vehicle emissions from the road segment, g/s-m
u	Wind speed, m/s
α	Angle that expected for a due north-south roadway, degree
β	Concentration-response coefficient describing the effects of PM on health outcome, m^3/μg
β	Concentration-response coefficient, m^3/μg
ω	Angle between the roadway and the wind direction, degree

CHAPTER 1

INTRODUCTION

It has been long recognized that integrating health considerations into decision-making in sectors outside the traditional healthcare industry is a key for chronic disease prevention and health promotion [1, 2]. Over the past decade, health impact assessment (HIA) has been more widely used in the United States due to increased awareness of chronic diseases associated with environmental risk factors that could be generated by projects, programs, plans, and policies in non-health-related sectors, such as urban planning, transportation, agriculture, education, and others [3]. Signs of the increased interest in HIA in the United States include the formation in 2011 of an official Society of Practitioners of Health Impact Assessment [4] and the release of a report on HIA by the U.S. National Research Council [1].

Over the past decade, more than 115 HIAs have been completed in the United States to help decision-makers identify and evaluate health consequences and mitigation options of proposals at various levels of government [5]. The majority of these HIAs are related to urban and transportation planning [3, 5]. Yet the current HIA practice employs mostly qualitative approaches, relying on literature reviews, stakeholder interviews, and HIA practitioner judgments to determine health impacts rather than quantitative estimation of the magnitude and distribution of the impacts. As a result, most previous HIAs have limited value for supporting cost-benefit analyses of alternative proposals. Two recent reviews revealed that only five previous HIAs of urban planning and transportation projects in the United States have quantified estimates of deaths and illnesses prevented or caused by the projects [5, 6]. These five

quantitative HIAs used deterministic approaches that overlooked potentially important sources of variability and uncertainty. As a result, the previous quantitative HIAs may not convey adequately the full range of potential impacts and the degree of certainty in the estimations [7–9] [10–14].

In contrast to HIA practitioners, risk assessors and policy analystshave long used quantitative methods to inform decisions about air quality policies. Such quantitative analysis to support policymaking is required under Presidential Executive Orders 12866 and 13563 for any regulatory action likely to have an economic impact of $100 million or more. As an example, the recent EPA revisions to the national ambient air quality standards for particulate matter employed a formal regulatory impact analysis (RIA) to quantify the health impacts of three different annual standards. This regulatory impact analysis estimated that the selected new standard would decrease annual cases of premature mortality by 460-1,000 by the year 2020 [15]. Nonetheless, the quantitative methods developed to support RIAs appear to receive little attention among HIA practitioners. Furthermore, most HIAs focus on local decisions, whereas RIAs evaluate national policy decisions. Due to these differences in scale, the methods appropriate for HIAs will of necessity differ from methods used for RIAs.

This dissertation aims to expand the evidence base for quantitative HIAs of local planning and transportation decisions by developing a new modeling approach accounting for potentially important sources of variability and uncertainty. Potential sources of variability relevant to quantifying health impacts include exposure concentrations, concentration-response functions for health effects of concern, age, and baseline health status of the exposed population; potentially important sources of uncertainty include the form and parameters of concentration-response functions and air quality model prediction error [16–18]. Moreover, the research also

demonstrates methods for sensitivity analysis relevant to such local-scale decisions, including an investigation of how changes to vehicle activities, vehicle speeds, or road grades over a roadway segment may influence HIA results. As Frey and Patil note, sensitivity analyses of risk models offer important benefits for decision-making, including helping to identify key risk factors and prioritize additional data collection activities [8]. Furthermore, as an expert review of processes for modeling air emissions to support air quality management in North America notes, "Uncertainty quantification is useful . . . for helping decision-makers to make robust decisions in the face of limited information" [9]. The modeling framework and findings of this dissertation should benefit HIA practitioners and others conducting quantitative, local-scale HIAs of the built environment and transportation projects by helping them identify the most at-risk populations and risk sources, prioritize data collection needs, and make robust decisions in the face of uncertainty.

This dissertation uses a case study transportation corridor to test and demonstrate the improved modeling approach. The transportation corridor is Martin Luther King, Jr., Boulevard in Chapel Hill, North Carolina. Specifically, the dissertation focuses on the potential effects on near-roadway air quality and public health of a new development proposed by The University of North Carolina at Chapel Hill: the proposed Carolina North campus. The proposed project would build an approximately 250-acre new research and mixed-use academic campus on the Horace Williams tract at north of Estes Drive and west of Martin Luther King Jr. Boulevard, about two miles north from the main campus [19]. It is expected to bring major changes to Chapel Hill and neighboring areas. The University has outlined two development scenarios in 2015 and 2025 for evaluating the future impacts on transportation in the proximity of Carolina North. The 2015 development scenario is an 0.8 million-square-foot development with 1,525

parking spaces, while the 2025 development scenario is a 3 million-square-foot development with 5,835 parking spaces. The approximate size of the population living or working in this new campus is expected to be 1,780 and 7,100 persons for the 2015 and 2025 development scenarios, respectively. A previous analysis of traffic impacts indicated that Carolina North would generate 9,734 and 39,746 trips per day for the 2015 and 2025 development scenarios, respectively, with private vehicles accounting for more than 50% of trips and the majority trips related to the health care, academic, and private sectors [20]. These additional trips are expected to cause heavier traffic in the vicinity of Carolina North. However, the changes in the population exposure to traffic-related air pollution and its related health impacts due to increased traffic have not been investigated prior to this dissertation.

The improved modeling approach is applied to the traffic conditions on the north-south corridor extending between the intersection of Martin Luther King, Jr. Boulevard and Whitfield Road and the intersection of South Columbia Street and Mt. Carmel Church Road for three development scenarios: (1) 2009 baseline scenario; (2) 2025 without Carolina North scenario; and (3) 2025 with the new campus scenario. According to the previous transportation impact analysis (TIA) for the project [20], the major impacts of increased traffic due to Carolina North are expected along this corridor, which is the main route connecting Carolina North to the main campus, downtown Chapel Hill, and the highway interchanges. Moreover, 2010 census data indicate that approximately 16,000 people (more than one-fourth of total population in Chapel Hill) live in the census blocks located within 500 meters from the corridor[21].

For this research, current and anticipated future traffic conditions on the study corridor are obtained from the Carolina North TIA. Briefly, the Carolina North TIA simulated the 2009 traffic conditions primarily based on 2008 traffic count data from the University of North

Carolina at Chapel Hill Development Plan, the Town of Chapel Hill's traffic signal system database, and the traffic studies of other development proposals. It assumed that the traffic growth from 2008 to 2009 was about 2%. For the 2025 without Carolina North scenario, the future traffic growth due to regional developments was simulated using the Triangle Regional Travel Demand Model (TRM). The estimated annual growth rates were approximately 2.25% from 2009 to 2015, and 1.25% from 2015 to 2025. The future traffic growth due to other developments in the vicinity of Carolina North was obtained from traffic studies of those development proposals. For 2025 with the new campus scenario, the Carolina North TIA simulated the future traffic growth due to the project using four-step models that included trip generation, mode choice, trip distribution, and route assignment; details are provided in the TIA.

This research focuses on the health impacts of exposure to traffic-related fine particulate matter (i.e., particles with diameter less than 2.5 μm, PM2.5). PM2.5 was used as a proxy for traffic-related air pollution in four of the five previous quantitative HIAs [10–14]. In Orange County, North Carolina, where Carolina North is located, emissions inventory data reveal that traffic contributed approximately 21% of total primary emissions in 2008 [22]. Health studies have reported the relationship between exposures to PM2.5, either short- or long-term, and various adverse health effects [23–26]. EPA's Integrated Science Assessments (ISAs) for Particulate Matter has reviewed recent evidence from epidemiologic and toxicological literature and suggested the causal or likely causal relationships between short- or long-term exposure to PM2.5 and premature morality along with adverse cardiovascular and respiratory health effects. Moreover, no threshold exposure can be considered as risk-free [27]. Recent community health assessments have shown that diseases related to the cardiovascular and respiratory systems—the

systems most affected by PM2.5 exposure—are the leading causes of death and hospitalization in both Orange County and North Carolina [28].

The subsequent chapters of this dissertation are structured around three objectives:

Objective 1, as presented in **Chapter 2**, is to develop an improved modeling approach for estimating population exposure to traffic-related PM2.5 that better represents the effects of vehicle activities, vehicle speeds, road grades, and temperatures on traffic emissions than the conventional approach of previous HIAs. The performance of the developed modeling approach is evaluated by comparing it against roadside measurements. This chapter has been accepted for publication: *Chart-asa, C., Sexton, K.G., MacDonald Gibson, J. 2013, in press. Traffic Impacts on Fine Particulate Matter Air Pollution at the Urban Project Scale: A Quantitative Assessment.* Journal of Environmental Protection [29].

Objective 2, as presented in **Chapter 3**, is to demonstrate a new modeling approach for quantifying health impacts of traffic-related PM2.5 at the urban project scale that improves on the conventional approach of previous HIAs by incorporating (1) variability in exposure concentration, concentration-response coefficients, and demographic characteristics of the exposed population and (2) uncertainty in air quality model accuracy and concentration-response coefficients into the model predictions. The modeling approach can be used to assess health disparities in exposure to risks from the traffic-related PM2.5. This chapter has been submitted as an article to Science of the Total Environment: *Health Impact Assessment of Traffic-Related Air Pollution at the Urban Project Scale: Influence of Variability and Uncertainty*.

Objective 3, as presented in **Chapter 4**, is to develop a simplified framework that can be more easily used by HIA practitioners to quantify the air quality and health impacts of motor vehicle emissions, while accounting for variability in vehicle activity, vehicle speed, and road

grade changes over roadway segments as well as for the previously mentioned uncertainty sources. The framework can be used to assist HIA practitioners who may not have the resources to run air quality dispersion models.

REFERENCES

[1] National Research Council, *Improving Health in the United States: The Role of Health Impact Assessment*. Washington, DC: The National Academies Press, 2011.

[2] A. Wernham, "Health Impact Assessments are Needed in Decision Making about Environmental and Land-Use Policy," *Health Aff. (Millwood).*, vol. 30, no. 5, pp. 947–56, 2011.

[3] A. L. Dannenberg, R. Bhatia, B. L. Cole, S. K. Heaton, J. D. Feldman, and C. D. Rutt, "Use of Health Impact Assessment in the U.S.: 27 Case Studies, 1999-2007," *Am. J. Prev. Med.*, vol. 34, no. 3, pp. 241–56, 2008.

[4] Society of Practitioners of Health Impact Assessment, "Society of Practitioners of Health Impact Assessment (SOPHIA)," 2013. http://www.hiasociety.org/.

[5] L. Singleton-baldrey, "The Impacts of Health Impact Assessment: A Review of 54 Health Impact Assessments, 2007-2012," University of North Carolina at Chapel Hill, 2012.

[6] R. Bhatia and E. Seto, "Quantitative Estimation in Health Impact Assessment: Opportunities and Challenges," *Environ. Impact Assess. Rev.*, vol. 31, no. 3, pp. 301–309, 2011.

[7] H. C. Frey and D. E. Burmaster, "Methods for Characterizing Variability and Uncertainty: Comparison of Bootstrap Simulation and Likelihood-Based Approaches," *Risk Anal.*, vol. 19, no. 1, pp. 109–130, Feb. 1999.

[8] H. C. Frey and S. R. Patil, "Identification and review of sensitivity analysis methods.," *Risk Anal.*, vol. 22, no. 3, pp. 553–78, Jun. 2002.

[9] The NARSTO Emission Inventory Assessment Team, "Improving Emission Inventories for Effective Air Quality Management Across North America," Oak Ridge, Tennessee, 2005.

[10] Human Impact Partners, "Pittsburg Railroad Avenue Specific Plan Health Impact Assessment," Oakland, CA, 2008.

[11] Human Impact Partners, "Pathways to Community Health: Evaluating the Healthfulness of Affordable Housing Opportunity Sites Along the San Pablo Avenue Corridor Using Health Impact Assessment," Oakland, CA, 2009.

[12] UC Berkeley Health Impact Group, "Oak to Ninth Avenue Health Impact Assessment," Berkeley, CA, 2006.

[13] UC Berkeley Health Impact Group, "MacArthur BART Health Imapct Assessment," Berkeley, CA, 2007.

[14] UC Berkeley Health Impact Group, "Health Impact Assessment of the Port of Oakland," Berkeley, CA, 2010.

[15] U.S. Environmental Protection Agency, "Regulatory Impact Analysis for the Final Revisions to the National Ambient Air Quality Standards for Particulate Matter," Research Triangle Park, NC, 2012.

[16] B. Ostro and L. Chestnut, "Assessing the health benefits of reducing particulate matter air pollution in the United States.," *Environ. Res.*, vol. 76, no. 2, pp. 94–106, 1998.

[17] A. Prüss-Üstün, C. Mathers, C. Corvalán, and A. Woodward, *Introduction and methods: assessing the environmental burden of disease at national and local levels*, no. 1. Geneva, Switzerland: World Health Organization, 2003.

[18] J. MacDonald Gibson, A. Brammer, C. Davidson, T. Folley, F. Launay, and J. Thomsen, *Environmental Burden of Disease Assessment: A Case Study in the United Arab Emirates*. Dordrecht, Heidelberg, London, New York: Springer, 2013.

[19] University of North Carolina at Chapel Hill, "Carolina North Plan report," Chapel Hill, NC, 2007.

[20] Vanasse Hangen Brustlin Inc., "Transportation Impact Analysis for the Carolina North Development," Watertown, MA, 2009.

[21] US Census Bureau, "Census Block Shapefiles with 2010 Census Population and Housing Unit Counts," 2011. .

[22] US Environmental Protection Agency, "2008 National Emissions Inventory: Data & Documentation," 2013. .

[23] C. A. Pope III and D. W. Dockery, "Health Effects of Fine Particulate Air Pollution: Lines that Connect," *J. Air Waste Manage. Assoc.*, vol. 56, no. 6, pp. 709–742, Jun. 2006.

[24] D. W. Dockery, "Health effects of particulate air pollution," *Ann. Epidemiol.*, vol. 19, no. 4, pp. 257–63, Apr. 2009.

[25] R. D. Brook, S. Rajagopalan, C. A. Pope III, J. R. Brook, A. Bhatnagar, A. V Diez-Roux, F. Holguin, Y. Hong, R. V Luepker, M. a Mittleman, A. Peters, D. Siscovick, S. C. Smith, L. Whitsel, and J. D. Kaufman, "Particulate matter air pollution and cardiovascular disease: An update to the scientific statement from the American Heart Association," *Circulation*, vol. 121, no. 21, pp. 2331–78, 2010.

[26] World Health Organization, *Health effects of transport-related air pollution.* Copenhagen Ø, Denmark: WHO Regional Office for Europe, 2005.

[27] US Environmental Protection Agency, “Integrated Science Assessment for Particulate Matter, EPA/600/R-08/139F,” Research Triangle Park, NC, 2009.

[28] Orange County Health Department and Healthy Carolinians of Orange County, “2011 Orange County Community Health Assessment,” Hillsborough, NC, 2011.

[29] C. Chart-asa, K. G. Sexton, and J. MacDonald Gibson, “Traffic Impacts on Fine Particulate Matter Air Pollution at the Urban Project Scale: A Quantitative Assessment,” *J. Environ. Prot. (Irvine,. Calif).*, vol. 4, no. December, 2013.

CHAPTER 2

TRAFFIC IMPACTS ON FINE PARTICULATE MATTER AIR POLLUTION AT THE URBAN PROJECT SCALE: A QUANTITATIVE ASSESSMENT[1]

Introduction

The World Health Organization and other public health advocates have long stressed the need for formal health impact assessment (HIA) to inform decision-making in sectors outside the health-care industry [1–3]. The rationale is that chronic diseases that pose major health burdens in the post-industrial world are driven largely by policy, program, and planning decisions in transportation, agriculture, urban planning, and other sectors that ordinarily do not include population health as an objective in their decision processes. Commonly cited examples include the effects of government agricultural subsidies on the availability of healthy foods and the effects of transportation plans on population exposure to noise and air pollution. HIA is intended to encourage decision-makers in these and other sectors to make choices that minimize negative and maximize positive impacts on public health, within budgetary and other constraints. The intent of HIA is to prevent the chronic, noninfectious diseases—including heart disease, stroke, and diabetes—that have replaced infectious diseases as the leading health concerns in post-industrialized nations [4]. Health practitioners have long recognized that exposures to risk factors for these chronic diseases are driven by a wide range of policy, planning, and program

[1] *Chart-asa, C., Sexton, K.G., MacDonald Gibson, J. 2013, in press. Traffic Impacts on Fine Particulate Matter Air Pollution at the Urban Project Scale: A Quantitative Assessment.* Journal of Environmental Protection

decisions in multiple sectors and that prevention through better-informed decision-making in all sectors is likely to be less costly than treating the symptoms [2].

While the practice of HIA is well established in the European Union and some other nations, in the United States HIA practice is relatively new [2, 5, 6]. The first U.S. HIA, which evaluated the health impacts of a proposed policy to increase the minimum wage in San Francisco, was completed in 1999 [2, 7]. By the end of 2012, at least 114 additional HIAs had been completed in the United States [8]. However, only 14 of these HIAs provided quantitative estimates of the impacts of alternative choices on health [9]. The rest are qualitative, relying on the judgment of the HIA practitioner to determine whether one choice will be more or less detrimental or beneficial to population health, in comparison with other options. In the US urban planning and transportation sectors, such qualitative HIAs are of little use. In order to prioritize urban planning and transportation projects, state and local planning and transportation agencies employ cost-benefit analysis. To be able to include health impacts in these cost-benefit analyses, quantitative estimates of health impacts—in terms of numbers of illnesses and premature deaths—are essential. Yet, a recent review found that only four HIAs in the transportation and urban planning sectors in the United States had employed quantitative methods, and all of these were conducted in major metropolitan areas in California [9].

In order to expand the evidence base for the use of quantitative HIA to support planning and transportation decisions in the United States, this paper presents an improved approach for quantifying the future air quality effects of increased traffic brought by new urban or suburban development projects. We focus specifically on predicting exposure to airborne fine particulate matter (i.e., particles with diameter less than or equal to 2.5 μm, denoted as PM2.5), which often is used as a marker of near-roadway air pollution to support health effects estimates. We then

demonstrate the modeling approach for a case study site: a proposed extension to the campus of the University of North Carolina (UNC) at Chapel Hill, in the United States.

Our modeling approach improves on those in the previous four US transportation-related HIAs in several ways. First, it accounts for the effects of acceleration, deceleration, and idling on all roadway links in the study corridor using an approach recommended by Ritner et al. but not previously employed in an HIA [10]. Second, it compares model predictions to measured pollutant concentrations along the roadway corridor. According to Ritner et al., such a performance evaluation has not been previously completed. Third, it improves on the Ritner et al. approach by developing a new algorithm to incorporate daily temperature variability.

The planned future project used as the case study for demonstrating the new modeling method is known as "Carolina North," which is planned as an extension to the current UNC campus. UNC-Chapel Hill is the oldest public university in the United States and has a current student population of more than 29,000 [11]. The campus is located in the town of Chapel Hill, which has a population just over 57,000 [12]. The planned new campus will be located about 3 km (2 miles) north of the existing campus (**Figure 2.1**). If constructed, it is expected to increase the number of trips to the area by 10,000 per day by 2015—half of those by private vehicle—and, accordingly, to substantially increase traffic in the surrounding neighborhoods [13]. By 2025, the number of additional daily trips to the campus is expected to increase by as many as 40,000 [13]. The main traffic effects are expected along Martin Luther King Jr. Boulevard, the main thoroughfare connecting the new campus to both the existing campus (to the south) and the nearest highway interchange (to the north).

UNC commissioned a transportation impact analysis in 2009 in order to estimate the anticipated increases in traffic volumes, but the air quality impacts of the increased traffic were

not evaluated. Hence, the transportation impact analysis cannot be used directly to support decision-making about whether alternative transportation network designs (including, for example, new or expanded public transit routes) may be needed to prevent traffic-related air quality degradation and associated health impacts. By quantifying the air quality effects of additional traffic generated by the future campus, this paper can support a future quantitative HIA to inform local transportation and planning decisions.

Materials and Methods

Our process for modeling population exposure to excess PM2.5 attributable specifically to increased traffic from the Carolina North campus builds on a new approach recommended by Ritner et al. [10], who proposed an algorithm to account for vehicle acceleration, deceleration, and idling at intersections in modeling of near-roadway pollutant concentrations. We improved on the Ritner et al. approach by developing a new algorithm for incorporating hourly temperature variability in the estimation. We then tested our predictions against roadside air quality measurements. We analyzed near-roadway air quality for three different scenarios: 2009 conditions, 2025 conditions assuming the new campus is not built, and 2025 conditions assuming the campus is built. Information on traffic counts for all these scenarios came from the previously completed transportation impact analysis [14]. We modeled air quality effects only for daytime traffic (6 a.m. to 7 p.m.), since we assume that the major impacts will occur during these hours.

We modeled PM2.5 concentrations at each of the 160 census blocks located within 500 m of the study corridor (following guidance from the Health Effects Institute suggesting that key traffic-related pollution impacts occur within 300–500 m of major roadways) [15]. Approximately 16,000 people live within these census blocks [16]. In this study, the population

exposures in each census block are represented by the estimated 24-hour PM2.5 concentrations at each receptor.

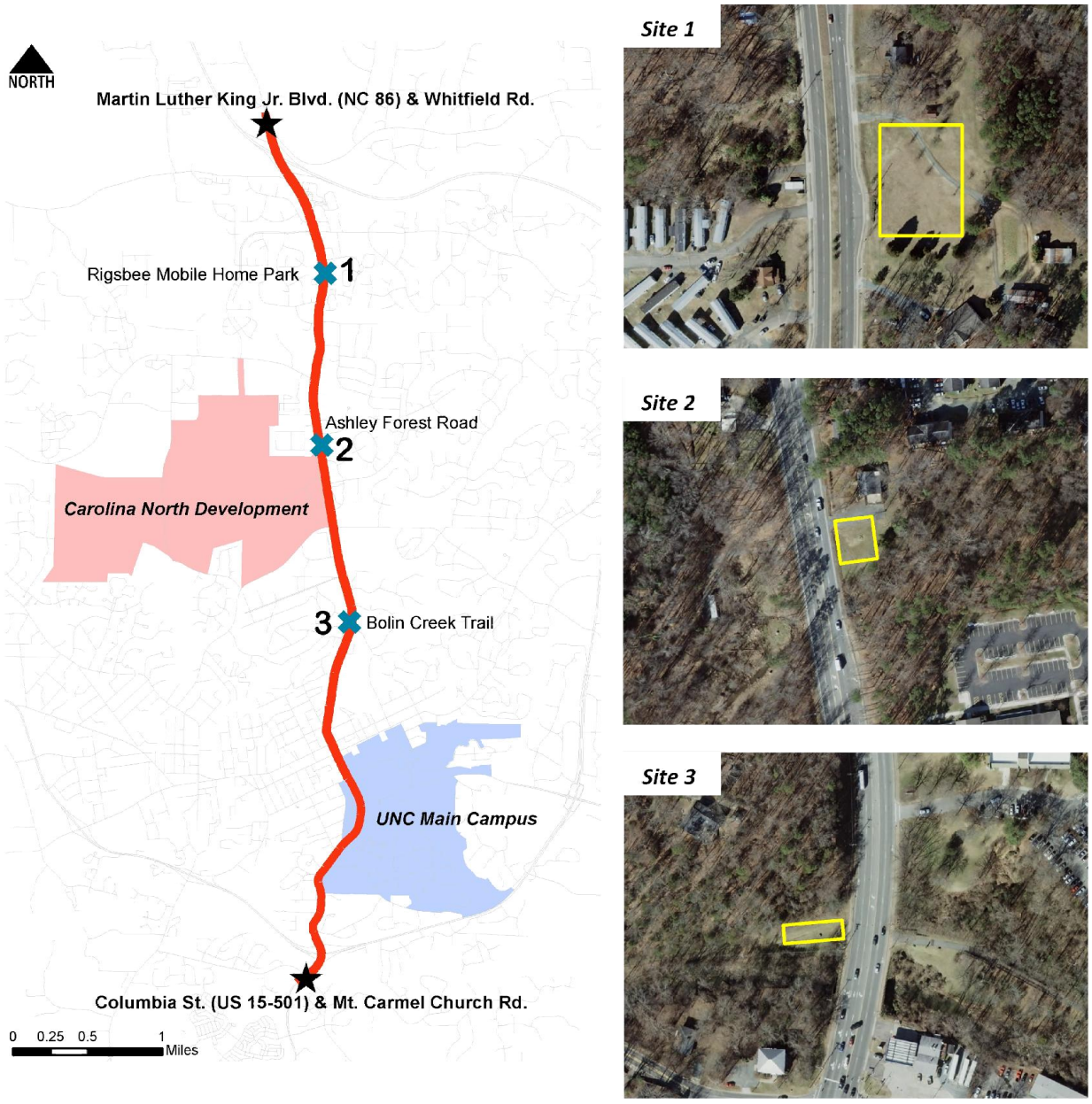

Figure 2.1 The study corridor runs from the intersection of Martin Luther King Jr. Boulevard and Whitfield Road to the intersection of South Columbia Street and Mt. Carmel Church Road, Chapel Hill, NC. This map also shows the locations of the three selected study sites. Site 1 is on the east side of Martin Luther King Jr. Blvd., opposite the Rigsbee Mobile Home Park. Site 2 is on the east side of Martin Luther King Jr. Blvd. near Ashley Forest Rd. Site 3 is on the west side of Martin Luther King Jr. Blvd., opposite the entrance to Bolin Creek.

Modeling Approach

Our modeling framework includes nine steps (**Figure 2.2**):

Step 1: Divide roadway into links for analysis. Air emissions from any single vehicle depend substantially on the vehicle speed, vehicle acceleration, time spent idling, and road grade. To account for these effects, we followed the approach of Ritner et al. by dividing the study corridor roadway into very short links [10]. In total, we modeled 1200 links along the 8.2 km (5.1 mile) study corridor. Each link has a roughly constant road grade; fraction of vehicle time spent decelerating, idling or accelerating; and moving speed. We used ArcGIS 9.3.1 (ESRI, Redlands, CA) and 2010 aerial photos from the Orange County Geographic Information Systems (GIS) Division to draw the series of links [17]. Link-specific traffic activities were determined based on the simulated traffic data for 2009, 2025 no-build, and 2025 build scenarios from the transportation impact analysis [14]. Link-specific average speeds were assumed to be equal to speed limits based on GIS street maps from the Town of Chapel Hill [18]. The speed limit was 25 mph for 17% of the links, 35 mph for 68% of the links, and 45 mph for the remaining 15%. Link-specific grades were derived from GIS contour maps from the Town of Chapel Hill [19] and ranged from 0%–10%.

Step 2: Estimate vehicle emissions factors for six different temperatures for each link using MOVES. As suggested by both Ritner et al. [10] and the U.S. Environmental Protection Agency's (EPA) "Guidance on Quantitative PM Hot-Spot Analyses for Transportation Conformity" [20], we used MOVES 2010b (Motor Vehicle Emission Simulator, EPA, Washington, DC) to develop 2009 and 2025 link-specific emission rates of PM2.5 (grams/vehicle-mile), according to link-specific traffic activities, average speeds, and grades. The MOVES model was developed by the EPA based on laboratory tests that measured

emissions from different kinds of vehicles under conditions designed to represent typical driving behaviors. Unlike its predecessor, known as MOBILE6, MOVES can provide separate emissions factors for different vehicle operation modes: acceleration, deceleration, idling, and cruising [10].

MOVES models emissions for 13 vehicle types: motorcycle, passenger car, passenger truck, light commercial truck, intercity bus, transit bus, school bus, refuse truck, single unit short-haul truck, single unit long-haul truck, motor home, combination short-haul truck, and combination long-haul truck. It also considers three fuel types: gasoline, diesel, and compressed natural gas. Hence, in order for the model to provide accurate estimates for any specific roadway segment, the fraction of vehicles in each class and fuel type category must be estimated. For this analysis, we used vehicle fleet distribution data from Guilford County, NC [21] (county seat: Greensboro), since data specific to Chapel Hill were unavailable. The fuel type distributions as well as fuel supply and formulation in the project areas were based on national defaults. These data (fleet distributions and fuel types) were fixed in all MOVES runs.

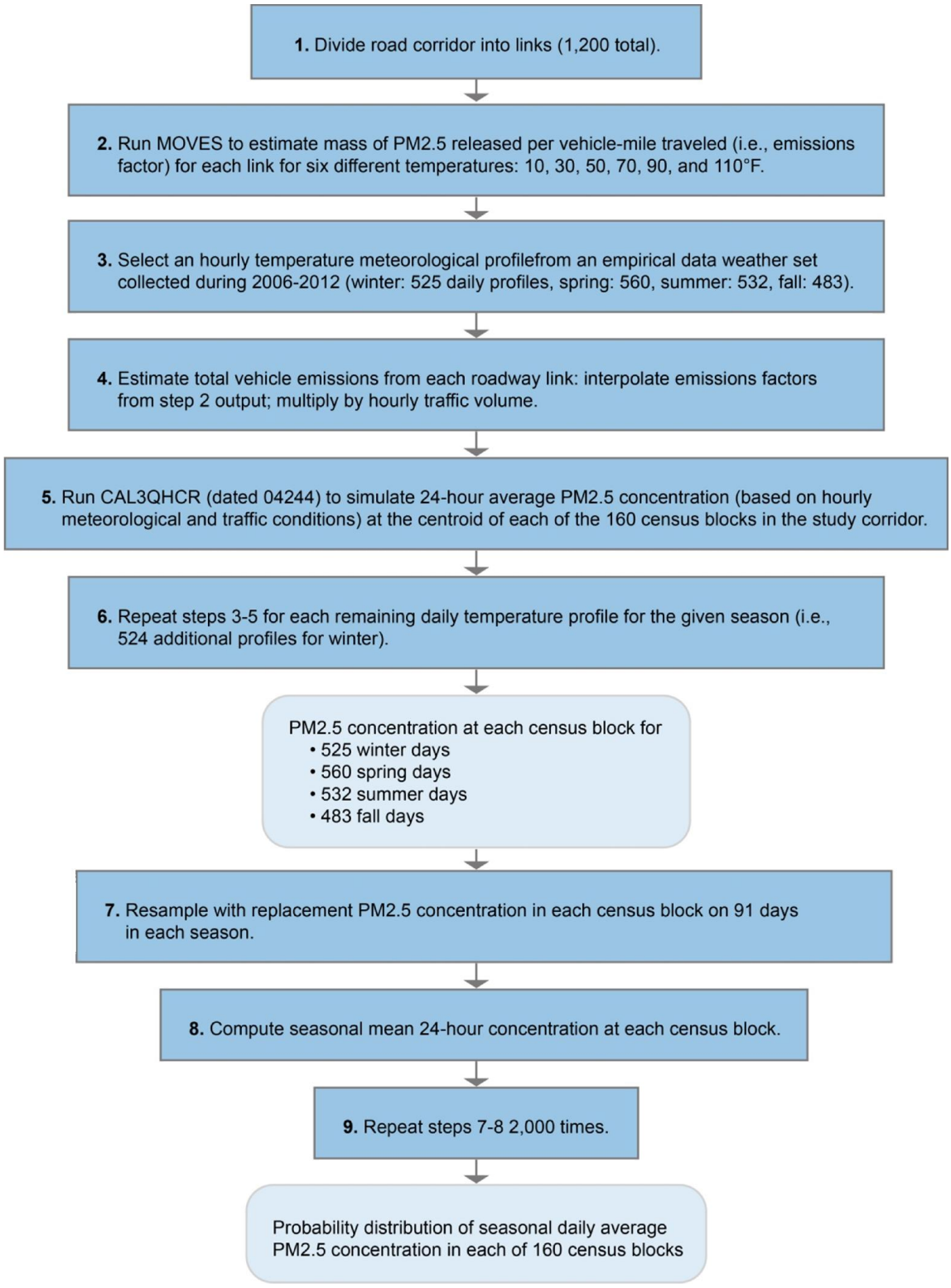

Figure 2.2 Flowchart showing the nine steps of our modeling framework

The EPA's PM hot-spot guidance recommends that the link-specific emission rates should be prepared based on average temperatures for four different time periods in a day for each season, meaning that each development scenario would require 16 MOVES runs. However, this approach does not fully account for daily temperature variability within a given season. Previous studies have shown that PM emission rates are highlight sensitive to temperature, and hence omitting temperature variability could decrease the accuracy of modeled emissions factors [22, 23]. Our new algorithm for representing intra-seasonal variability in temperature and meteorological conditions runs MOVES for six different temperatures: 10, 30°F, 50°F, 70°F, 90°F, and 110°F [23]. Later steps of the algorithm (described below) interpolate between these six estimates to determine temperature-specific emissions factors for each roadway link. For example, if a wintertime simulation of any given hour yielded a temperature of 40°F for that hour, we then estimated the vehicle emissions factors to be the average of the emissions factors for 30 and 50 degrees.

Step 3: Select an hourly temperature and meteorological profile from empirical weather data. The meteorological data to estimate probability distributions of the effects of weather on PM2.5 concentrations for each season were obtained from the EPA's Meteorological Processor for Regulatory Models, using 2006–2012 surface and upper air data at the national weather stations in Chapel Hill and Greensboro respectively [24, 25]. A total of 2,100 days with complete required data were used in the modeling, including 525 days for winter, 560 days for spring, 532 days for summer, and 483 days for fall. Seasonal temperature profiles are shown in **Figure 2.3**. **Figure 2.4** shows the distributions of seasonal wind speed and direction. In this third step, we selected one day from these 2,100 days to support the modeling in steps 4–5 below, and

then we repeated this selection (step 6) without replacement 2099 times until we had estimated PM2.5 concentrations in each census block for each day having a complete weather record.

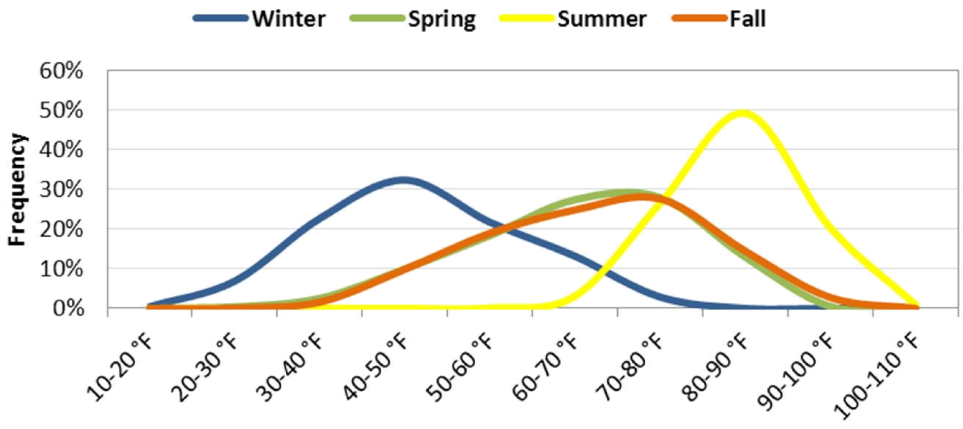

Figure 2.3 Seasonal temperature profiles from 6 a.m. to 7 p.m., according to the meteorological data used in the CAL3QHCR modeling

Step 4: Estimate the total emissions from vehicles traveling on each roadway link.

The MOVES model estimates average per-vehicle emissions in grams per vehicle-mile, accounting for the specific distribution of vehicle types, ages, and fuel sources at the study site. The next step was to compute the total mass of PM2.5 emitted from each vehicle on each roadway link. For this step, vehicle counts were needed. The link-specific traffic volumes were based on the simulated traffic data for 2009, 2025 no-build, and 2025 build scenarios from the Carolina North Traffic Impact Analysis [14]. For the temperature profile selected in step 3, we estimated emissions factors by interpolating between the outputs of step 2 for the nearest two temperatures.

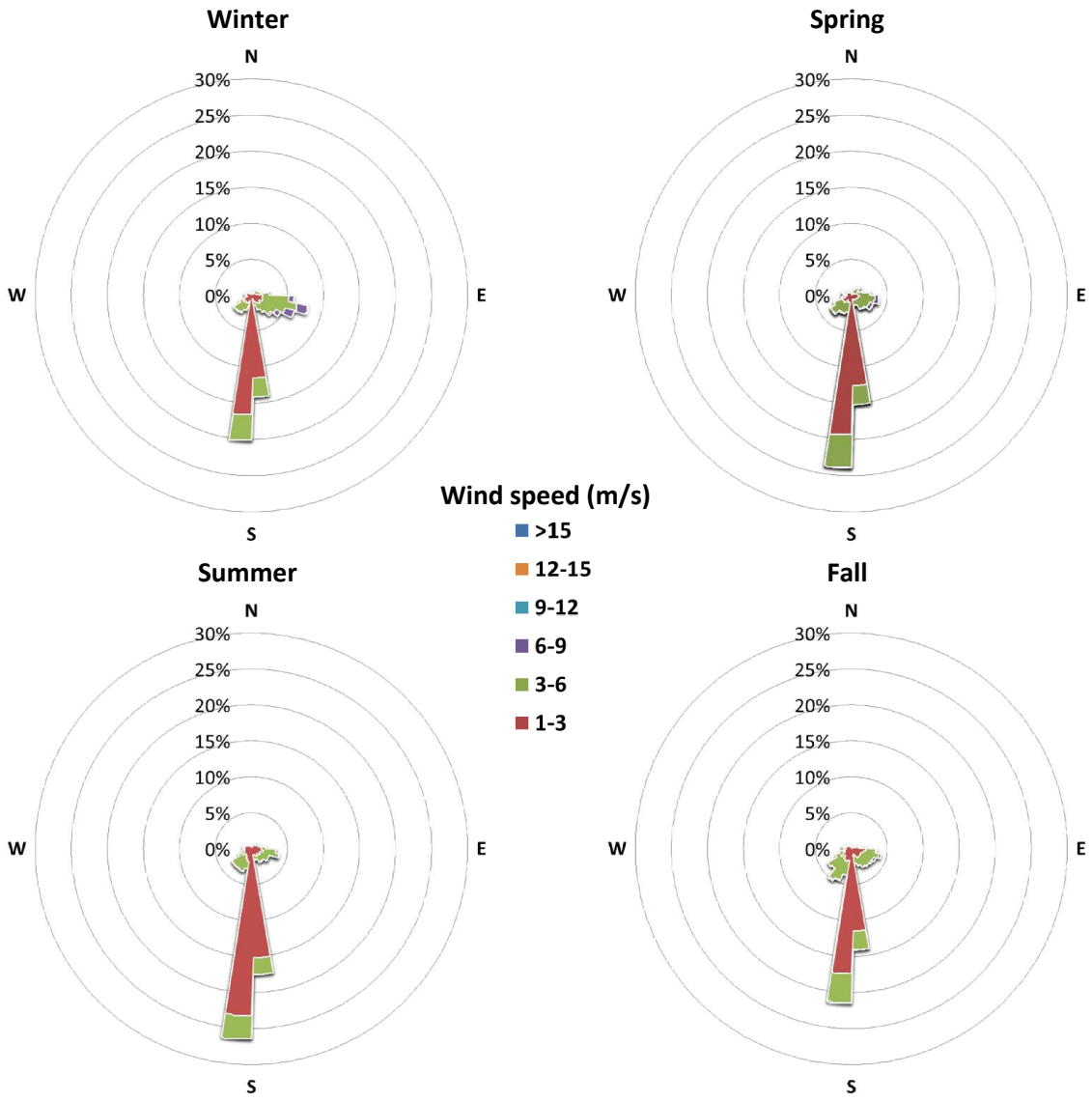

Figure 2.4 Seasonal wind roses from 6 a.m. to 7 p.m., according to the meteorological data used in the CAL3QHCR modeling

Step 5: Model dispersion of PM2.5 from roadway emissions into the surrounding neighborhoods using CAL3QHCR. The PM hot-spot guidance suggests two air pollution dispersion models—CAL3QHCR (EPA, Research Triangle Park, NC) or AERMOD (EPA, Research Triangle Park, NC)—for simulating PM2.5 pollution dispersion from roadways. Both models are based on Gaussian plume dispersion. However, a recent model comparison study suggested that CAL3QHCR requires less meteorological data and user effort and appears to

perform better than AERMOD for analyses at the urban project scale [26]. In this study, we tested and used CAL3QHCR for estimating population exposure to PM2.5 ($\mu g/m^3$) from the study corridor. As described below under "model validation approach," we tested two different versions of CAL3QHCR: one dated 13196 and the other dated 04244. We then used the best-performing of the two in subsequent simulations. We ran CAL3QHCR for each roadway link using the meteorological profile from step 3 and the per-link total PM2.5 emissions from step 4. We modeled concentrations at an elevation of 1.5 m, corresponding to the elevation of the adult breathing zone.

Steps 6-9: Generate probability distribution of seasonal average 24-hour PM2.5 concentration. As **Figure 2.2** outlines, we first repeated steps 3–5 for each of the days (2,100 in total) for which historical empirical weather data were available. The result was 2,100 separate daily estimates of the PM2.5 concentration at each of the 160 census block centroids: 525 winter day estimates and 560, 532, and 483 spring, summer, and fall estimates, respectively. We then used a bootstrap technique to estimate a probability distribution for the average daily PM2.5 concentration in each season. Specifically, for each season, we resampled with replacement 91 days from the simulated daily PM2.5 concentration estimates. We then computed the mean value of these 91 daily estimates for each receptor. Then, we repeated this process of computing a seasonal mean 1,999 times, in order to generate a sample of 2,000 seasonal mean 24-hour PM2.5 concentrations. This sample then served as the basis for developing a probability distribution of the mean concentration for each season.

Model Validation Approach

This study tested the performance of the combined MOVES-CAL3QHCR modeling approach by comparing model predictions against roadside measurements at three selected sites

along the study corridor (**Figure 2.1**). Furthermore, we compared the predictive validity of two versions of CAL3QHCR (dated 04244 and dated 13196) According to the model change bulletin, the mixed mode rounding in the internal calculations of CAL3QHCR dated 04244 was removed from CAL3QHCR dated 13196. Consequently, the simulated concentrations from these two model versions are different in some cases.

We used a DustTrak DRX Aerosol Monitor Model 8534 (TSI, Shoreview, MN) to measure total PM2.5 concentrations at each of the three sites The DustTrak DRX instrument or similar models have been used in roadside measurements in several previous studies [27–29]. The DustTrak can detect concentrations from 1 to 150,000 $\mu g/m^3$ with an error of ±0.1% of the monitored concentration [30]. All of these instruments are calibrated at the factory with a known mass concentration of Arizona Test Dust (ISO 12103-1, A1 test dust) [31]. In addition, in each sampling period, we calibrated the instrument before taking measurements. During all sampling events, the DustTrak was held about 1.5 m above the ground (the adult breathing zone height) and programmed to record the total concentration every five seconds.

We collected samples on two separate days at Site 1 and on one day at Sites 2 and 3 for a total of four sampling days in the study corridor. During three of the four sampling days, we monitored PM2.5 concentrations during the morning and evening peak traffic periods and also in the middle of the day four an hour at a time (roughly 8:00–9:00 a.m., noon–1:00 p.m., and 5:00–6:00 p.m.). At Site 2, the property owner requested that we not collect samples in the evening, so we only sampled during the morning and noon hours. **Table 2.1** shows sample collection dates and measured PM2.5 concentrations.

During each sampling event, we drew continuous air samples for three minutes at 10 m from the roadway and then repeated the three-minute sampling at locations of 30 m and 50 m

from the roadway (except at Site 2, where obstructions prevented sampling at 50 m). Then, we repeated this process over the course of about one hour. As a result, at each site and during each sampling event, we collected PM2.5 concentrations for six three-minute intervals at 10 m, 30 m, and 50 m perpendicular distances from the roadway, as **Figure 2.5** illustrates. For each event, we then computed the average PM2.5 concentration measured during these three-minute intervals; **Table 2.1** shows the resulting estimated one-hour average concentrations.

During each sampling event, we simultaneously collected traffic counts and meteorological data. Traffic was monitored with a hand-held counter, and the counts were confirmed by viewing digital video recordings from a portable video recorder positioned on a tripod to film the roadway during sampling. We measured wind speed using a Skymate model SM-18 wind meter with accuracy within 3% (Campbell Scientific, Inc, Logan Utah); wind direction using a windsock and compass; and temperature, dewpoint, and relative humidity using an Extech model 445814 thermometer-psychrometer with temperature accuracy of ±1.8° F and relative humidity accuracy of ±4%. Data on atmospheric stability class and mixing height were estimated using EPA's Meteorological Processor for Regulatory Models. **Table 2.2** shows the traffic counts and meteorological conditions for each sampling event.

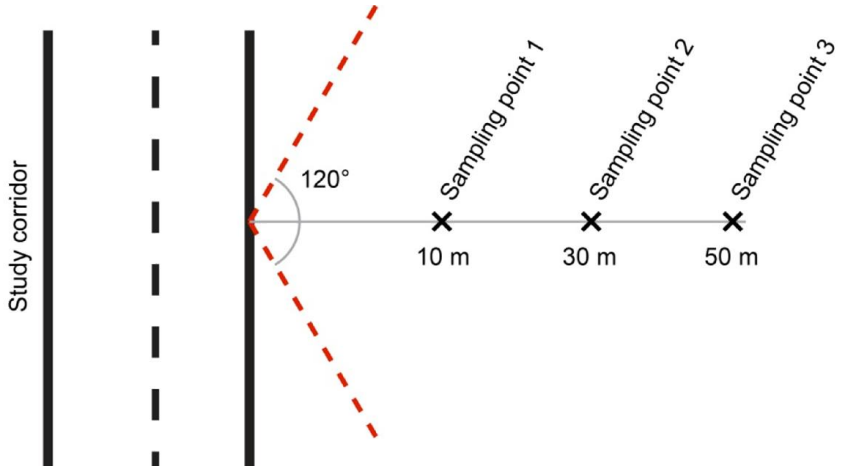

Figure 2.5 Diagram of sampling points along the study corridor

The measured concentrations at each sampling point represent the sum of background concentrations, PM2.5 contributions from other nearby sources, and traffic-related PM2.5. Therefore, in order to evaluate the performance of the CAL3QHCR model, concentrations of PM2.5 attributable to background and other sources must be subtracted from the monitored concentrations, in order to determine how much of the measured PM2.5 comes from the roadway. In testing model performance, other studies have used background concentrations measured at an upwind location or central air quality monitor [26, 32, 33]. However, Chapel Hill does not have an active PM2.5 monitor; the nearest PM2.5 monitor is about 45 km away, in Raleigh. Furthermore, due to resource limitations, we were able to use only one DustTrak monitor and hence were unable to capture background concentrations while simultaneously measuring near-road concentrations. Hence, we accounted for the effect of background PM2.5 by characterizing the differentials between the measured concentrations at pairs of sampling points at distances 10 m and 30 m, 10 m and 50 m, and 30 m and 50 m from the roadway. **Table 2.1** shows these differentials, as computed from the measured concentrations.

A factor-of-two plot has been commonly used to evaluate the performances of the CALINE series of dispersion models (e.g., CALINE3, CAL3QHC/CAL3QCHR, and CALINE4) [26, 32–35]. That is, modeled PM concentrations are plotted against measured concentrations to see whether the model estimates are within a factor of two of measured concentrations. Typically, the model is considered valid in predicting the traffic-related concentrations if at least 75% of the comparing pairs are within a factor-of-two envelope. This criterion was also applied in this study. We adopted this approach, comparing measured PM2.5 concentration differences between pairs of points with differences predicted by the two different CAL3QHCR model versions.

Data Cleaning

In total, the sampling events shown in **Table 2.1** yielded 29 data points. Of these, five points had to be eliminated because the wind direction was outside of a 120° degree arc from a line drawn perpendicular to the roadway (see **Figure 2.5**). In such conditions, the monitoring locations were not downwind of the roadway and therefore could not capture roadway contributions to PM2.5 [36]. Four additional data points were eliminated because they indicated negative dispersion (that is, PM2.5 concentrations increased rather than decreased with distance from the roadway). This data cleaning process left 20 data points for comparing measured PM2.5 concentrations to modeled concentrations.

Table 2.1 Measured and predicted PM2.5 concentrations ($\mu g/m^3$)

			Measured concentrations*			Measured concentration difference**			Predicted concentration differences: CAL3QHCR (dated 04244)			Predicted concentration differences: CAL3QHCR (dated 13196)		
Site	Date	Time period	10 m	30 m	50 m	10 vs. 30 m	10 vs. 50 m	30 vs. 50 m	10 vs. 30 m	10 vs. 50 m	30 vs. 50 m	10 vs. 30 m	10 vs. 50 m	30 vs. 50 m
1	16-May	Morning	14.9	13.8	13.9	1.1	1	NEG	0.7	0.9	0.2	0.7	1	0.3
		Noon	9	8.7	8.3	0.3	0.7	0.4	0.5	0.8	0.3	0.4	0.6	0.1
		Evening	9.7	10	9.7	NEG	NEG	0.3	1	1.3	0.3	0.9	1.3	0.3
	31-May	Morning	5.1	5.1	4.9	0	0.2	0.2	0.7	0.8	0.1	0.7	0.9	0.2
		Noon	2.6	2.2	1.6	0.4	1	0.6	0.5	0.8	0.3	0.5	0.6	0.2
		Evening	3	2.6	2.4	0.4	0.6	0.2	1.1	1.4	0.3	1	1.3	0.4
2	24-Apr	Morning	21.4	20.8	NA	WD	NA	NA	0.5	NA	NA	0.5	NA	NA
		Noon	10.5	10.4	NA	WD	NA	NA	0.7	NA	NA	0.6	NA	NA
3	16-Apr	Morning	10.8	10.8	10.5	NEG	0.3	0.3	0.7	0.9	0.2	0.6	0.8	0.2
		Noon	9.7	9.2	9	0.5	0.7	0.2	0.6	1	0.4	0.5	0.7	0.2
		Evening	9.2	8.9	8.5	WD	WD	WD	0	0	0	0.1	0.1	0

* NA indicates PM2.5 could not be measured at this location due to a physical obstruction.

** Negative values excluded during data cleaning are labeled as "NEG;" those excluded due to unfavorable wind direction are labeled as WD.

Table 2.2 Traffic and meteorological data used in CAL3QHCR modeling									
Site	Date	Time period	Average Traffic Count (veh/min)	Average wind Direction (deg)	Average wind direction within 120° arc from study corridor?	Average wind Speed (m/s)	Average Temperature (°F)	Stability Class*	Mixing height (m)*
1	16-May	Morning	34	80	Yes	0.8	73.7	Slightly unstable	678
		Noon	26	83*	Yes	1.4	85.9	Unstable	1315
		Evening	42	91	Yes	0.7	80.5	Slightly unstable	1395
	31-May	Morning	34	91	Yes	0.9	77.5	Slightly unstable	878
		Noon	29	55	Yes	1.5	88.6	Unstable	1676
		Evening	38	41	Yes	0.8	99.4	Slightly unstable	1776
2	24-Apr	Morning	32	349	No	0.6	56.9	Slightly unstable	670
		Noon	27	37	No	1.1	74.8	Unstable	1360
3	16-Apr	Morning	24	252	Yes	0.2	68.5	Neutral	1869
		Noon	22	264	Yes	0.7	80	Very unstable	1939
		Evening	31	20*	No	0.7	77.8	Neutral	1944

Wind speeds below 1 m/s were reset to 1 m/s when used in the CAL3QHCR modeling, as suggested in EPA's Meteorological Monitoring Guidance for Regulatory Modeling Applications [37].

* Data obtained from MPRM.

Results

Vehicle Emission Rates

The output from MOVES can provide useful insights about the vehicle classes contributing most to roadside pollution, the effects of meteorological and road characteristics on per-vehicle emissions, and the effects of future vehicle technologies.

To identify the vehicle classes contributing most to roadway emissions, we ran MOVES for a study corridor link with 0% grade, a 35 mph speed limit, and an ambient temperature of 90°F. **Figure 2.6** shows the results. This analysis reveals that trucks are the major contributors to roadside emissions for this corridor. In total, trucks of all categories contribute 79% of emissions: 19% from passenger trucks (e.g., sport utility vehicles) and the remaining 60% from

various kinds of commercial trucks. Consistent with this result, diesel-fueled vehicles account for nearly two-thirds (64%) of emissions whereas gasoline-fueled vehicles account for 36%. As well, vehicles more than 10 years old account for half of the roadside emissions. Hence, improving emissions controls or engine efficiency in diesel-fueled trucks, plus retiring older vehicles, could greatly reduce roadside emissions in the study corridor.

MOVES output also shows the important effects of temperature, road grade, and vehicle speed on roadway emissions. As **Figure 2.7** shows, emissions decrease as temperature increases, increase as road grade increases, and decrease as vehicle speed increases. These results illustrate the importance for modeling of accurately capturing temperature, vehicle speed, and especially road grade—hence the importance of dividing a study corridor into short links as in our study.

Interestingly, the results show that 2009 link-specific emission rates (ranging from 0.02–0.50 g/veh-mile) are higher than 2025 link-specific emission rates (ranging from 0.01–0.26 g/veh-mile). The differences result from the assumption, built into MOVES, that future vehicles will have more efficient engines that reduce emissions and will use cleaner fuels.

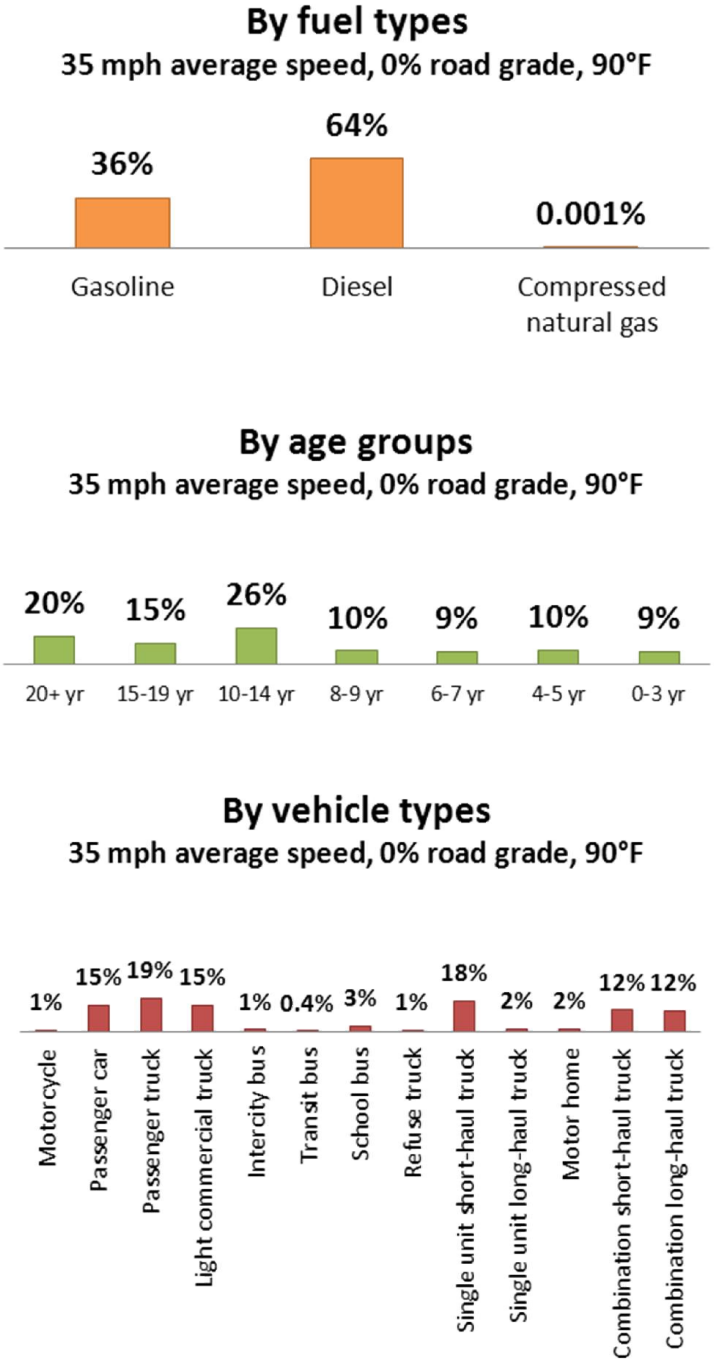

Figure 2.6 Example of 2009 link-specific emission rate fractions (%) at 35 mph average speed, 0% grade, and 90°F by fuel types, age groups, and vehicle types

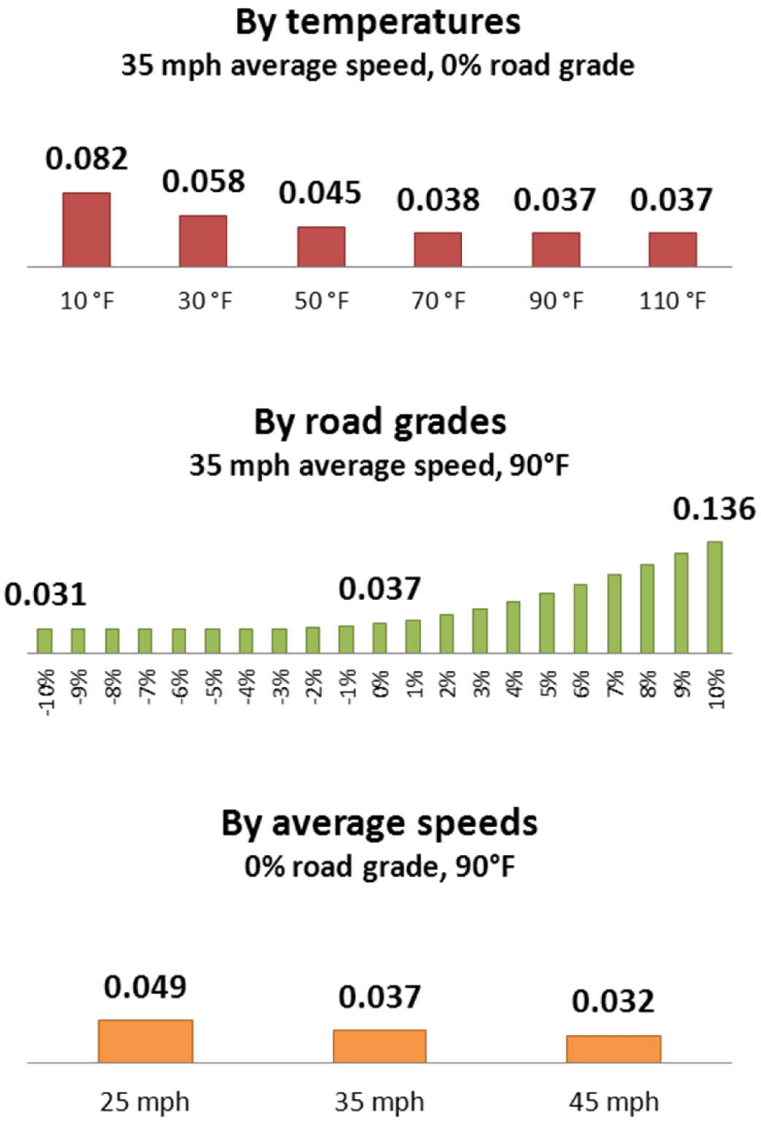

Figure 2.7 Examples of 2009 link-specific emission rate (g/veh-mile) changes by average speeds, grades, and temperatures

Model Performance Evaluation

Figure 2.8 compares the predictions of the two CAL3QHCR model versions to measurements of pollutant dispersion along the roadway corridor. The figure also shows the "factor-of-two envelope:" that is, the range of predictions that are within a factor of two of the measured dispersion. As shown, the models contain both under-predictions of the amount of dispersion (i.e., data points below the factor-of-two envelope) and over-predictions (data points more than twice the measured amount). However, both models are more likely to over-predict than to under-predict dispersion: that is, to predict greater concentration differences as one moves away from the roadway than were actually measured. Possible reasons for this prediction error include physical obstacles to dispersion (for example, at site 3, a large rock outcropping may interfere with dispersion) and intermittent winds. Previous model evaluations also have observed that the predecessor to CAL3QHCR did not perform well in the presence of street canyons or other physical obstacles or when winds are intermittent [32].

Of the two models, model 1 (the version dated 04244) performs better than model 2 (the version dated 1196). For model 1, 15 modeled estimates (75%) were within a factor of two of the measured value. Previous studies have suggested that a 75%, factor-of-two prediction capability indicates reasonable model performance, and model 1 achieves this metric [32]. For model 2, 13 observations (65%) were within a factor of two of observed values. Because model 1 better predicted the observed data than model 2, we used model 1 for our exposure predictions.

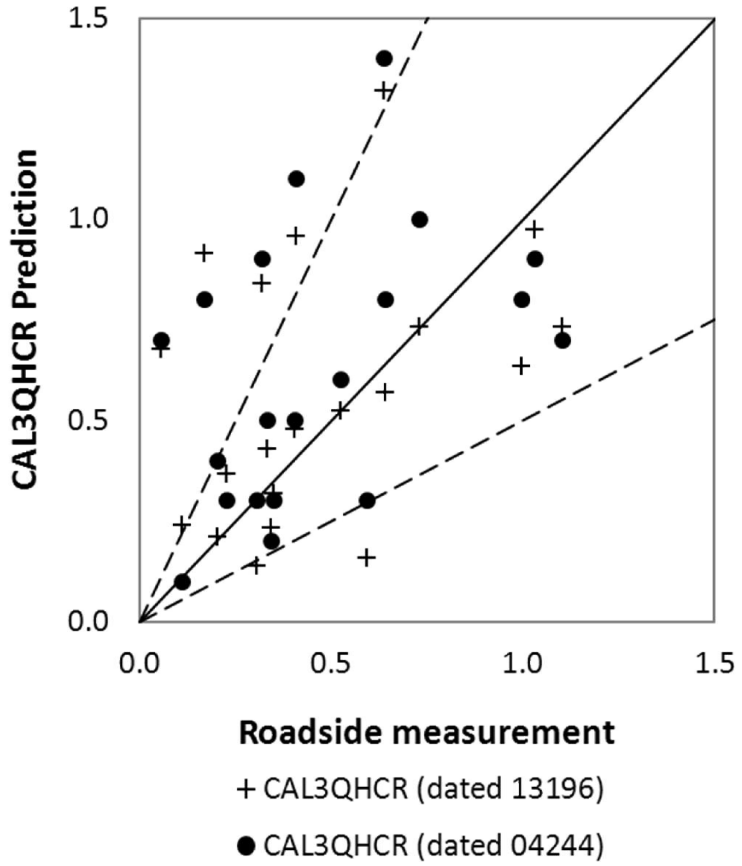

Figure 2.8 Factor-of-two plots of concentration differences (μg/m3) observed during roadside measurements and predicted byCAL3QHCR (dated 13196 and dated 04244)

Estimated PM2.5 Exposure under Current and Future Scenarios

Our modeling approach can be used to predict the effects of the Carolina North campus on ambient PM2.5 concentrations in census blocks in the study corridor if the campus is built.

Even if the new campus is built, the roadway contribution to ambient PM2.5 levels in the study corridor is predicted to be very low by 2025. The maximum contribution of traffic to any one census block occurs in winter and is predicted to be 0.11 $\mu g/m^3$, which is quite low in comparison with the ambient air quality standard (12 $\mu g/m^3$ annual average PM2.5 concentration). In comparison, if the new campus is not built, the maximum PM2.5 concentration in any one census block is 0.085 $\mu g/m^3$, which is 24% lower than if the campus is

built. In both cases, though, the maximum concentration is higher under current conditions than under future conditions, despite the anticipated traffic growth. Under current conditions, the model predicts that the maximum roadway contribution to seasonal PM2.5 in any one census block is 0.14 μg/m^3, which is 24% higher than expected in 2025, even if the new campus is built. These future emissions reductions reflect the built-in assumptions of MOVES that the future vehicle fleet will become more efficient (less polluting) and that fuels will be cleaner. The results thus illustrate the value of ensuring continued improvements in vehicle fuel economy and emissions standards.

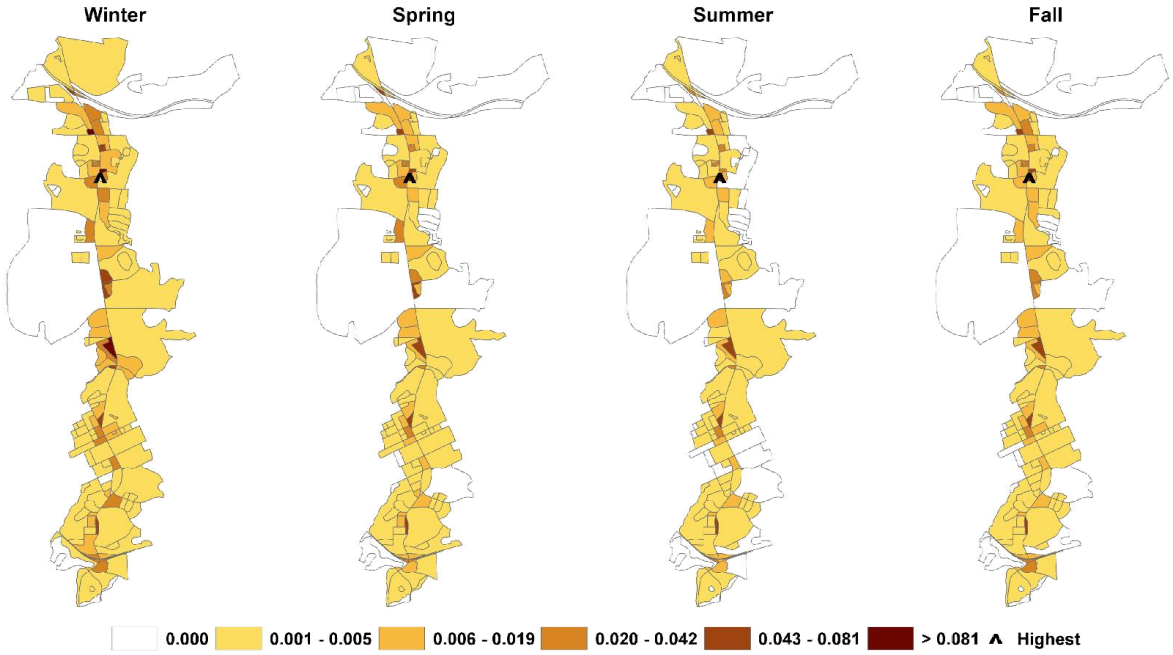

Figure 2.9 PM2.5 concentrations attributable to roadway emissions from the study corridor, as predicted by the combined MOVES-CAL3QHCR approach (μg/m^3) by season for the year 2009

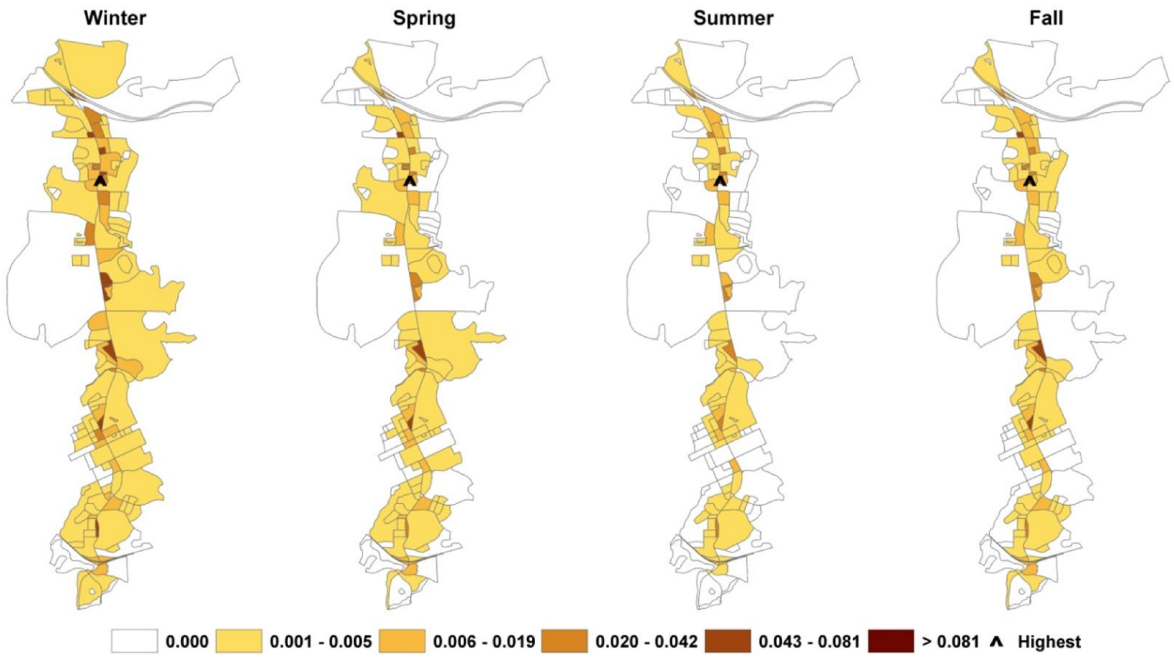

Figure 2.10 PM2.5 concentrations attributable to roadway emissions, as predicted by the combined MOVES-CAL3QHCR approach ($\mu g/m^3$) by season for the year 2025, assuming the Carolina North Campus is built

Our modeling approach included a new method for representing meteorological variability. Our results illustrate that variability can be important in some locations. Overall, the daily meteorological variability caused little change in seasonal daily mean PM2.5 concentrations. For example, in the 2025 scenario in which the Carolina North campus is built, the average coefficient of variation (i.e., standard deviation of the predicted seasonal mean divided by average of the seasonal mean) is 0.06, meaning that seasonal variability on average has a relatively small effect on model predictions. The maximum coefficient of variation in this scenario was less than 0.5, which means that 95% of the time, meteorological variability will change the predicted seasonal mean by less than a factor of 2. (According to the Central Limit Theorem, the seasonal mean converges to a normal distribution, and hence 95% of the time, the seasonal mean should be within two standard deviations of the actual mean, and in this case the standard deviation is about half the mean.) Thus, this meteorological variability is less important than the model uncertainty shown in **Figure 2.8**.

The modeling approach can be used to characterize spatial variability in roadway emissions effects on surrounding neighborhoods. **Figure 2.9** shows the resulting spatial variability for current conditions, and **Figure 2.10** shows the spatial variability for future conditions. In both instances (because both models rely on the same set of meteorological data), the census block with the maximum concentration is in the same location and also (despite changes in wind directions) does not vary seasonally. The most affected census block (shown with arrows in **Figures 2.9 and 2.10**) is located on the east side of Martin Luther King Jr. Boulevard at Blossom Lane. Such information could be useful for zoning decisions (e.g., decisions about locations for schools, retirement homes, or other land uses attracting sensitive populations).

Discussion

Our results are consistent with the few empirical evaluations of the accuracy in predicting roadway PM2.5 concentrations of CAL3QHCR and its predecessor, known as CALINE. Yura et al. compared CALINE predictions of PM2.5 to measured PM2.5 concentrations at a busy intersection in a suburban community in Sacramento, California, and an urban site along a six-lane road in London, England [32]. They found that 80% of model predictions were within a factor-of-two envelope of measured concentrations at the suburban site but that only 56% of predictions were within the factor-of-two envelope for the urban site. They attributed the poor performance at the urban site to limitations of the emissions factors they used (they relied on scaling United Kingdom PM10 emissions factors) and to street canyon effects. Chen et al. extended Yura's work by comparing the performance of the CAL3QHC model to that of the CALINE model for the same two sites (although during a different time period) as Yura used [26]. Chen et al. found that predicted PM2.5 concentrations were within the factor-of-two

envelope for 69% of the Sacramento data points and for 59% of the London data points. In both cities, CAL3QHC outperformed CALINE. Gokhale and Raokhande compared the CALINE and CAL3QHC models' ability to predict roadside PM2.5 concentrations at a busy intersection in Guwahati, India [38]. They found that the CAL3QHC model predictions were within a factor-of-two envelope for 65% of (66 of 102) hourly PM2.5 observations during winter and that the CAL3QHC model outperformed the CALINE model (the latter of which produced predictions within the factor-of-two envelope for 46 of 102 data points).

Our findings about the amount of PM2.5 contributed to a given location by a single busy roadway also are consistent with findings of the few modeling studies and quantitative HIAs of local effects of traffic in the United States. In a modeling study, Zhang and Batterman used CALINE along with the predecessor to MOVES, known as MOBILE6.2, to estimate the amount of PM2.5 pollution contributed by a busy roadway in Detroit, Michigan [33]. They found that the local roadway contributed only a small amount of the measured PM2.5: total measured PM2.5 concentrations averaged 16.8 $\mu g/m^3$, but Zhang and Batterman attributed "no more than 0.5 $\mu g/m^3$" to the roadway. They attributed the majority of observed PM2.5 "to long range transport of sulfate and other aerosols from the Ohio River Valley." Chen et al. also found that roadways in Sacramento and London contributed relatively small fractions to observed PM2.5 concentrations at the study sites [26].

Of the four transportation-related quantitative HIAs identified in the comprehensive review by Bhatia and Seto et al., three predicted PM2.5 concentrations attributable to vehicles on roadways (the fourth predicted PM10 concentrations) [9]. All of these HIAs (including the HIA that estimated PM10 concentrations) focused on proposed new development projects in or near Oakland, California, and all used CAL3QHCR to support their predictions. The first, an HIA of a

proposed residential development to be constructed near a highway (with an average daily traffic volume of about 119,000 vehicles) in Pittsburg, California, used CAL3QHCR to estimate that traffic-attributable exposures adjacent to the highway are about 2 $\mu g/m^3$ but that these exposures decline rapidly with distance to about 0.2 $\mu g/m^3$ [39]; this estimate assumed a constant emissions factor of 0.15 g/vehicle-mile travelled, whereas our estimate employed MOVES to estimate link-specific emissions factors, resulting in a range of emissions factors of 0.02–0.5 g/vehicle-mile travelled. The second of these three quantitative HIAs considered the potential traffic-related health effects of potential affordable housing sites in Oakland, California; this HIA used CAL3QHCR to estimate that two major roadways with combined annual average daily traffic counts of about 225,000 vehicles would contribute about 0.4–0.5 $\mu g/m^3$ to PM2.5 exposures at the locations under consideration, all of which were within meters of the roadways [40]. The third HIA concerned a potential new residential development near a transit station in Oakland; it estimated that alongside a major highway (with daily traffic counts averaging 144,000 vehicles) neighboring the proposed development site, about 0.3 $\mu g/m^3$ of PM2.5 could be attributed to traffic but that this traffic-related contribution decreased to 0.1 $\mu g/m^3$ at a distance of 150 m from the highway [41]. In summary, these HIAs estimate that directly adjacent to highways running through the Oakland area, traffic contributes anywhere from about 0.3–2 $\mu g/m^3$. All of these highways have daily traffic counts at least five times as high as the current traffic along the roadway corridor analyzed in the present study. The estimated roadway contributions that our modeling approach yielded (with the maximum roadway-contributed concentration of 0.14 $\mu g/m^3$ under current conditions) hence are quite consistent with these previous estimates when traffic volumes and distances of census block centroids to the roadway are considered. That is, if one multiplies the maximum estimate from our modeling approach by 5, then the estimated

maximum predicted concentration in any census block in the study corridor is 0.7 $\mu g/m^3$. This is within the range of concentrations predicted in the California studies.

Conclusions

In this study, a new modeling framework to quantify the project traffic growth impacts on population exposure to PM2.5 air pollution was proposed and then demonstrated by quantifying exposure to roadway PM2.5 emissions that may occur in the future due to the Carolina North development in Chapel Hill, North Carolina. This modeling framework should benefit others conducting quantitative HIAs of the built environment and transportation projects. Whereas previous HIAs employing air dispersion models have used average meteorological data and have assumed that vehicles move at a constant cruising speed along roadway links, our approach considers link- by-link variation in vehicle behavior and hourly meteorological variability.

Our results reveal that improvements in vehicle technologies and fuels will be a key factor in protecting public health from the air pollution generated by increases in traffic expected to occur due to local and regional developments in the future. In fact, the models we employed predict that traffic-related PM2.5 in the study corridor may actually decrease in the future, even if traffic increases, due to improved vehicle technologies and fuels.

Our results also reveal the need for improve models to predict near-road PM2.5 concentrations. While the integrated air quality model was able to predict dispersion reasonably well, about 25% of model predictions over-estimated dispersion. This over-estimation bias results in under-estimates of pollutant exposure. Hence, reducing model bias is critical to ensuring that decision-makers are adequately informed about air quality and health risks associated with roadway traffic.

REFERENCES

[1] J. Kemm, "Perspectives on Health Impact Assessment," *Bull. World Health Organ.*, vol. 81, no. 6, p. 387, 2003.

[2] National Research Council, *Improving Health in the United States: The Role of Health Impact Assessment*. Washington, DC: The National Academies Press, 2011.

[3] A. Wernham, "Health Impact Assessments are Needed in Decision Making about Environmental and Land-Use Policy," *Health Aff. (Millwood).*, vol. 30, no. 5, pp. 947–56, 2011.

[4] R. Lozano, M. Naghavi, K. Foreman, S. Lim, K. Shibuya, V. Aboyans, …, and C. J. L. Murray, "Global and Regional Mortality from 235 Causes of Death for 20 Age Groups in 1990 and 2010: A Systematic Analysis for the Global Burden of Disease Study 2010," *Lancet*, vol. 380, no. 9859, pp. 2095–128, 2012.

[5] A. L. Dannenberg, R. Bhatia, B. L. Cole, S. K. Heaton, J. D. Feldman, and C. D. Rutt, "Use of Health Impact Assessment in the U.S.: 27 Case Studies, 1999-2007," *Am. J. Prev. Med.*, vol. 34, no. 3, pp. 241–56, 2008.

[6] M. Wismar, J. Blau, K. Ernst, and J. Figueras, "The Effectiveness of Health Impact Assessment: Scope and Limitations of Supporting Decision-Making in Europe," Copenhagen Ø, Denmark.

[7] R. Bhatia and M. Katz, "Estimation of Health Benefits From a Local Living Wage Ordinance," *Am. J. Public Health*, vol. 91, no. 9, pp. 1398–402, 2001.

[8] L. Singleton-baldrey, "The Impacts of Health Impact Assessment: A Review of 54 Health Impact Assessments, 2007-2012," University of North Carolina at Chapel Hill, 2012.

[9] R. Bhatia and E. Seto, "Quantitative Estimation in Health Impact Assessment: Opportunities and Challenges," *Environ. Impact Assess. Rev.*, vol. 31, no. 3, pp. 301–309, 2011.

[10] M. Ritner, K. K. Westerlund, C. D. Cooper, and M. Claggett, "Accounting for Acceleration and Deceleration Emissions in Intersection Dispersion Modeling Using MOVES and CAL3QHC," *J. Air Waste Manage. Assoc.*, vol. 63, no. 6, pp. 724–736, 2013.

[11] University of North Carolina at Chapel Hill, "About UNC," 2013. http://www.unc.edu/about/.

[12] Town of Chapel Hill, "Snapshot of the Town of Chapel Hill," 2012. http://www.townofchapelhill.org/Modules/ShowDocument.aspx?documentid=12177.

[13] K. Ross, “Carolina North Hearing Highlights Traffic Impact,” *The Carrboro Citizen*, 2009. http://www.carrborocitizen.com/main/2009/05/14/carolina-north-hearing-highlights-traffic-impact/.

[14] Vanasse Hangen Brustlin Inc., “Transportation Impact Analysis for the Carolina North Development,” Watertown, MA, 2009.

[15] Health Effects Institute, “Traffic-Related Air Pollution: A Critical Review of The Literature on Emissions, Exposure, and Health Effects, HEI Special Report 17,” Boston, MA, 2010.

[16] US Census Bureau, “Census Block Shapefiles with 2010 Census Population and Housing Unit Counts,” 2011.

[17] Orange County, “Aerials2010,” 2012.

[18] Town of Chapel Hill, “Street Centerline,” 2009.

[19] Town of Chapel Hill, “2ft Elevation Contours,” 2009.

[20] US Environmental Protection Agency, “Guidance on Quantitative PM Hot-Spot Analyses for Transportation Conformity,” 2011. http://www.epa.gov/otaq/stateresources/transconf/policy/pm-hotspot-guide.pdf.

[21] N.C. Division of Air Quality, “MOVES Input and Output Files: Hickory and Triad PM2.5 Redesignation Demonstration and Maintenance Plan,” 2011. .

[22] P. A. Mulawa, S. H. Cadle, K. Knapp, R. Zweidinger, R. Snow, R. Lucas, and J. Goldbach, “Effect of Ambient Temperature and E-10 Fuel on Primary Exhaust Particulate Matter Emissions from Light-Duty Vehicles,” *Environ. Sci. Technol.*, vol. 31, no. 5, pp. 1302–1307, 1997.

[23] D. Choi, M. Beardsley, D. Brzezinski, J. Koupal, and J. Warila, “MOVES Sensitivity Analysis: The Impacts of Temperature and Humidity on Emissions,” in *The MOVES Workshop 2011*, 2011.

[24] National Climatic Data Center, “Quality Controlled Local Climatological Data (QCLCD),” 2013.

[25] National Oceanic and Atmospheric Administration, “NOAA/ESRL Radiosonde Database,” 2013.

[26] H. Chen, S. Bai, D. Eisinger, D. Niemeier, and M. Claggett, “Predicting Near-Road PM2.5 Concentrations,” *Transp. Res. Rec. J. Transp. Res. Board*, vol. 2123, pp. 26–37, 2009.

[27] M. G. Boarnet, D. Houston, R. Edwards, M. Princevac, G. Ferguson, H. Pan, and C. Bartolome, "Fine Particulate Concentrations on Sidewalks in Five Southern California Cities," *Atmos. Environ.*, vol. 45, no. 24, pp. 4025–4033, 2011.

[28] J. S. Wang, T. L. Chan, Z. Ning, C. W. Leung, C. S. Cheung, and W. T. Hung, "Roadside Measurement and Prediction of CO and PM2.5 Dispersion from On-Road Vehicles in Hong Kong," *Transp. Res. Part D Transp. Environ.*, vol. 11, no. 4, pp. 242–249, 2006.

[29] Y. Wu, J. Hao, L. Fu, Z. Wang, and U. Tang, "Vertical and Horizontal Profiles of Airborne Particulate Matter Near Major Roads in Macao, China," *Atmos. Environ.*, vol. 36, no. 31, pp. 4907–4918, 2002.

[30] TSI Inc., "Spec Sheet Model 8533/8534 DustTrak DRX Aerosol Monitor," 2012.

[31] TSI Inc., "DustTrak DRX Aerosol Monitor Theory of Operation (EXPMN-002)," 2012.

[32] E. A. Yura, T. Kear, and D. Niemeier, "Using CALINE Dispersion to Assess Vehicular PM2.5 Emissions," *Atmos. Environ.*, vol. 41, no. 38, pp. 8747–8757, 2007.

[33] K. Zhang and S. Batterman, "Near-Road Air Pollutant Concentrations of CO and PM2.5: A Comparison of MOBILE6.2/CALINE4 and Generalized Additive Models," *Atmos. Environ.*, vol. 44, no. 14, pp. 1740–1748, 2010.

[34] P. E. Benson, "CALINE3, A Versatile Dispersion Model for Predicting Air Pollutant Levels Near Highways and Arterial Streets," Sacramento, CA, 1979.

[35] P. E. Benson, "CALINE4, A Dispersion Model for Predicting Air Pollutant Concentrations Near Roadways," Sacramento, CA, 1989.

[36] Battelle, "Detailed Monitoring Protocol for US 95 Settlement Agreement," Columbus, OH, 2006.

[37] US Environmental Protection Agency, "Meteorological Monitoring Guidance for Regulatory Modeling Applications, EPA-454/R-99-005," Research Triangle Park, NC, 2000.

[38] S. Gokhale and N. Raokhande, "Performance Evaluation of Air Quality Models for Predicting PM10 and PM2.5 Concentrations at Urban Traffic Intersection During Winter Period," *Sci. Total Environ.*, vol. 394, no. 1, pp. 9–24, 2008.

[39] Human Impact Partners, "Pittsburg Railroad Avenue Specific Plan Health Impact Assessment," Oakland, CA, 2008.

[40] Human Impact Partners, "Pathways to Community Health : Evaluating the Healthfulness of Affordable Housing Opportunity Sites Along the San Pablo Avenue Corridor Using Health Impact Assessment," Oakland, CA, 2009.

[41] UC Berkeley Health Impact Group, “MacArthur BART Health Imapct Assessment,” Berkeley, CA, 2007.

CHAPTER 3

HEALTH IMPACT ASSESSMENT OF TRAFFIC-RELATED AIR POLLUTION AT THE URBAN PROJECT SCALE: INFLUENCE OF VARIABILITY AND UNCERTAINTY[2]

Introduction

In the United States, nonprofit organizations and public health practitioners increasingly advocate for formal health impact assessments (HIAs) to inform land-use and transportation planning decisions [1, 2]. Signaling the heightened interest in HIAs in the United States, the U.S. National Academy of Sciences in 2011 published a report, *Improving Health in the United States: The Role of Health Impact Assessment*, concluding that "HIA is a particularly promising approach for integrating health implications into decision-making" [3]. The report offered the following formal definition of HIA:

> "HIA is a systematic process that uses an array of data sources and analytic methods and considers input from stakeholders to determine the potential effects of a proposed policy, plan, program, or project on the health of a population and the distribution of those effects within the population. HIA provides recommendations on monitoring and managing those effects."

As the National Academies report explains, the increasing demand for U.S. HIAs is driven by the growing recognition that reducing obesity and chronic disease rates will require

[2] *Chart-asa, C., & MacDonald Gibson, J. 2013. In preparation for* Science of the Total Environment

substantial changes to decision-making processes in arenas outside the traditional healthcare sector. For example, decisions by transportation and municipal planning organizations can promote or limit opportunities for physical activity and can exacerbate or decrease exposure to ambient air pollution. While HIAs have been used in Europe, Australia, Canada, and Thailand for decades, the first U.S. HIA was completed in 1999 by the San Francisco Department of Public Health [2, 3]. By the end of 2012, however, at least 115 U.S. HIAs had been completed, and another 64 were under way [4]. Of the completed HIAs, 70 (more than 60%) focused on proposed changes to the built environment and/or transportation networks [4, 5].

To have maximum impact on land-use and transportation decisions, HIAs ideally would provide quantitative estimates of the health effects of the decision alternatives under consideration. That is, they would estimate the number of deaths and illnesses prevented or caused by each alternative. This information then could be used to quantify the health costs (positive or negative) of each alternative. Such quantitative cost and benefit estimates are needed, because cost-benefit analysis drives major transportation and land-use decisions in the United States [6]. However, only 5 of the 70 transportation-related HIAs in the United States carried out prior to 2013 quantified the expected health impacts [4, 7]. **Table 3.1** summarizes these HIAs. The remaining HIAs expressed qualitative conclusions.

The *Aerotropolis Atlanta Brownfield Redevelopment HIA* [8] illustrates the qualitative approach used by most previous U.S. HIAs. This HIA evaluated a plan to convert a former Ford assembly plant near Atlanta, Georgia, to a new community called "Aerotropolis Atlanta." The HIA's analysis of air quality impacts was based on a review of previous studies (not associated with this project) of traffic impacts on air quality and health. It concluded, "Aerotropolis may lead to a change in traffic volume around the site . . . , potentially impacting people who live,

work, or visit within the air-shed of the affected streets." The HIA recommended several mitigation measures to reduce air pollution exposures: congestion pricing, increased public transit, zoning of sensitive uses away from roadways, and vegetation buffers around roadways. The HIA did not quantify the air quality or health impacts of the proposed new development or these mitigation alternatives.

While the above-mentioned five previous quantitative HIAs estimate the magnitude of air quality and related health impacts, none considers the potential variability and uncertainty of the estimates. Rather, these HIAs each provide a single, deterministic prediction of traffic-related air quality and health impacts for each decision option (see **Table 3.1**). The reliance on deterministic estimates is a major limitation because it fails to consider the full range of potential risks, including, for example, impacts on highly exposed or vulnerable populations or impacts under extreme weather conditions. The deterministic approach also fails to provide information to decision-makers about the degree of certainty in the predictions. **Box 3.1** highlights potentially important sources of variability and uncertainty. Previous quantitative HIAs have not considered the effects of these uncertainty and variability sources on their health impact estimates.

This paper aims to strengthen the tool set available to HIA practitioners by developing a new approach for incorporating variability and uncertainty in quantitative, transportation-related HIAs. Like four of the five HIAs in **Table 3.1**, we use airborne particulate matter having diameter less than 2.5 μm (denoted as PM2.5) as an indicator of traffic-related air pollution (the third HIA evaluated PM_{10}, particulate matter having diameter less than 10 μm). We first assess the effects on health impact estimates when including some or all of the variability and uncertainty sources listed in **Box 3.1**, in comparison to relying on the current, deterministic

approach. Then, we apply the method to a case study site to illustrate how it could be used in future HIAs. The results highlight the limitations of the current HIA approach and offer potential solutions to increase the usefulness of future HIAs for practical decision-making.

Table 3.1 Previous quantitative transportation-related HIAs in the United States

Title	Project analyzed	Traffic-related air pollutants considered	Study area population	Estimated annual health impacts
Pittsburg Railroad Avenue Specific Plan HIA [9]	New Bay Area Rapid Transit (BART) station and mixed-use village in Pittsburg, CA, including 1,600 housing units and 450,000 sq. ft. of retail, commercial, and public service spaces	PM2.5	4,770	• 6 deaths (age ≥ 30) • 5 hospital admissions for asthma (age < 65) • 12 lower respiratory symptom days (ages 7–14)
Evaluating the Healthfulness of Affordable Housing Opportunity Sites Along the San Pablo Avenue Corridor Using HIA [10]	Affordable housing sites in El Cerrito and Richmond, CA	PM2.5	1,000,000	• 33–41 deaths (all ages)
Oak to Ninth Avenue HIA [11]	New waterfront development in Oakland, CA, including 3,100 housing units and 200,000 sq. ft. of retail, commercial, and public service spaces	PM10	10,000	• 0.8 deaths (age ≥ 30) • 0.4 chronic bronchitis cases (age ≥ 27) • 10.6 emergency room visits for asthma (age < 65)
MacArthur BART Transit Village HIA [12]	Redevelopment of parking lot into a mixed-use village in Oakland, CA, including 625 housing units and 30,000 sq. ft. of retail, commercial, and public service spaces	PM2.5	100,000	• 2.7 deaths (age ≥ 30) • 1.0 chronic bronchitis cases (age ≥ 27) • 34.2 acute bronchitis cases (ages 8–12) • 0.1 hospital admissions for asthma (age < 65) • 26.9 lower respiratory symptom days (ages 7–14)
Health Impact Assessment of the Port of Oakland [13]	Ongoing growth of port operations in West Oakland, CA	PM2.5	22,000	• 1.3 deaths (age ≥ 30)

Box 3.1 Sources of variability and uncertainty in estimating health effects of PM2.5 from traffic

Sources of uncertainty

PM2.5 exposure concentration

- Air quality model prediction accuracy

Dose-response function

- Shape of dose-response function
- Dose-response coefficient

Sources of variability

PM2.5 exposure concentration

- Meteorology
- Vehicle fleet composition (vehicle type and age)
- Vehicle fuel
- Traffic volume
- Traffic speed
- Road grade
- Traffic behavior at intersections

Dose-response function

- Seasonal variability
- Population susceptibility

Demographic characteristics of exposed population

- Age
- Race
- Gender
- Health status

Case Study Site

We demonstrate the suggested new assessment process for a case study transportation corridor—Martin Luther King, Jr., Blvd.—in Chapel Hill, North Carolina. Traffic along this four-lane roadway is expected to increase in the future due to the planned construction of a new campus for the University of North Carolina at Chapel Hill (UNC). UNC, the oldest public university in the United States, has a current student population of about 29,000. The new campus, called "Carolina North," is intended to increase the university's capability to translate research into applications. It will be located about 3 km (2 miles) north of the existing campus (**Figure 3.1**). If constructed, it is expected to increase the number of trips to the area by 10,000 per day by 2015, with most of the increases expected to occur along Martin Luther King, Jr.,

Blvd., the main link between the new campus and the existing campus [14]. By 2025, the number of additional daily trips to the campus is expected to increase by as many as 40,000.

This analysis focuses on health effects of the expected additional traffic-related air pollution among residents living in census blocks within 500 meters of the study corridor. In all, this area encompasses 160 U.S. census blocks (see **Figure 3.1**) and has a total population of about 16,000—more than one-quarter of Chapel Hill's total population of 57,000.

We analyze the effects of traffic along Martin Luther King, Jr., Blvd. on ambient PM2.5 concentrations and population health under three different scenarios: (1) the year 2009, (2) 2025, assuming the new campus is not built, and (3) 2025, with the new campus. The baseline comparison year is 2009, because the most comprehensive transportation analysis of the study corridor was conducted using 2009 data [14]. **Table 3.2** provides summary information about the population size and traffic volumes under these three scenarios.

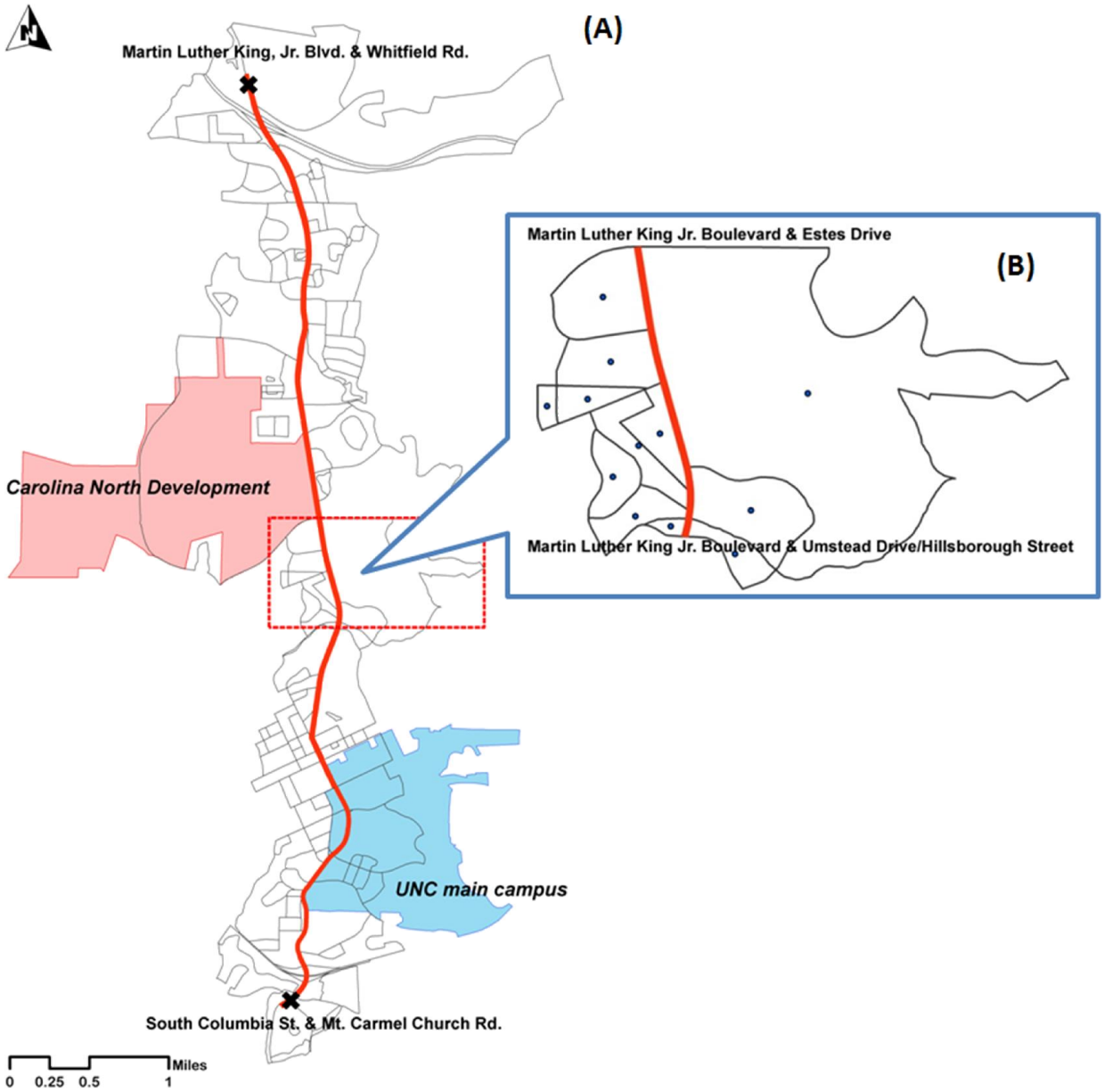

Figure 3.1 (A) The study corridor between the intersection of Martin Luther King, Jr., Blvd. and Whitfield Rd and the intersection of South Columbia St. and Mt. Carmel Church Rd., Chapel Hill, NC, and the census blocks located within 500 meters from the study corridor. (B) The road segment and census blocks for simulations to demonstrate differences in health burden estimates when including the variability and the uncertainty into the modeling approach. Circle dots represent census block centroids.

Table 3.2 Highest traffic volume and population size under three scenarios considered		
Scenario	Highest traffic volume of road segments on study corridor (veh/hr)	Total population of 160 census blocks located within 500 meters from study corridor
2009	1,758	16,042*
2025 without the new campus	2,443	19,140*
2025 with the new campus	2,832	19,140*

* Computed based on the same growth rates forecasted by the North Carolina Capital Area Metropolitan Planning Organization [15]

Method for Quantifying Health Impacts

This analysis has two main parts:

1) Analyze the effects of including variability and uncertainty in the HIA: First, we investigate in the effects on health impact estimates of including uncertainty and variability, as compared to results obtained using the conventional deterministic approach. For this analysis, we focus on the 12 census blocks highlighted in **Figure 1B**, which our prior air quality modeling indicated are more vulnerable to traffic-related PM2.5 than most other census blocks in the corridor [16].

2) Quantify the health impacts of traffic from the proposed new campus in the study corridor: Second, we quantify traffic-related air quality and health effects along the entire study corridor for the three development scenarios in **Table 3.2**. This analysis includes all the variability and uncertainty sources in **Box 3.1** except for uncertainty in the shape of the dose-response function, although we do consider uncertainty in the parameter of this function.

Both analyses use the same modeling framework, described in detail in the following sections.

Overview of Modeling Framework

Quantifying the health impacts of traffic-related air pollution requires three key categories of information: (1) an estimate of the PM2.5 concentration to which the population is

exposed, (2) concentration-response functions relating the exposure concentration to the probability of experiencing adverse health impacts, and (3) the baseline number of cases of the health effects of concern (from all causes) in the exposed population [17–19]. **Figure 2** summarizes how this analysis combines these three information categories (in shaded boxes in the figure) to yield health impact estimates. The unshaded boxes show sources of variability and uncertainty relevant to each information category. The subscript notation in the figure indicates that we conduct our analysis at the census block scale, where i represents an individual block. That is, we characterize health risks separately for each census block, considering variability in PM2.5 exposure concentrations and population demographic characteristics within each census block. The subscripts j, k, and l indicate that we also consider differences in baseline health status by age (j), gender (k), and race (l). We consider differences in effects by season (subscript m), as well, since epidemiologic evidence suggests seasonal differences in dose-response functions [20, 21]. While the five previous quantitative HIAs used similar concentration-response functions as those in this analysis, none considered fine-scale exposure variability, differences in effects among demographic groups, or seasonal effects, nor did they consider the other sources of variability and uncertainty listed in **Box 3.1** and illustrated in **Figure 3.2**. The following sections provide details on how we estimated PM2.5 exposure concentrations, concentration-response functions, and baseline incidence rates of adverse health outcomes and how we incorporated variability and uncertainty into the analysis.

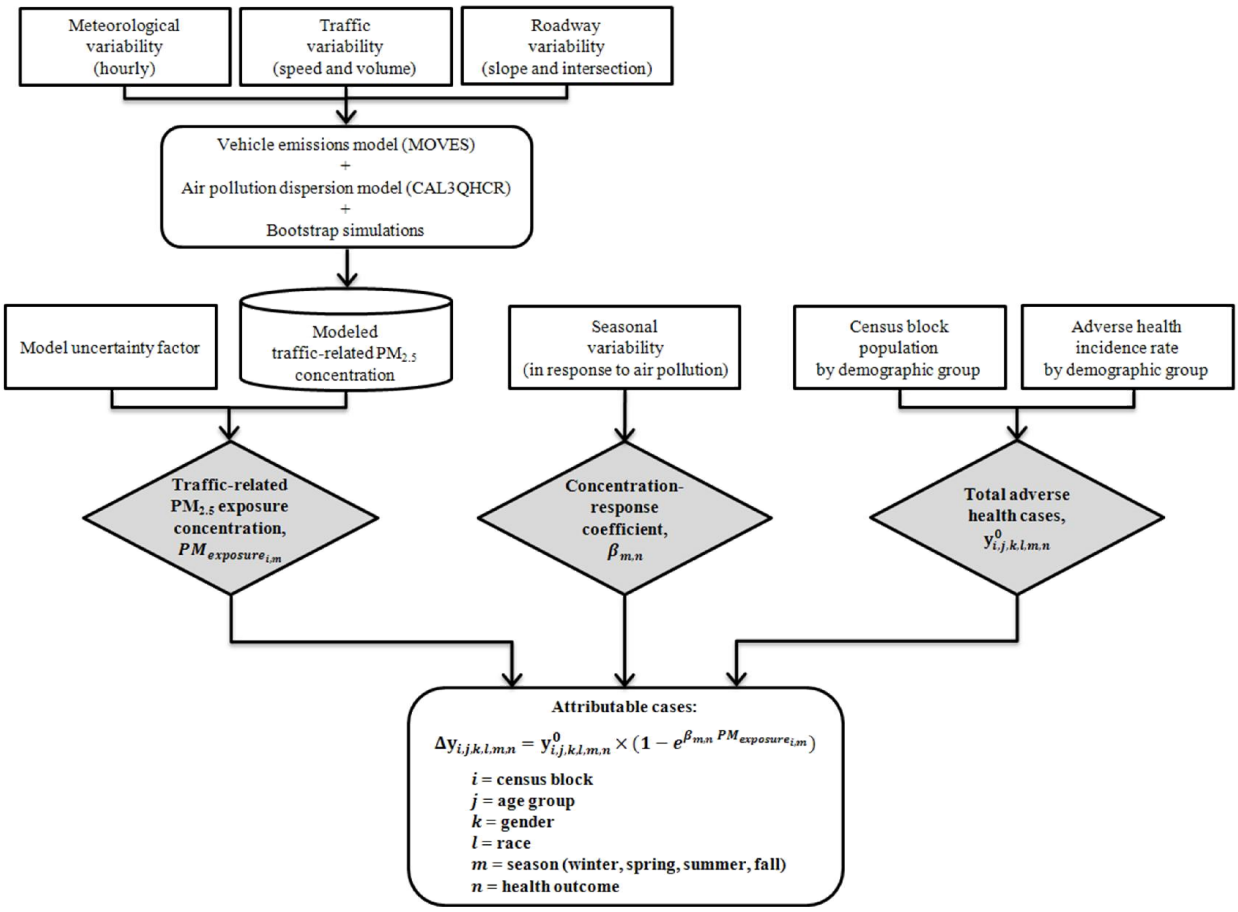

Figure 3.2 Overview of framework for incorporating variability and uncertainty into assessment of the health impacts of traffic-related PM2.5. The rectangles show sources of variability and uncertainty. The shaded diamonds show the three major information categories needed for quantitative health impact assessment.

PM2.5 Exposure Concentration

The 24-hour exposures to traffic-related PM2.5 at each census block were estimated using an integrated air quality modeling approach described in Chart-asa, Sexton, and MacDonald Gibson [16]. In brief, the approach employs standard traffic emissions and air quality dispersion modeling tools, but it adds a novel approach for modeling variability in exposure due to hourly meteorological variability. The linked models used to predict traffic-related air quality effects are MOVES 2010b, commonly used in the United States to estimate vehicle emissions factors (g/vehicle-mile) on different roadway links, and CAL3QHCR, used to

model the dispersion of pollutants away from roadways. Using these two models, we simulated the 24-hour PM2.5 concentration at the centroid of each of the 160 census blocks for 91 days in each of the four seasons, using hourly temperature profiles selected at random from 2006–2012 data obtained from the national weather stations in Chapel Hill and Greensboro [22, 23]. All simulations used meteorological profiles generated from EPA's Meteorological Processor for Regulatory Models from 6 a.m. to 7 p.m., since the traffic emissions during these hours are assumed to contribute the major impacts. The meteorological profiles contained a total of 2,100 days with complete required data (i.e., 525 days for winter, 560 days for spring, 532 days for summer, and 483 days for fall). For each census block and season, we computed the mean value of the estimated 24-hour PM2.5 concentration (i.e., the mean of the 91 separately estimated 24-hour concentrations), then repeated this process 2,000 times for each season. The result was an estimated probability distribution for the seasonal PM2.5 24-hour-average concentration in each census block. The simulations were based on 2009 and 2025 emission factors from MOVES modeling and simulated traffic data for 2009 and 2025 scenarios with or without Carolina North from the Transportation Impact Analysis (TIA) for the Carolina North Development [14]. The simulated concentrations in each census block were used as a surrogate for the 24-hour population exposures to PM2.5 in each census block.

In addition to considering variability in PM2.5 exposure concentrations, we included in the analysis an estimate of the effects of uncertainty in the accuracy of the air quality model predictions. Our own previous research on the integrated air quality modeling approach, as well as previous work by others, suggests that the combined MOVES-CAL3QHCR modeling approach generally predicts PM2.5 concentration within a factor of two of measured concentrations (although of course accuracy varies depending on local conditions and the quality

of data available to support the model). Hence, we represented model uncertainty with an uncertainty factor (*UF*) represented by a triangular probability distribution with lower limit = 0.5, upper limit = 2.0, and mode =1.0 (representing the expected factor-of-two uncertainty in the model). Correspondingly, in each census block, the PM2.5 24-hour average exposure concentration was estimated for each season as

$$PM_{exposure_{i,m}} = UF \times PM_{model_{i,m}} \quad (1)$$

where $PM_{exposure_{i,m}}$ represents the average 24-hour PM2.5 concentration in census block i (i = 1–160) and season m (m =winter, spring, summer, fall); UF is the model uncertainty factor; and $PM_{model_{i,m}}$ is the corresponding model-predicted seasonal average PM2.5 concentration.

Concentration-Response Functions

This study considers the effects of short-term exposure to traffic-related PM2.5 on cardiovascular and respiratory mortality (all ages) and unscheduled hospital admissions (age 65 and over). These four health outcomes were previously selected for the core analysis in the U.S. Environmental Protection Agency's (EPA's) quantitative health risk assessment for supporting the review of the U.S. National Ambient Air Quality Standards for PM [24]. For this analysis, as recommended by the World Health Organization and others [17, 25, 26], we use the following relationship to describe the link between seasonal daily average PM2.5 concentrations and the relative risk of a specific adverse health effect (that is, the probability of the adverse event occurring in the exposed population divided by the probability in an unexposed population):

$$RR_{i,m,n} = e^{\beta_{m,n} PM_{exposure_{i,m}}} \quad (2)$$

where $\beta_{m,n}$ is the concentration-response coefficient describing the effects of PM on health outcome n during season m and $RR_{i,m,n}$ is the relative risk of health outcome n during season m

in census block i. The number of adverse health cases in the population attributable to traffic-related PM2.5 then can be determined from the following relationship:

$$\Delta y_{i,j,k,l,m,n} = y^0_{i,j,k,l,m,n} \times AF_{i,j,k,l,m,n} \quad (3a)$$

$$= y^0_{i,j,k,l,m,n} \times \frac{(RR_{i,m,n} - 1)}{RR_{i,m,n}} \quad (3b)$$

$$= y^0_{i,j,k,l,m,n} \times \frac{(e^{\beta_{m,n} PM_{exposure_{i,m}}} - 1)}{e^{\beta_{m,n} PM_{exposure_{i,m}}}} \quad (3c)$$

$$= y^0_{i,j,k,l,m,n} \times (1 - e^{-\beta_{m,n} PM_{exposure_{i,m}}}) \quad (3d)$$

where $AF_{i,j,k,l,m,n}$ and $\Delta y_{i,j,k,l,m,n}$ are the fraction and number of cases of adverse health event n attributable to traffic-related PM2.5 in season m in census block i for age group j, gender k, and race l and where $y^0_{i,j,k,l,m,n}$ is the observed total number of cases in the same location and among the same population group. Equations (3a) and (3b) are the standard equations used in analyses by the WHO and other organizations to attribute observed cases of adverse health events to specific risk factors [17, 18, 27, 28], and equations (3c) and (3d) combine these with equation (2).

The β values in equations (2), (3a), (3b), (3c), and (3d) (known as dose-response coefficients) were drawn from the U.S. Environmental Protection Agency guidance document entitled Quantitative Health Risk Assessment for Particulate Matter [20, 21, 24]. **Table 3.3** shows the coefficient values used in this analysis. EPA retrieved these coefficients from peer-reviewed epidemiologic studies that met certain quality-assurance criteria, including, for example, the estimation of exposure from measured rather than modeled PM2.5 data. The coefficients are specific to 15 U.S. metropolitan areas (e.g., Atlanta, Detroit, Houston, Los Angles, New York, and so on) or to four regions (Northeast, Southeast, Northwest, and Southwest). This study employed the coefficients for the mortality effects for Atlanta, which is

the nearest city for which the concentration-response coefficients are available, and the coefficients for the morbidity effects for Southeast region, in which Chapel Hill is located.

Baseline Incidence Rates of Adverse Health Effects

Data on baseline incidence rates of the adverse health effects of interest in this study were obtained from North Carolina public health databases. Annual mortality rates for each age group (shown in **Table 3.4**) were calculated by dividing 2010 deaths in Orange County (where Chapel Hill is located) from the detailed mortality statistics report [29] by the 2010 census population in Orange County from the National Historical Geographic Information System [30]. The annual unscheduled hospital admissions rates (**Table 3.5**) were obtained from 2009 emergency department visit data reported by the North Carolina Disease Event Tracking and Epidemiologic Collection Tool (NC DETECT) [31]. We were unable to obtain data on incidence rates by gender and race, so we assume incidence rates are the same for both genders and all races (which is a limitation of this analysis). It should be noted as well that the ICD codes specific to concentration-response coefficients may not be entirely matched to the ICD codes specific to the incidence rates used in this study, depending on reported data. Moreover, the emergency department visits may not result in hospital admissions, and some hospital admissions may occur without first visiting the emergency department.

To reflect seasonal variation, we adjusted the incidence rates for cardiovascular and respiratory mortality and unscheduled hospital admissions using data on temporal variability in cardiovascular and respiratory deaths in Orange County during 1999–2010 from the CDC WONDER database [32]. The fractions for cardiovascular events are 0.25, 0.31, 0.20, and 0.24 for winter, spring, summer, and fall respectively, while the fractions for respiratory events are 0.30, 0.26, 0.21, and 0.23 for winter, spring, summer, and fall respectively.

To determine the total number of cases in any given season (i.e., $y^0_{i,j,k,l,m,n}$ in equation 3), we multiplied the given incidence rate by the corresponding size of each demographic group in each census block.

Table 3.3 Mean concentration-response coefficient (95% CI) used in this study

Health outcome	Disease category	ICD-9 or ICD-10 code[a]	Age group	Season	Mean concentration-response coefficient (95% CI)[b]
Mortality	Cardiovascular	I01–I59	All ages	All-year[c]	0.00066 (-0.00066, 0.00198)
				Winter	0.00135 (-0.00193, 0.00462)
				Spring	0.00076 (-0.00273, 0.00425)
				Summer	0.00062 (-0.00222, 0.00347)
				Fall	-0.00018 (-0.00293, 0.00257)
	Respiratory	J00–J99	All ages	All-year[c]	0.00121 (-0.00048, 0.00290)
				Winter	0.00093 (-0.00144, 0.00329)
				Spring	0.00035 (-0.00205, 0.00275)
				Summer	0.00077 (-0.00155, 0.00310)
				Fall	0.00096 (-0.00134, 0.00325)
Unscheduled hospital admissions	Cardiovascular	410–414, 426–429, 430–438, and 440–449	65 and over	All-year[c]	0.00029 (-0.00019, 0.00077)
				Winter	0.00105 (-0.00007, 0.00219)
				Spring	0.00075 (-0.00026, 0.00176)
				Summer	-0.00067 (-0.00161, 0.00026)
				Fall	0.00017 (-0.00072, 0.00106)
	Respiratory	464–466, 480–487, and 490–492	65 and over	All-year[c]	0.00035 (-0.00044, 0.00113)
				Winter	0.00040 (-0.00146, 0.00224)
				Spring	0.00075 (-0.00082, 0.00231)
				Summer	-0.00052 (-0.00209, 0.00105)
				Fall	0.00014 (-0.00130, 0.00158)

[a] ICD-10 for mortality, and ICD-9 for unscheduled hospital admissions

[b] Coefficients were originally from Zanobetti and Schwartz, 2009 [20], and Bell et al., 2008 [21] respectively

[c] Used only in simulation 1

Method for Testing Effects of Variability and Uncertainty on Predicted Health Impacts

Five simulations of 2,000 iterations each were run using Matlab to demonstrate differences in health burden estimates when including variability and uncertainty in the modeling approach. To facilitate computation, we focused this analysis on 12 census blocks (highlighted in **Figure 3.1**) shown from our previous research to include the highest exposures. The total population in the 12 blocks is 1,117 (about 7% of the total population in the study corridor).

Table 3.6 lists the five simulations and the variability and uncertainty considered in each. The first simulation (1a) follows the deterministic approach of previous HIAs, using average traffic volumes and a constant traffic emission factor corresponding to traffic cruising at 35 mph on a flat roadway under a constant ambient temperature of 70°F. Like previous HIAs, simulation 1a accounts for neither uncertainty in the concentration-response coefficient (using the mean value as a deterministic estimate) nor seasonal variability. Simulation 1b is identical to simulation 1a, except that it uses seasonal concentration-response coefficients (also deterministic). Simulations 2–4 systematically include (one at a time) variability in PM2.5 exposure concentrations (simulations 2–4), uncertainty in concentration-response coefficients (simulations 3–4), and air quality model prediction error (simulation 4).

Method for Comparing Health Impacts under Alternative Scenarios

As noted previously, we simulated health impacts for the full study corridor (160 census blocks) for the three different scenarios in **Table 3.2**. For each scenario, 2,000 simulations were run in Matlab and also in Analytica[3] (to check for errors). Traffic patterns (traffic volumes along each roadway link in the corridor) for each scenario were taken from a previous traffic impact analysis conducted for the Town of Chapel Hill [14]. The 2025 census block populations were

[3] Lumina Decision systems, Los Gatos, Calif.

computed by multiplying the 2010 census block populations by growth rates forecasted by the North Carolina Capital Area Metropolitan Planning Organization [15]. Additionally, due to lack of better information, it assumed that the 2009 and 2025 population demographic characteristics (age, race, and gender) are identical to those in 2010.

Table 3.4 Annual mortality rates by race, gender, and age group for Orange County

Cause of death	ICD-10 code	Age group	Race and gender					
			W M	W F	B M	B F	O M	O F
Cardiovascular disease	I05–I09, I10–I15, I20–I25, I26–I28, and I30–I52	0 to 4	0	0	0	0	0	0
		5 to 9	0	0	0	0	0	0
		10 to 14	0	0	0	0	0	0
		15 to 19	0	0	0	0	0	0
		20 to 24	0	0	0	0	0	0
		25 to 34	0	0	0	0	0	0
		35 to 44	0.00017	0	0	0.00095	0	0
		45 to 54	0.00029	0.00013	0.00272	0.00153	0	0
		55 to 64	0.00179	0.00091	0.00235	0.00105	0.00257	0
		65 to 74	0.00343	0.00244	0.00725	0	0	0
		75 to 84	0.01647	0.00770	0.01724	0.02065	0	0
		85 and over	0.05251	0.03034	0.02632	0.02299	0.12500	0
Respiratory disease	J00–J99	0 to 4	0	0	0	0	0	0
		5 to 9	0	0	0	0	0	0
		10 to 14	0	0	0	0	0	0
		15 to 19	0	0	0	0	0	0
		20 to 24	0	0	0	0	0	0
		25 to 34	0	0	0	0	0	0
		35 to 44	0	0	0	0	0	0
		45 to 54	0	0	0	0	0	0
		55 to 64	0.00049	0.00045	0	0.00105	0	0
		65 to 74	0.00206	0.00183	0.00483	0.00345	0	0
		75 to 84	0.00524	0.00495	0.00575	0.00590	0.00116	0
		85 and over	0.03580	0.00787	0.01316	0.01149	0	0

W M = white male, W F = white female, B M = black or African American male, B F = black or African American female, O M = other races male, and O F = other races female

Table 3.5 Annual emergency department visits rates for North Carolina State			
Cause of visit	ICD 9 code	Age group	Annual rate
Cardiovascular disease	427.5, 428 and 518.4 (excluding failure due to fumes and vapors), 430–435, and 437.0–437.1	65 and over	0.0856
Respiratory disease	466, and 480–486	65 and over	0.0355

Table 3.6 Sources of uncertainty and variability included in the five simulations					
Uncertainty and variability sources	Simulation number				
	1a	1b	2	3	4
Sources of uncertainty					
PM2.5 exposure concentration					
• Air quality model prediction accuracy					x
Dose-response function					
• Shape of dose-response function					
• Dose-response coefficient				x	x
Sources of variability					
PM2.5 exposure concentration					
• Meteorology			x	x	x
• Vehicle fleet composition (vehicle type and age)			x	x	x
• Vehicle fuel			x	x	x
• Traffic volume			x	x	x
• Traffic speed			x	x	x
• Road grade			x	x	x
• Traffic behavior at intersections			x	x	x
Dose-response function					
• Seasonal variability		x	x	x	x
• Population susceptibility					
Demographic characteristics of exposed population					
• Age			x	x	x
• Race			x	x	x
• Gender			x	x	x
• Health status			x	x	x

Results and Discussion

Effect of Including Variability and Uncertainty

Incorporating variability and uncertainty into the model predictions increased mean values of key input variables in equation (3d) substantially, compared to the conventional deterministic method, at least with this case. **Table 3.7** shows averages of seasonal mean values of $PM_{exposure}$ for the 12 selected census blocks in **Figure 3.1 (B)**; seasonal mean values of β; and seasonal incidence fractions used to adjust y^0 for cardiovascular and respiratory mortality and unscheduled hospital admissions in five simulations including different uncertainty and variability sources. **Table 3.8** shows the ratios of these variables in the simulations 1b, 2, 3, and 4 to the values in simulation 1a. It is important to note that the averages of seasonal mean values of $PM_{exposure}$ were used as examples for explanation of the effects of including variability in traffic emissions and uncertainty in model prediction error only. The actual calculation of health burdens used distinct values at each of the 12 census blocks (as in **Figure 3.3**).

At least with this case, these results illustrates that including the variability in traffic emissions caused by traffic volume, traffic activity, average traffic speed, road grade, and temperature into the modeling approach (simulation 2 and 3) increases the averages of seasonal mean values of $PM_{exposure}$ by approximately a factor of 2.3 to 3.7, depending on season. In addition to the variability in traffic emissions, simulation 4 also included uncertainty in model prediction accuracy and, in turn, the new seasonal mean values of $PM_{exposure}$ increased by about an additional factor of 0.4 to 0.6, depending on season. The largest changes occur in winter reflecting the increases in traffic emissions due to cold temperatures.

Table 3.7 Averages of seasonal mean values of $PM_{exposure}$ for the 12 selected census blocks; seasonal mean values of β; and seasonal incidence fractions used to adjust y^0 for cardiovascular and respiratory mortality and unscheduled hospital admissions in five simulations including different uncertainty and variability sources shown in Table 3.6

Season	Simulation 1a	Simulation 1b	Simulation 2	Simulation 3	Simulation 4
Averages of mean values of $PM_{exposure}$ across the selected 12 census blocks (μg/m^3)					
Winter	3.91×10^{-3}	3.91×10^{-3}	1.45×10^{-2}	1.45×10^{-2}	1.69×10^{-2}
Spring	3.96×10^{-3}	3.96×10^{-3}	1.10×10^{-2}	1.10×10^{-2}	1.28×10^{-2}
Summer	3.41×10^{-3}	3.41×10^{-3}	7.79×10^{-3}	7.79×10^{-3}	9.11×10^{-3}
Fall	4.25×10^{-3}	4.25×10^{-3}	1.04×10^{-2}	1.04×10^{-2}	1.21×10^{-2}
Mean values of β for cardiovascular mortality (for a 1 μg/m^3 increased in $PM_{exposure}$)					
Winter	6.60×10^{-4}	1.35×10^{-3}	1.35×10^{-3}	2.00×10^{-3}	2.00×10^{-3}
Spring	6.60×10^{-4}	7.60×10^{-4}	7.60×10^{-4}	1.70×10^{-3}	1.70×10^{-3}
Summer	6.60×10^{-4}	6.20×10^{-4}	6.20×10^{-4}	1.40×10^{-3}	1.40×10^{-3}
Fall	6.60×10^{-4}	-1.80×10^{-4}	-1.80×10^{-4}	1.10×10^{-3}	1.10×10^{-3}
Mean values of β for respiratory mortality (for a 1 μg/m^3 increased in $PM_{exposure}$)					
Winter	1.21×10^{-3}	9.30×10^{-4}	9.30×10^{-4}	1.40×10^{-3}	1.40×10^{-3}
Spring	1.21×10^{-3}	3.50×10^{-4}	3.50×10^{-4}	1.10×10^{-3}	1.10×10^{-3}
Summer	1.21×10^{-3}	7.70×10^{-4}	7.70×10^{-4}	1.30×10^{-3}	1.30×10^{-3}
Fall	1.21×10^{-3}	9.60×10^{-4}	9.60×10^{-4}	1.40×10^{-3}	1.40×10^{-3}
Mean values of β for cardiovascular hospital admission (unscheduled) (for a 1 μg/m^3 increased in $PM_{exposure}$)					
Winter	2.90×10^{-4}	1.05×10^{-3}	1.05×10^{-3}	1.10×10^{-3}	1.10×10^{-3}
Spring	2.90×10^{-4}	7.50×10^{-4}	7.50×10^{-4}	8.27×10^{-4}	8.27×10^{-4}
Summer	2.90×10^{-4}	-6.70×10^{-4}	-6.70×10^{-4}	2.17×10^{-4}	2.17×10^{-4}
Fall	2.90×10^{-4}	1.70×10^{-4}	1.70×10^{-4}	4.30×10^{-4}	4.30×10^{-4}
Mean values of β for cardiovascular mortality (for a 1 μg/m^3 increased in $PM_{exposure}$)					
Winter	3.50×10^{-4}	4.00×10^{-4}	4.00×10^{-4}	9.13×10^{-4}	9.13×10^{-4}
Spring	3.50×10^{-4}	7.50×10^{-4}	7.50×10^{-4}	9.96×10^{-4}	9.96×10^{-4}
Summer	3.50×10^{-4}	-5.20×10^{-4}	-5.20×10^{-4}	4.82×10^{-4}	4.82×10^{-4}
Fall	3.50×10^{-4}	1.40×10^{-4}	1.40×10^{-4}	6.40×10^{-4}	6.40×10^{-4}
Fraction of annual cardiovascular mortality and hospital admissions (unscheduled) in each season					
Winter	0.25	0.25	0.25	0.25	0.25
Spring	0.25	0.31	0.31	0.31	0.31
Summer	0.25	0.20	0.20	0.20	0.20
Fall	0.25	0.24	0.24	0.24	0.24
Fraction of annual respiratory mortality and hospital admissions (unscheduled) in each season					
Winter	0.25	0.30	0.30	0.30	0.30
Spring	0.25	0.26	0.26	0.26	0.26
Summer	0.25	0.21	0.21	0.21	0.21
Fall	0.25	0.23	0.23	0.23	0.23

Table 3.8 Ratios of averages of seasonal mean values of $PM_{exposure}$ for the 12 selected census blocks; seasonal mean values of β; and seasonal incidence fractions used to adjust y^0 in simulations 1b, 2, 3, and 4 to those in simulation 1a				
Season	Simulation 1b/1a	Simulation 2/1a	Simulation 3/1a	Simulation 4/1a
Ratios of averages of mean values of $PM_{exposure}$				
Winter	1.00	3.70	3.70	4.32
Spring	1.00	2.76	2.76	3.23
Summer	1.00	2.29	2.29	2.67
Fall	1.00	2.45	2.45	2.86
Ratios of mean values of β for cardiovascular mortality				
Winter	2.05	2.05	3.03	3.03
Spring	1.15	1.15	2.58	2.58
Summer	0.94	0.94	2.12	2.12
Fall	0*	0*	1.67	1.67
Ratios of mean values of β for respiratory mortality				
Winter	0.77	0.77	1.16	1.16
Spring	0.29	0.29	0.91	0.91
Summer	0.64	0.64	1.07	1.07
Fall	0.79	0.79	1.16	1.16
Ratios of mean values of β for cardiovascular hospital admission				
Winter	3.62	3.62	3.79	3.79
Spring	2.59	2.59	2.85	2.85
Summer	0*	0*	0.75	0.75
Fall	0.59	0.59	1.48	1.48
Ratios of mean values of β for respiratory hospital admission				
Winter	1.14	1.14	2.61	2.61
Spring	2.14	2.14	2.84	2.84
Summer	0*	0*	1.38	1.38
Fall	0.40	0.40	1.83	1.83
Ratios of incidence fractions for cardiovascular mortality and hospital admission (unscheduled)				
Winter	1.01	1.01	1.01	1.01
Spring	1.22	1.22	1.22	1.22
Summer	0.80	0.80	0.80	0.80
Fall	0.97	0.97	0.97	0.97
Ratios of incidence fractions for respiratory mortality and hospital admission (unscheduled)				
Winter	1.21	1.21	1.21	1.21
Spring	1.05	1.05	1.05	1.05
Summer	0.84	0.84	0.84	0.84
Fall	0.90	0.90	0.90	0.90

* The negative values of β are recoded to zero, since exposure to traffic-related PM2.5 would not benefit population health.

Including the variability in seasonal concentration-response coefficient functions (simulation 1b and 2) increased mean values of β in some seasons and decreased mean values of β in other seasons, depending on health outcome and season, compared to the mean values of β derived from all-year concentration-response functions (simulation 1a). The changes range from a factor of 0 to 3.6. In addition to the variability in seasonal concentration-response coefficient functions, simulations 3 and 4 also included uncertainty in concentration-response coefficients (represented by the zero-truncated normal distribution in order to avoid negative values of β,which would imply that exposure to traffic-related PM2.5 would benefit population health). The new mean values of β changed by a factor of 0.8 to 3.8, depending on health outcome and season, compared to the mean values of β in simulation 1a.

Including the variability in seasonal incidence fractions (simulations 1b, 2, 3, and 4) increased y^0 in some seasons and decreased y^0 in other seasons, depending on health outcomes and seasons, compared to not including this variability (simulation 1a). The changes range from a factor of 0.8 to 1.2.

Based on the above information, the effects of including variability and/or uncertainty are heavily dependent on data and assumptions used in the integrated MOVES-CAL3QHCR modeling and the health impacts estimation. The effects of including variability in traffic emissions caused by traffic volume, traffic activity, average traffic speed, road grade, and temperature may be most influential on the health impacts estimates, compared to the effects of including other variability and uncertainty sources. Thus, these results suggest that the deterministic approach tend to under-estimate health impacts if the surrogate traffic volumes and traffic emission factor lead to lower traffic emission and, in turn, lower exposure concentrations,

compared to the approaches accounting for the effects of variability in traffic emissions along the roadway of interest.

Due to small values of β and $PM_{exposure}$ as in the case for this study, the equation (3d) can be approximated as $\Delta y = y^0 \times \beta \times PM_{exposure}$. So, the aggregate effects of including variability and/or uncertainty in each simulation approach can be approximated by multiplying the ratios to mean values in simulation 1a for each predictor variable shown in **Table 3.8**. The aggregate effects on health burdens estimates for the 12 selected census blocks in the simulation 1b, 2, 3, and 4 are summarized in **Table 3.9**.

Table 3.9 Aggregate effects of including variability and/or uncertainty in simulations 1b, 2, 3, and 4

Season	Simulation 1b	Simulation 2	Simulation 3	Simulation 4
Cardiovascular mortality				
Winter	2.1	7.6	11	13
Spring	1.4	3.9	8.7	10.2
Summer	0.75	1.7	3.9	4.5
Fall	0*	*0	4.0	4.6
Respiratory mortality				
Winter	0.93	3.4	5.2	6.0
Spring	0.30	0.84	2.7	3.1
Summer	0.53	1.2	2.0	2.4
Fall	0.71	1.8	2.6	3.0
Cardiovascular hospital admission (unscheduled)				
Winter	3.7	13	14	17
Spring	3.2	8.8	9.6	11
Summer	0*	0*	1.4	1.6
Fall	0.57	1.4	3.5	4.1
Respiratory hospital admission (unscheduled)				
Winter	1.4	5.1	12	14
Spring	2.3	6.2	8.3	9.7
Summer	0*	0*	2.6	3.1
Fall	0.36	0.88	4.0	4.7

* Zero aggregate effects are resulted from recoding the negative values of β to zero.

Figure 3.3 compares the sums of mean estimates of health burdens for the 12 selected census blocks over a year (annual excess cases) using the deterministic approach of previous HIAs (simulation 1a) to the results obtained when variability and uncertainty are introduced into the analysis (simulation 1b, 2, 3, and 4). Distinct values at each of the 12 census blocks were used in the calculations. The health burden estimates in simulation 4 accounting for variability and uncertainty in traffic emissions, model prediction accuracy, seasonal concentration-response function, and seasonal incidence variation were greater than those in simulation 1a by a factor of 7.2, 3.4, 8.7, and 8.0 for cardiovascular mortality, respiratory mortality, cardiovascular hospital admission (unscheduled), and respiratory hospital admission (unscheduled), respectively. In fact, the estimates without considering variability and uncertainty are biased so low that they are outside the 95% confidence intervals of estimates including variability and uncertainty. These biased predictions could have important implications for decision-making. For example, it is possible that excluding variability and uncertainty, and hence producing unrealistically low estimates of health impacts, could result in a decision not to pursue mitigation measures that would have been determined cost-effective had the full impacts of variability and uncertainty been considered in the analysis.

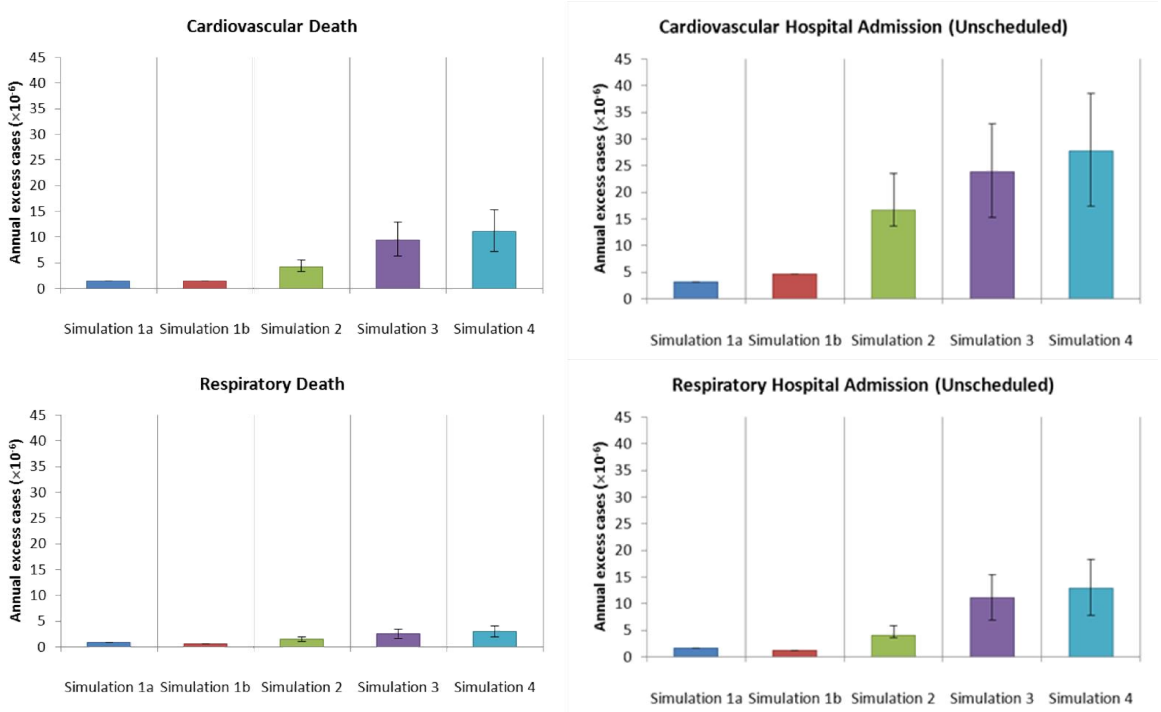

Figure 3.3 Sums of mean estimates of health burdens for the 12 selected census blocks over a year (annual excess cases) using five simulation approaches accounting for different uncertainty and variability sources shown in Table 3.6. Error bars represent 95% confidence intervals.

Population Health Risks at the Case Study Site

Figures 3.4, 3.5, and 3.6 show the estimated health impacts of traffic-related PM2.5 under the three development scenarios listed in **Table 3.2**. The figures show maps of cases of each health outcome in each census block by season along with bar charts depicting total cases in the study corridor by season. As the bar charts and maps illustrate, effects are highest in winter for all scenarios, due to the influences of high concentration-response coefficients, seasonal incidence variations, and traffic emission factors during low temperatures. The maps also illustrate considerable spatial variation in the distribution of adverse health effects, due to both population and exposure concentration differences (the latter resulting from differences in distances from census blocks to the roadway and differences in traffic, meteorological, and road characteristic variability). Some census blocks show zero excess health effects.

Table 3.10 compares the results for each scenario by a number of metrics: number of census blocks with health impacts, range of exposure concentrations across census blocks, and total number of adverse health effects across all blocks. Notably, even though the population increases in 2025, the total number of adverse health cases attributable to traffic-related PM2.5 decreases relative to 2009, ***with or without the Carolina North Development*** (although the decrease is lower with the development). These decreases are due to the built-in assumptions of MOVES that future vehicles will be cleaner than today's fleet, resulting in traffic emissions that drop by about 50%, on average.

Table 3.10 Comparison of HIA results by development scenario

Scenario	Number of census blocks affected[a]	Range of mean exposure concentrations in affected blocks ($\mu g/m^3$)[b]	Total excess cases in winter ($\times 10^{-6}$)			
			CVD mortality	CVD hospital admissions	Respiratory mortality	Respiratory hospital admissions
2009	118–148	0.0002–0.16	45	150	13	67
2025 without Carolina North	75–122	0.0002–0.10	20	66	5.6	30
2025 with Carolina North	84–137	0.0002–0.13	28	94	8.0	43

[a] Number of census blocks with exposure concentrations greater than zero (varies by season).

[b] Lowest and highest mean seasonal exposure concentration in affected census blocks (also varies by season).

Figure 3.4 The spatial distributions and the total excess cases of adverse health effects of traffic-related PM2.5 in each season in the 2009 scenario. Error bars represent the lower and upper limits that were computed based on the 95% CI of attributable fractions. The estimates less than zero at any census block were recoded to zero.

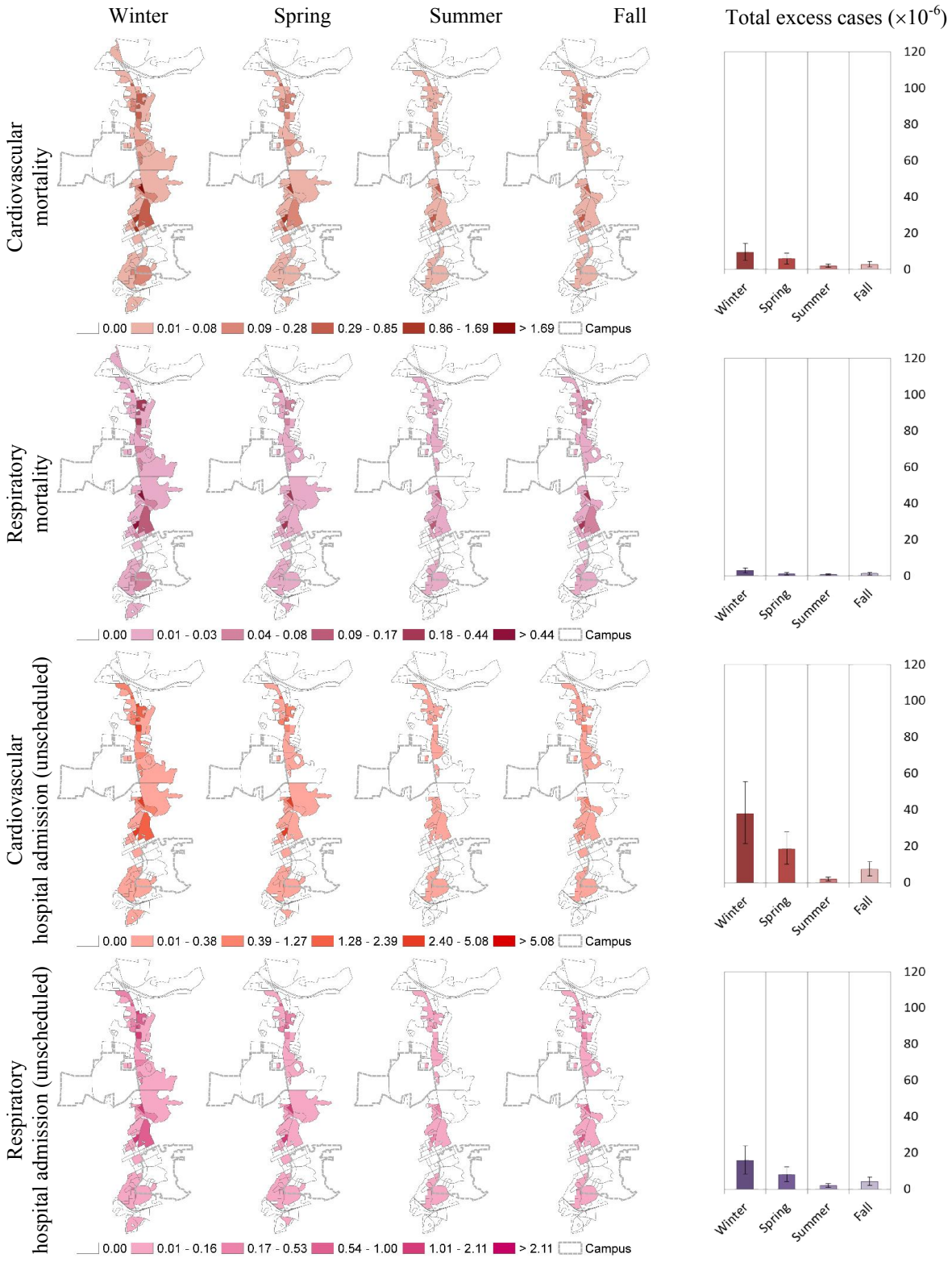

Figure 3.5 The spatial distributions and the total excess cases of adverse health effects of traffic-related PM2.5 in each season in the 2025 scenario without the Carolina North development. Error bars represent the lower and upper limits that were computed based on the 95% CI of attributable fractions. The estimates less than zero at any census block were recoded to zero.

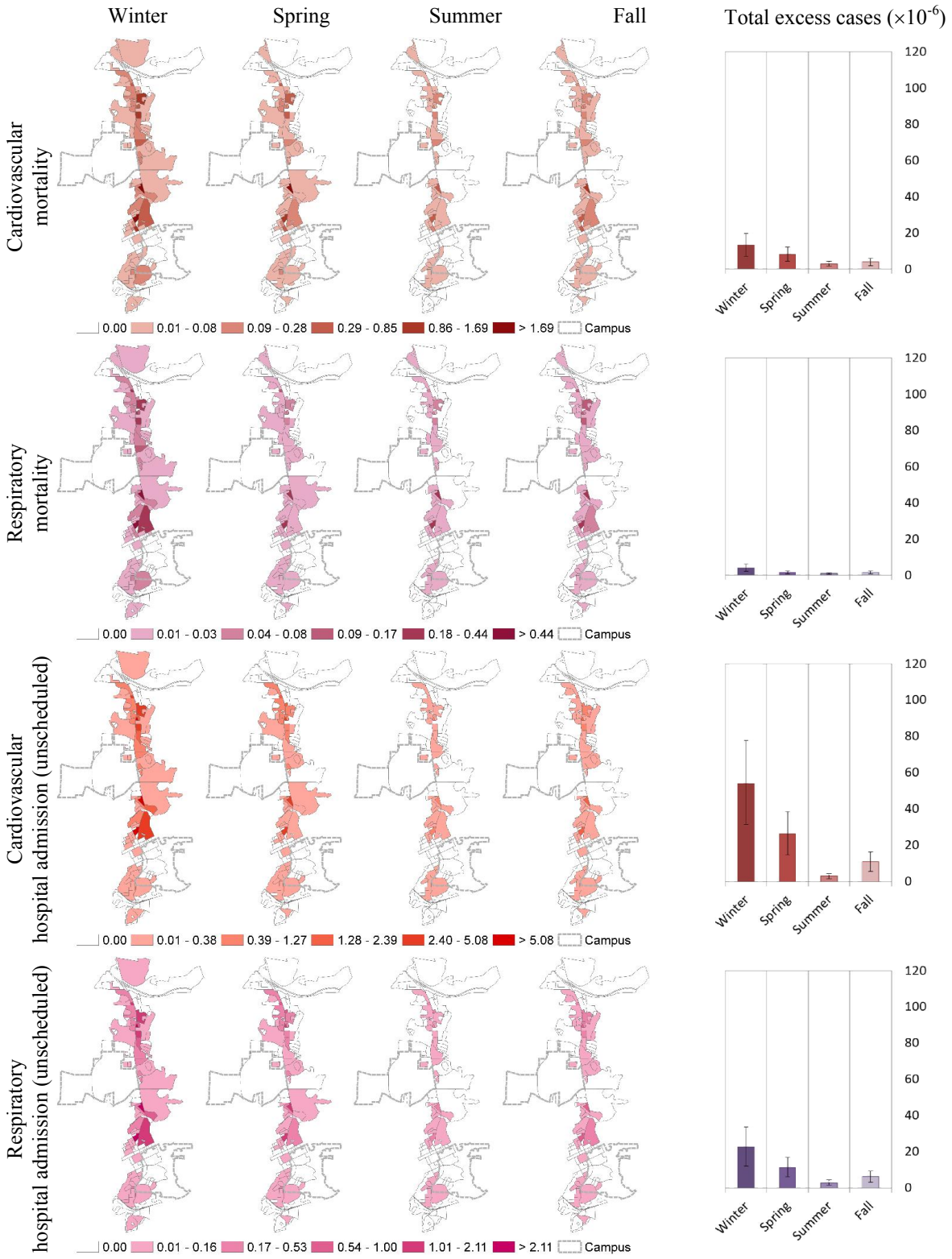

Figure 3.6 The spatial distributions and the total excess cases of adverse health effects of traffic-related PM2.5 in each season in the 2025 scenario with the Carolina North development. Error bars represent the lower and upper limits that were computed based on the 95% CI of attributable fractions. The estimates less than zero at any census block were recoded to zero.

Figure 3.7 shows the predicted health effects of traffic-related PM2.5 from the Carolina North campus with and without the assumption that future vehicles will be less polluting than today's fleet. The figure shows the excess cases of each health effect beyond what is expected if the campus is not built (in other words, the difference between scenario 3 and scenario 2 for each health outcome). These results illustrate that cleaner vehicle technologies and fuels are expected to have a substantial impact on population health risks from future traffic-related PM2.5 pollution.

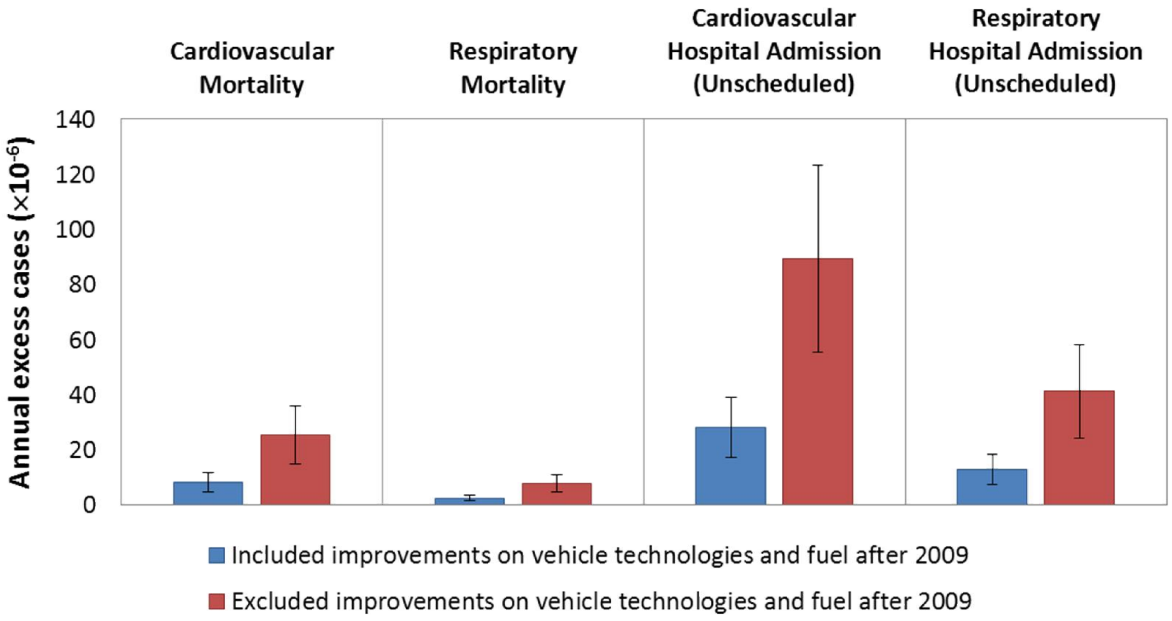

Figure 3.7 Comparisons of total annual excess cases of adverse health effects of traffic-related PM2.5 from the Carolina North campus by the year 2025 with and without cleaner vehicle technologies and fuels. The numbers of cases shown are those predicted to occur if the campus is built, minus the number predicted in 2025 if the campus is not built.

There is some evidence of existing racial disparities in exposure to risks from traffic-related PM2.5 pollution. The census block having the highest number of total deaths attributable to traffic on the study corridor under current conditions (block number 371350118002002, which has a population of 201) also has a very high percentage of black residents, at 47%, compared to 9% black population in the study area as a whole. This census block is the home of a public

housing community, Airport Gardens, intended for low-income families. Of the 10 census blocks with the highest number of attributable deaths, seven have much higher percentage black populations than the average for the study area, ranging from 17–47%. The correlation between percent black and total extra deaths in each census block for blocks with nonzero population is 0.37 ($t(114)=4.2$, $p<0.0001$), and for total hospital admissions it is 0.24 ($t(114)=2.6$, $p<0.005$); as the p-values indicate, these correlations (while not large) are highly significant.

This analysis also shows evidence of substantial risk differences by age. **Figure 3.8** shows the distribution of results by age for scenario 1 (the others show similar proportionate distributions since population distribution assumptions are identical). As shown, effects are predicted only in adults aged 35 and over. For hospital admissions effects, this results is expected, since the epidemiologic studies we used do not provide evidence of a significant association between hospital admissions for respiratory and cardiovascular illnesses in age groups younger than 65. However, the mortality estimates include all ages. The lack of attributable mortality among those aged less than 35 is due to the lack of observed mortality for cardiovascular and respiratory causes in these age groups (see **Table 3.4**).

Overall, future risks attributable to traffic-related PM2.5 from construction of the new campus in this study corridor are extremely low, even if one assumes that the vehicle fleet and fuels of the future will be identical to those used today. Assuming no vehicle technology or fuel improvements, then the total premature mortality attributable to traffic-related PM2.5 from the new campus in the study corridor, compared to if the campus is not built, is 3 x 1 10^{-5} CVD deaths plus 9 x 10^{-6} respiratory deaths. Summing these two estimates and dividing by the future study corridor population of 19,000 yields a per-person annual risk of about 2 x 10^{-9}. If vehicle improvements are included in the analysis, then the per-person risk drops to 6 x 10^{-10}. These are

annual risks, but are low even if one assumes a resident is exposed to such a risk level for a life-time. For a 70-year lifetime, the total per-person annual risk (assuming cleaner technologies) is 4×10^{-8}. Even in the most-exposed census block, lifetime risks attributable to the new campus are relatively low (about 1×10^{-8} per year, or less than one-in-one-million over a lifetime).

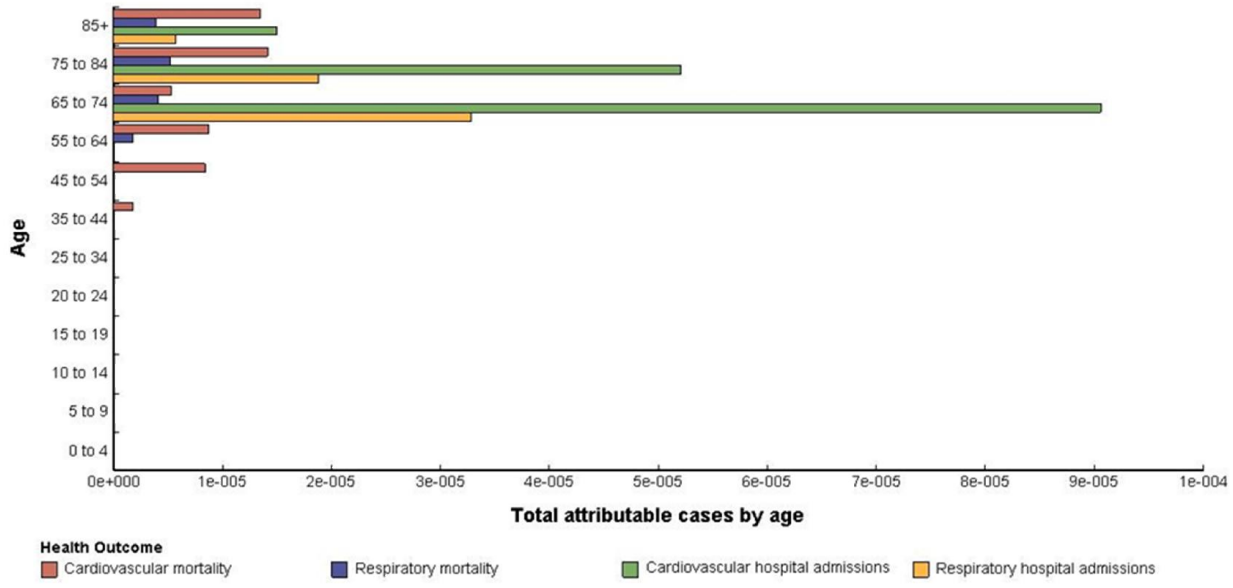

Figure 3.8 Age distribution of traffic-related health impacts in the 2009 scenario

There are limitations to be noted about the concentration-response functions used in this study. Even though these functions have been evaluated to be sufficient to support quantitative risk assessment by EPA, the coefficients are not specific to the study area. That is, these coefficients may not properly represent the population exposure to PM2.5, the composition of PM2.5 to which populations are exposed, and the adverse health events associated with PM2.5 in the exposed population in the study area. Furthermore, the concentration-response functions used in this study were developed using the ambient concentrations measured at central monitoring stations as a surrogate for population exposures to PM2.5. As a result, these functions may be more appropriate for health impact assessment at coarse spatial resolution, e.g. county

level, than for the local-scale application in this research. To improve health impact assessment, future work may consider using specific coefficients accounting for personal exposures at a finer spatial resolution, as demonstrated in Chang, Fuentes, and Frey [33].

Sensitivity and Uncertainty Analysis

Figure 3.9 shows the sensitivity of the predicted CVD deaths to very low or very high values of the variables that are either uncertain or variable in this analysis and hence are treated as random variables: modeled PM2.5 concentration, air dispersion model uncertainty factor, and exposure-response coefficient. (The modeled PM2.5 concentration incorporates multiple sources of variability, including variability in meteorological conditions, road grade, queuing at intersections, and vehicle speed.) In **Figure 3.9**, 1,000 simulations were run for the 2009 scenario, holding each random variable at the lower bound and then upper bound of its 95% confidence interval while representing all other variables as in simulation 4. As shown, the health impact estimates are most sensitive to uncertainty in the exposure-response coefficient and second-most sensitive to air quality model uncertainty. Variability in PM2.5 exposure concentrations attributable to weather, traffic, and road conditions contributes less to the spread in results, causing the predicted impacts to vary by only about plus or minus 30%, compared to about a factor of three difference in results when the concentration-response coefficient increases to the upper end of its confidence interval. Sensitivity analysis results were similar for the other three health effects. These results illustrate the importance for future transportation-related HIAs of decreasing uncertainty in epidemiologic estimates of the concentration-response coefficient.

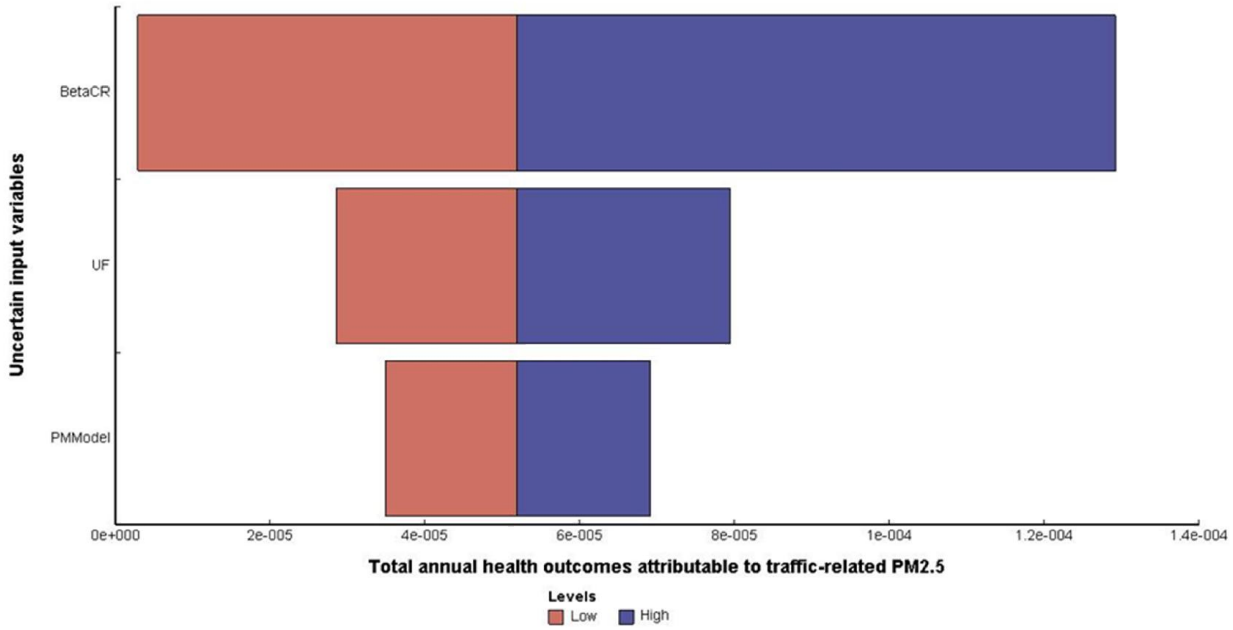

Figure 3.9 Sensitivity of predicted CVD deaths attributable to traffic-related PM2.5 to changing random variables in the model to extreme values representing the upper and lower ends of the 95% confidence intervals

Conclusions

This study developed an improved modeling approach for estimating the health impacts of traffic-related PM2.5 air pollution under alternative future urban development scenarios. We then demonstrated the approach by quantifying health impacts in a case study roadway corridor that could be affected by a new UNC campus extension in Chapel Hill. The new approach accounts for the effects of variability in traffic emissions factors and in concentration-response coefficients throughout the analysis period. It also accounts for uncertainty in concentration-response coefficients and air quality model prediction error. The approach could benefit others conducting environmental and health impact analyses of traffic-related PM2.5.

Comparisons to the conventional modeling approach used in other quantitative HIAs revealed that those HIAs could under-estimate potential health burdens by failing to consider variability and uncertainty in input variables used to generate the health impact estimates. Our

analysis showed that in the case study corridor the conventional approach under-predicted health impacts by a factor of 3.4–8.7, depending on the health endpoint. As such, the conventional HIA approach could in some circumstances lead to decisions that are not cost effective and/or are not sufficiently protective of public health.

This analysis also showed that a fine-scale approach that quantifies impacts over a small grid (in this case, U.S. census blocks), accounting for demographic variability in each grid cell along with the previously mentioned variability and uncertainty in model inputs, can be useful for identifying health disparities. For example, this analysis reveals that the neighborhood in the study area with the highest health burden also has a very high minority population, compared to that in the rest of the study area. In addition, this method of accounting for demographic variability can be used to analyze differences in risks among age and gender groups. It could be extended to analyze impacts among populations with pre-existing health conditions, as well.

Overall, the risks of traffic-related PM2.5 from the proposed new campus are very low (less than 1×10^{-8}) even for the most-exposed populations. Nonetheless, it is important to recognize that we consider only one type of traffic-related pollutant and one roadway corridor. Risks would be higher if including all roadways affected by traffic from the new campus and all traffic-related pollutants. Furthermore, it is important to keep in mind the many other sources of ambient air pollution exposure in the study area and the cumulative effects of multiple exposures. Taking steps to reduce traffic from the new campus (e.g., increasing the frequency of public transit service, encouraging carpooling, charging for parking, and other steps) will reduce air pollution exposures and produce benefits beyond those along the single roadway considered in this case study.

Overall, this work highlights the sensitivity of traffic-related health impact assessments to uncertainty and variability in concentration-response coefficients, air quality model prediction accuracy, and traffic emissions factors. Future HIAs should account for these influential variability and uncertainty sources.

REFERENCES

[1] A. Wernham, "Health Impact Assessments are Needed in Decision Making about Environmental and Land-Use Policy," *Health Aff. (Millwood).*, vol. 30, no. 5, pp. 947–56, 2011.

[2] R. Bhatia and J. Corburn, "Lessons from San Francisco: health impact assessments have advanced political conditions for improving population health.," *Health Aff. (Millwood).*, vol. 30, no. 12, pp. 2410–8, 2011.

[3] National Research Council, *Improving Health in the United States: The Role of Health Impact Assessment*. Washington, DC: The National Academies Press, 2011.

[4] L. Singleton-baldrey, "The Impacts of Health Impact Assessment: A Review of 54 Health Impact Assessments, 2007-2012," University of North Carolina at Chapel Hill, 2012.

[5] A. L. Dannenberg, R. Bhatia, B. L. Cole, S. K. Heaton, J. D. Feldman, and C. D. Rutt, "Use of Health Impact Assessment in the U.S.: 27 Case Studies, 1999-2007," *Am. J. Prev. Med.*, vol. 34, no. 3, pp. 241–56, 2008.

[6] Federal Highway Administration, "Economic Analysis Primer: Benefit-Cost Analysis," Washington, DC, 2003.

[7] R. Bhatia and E. Seto, "Quantitative Estimation in Health Impact Assessment: Opportunities and Challenges," *Environ. Impact Assess. Rev.*, vol. 31, no. 3, pp. 301–309, 2011.

[8] C. L. Ross, M. L. Elliott, M. M. Rushing, J. Barringer, S. Cox, A. Frackelton, J. Kent, and A. Rao, "Aerotropolis Atlanta Brownfield Redevelopment Health Impact Assessment," Alanta, 2011.

[9] Human Impact Partners, "Pittsburg Railroad Avenue Specific Plan Health Impact Assessment," Oakland, CA, 2008.

[10] Human Impact Partners, "Pathways to Community Health : Evaluating the Healthfulness of Affordable Housing Opportunity Sites Along the San Pablo Avenue Corridor Using Health Impact Assessment," Oakland, CA, 2009.

[11] UC Berkeley Health Impact Group, "Oak to Ninth Avenue Health Impact Assessment," Berkeley, CA, 2006.

[12] UC Berkeley Health Impact Group, "MacArthur BART Health Imapct Assessment," Berkeley, CA, 2007.

[13] UC Berkeley Health Impact Group, "Health Impact Assessment of the Port of Oakland," Berkeley, CA, 2010.

[14] Vanasse Hangen Brustlin Inc., “Transportation Impact Analysis for the Carolina North Development,” Watertown, MA, 2009.

[15] NC Capital Area Metropolitan Planning Organization, “Socio-Economic Demographic Forecasts shapefile. 2030 Long Range Transportation Plan.,” 2005.

[16] C. Chart-asa, K. G. Sexton, and J. MacDonald Gibson, “Traffic Impacts on Fine Particulate Matter Air Pollution at the Urban Project Scale : A Quantitative Assessment,” *J. Environ. Prot. (Irvine,. Calif).*, vol. 4, 2013.

[17] B. Ostro and L. Chestnut, “Assessing the health benefits of reducing particulate matter air pollution in the United States.,” *Environ. Res.*, vol. 76, no. 2, pp. 94–106, 1998.

[18] A. Prüss-Üstün, C. Mathers, C. Corvalán, and A. Woodward, *Introduction and methods: assessing the environmental burden of disease at national and local levels*, no. 1. Geneva, Switzerland: World Health Organization, 2003.

[19] J. MacDonald Gibson, A. Brammer, C. Davidson, T. Folley, F. Launay, and J. Thomsen, *Environmental Burden of Disease Assessment: A Case Study in the United Arab Emirates*. Dordrecht, Heidelberg, London, New York: Springer, 2013.

[20] A. Zanobetti and J. Schwartz, “The effect of fine and coarse particulate air pollution on mortality: a national analysis.,” *Environ. Health Perspect.*, vol. 117, no. 6, pp. 898–903, 2009.

[21] M. L. Bell, K. Ebisu, R. D. Peng, J. Walker, J. M. Samet, S. L. Zeger, and F. Dominici, “Seasonal and regional short-term effects of fine particles on hospital admissions in 202 US counties, 1999-2005,” *Am. J. Epidemiol.*, vol. 168, no. 11, pp. 1301–10, 2008.

[22] National Climatic Data Center, “Quality Controlled Local Climatological Data (QCLCD),” 2013.

[23] National Oceanic and Atmospheric Administration, “NOAA/ESRL Radiosonde Database,” 2013.

[24] US Environmental Protection Agency, “Quantitative health risk assessment for particulate matter, EPA-452/R-10-005,” Research Triangle Park, NC, 2010.

[25] K. Aunan, “Exposure-response functions for health effects of air pollutants based on epidemiological findings,” *Risk Anal.*, vol. 16, no. 5, pp. 693–709, 1996.

[26] Y. Li, J. MacDonald Gibson, P. Jat, G. Puggioni, M. Hasan, J. J. West, W. Vizuete, K. Sexton, and M. Serre, “Burden of disease attributed to anthropogenic air pollution in the United Arab Emirates: estimates based on observed air quality data.,” *Sci. Total Environ.*, vol. 408, no. 23, pp. 5784–93, 2010.

[27] C. J. Murray, M. Ezzati, A. D. Lopez, A. Rodgers, and S. Vander Hoorn, "Comparative quantification of health risks conceptual framework and methodological issues," *Popul. Health Metr.*, vol. 1, no. 1, p. 1, 2003.

[28] C. Mathers, T. Vos, A. Lopez, J. Salomon, and M. Ezzati, "National Burden of Disease Studies: A Practical Guide. Edition 2.0. Global Program on Evidence for Health Policy," Geneva, Switzerland, 2001.

[29] North Carolina State Center for Health Statistics, "Detailed Mortality Statistics, 2010," 2012.

[30] Minnesota Population Center, "National Historical Geographic Information System: Version 2.0." Minneapolis, MN: University of Minnesota, 2011.

[31] University of North Carolina at Chapel Hill, "The UNC Department of Emergency Medicine Carolina Center for Health Informatics Report, Overview and Analysis of NC DETECT Emergency Department Data: 2009," Chapel Hill, NC, 2011.

[32] Centers for Disease Control and Prevention, "CDC WONDER," 2013. http://wonder.cdc.gov/.

[33] H. H. Chang, M. Fuentes, and H. C. Frey, "Time series analysis of personal exposure to ambient air pollution and mortality using an exposure simulator.," *J. Expo. Sci. Environ. Epidemiol.*, vol. 22, no. 5, pp. 483–8, 2012.

CHAPTER 4

SIMPLIFIED APPROACH FOR QUANTIFYING HEALTH IMPACTS OF TRAFFIC-RELATED AIR POLLUTION AT THE URBAN PROJECT SCALE

Introduction

Motivated by increasing rates of preventable chronic diseases, public health practitioners in the United States increasingly are advocating for formal health impact assessments (HIAs) of urban and transportation planning decision[1, 2]. The long-term goal of these advocates is to change the way road networks and cities are designed, taking into account the effects of design choices on people's decisions about how to move from place to place—whether by private car, public bus or train, bicycle, or walking. These transportation behavior choices, in turn, have impacts on both air quality and physical activity. For example, increased travel by foot or bicycle not only decreases motor vehicle pollutant emissions and the associated health risks of exposure to these emissions but also the risk of obesity and multiple chronic diseases. For example, a recent study in Charlotte, North Carolina, showed that after the construction of a new light rail system, residents who used the system lost more than six pounds, on average, a year after the system was completed; the change was attributed to residents' walking to reach the rail station, whereas previously they had travelled by private car [3].

Choices among alternative transportation system designs and urban development options often are driven by cost-benefit analyses: choices that cost more than the benefits they yield are often rejected in favor of alternatives with higher benefit-cost ratios. Hence, ideally, HIAs

would quantify the health effects of alternative transportation and urban planning decisions, so that any health benefits or costs are factored into the decision-making. However, of more than 70 transportation-related HIAs completed in the United States between 1999 and the end of 2012, only 5 quantified health effects [4, 5]. The others provided qualitative descriptions of potential health impacts, indicating whether the alternative was expected to increase or decrease health risks but not the magnitude of the increase or decrease. While such qualitative analyses may alert decision-makers to potential unintended consequences of their choices, they cannot be used in cost-benefit analyses. Hence, the potential for HIAs to impact decision-making is diminished.

The goal of this research is to develop a simplified approach for quantifying the potential health effects of alternative urban transportation and planning decisions on air quality and public health. Specifically, the research develops a prototype streamlined approach for forecasting how changes in traffic patterns (for example, due to new urban developments) will affect the concentration of particulate matter having diameter less than 2.5 μm (PM2.5) in near-roadway neighborhoods and, in turn, how residents' health will be affected. To make such predictions, the five previous quantitative HIAs as well the previous chapters of this dissertation have linked models that predict automotive fleet emissions of PM2.5 to models that predict dispersion of emitted PM2.5 away from the roadway. However, such models are demanding in terms of expertise, computing resources, and time and hence are costly to implement, putting them beyond the reach of many HIA practitioners [6]. For example, to run linked emissions-dispersion models, the roadway of interest must be divided into a series of short links with similar traffic conditions, and the pollution dispersion from these links is simulated based on

road geometry, traffic volume, traffic emission rates, and meteorological conditions. Large numbers of links lead to a very time-consuming simulation.

This research seeks to improve on previous attempts to develop simplified approaches for predicting near-roadway PM2.5 concentrations and the associated health risks. For example, Batterman et al. developed a simplified model for predicting near-road dispersion by fitting a function with 13 parameters to the output of a line-source Gaussian dispersion model, CALINE4 [7]. Using this simplified model requires finding the values of the 13 parameters for different wind angles in a look-up table developed by Batterman et al. and then multiplying the result of the 13-parameter expression by the PM2.5 emission rate (g/vehicle-mile) on the roadway of interest. Estimating the emissions rate requires running another complex model (such as the MOVES model, developed by the U.S. Environmental Protection Agency) to predict fleet emissions. The New Zealand Transport Agency (NZTA) also has attempted to develop a simplified dispersion model[8]. Like Batterman et al., NZTA fitted a simplified equation to output from CALINE, but they used a two-parameter power-law model rather than a 13-parameter model. Like Batterman, the simplified NZTA approach requires running a separate emissions model, such as MOVES. Another example of a simplified modeling approach is development by the Sacramento Metropolitan Air Quality Management District (SMAQMD) of screening tables showing how changes to peak traffic volumes may affect increased lifetime cancer risks due to diesel particulate matter exposure at perpendicular distances from the middle of the roadway edges. If the proposed project is located within the distance associated with an increased cancer risk higher than the design criterion, then the site-specific HIA is required [9]. However, the SMAQMD approach does not consider how exposure and health impacts may be affected by traffic activity (such as idling or accelerating), traffic speed, or road grade changes.

This research seeks to develop an approach to support HIAs of transportation-related impacts on air quality and public health at the local scale that strikes a balance between complexity and accuracy. The measure of success in the simplified approach is its ability to reproduce the results of estimates generated by full implementation of a linked emissions-dispersion model. The simplified model is then extended to incorporate a health impact function, further simplifying the computational burden of conducting quantitative HIAs. The resulting predicted health impacts are compared to those generated by a full linked emissions-dispersion-health effects model for a case study site.

Modeling Method

Conceptual Approach

The simplified model chosen for this research follows the form Ax^B, where x indicates the horizontal distance between the modeled roadway and an exposure location of interest. In this research, parameters A and B for each season and each side of the roadway are estimated by fitting output obtained from the emissions model MOVES and the dispersion model CAL3QHCR, both of which are described in further detail below. That is, this research runs the linked MOVES-CAL3QHCR model for different distances x and then fits the resulting output to an equation of the form Ax^B, in order to estimate A and B. To use the simplified model, an HIA practitioner could look up values of A and B for the relevant season and then determine the PM2.5 exposure concentration at any perpendicular distance x from the roadway. This simplified approach would greatly reduce the time, expertise, and computational resources needed for an HIA.

This section first describes the basis for choosing a model of the form Ax^B. Then, it explains the process for estimating parameters A and B using output from MOVES and

CAL3QHCR. It then describes an approach for adapting the Ax^B model form to account for varying traffic conditions and road grades and also to provide direct estimates of health impacts. Finally, it discusses a process for validating the simplified model, where the measure of validation is a comparison with estimates produced through full MOVES-CAL3QHCR implementation.

Reduced-Form Model Rationale

The choice of the functional form Ax^B derives directly form the mass-balance model underlying all Gaussian line-source dispersion models (including CAL3QHCR). From basic principles of mass conservation [10], it can be shown that the for a road segment of finite length, the ground-level concentration of a pollutant at any perpendicular distance *x* from the road can be estimated from

$$C_{(x,0)} = \frac{2q}{(2\pi)^{1/2}\sigma_z u} exp\left[-\frac{1}{2}\left(\frac{H}{\sigma_z}\right)^2\right] \int_{p_1}^{p_2} \frac{1}{(2\pi)^{1/2}} \exp(-0.5p^2)\, dp \quad (1)$$

where q represents the total mass of vehicle emissions from the road segment per unit time; σ_y and σ_z represent the contaminant diffusivity in the cross-wind and vertical directions, respectively; u represents the wind speed; H represents the roadway height; and $p_i = y_i/\sigma_{y_i}$ (i = 1,2), where y_i are the positions of the ends of the line source in the cross-wind direction.

For a roadway at ground level, as in the case study in this research, H = 0, so the first exponential term in equation (1) reduces to unity. Furthermore, using empirical tables of σ_y from Wark and Warner [10], and recognizing that the integral on the right side of equation 1 is the probability distribution function for a standard normal random variable, it can be easily shown that this integral evaluates greater than 0.96 (and less than 1.0) for y_1 = -250 ft, y_2 = 250 ft (as in the road segment in this research) and all x distances and stability classes relevant to this research. In other words, equation 1 is equivalent to

$$C_{(x,0)} = \frac{2q}{(2\pi)^{1/2}\sigma_z u} P(p_1 < Z < p_2) \quad (2)$$

where Z is a standard normal random variable. For a road segment of length 500 ft, the maximum value of p_1 (which is less than zero) and the minimum value of p_2 occur for stability class *A*. For a perpendicular distance of 500 ft from the roadway, the value of σ_y is about 120 ft. Hence, p_1 = -250 ft/120 ft =-2.08, and p_2 = 250 ft/120 ft = 2.08. The right-most term in equation 2 is then $P(-2.08 < Z < 2.08) = 0.96$. For all other stability classes and distances *x* relevant to this research, $p_1 < -2.08$ and $p_2 > 2.08$, so that $0.96 < P(p_1 < Z < p_2) < 1.0$, and equation (2) can be approximated as

$$C_{(x,0)} = \frac{2q}{(2\pi)^{1/2}\sigma_z u} \quad (3)$$

From the empirically based charts in Wark and Warner [10], for all stability classes and distances x, $\ln(\sigma_z)$ is a linear function of $\ln(x)$, so

$$\sigma_z = Cx^{B'} \quad (4)$$

Combining equations (3) and (4),

$$C_{(x,0)} = \frac{2q}{(2\pi)^{1/2}Cu} x^{-B'} = Ax^B \quad (5)$$

where *A* represents the combination of the effects of the emissions rate and wind speed. Hence, the simplified equation fitted to the combined output from MOVES and CAL3QHCR is consistent with the fundamental principles of mass conservation upon which Gaussian dispersion models are based.

Wark and Warner [10] note that equations (1) and (2) assume the wind is perpendicular to the road and that, if this is not the case, then these equations should be divided by sin ω, where ω is the angle between the roadway and the wind direction. These corrections for wind direction already are made in CAL3QHCR. However, to use equation (5), a further correction is needed

for roads that are not due north-south, since the baseline case in the CAL3QHCR modeling assumes a north-south roadway. For a due north-south road, equation (5) can be corrected as follows:

$$C(X)_{NS} = \frac{Ax^B}{\sin(\omega)} \tag{6}$$

For a roadway that is at an angle α from due north-south, the equivalent correction for wind direction gives

$$C(X)_{\alpha} = \frac{Ax^B}{\sin(\omega+\alpha)} \tag{7}$$

Therefore, for a given perpendicular distance x from a roadway, the ratio of the pollutant concentration from a roadway at angle α to that expected for a due north-south roadway is given by the ratio of equations (6) and (7):

$$C(X)_{\alpha} = \frac{\frac{Ax^B}{\sin(\omega+\alpha)}}{\frac{Ax^B}{\sin(\omega)}} = \frac{\sin(\omega)}{\sin(\omega+\alpha)} \tag{8}$$

Equation (8) provides a means to correct equation (5) as estimated for a north-south road, so that it can be applied to roads at any angle α from due north-south, given wind direction ω.

Linked MOVES-CAL3QHCR Modeling

As noted above, to estimate parameters A and B for equation 5, this dissertation runs MOVES to estimate vehicle emissions and CAL3QHCR to estimate pollutant concentrations at different horizontal distances from a hypothetical road link of length 500 ft. MOVES was developed by EPA to replace its predecessor model, MOBILE, for regulatory vehicle emissions estimations outside California [11]. It applies a modal-based approach that derives emissions based on a distribution of vehicle operating modes associated with vehicle speeds and vehicle specific powers (VSP, the power demand placed on a vehicle operating under various modes and speeds) of each vehicle class. The vehicle activity on each roadway link varies by time fractions

spent in each operating mode [12]. This would allow the option of more accurately estimating emissions at a link-level analyses [13]. CAL3QHCR was developed by EPA as an enhanced version of CAL3QHC, which in turn updated the CALINE model previously used to predict pollutant dispersion from roadways. CAL3QHCR applies the same main dispersion and queuing algorithms for estimating traffic-related CO and PM as in CAL3QHC but also includes additional features to process up to a year of hourly local meteorological data [14]. It is a steady-state Gaussian plume model; that is, it is based on underlying equations similar to equation 1, and it assumes constant meteorological conditions in any given hour [15]. EPA recommends using CAL3QHCR for estimating near-road particulate pollution at the project scale [11].

Fitting of Reduced-Form Model

To provide data necessary to estimate parameters A and B for the reduced-form model, the combined MOVES-CALQHCR model was run for the hypothetical four-lane road link illustrated in **Figure 4.1** using meteorological and traffic fleet composition data for the Town of Chapel Hill. The hypothetical road is oriented in the north-south direction; has four travel lanes (two in each direction) of 12 feet in width each; and has a total length of 500 feet. For the baseline parameter fitting, the following conditions were assumed: 1600 vehicles/hour traveling under cruise conditions (with no idling or acceleration) at 35 mph on a flat roadway.

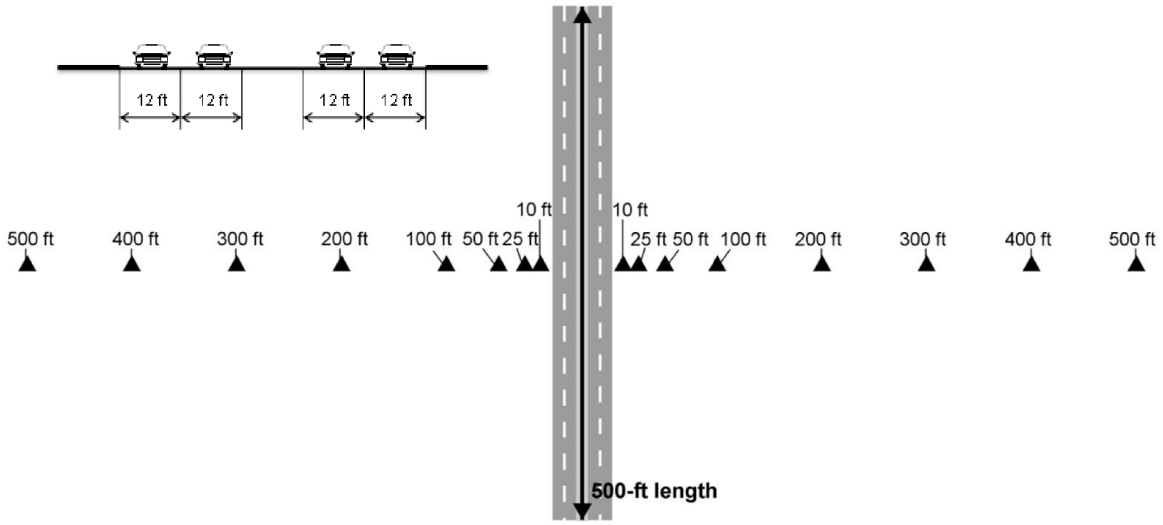

Figure 4.1 Illustration of hypothetical roadway and receptors at eight perpendicular distances from the middle of the roadway edges (10, 25, 50, 100, 200, 300, 400, and 500 feet)

This study also considered for different traffic conditions and road grades. Vehicle operating mode distributions were varied by three traffic activities (cruise, queue, and acceleration), three average traffic speeds (25, 35, and 45 mph), and 21 unit road grades (one-degree increments between -10 and +10 %).

According to EPA's quantitative PM hot-spot analysis guidance [11], cruise traffic activity refers to vehicles travelling at the average road speed and grade. Queue traffic activity includes cruise traffic activity plus idling at a stop. Similarly, the acceleration traffic activity is characterized as cruise traffic activity plus accelerating from a stop to the average speed. This study derived the operating mode distributions for cruise traffic activity based on the model default driving cycles. The operating mode distributions for the queue traffic activity were assumed equal to the operating mode distributions for cruise traffic activity plus the time fraction of idling (Op-Mode 1). The operating mode distributions for acceleration traffic activity were calculated by summing the operating mode distributions for cruise traffic activity and the

operating mode distributions for vehicle driving at half of the average speed minus the time fraction spent idling and braking (Op-Mode 0, 1, and 501).

The hourly average traffic volume were determined as factors of the threshold capacity of a major arterial in Chapel Hill, including 800 (0.5), 1600 (1.0), 2400 (1.5), and 3200 (2.0) veh/hr [16] and held constant over the analysis period.

Parameters *A* and *B* were estimated by bootstrapping from the output of thousands of runs of MOVES-CAL3QHCR, using an approach similar to that described in **Chapters 2 and 3** plus a modeling concept to predict and scale roadside exposure for various traffic scenarios from one set of emission rate and traffic volume that described in Liu and Frey [17]. **Figure 4.2** illustrates the ten steps of this process. In brief, MOVES-CAL3QHCR was run for each of 2,100 daily weather patterns from meteorological data sets covering the period 2006–2012, including 525 winter days, 560 spring days, 532 summer days, and 483 fall days, obtained from the national weather stations in Chapel Hill and Greensboro (with the former providing surface data and the latter providing data for upper atmospheric layers) [18, 19]. Hourly "unit" concentration estimates were simulated for eight different perpendicular distances from the middle of the roadway (i.e., 10, 25, 50, 100, 200, 300, 400, and 500 feet) on each side of the roadway using an emission rate of 1.0 g/veh-mile and a traffic volume of 10,000 veh/hr. The hourly "unit" concentration estimates were scaled by the traffic volume and emission rates corresponding to the traffic condition of interest and the resulting hourly predictions were averaged to 24-hour average concentrations. This process generated 2,100 daily estimates of 24-hour-average concentrations at each receptor location corresponding to the traffic condition of interest. For each season, receptor location, 91 samples of the estimated daily average PM2.5 concentration were randomly selected from the appropriate subset of daily estimates, and these were adjusted

by model prediction error factors randomly sampled from the triangular distribution with lower limit = 0.5, upper limit = 2.0, and mode =1.0, since the previous evaluation (see **Chapter 2**) of integrated MOVES-CAL3QHCR modeling indicated that modeled concentrations can be considered as good approximations within a factor of two of measured concentrations. Then, the 91 samples of the adjusted daily average PM2.5 concentration were averaged to obtain a seasonal daily mean PM2.5 concentration at each location. This process of sampling 91 daily concentration profiles for each season and averaging the results was repeated 2,000 times, in order to obtain 2,000 estimates of the seasonal average daily PM2.5 concentration at each receptor location. The parameters Ax^B were estimated by fitting curves to the mean values of these 2,000 samples for each receptor location (designated in **Figure 4.1** as *x*). To obtain upper and lower bound estimates, parameters A and B also were estimated by curve fitting to the lower and upper 95th percentiles of the predicted concentrations.

In MOVES modeling, traffic-related PM2.5 emission rates (g/veh-mile) for the hypothetical roadway considered thirteen vehicle types (i.e., motorcycle, passenger car, passenger truck, light commercial truck, intercity bus, transit bus, school bus, refuse truck, single unit short-haul truck, single unit long-haul truck, motor home, combination short-haul truck, and combination long-haul truck) and three fuel types (i.e., gasoline, diesel, and compressed natural gas). The distribution of vehicle types were represented by the vehicle mix for Guilford County, NC [20]. The distributions of vehicle age and fuel type were based on the model national defaults. MOVES was run for six temperatures (i.e., 10, 30, 50, 70, 90, and 110 °F) in order to characterize the emission rate variation due to temperature changes. For any selected temperature profile, emissions rates were interpolated based on the nearest two of the estimated

six temperatures. The estimated emission rates were used as the basis to determine hourly emission rates as the key input to CAL3QHCR.

In CAL3QHCR modeling, the hypothetical roadway was represented by two model links, each for one traffic way. Meteorological data were prepared for input into CAL3QHCR using the EPA's Meteorological Processors and Accessories Programs. The analysis period was limited to day-time hours during 6 a.m. to 7 p.m., since the traffic emissions during these hours are assumed to contribute the major near-road pollution and health impacts. Then, these hourly concentrations were averaged over 24 hours, assuming roadway contributions between the hours of 7 p.m. and 6 a.m. were zero.

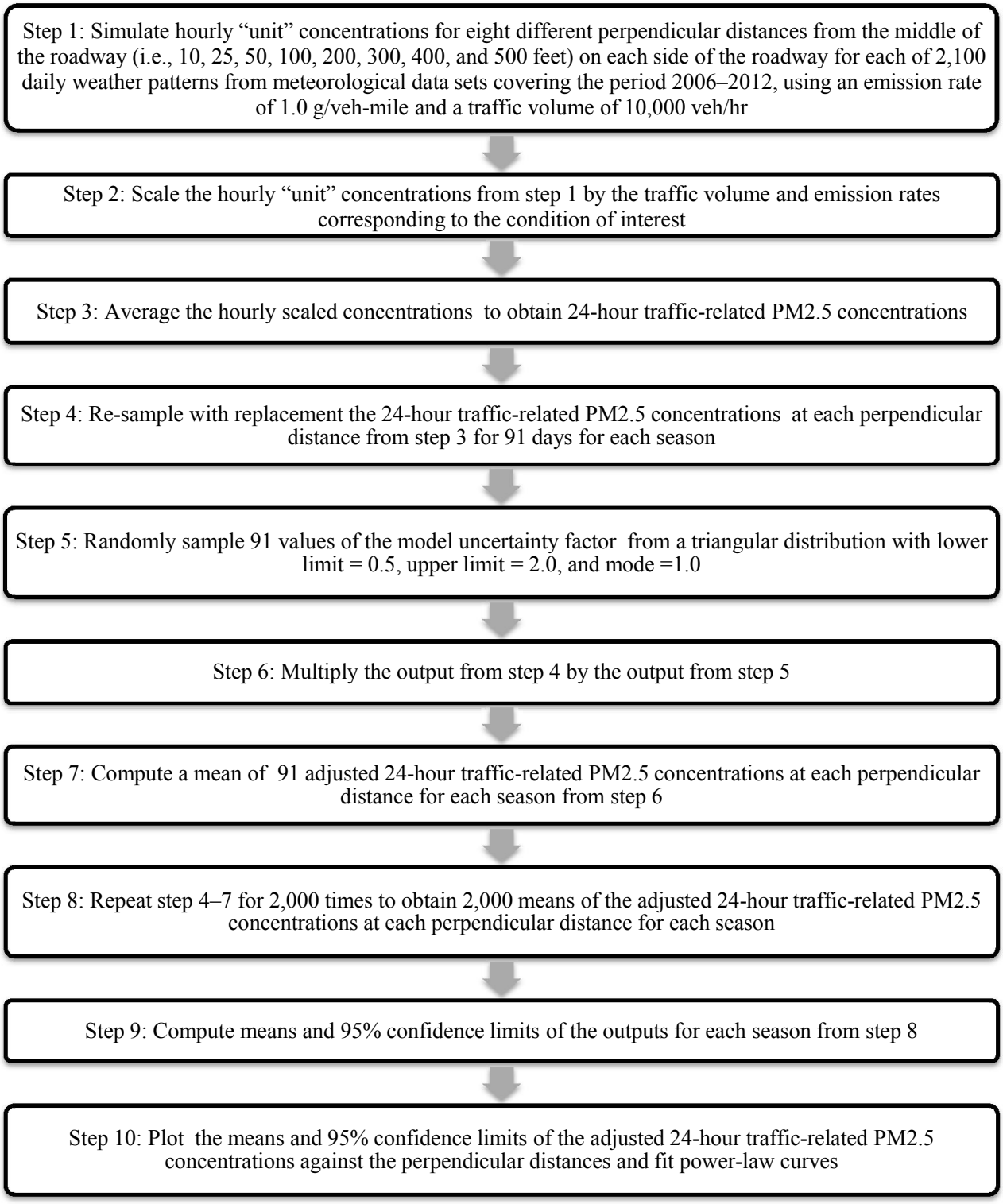

Figure 4.2 Flow chart showing ten steps for estimating parameters *A* and *B* for traffic-related PM2.5

Incorporation of Health Impacts

This project also estimated separate parameters A' for determining directly the health effects of roadway-related air pollution at specific distances from the road. These parameters can be used directly to determine the fraction of observed cases of a specific health outcome in a population living within distance x of the roadway that is attributable to PM2.5 pollution from the roadway—that is, to determine the attributable fraction (AF) directly. As in **Chapters 2 and 3**, this analysis focused on the attributable fractions of cardiovascular and respiratory mortality (all ages) and unscheduled hospital admissions (ages over 65) due to short-term PM2.5 exposure. These health effects were considered as the major health impacts being estimated in EPA's quantitative health risk assessment for supporting the review of National Ambient Air Quality Standards for PM [21]. The season- specific concentration-response functions were retrieved from the EPA's health risk assessment that have been evaluated and judged adequate to be used for health risk assessment of PM2.5 pollution. The retrieved concentration-response functions for mortality and morbidity effects were specific to Atlanta and Southeast region, which are the closet areas for which the functions are available and which has similar meteorological condition as Chapel Hill. These functions were developed based on the log-linear model, which the attributable fraction can be described by the following equation [22]:

$$AF = \frac{e^{\beta C(x)} - 1}{e^{\beta C(x)}} = 1 - e^{-\beta C(x)} \quad (9)$$

where AF is the attributable fraction; β is concentration–response coefficient; and $C(x)$ is the seasonal average 24-hour traffic-related PM2.5 concentrations at an exposure point at distance x from the roadway. The season-specific means and standard deviations for the concentration-response coefficients are shown in **Table 1**.

Table 4.1 Season-specific means and standard deviation used in the disease burden assessment					
Health effects	ICD-9 or ICD-10 code	Age group	Season	Concentration-response coefficient	
				Mean	Standard Deviation
Cardiovascular mortality	I01–I59	All ages	Winter	0.00135	0.00167
			Spring	0.00076	0.00178
			Summer	0.00062	0.00145
			Fall	-0.00018	0.00140
Respiratory mortality	J00–J99	All ages	Winter	0.00093	0.00121
			Spring	0.00035	0.00122
			Summer	0.00077	0.00119
			Fall	0.00096	0.00117
Unscheduled cardiovascular hospital admissions	410–414, 426–429, 430–438, and 440–449	65 and over	Winter	0.00105	0.00058
			Spring	0.00075	0.00052
			Summer	-0.00067	0.00048
			Fall	0.00017	0.00045
Unscheduled respiratory hospital admissions	464–466, 480–487, and 490–492	65 and over	Winter	0.00040	0.00094
			Spring	0.00075	0.00080
			Summer	-0.00052	0.00080
			Fall	0.00014	0.00073

EPA derived the concentration-response coefficients of the mortality effects from Zanobetti and Schwartz [23] and the morbidity effects from Bell et al. [24].

Recognizing that for small values of $\beta C(x)$ (as is the case for this assessment), equation (9) can be approximated as $\beta C(x)$, AF can be estimated as:

$$AF = \beta A x^B = A' x^B \tag{10}$$

Parameters A' for each health outcome were estimated using a similar process as that for estimating parameter A: the resulting daily concentration estimates at each receptor location x for each of the 2,100 days for which weather data were available were multiplied by a value of β randomly sampled from the zero-truncated normal distribution with mean and stand deviation as shown in **Table 4.1**. For each season, 91 daily AFs were then sampled at random and averaged, and this process was repeated 2,000 times to obtain 2,000 estimates of the seasonal AFs. The mean value and upper and lower confidence interval values of these seasonal AFs were then fitted to equation (10).

Reduced-Form Model Validation Approach

The reduced-form model was validated by comparing the predicted PM2.5 concentrations and AFs for four census blocks within 500 meters of a segment of Martin Luther King, Jr., Boulevard in Chapel Hill, North Carolina, between the intersections with Estes Drive and Piney Mountain Road/ Municipal Drive. Predictions were developed for both the years 2009 and for 2025, based on future traffic projections obtained from the Town of Chapel Hill [25]. The validation compared estimates from the reduced-form approach with those obtained from a full implementation of MOVES-CAL3QHCR as described in **Chapters 2 and 3**.

Results and Discussion

Simplified Equations for Quantifying Near-Road Traffic-Related PM2.5 Pollution and Related Health Impacts

Figure 4.3 and 4.4 showed 2009 and 2025 horizontal profiles of near-road traffic-related PM2.5 pollution and related health impacts simulated by assigning both traffic ways the base traffic condition. Points and error bars represent mean and 95% CI of the estimates. According to the meteorological data used in this study, the prevailing winds were from north to south with low speeds, thus the traffic pollution tended to be dispersed along the hypothetical roadway. Consequently, the estimates were highly elevated near the roadway edges, and decreased rapidly within 100 feet. The magnitude estimates on both sides of the roadway were at similar levels, except for winter that the estimates on the east side were higher than those on the west side due to more frequent occurrences of winds blowing to east. Moreover, winter appeared to be the most polluted season, due to the influence of increased emission rates at low temperatures [26]. When breaking down the estimates by the emission sources as vehicle fuel types, vehicle age groups, and vehicle types, the average percentage contributions of each vehicle classes were

shown in **Figure 4.5**. For 2009, the major contributions were from diesel vehicles; vehicle ages 10 years and older; or light-duty vehicles. For 2025, the main contributors were gasoline vehicles; vehicle age groups 0–3, 10–14, and 20 years or older; or also light-duty vehicles.

Table 4.2 and 4.3 showed curve parameters A and B for mean and 95% confidence limits of the estimates of near-road PM2.5 pollution and related health impacts. The estimates using the parameters in **Table 4.2 and 4.3** and equations (5) and (10) can be weighted by the average percentage contributions for vehicle class of interest in **Figure 4.5** to obtain the new estimates specific to such vehicle class as $\%\, contribution \times Ax^B$.

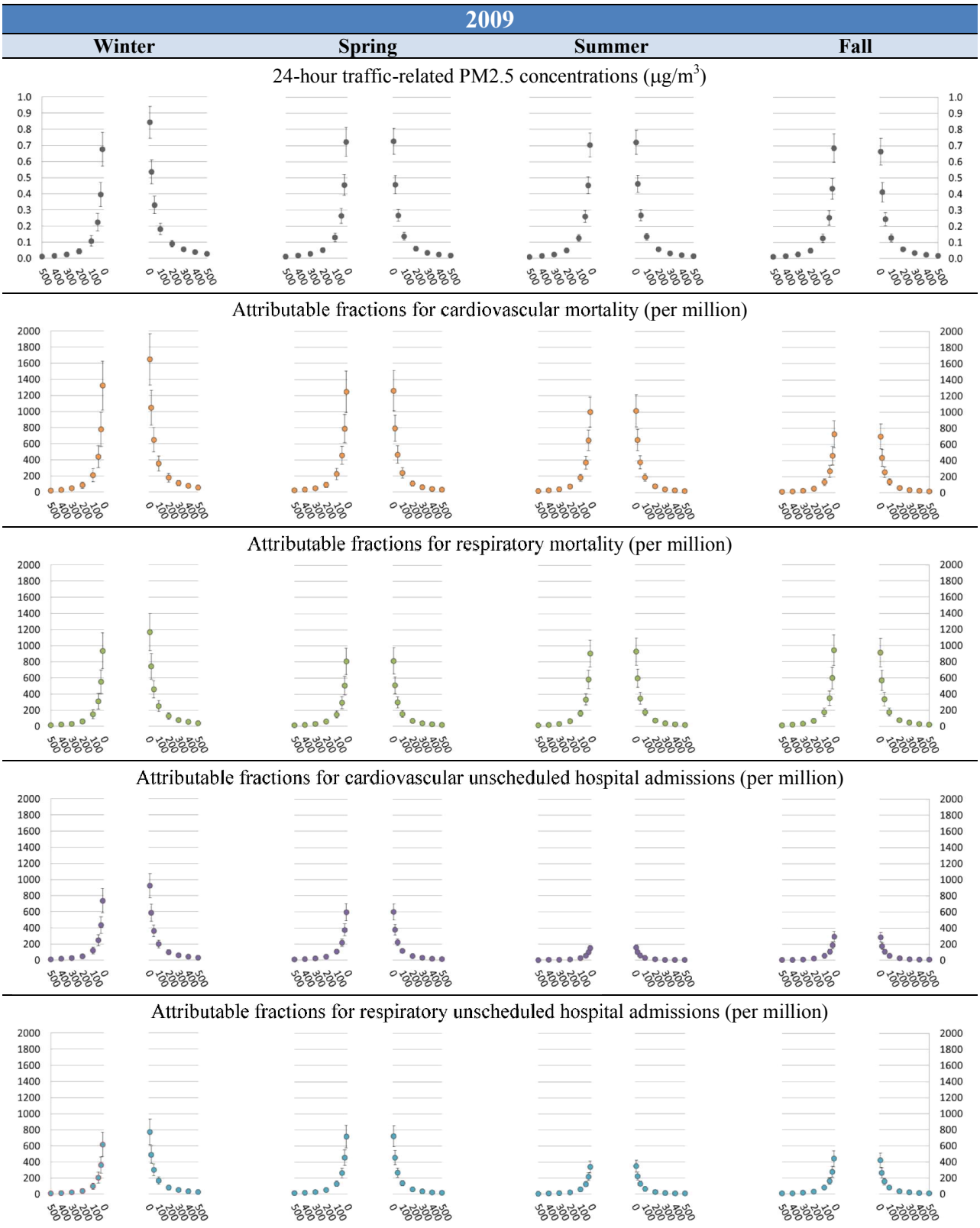

Figure 4.3 2009 horizontal profiles of 24-hour traffic-related PM2.5 concentrations (μg/m^3) and corresponding attributable fractions (per million) simulated by assigning both traffic way the base traffic condition. Points and error bars represent mean and 95% CI of the estimates. X-axis is distance from the roadway edges (feet).

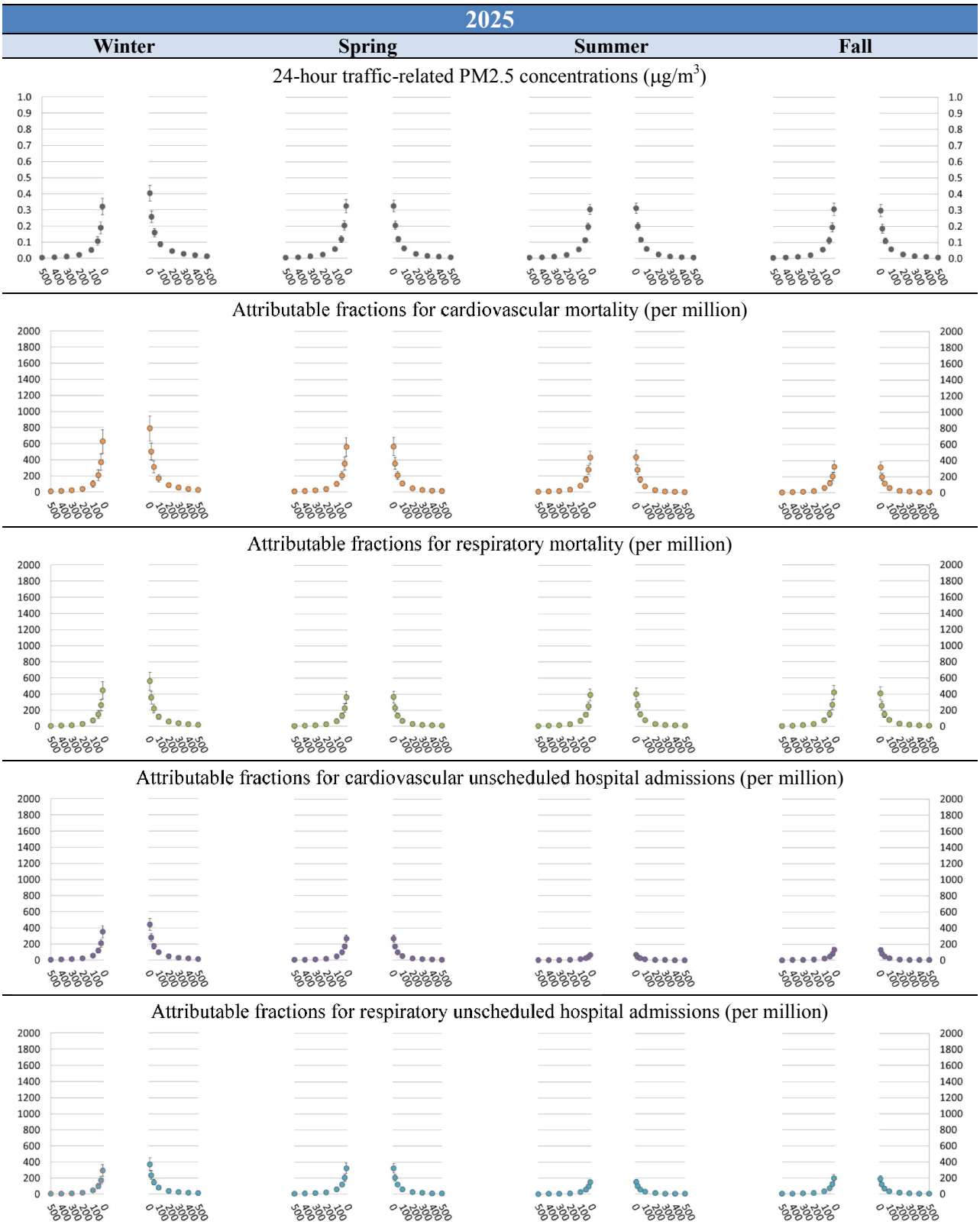

Figure 4.4 2025 horizontal profiles of 24-hour traffic-related PM2.5 concentrations (μg/m^3) and corresponding attributable fractions (per million) simulated by assigning both traffic way the base traffic condition. Points and error bars represent mean and 95% CI of the estimates. X-axis is distance from the roadway edges (feet).

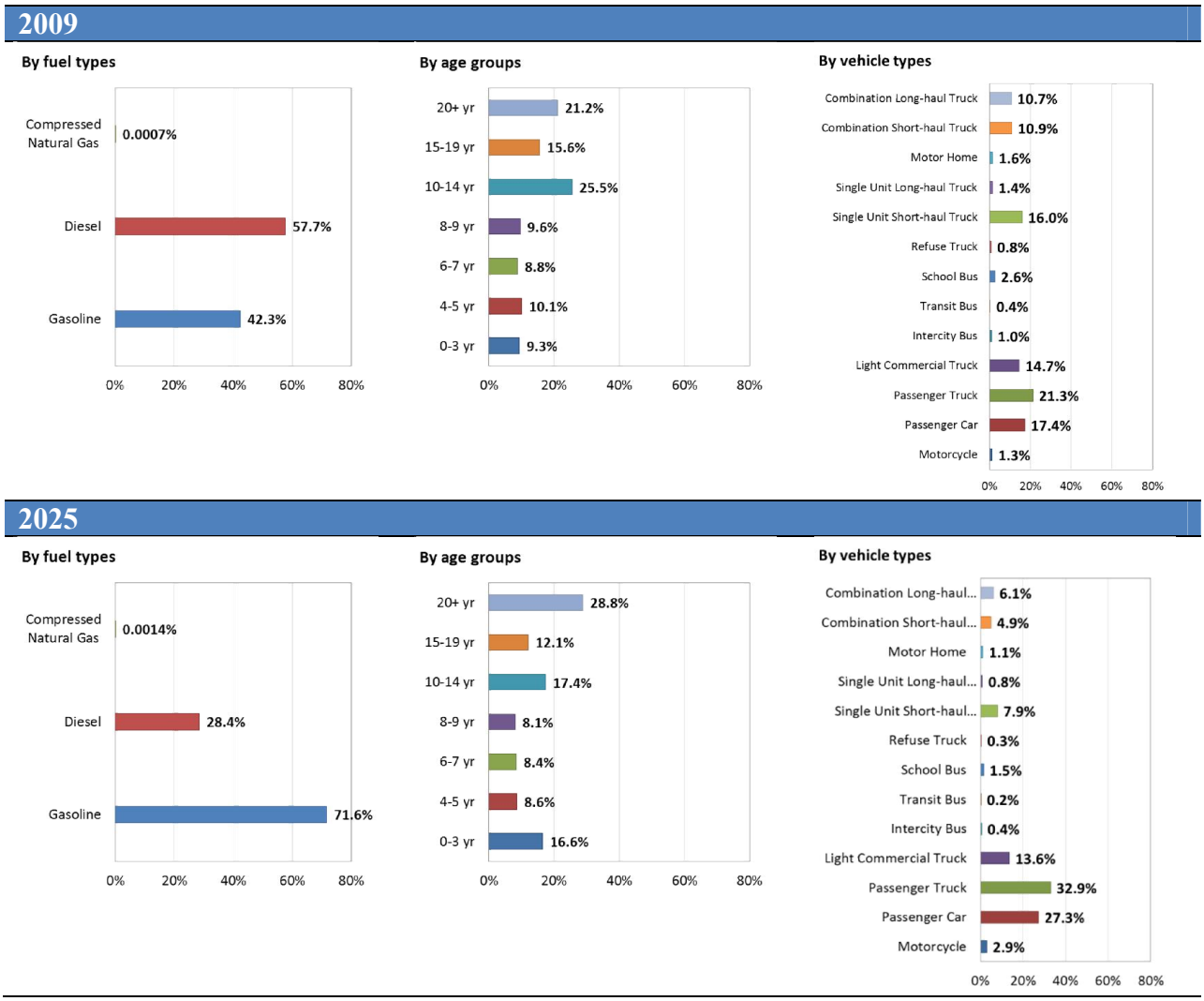

Figure 4.5 2009 and 2025 average percentage contributions of the 24-hour traffic-related PM2.5 concentrations and corresponding attributable fractions by fuel types, age groups, and vehicle types

Table 4.2 2009 power-law curve parameters for the 24-hour traffic-related PM2.5 concentrations (μg/m3) and corresponding attributable fractions (*AF*) of cardiovascular (CVD) and respiratory (RD) diseases events (per million) as a function of a perpendicular distance from the middle of road edge (feet)

Season	Indicator	Value	East-side			West-side		
			A	*B*	R^2	*A*	*B*	R^2
Winter	24-hour traffic-related PM2.5	Mean	8.5	-0.88	0.98	1.3×10^{1}	-1.10	0.97
		Lower	8.6	-0.93	0.98	1.6×10^{1}	-1.26	0.97
		Upper	8.7	-0.85	0.98	1.2×10^{1}	-1.03	0.97
	AF CVD mortality	Mean	1.7×10^{4}	-0.88	0.98	2.5×10^{4}	-1.10	0.97
		Lower	1.6×10^{4}	-0.94	0.98	3.3×10^{4}	-1.29	0.97
		Upper	1.8×10^{4}	-0.85	0.98	2.5×10^{4}	-1.03	0.97
	AF RD mortality	Mean	1.2×10^{4}	-0.88	0.98	1.8×10^{4}	-1.10	0.97
		Lower	1.1×10^{4}	-0.94	0.98	2.4×10^{4}	-1.30	0.96
		Upper	1.3×10^{4}	-0.85	0.98	1.8×10^{4}	-1.03	0.97
	AF unscheduled hospital admissions for CVD	Mean	9.2×10^{3}	-0.88	0.98	1.4×10^{4}	-1.10	0.97
		Lower	9.0×10^{3}	-0.94	0.98	1.9×10^{4}	-1.28	0.97
		Upper	9.8×10^{3}	-0.85	0.98	1.4×10^{4}	-1.03	0.97
	AF unscheduled hospital admissions for RD	Mean	7.8×10^{3}	-0.88	0.98	1.2×10^{4}	-1.10	0.97
		Lower	7.4×10^{3}	-0.94	0.98	1.5×10^{4}	-1.30	0.97
		Upper	8.5×10^{3}	-0.85	0.98	1.2×10^{4}	-1.03	0.97
Spring	24-hour traffic-related PM2.5	Mean	1.0×10^{1}	-0.99	0.97	1.4×10^{1}	-1.08	0.97
		Lower	1.1×10^{1}	-1.06	0.97	1.5×10^{1}	-1.17	0.96
		Upper	9.8	-0.95	0.98	1.3×10^{1}	-1.03	0.97
	AF CVD mortality	Mean	1.7×10^{4}	-0.99	0.97	2.3×10^{4}	-1.08	0.97
		Lower	1.7×10^{4}	-1.06	0.97	2.5×10^{4}	-1.19	0.96
		Upper	1.9×10^{4}	-0.95	0.98	2.4×10^{4}	-1.03	0.97
	AF RD mortality	Mean	1.1×10^{4}	-0.99	0.97	1.5×10^{4}	-1.08	0.97
		Lower	1.1×10^{4}	-1.07	0.97	1.6×10^{4}	-1.19	0.96
		Upper	1.2×10^{4}	-0.95	0.98	1.5×10^{4}	-1.03	0.97
	AF unscheduled hospital admissions for CVD	Mean	8.2×10^{3}	-0.99	0.97	1.1×10^{4}	-1.08	0.97
		Lower	8.5×10^{3}	-1.06	0.97	1.2×10^{4}	-1.19	0.96
		Upper	8.5×10^{3}	-0.95	0.98	1.1×10^{4}	-1.03	0.97
	AF unscheduled hospital admissions for RD	Mean	1.0×10^{4}	-0.99	0.97	1.4×10^{4}	-1.09	0.97
		Lower	1.0×10^{4}	-1.06	0.97	1.5×10^{4}	-1.19	0.96
		Upper	1.0×10^{4}	-0.95	0.98	1.4×10^{4}	-1.03	0.97
Summer	24-hour traffic-related PM2.5	Mean	1.1×10^{1}	-1.03	0.97	1.5×10^{1}	-1.12	0.96
		Lower	1.2×10^{1}	-1.08	0.97	1.7×10^{1}	-1.20	0.96
		Upper	1.1×10^{1}	-0.99	0.97	1.4×10^{1}	-1.07	0.96
	AF CVD mortality	Mean	1.6×10^{4}	-1.03	0.97	2.1×10^{4}	-1.12	0.96
		Lower	1.5×10^{4}	-1.08	0.97	2.3×10^{4}	-1.21	0.96
		Upper	1.7×10^{4}	-1.00	0.97	2.2×10^{4}	-1.07	0.96
	AF RD mortality	Mean	1.5×10^{4}	-1.03	0.97	1.9×10^{4}	-1.12	0.96
		Lower	1.4×10^{4}	-1.09	0.97	2.1×10^{4}	-1.22	0.96
		Upper	1.6×10^{4}	-0.99	0.97	2.0×10^{4}	-1.07	0.96
	AF unscheduled hospital admissions for CVD	Mean	2.5×10^{3}	-1.03	0.97	3.2×10^{3}	-1.12	0.96
		Lower	2.3×10^{3}	-1.09	0.97	3.4×10^{3}	-1.23	0.95
		Upper	2.7×10^{3}	-1.00	0.97	3.4×10^{3}	-1.07	0.96
	AF unscheduled hospital admissions for RD	Mean	5.5×10^{3}	-1.03	0.97	7.3×10^{3}	-1.12	0.96
		Lower	5.1×10^{3}	-1.09	0.97	7.8×10^{3}	-1.23	0.95
		Upper	6.0×10^{3}	-0.99	0.97	7.6×10^{3}	-1.07	0.96
Fall	24-hour traffic-related PM2.5	Mean	8.5	-0.97	0.98	1.3×10^{1}	-1.08	0.97
		Lower	9.0	-1.04	0.97	1.5×10^{1}	-1.19	0.96
		Upper	8.5	-0.92	0.98	1.2×10^{1}	-1.02	0.97
	AF CVD mortality	Mean	8.9×10^{3}	-0.97	0.98	1.4×10^{4}	-1.08	0.97
		Lower	8.8×10^{3}	-1.05	0.97	1.6×10^{4}	-1.23	0.96
		Upper	9.6×10^{3}	-0.92	0.98	1.4×10^{4}	-1.02	0.97
	AF RD mortality	Mean	1.2×10^{4}	-0.97	0.98	1.8×10^{4}	-1.08	0.97
		Lower	1.2×10^{4}	-1.05	0.97	2.1×10^{4}	-1.21	0.96
		Upper	1.2×10^{4}	-0.92	0.98	1.8×10^{4}	-1.02	0.97
	AF unscheduled hospital admissions for CVD	Mean	3.6×10^{3}	-0.96	0.98	5.5×10^{3}	-1.08	0.97
		Lower	3.6×10^{3}	-1.05	0.97	6.5×10^{3}	-1.22	0.96
		Upper	3.9×10^{3}	-0.92	0.98	5.6×10^{3}	-1.02	0.97
	AF unscheduled hospital admissions for RD	Mean	5.4×10^{3}	-0.97	0.98	8.2×10^{3}	-1.08	0.97
		Lower	5.5×10^{3}	-1.05	0.97	9.4×10^{3}	-1.22	0.96
		Upper	5.8×10^{3}	-0.92	0.98	8.4×10^{3}	-1.02	0.97

Table 4.3 2025 power-law curve parameters for the 24-hour traffic-related PM2.5 concentrations ($\mu g/m^3$) and corresponding attributable fractions (AF) of cardiovascular (CVD) and respiratory (RD) diseases events (per million) as a function of a perpendicular distance from the middle of road edge (feet)

Season	Indicator	Value	East-side			West-side		
			A	B	R^2	A	B	R^2
Winter	24-hour traffic-related PM2.5	Mean	4.0	-0.88	0.98	6.0	-1.10	0.97
		Lower	4.1	-0.93	0.98	7.8	-1.25	0.97
		Upper	4.1	-0.84	0.98	5.7	-1.03	0.97
	AF CVD mortality	Mean	7.8×10^3	-0.88	0.98	1.2×10^4	-1.10	0.97
		Lower	7.5×10^3	-0.94	0.98	1.5×10^4	-1.29	0.97
		Upper	8.5×10^3	-0.84	0.98	1.2×10^4	-1.03	0.97
	AF RD mortality	Mean	5.6×10^3	-0.88	0.98	8.4×10^3	-1.10	0.97
		Lower	5.2×10^3	-0.93	0.98	1.1×10^4	-1.30	0.96
		Upper	6.1×10^3	-0.84	0.98	8.4×10^3	-1.03	0.97
	AF unscheduled hospital admissions for CVD	Mean	4.4×10^3	-0.88	0.98	6.6×10^3	-1.10	0.97
		Lower	4.3×10^3	-0.93	0.98	8.7×10^3	-1.28	0.97
		Upper	4.7×10^3	-0.84	0.98	6.5×10^3	-1.03	0.97
	AF unscheduled hospital admissions for RD	Mean	3.7×10^3	-0.88	0.98	5.5×10^3	-1.10	0.97
		Lower	3.5×10^3	-0.94	0.98	7.2×10^3	-1.30	0.97
		Upper	4.1×10^3	-0.84	0.98	5.6×10^3	-1.03	0.97
Spring	24-hour traffic-related PM2.5	Mean	4.4	-0.99	0.98	6.0	-1.08	0.97
		Lower	4.8	-1.05	0.97	6.8	-1.17	0.96
		Upper	4.4	-0.94	0.98	5.8	-1.03	0.97
	AF CVD mortality	Mean	7.7×10^3	-0.99	0.97	1.0×10^4	-1.08	0.97
		Lower	7.7×10^3	-1.06	0.97	1.1×10^4	-1.19	0.96
		Upper	8.3×10^3	-0.94	0.98	1.1×10^4	-1.03	0.97
	AF RD mortality	Mean	5.0×10^3	-0.99	0.97	6.7×10^3	-1.08	0.97
		Lower	5.0×10^3	-1.06	0.97	7.3×10^3	-1.19	0.96
		Upper	5.3×10^3	-0.94	0.98	6.9×10^3	-1.02	0.97
	AF unscheduled hospital admissions for CVD	Mean	3.7×10^3	-0.98	0.97	4.9×10^3	-1.08	0.97
		Lower	3.8×10^3	-1.06	0.97	5.5×10^3	-1.19	0.96
		Upper	3.8×10^3	-0.94	0.98	5.0×10^3	-1.02	0.97
	AF unscheduled hospital admissions for RD	Mean	4.4×10^3	-0.99	0.97	6.0×10^3	-1.08	0.97
		Lower	4.5×10^3	-1.06	0.97	6.6×10^3	-1.19	0.96
		Upper	4.7×10^3	-0.94	0.98	6.2×10^3	-1.03	0.97
Summer	24-hour traffic-related PM2.5	Mean	4.9	-1.03	0.97	6.5	-1.12	0.96
		Lower	5.1	-1.08	0.97	7.3	-1.20	0.96
		Upper	4.9	-0.99	0.97	6.2	-1.07	0.96
	AF CVD mortality	Mean	7.0×10^3	-1.03	0.97	9.1×10^3	-1.12	0.96
		Lower	6.6×10^3	-1.08	0.97	9.8×10^3	-1.21	0.96
		Upper	7.6×10^3	-1.00	0.97	9.4×10^3	-1.07	0.96
	AF RD mortality	Mean	6.3×10^3	-1.03	0.97	8.3×10^3	-1.12	0.96
		Lower	6.1×10^3	-1.09	0.97	9.0×10^3	-1.22	0.96
		Upper	6.8×10^3	-0.99	0.97	8.5×10^3	-1.07	0.96
	AF unscheduled hospital admissions for CVD	Mean	1.1×10^3	-1.03	0.97	1.4×10^3	-1.12	0.96
		Lower	9.9×10^2	-1.09	0.97	1.5×10^3	-1.23	0.95
		Upper	1.2×10^3	-1.00	0.97	1.5×10^3	-1.07	0.96
	AF unscheduled hospital admissions for RD	Mean	2.4×10^3	-1.03	0.97	3.2×10^3	-1.12	0.96
		Lower	2.2×10^3	-1.09	0.97	3.4×10^3	-1.23	0.95
		Upper	2.6×10^3	-0.99	0.97	3.3×10^3	-1.07	0.96
Fall	24-hour traffic-related PM2.5	Mean	3.8	-0.96	0.98	5.7	-1.08	0.97
		Lower	4.0	-1.03	0.97	6.9	-1.20	0.96
		Upper	3.8	-0.92	0.98	5.4	-1.02	0.97
	AF CVD mortality	Mean	4.0×10^3	-0.96	0.98	6.1×10^3	-1.08	0.97
		Lower	3.9×10^3	-1.05	0.97	7.4×10^3	-1.24	0.96
		Upper	4.3×10^3	-0.92	0.98	6.2×10^3	-1.02	0.97
	AF RD mortality	Mean	5.2×10^3	-0.96	0.98	7.8×10^3	-1.08	0.97
		Lower	5.2×10^3	-1.05	0.97	9.3×10^3	-1.22	0.96
		Upper	5.5×10^3	-0.92	0.98	7.9×10^3	-1.02	0.97
	AF unscheduled hospital admissions for CVD	Mean	1.6×10^3	-0.96	0.98	2.5×10^3	-1.08	0.97
		Lower	1.6×10^3	-1.05	0.97	2.9×10^3	-1.22	0.96
		Upper	1.7×10^3	-0.92	0.98	2.5×10^3	-1.02	0.97
	AF unscheduled hospital admissions for RD	Mean	4.0	-0.88	0.98	6.0	-1.10	0.97
		Lower	4.1	-0.93	0.98	7.8	-1.25	0.97
		Upper	4.1	-0.84	0.98	5.7	-1.03	0.97

Sensitivity Analysis

Figures 4.6, 4.7, 4.8, 4.9, and 4.10 show the change in parameter *A* associated with different changes in traffic volume, traffic speed and behavior, and road grade. In the same way that the results of equation (5) can be adjusted to estimate the amount of air pollution contributed by each vehicle class, the estimates from these equations can be adjusted by the average percentage changes shown in **Figures 4.6, 4.7, 4.8, 4.9, and 4.10** to obtain the new estimates for other traffic conditions as $1 + \%\ \text{change} \times Ax^B$. A limitation of the simplified equations, however, is that the average percentage changes are only specific to the traffic condition analyzed and cannot be combined, except for the average percentage changes due to traffic volume. That is, the sensitivity analysis does not account for the simultaneous change of multiple parameters [27, 28]. This limitation could be addressed in the future by conducting additional simulations for different combinations of vehicle speed, traffic behavior, and road grade.

For the traffic volume influence, traffic volume is a direct multiplier in the Gaussian dispersion equation, thus percentage changes in this parameter are directly proportional to percentage changes in predicted concentrations at each receptor [29, 30]. The attributable fractions were estimated as an exponential function of the predicted concentration from CAL3QHCR. Thus, the percentage changes in traffic volume are directly proportional to percentage changes in the attributable fractions as well. As shown in **Figure 4.6**, the percentage changes in the 24-hour traffic-related concentrations and attributable fractions were -50%, +50%, and +100% when changing hourly average traffic volume on each way of the hypothetical roadway from 1600 veh/hr to 800, 2400, and 3200 veh/hr respectively.

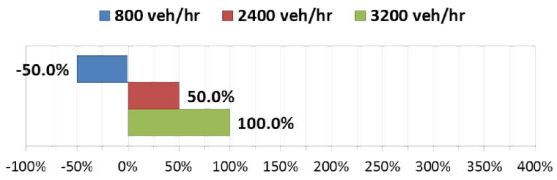

Figure 4.6 Average percentage changes in near-road traffic-related PM2.5 pollution and related health impacts when changing traffic volumes on the hypothetical roadway from 1600 veh/hr each way to 800, 2400, and 3200 veh/hr each way

For the traffic activity influence, this study used the vehicle operating mode distributions for cruise traffic activity as a basis to develop the vehicle operating mode distributions for queue and acceleration traffic activities. Additional time fractions in idling and running modes for the queue and the acceleration traffic activities resulted in increased emission rates. The results showed that the average percentage changes in 24-hour traffic-related PM2.5 concentrations and corresponding attributable fractions were approximately +10% in both 2009 and 2025 when changing cruise traffic activity on both traffic ways of the hypothetical roadway to queue traffic activity with 50% idling time fractions, and about +65 and +55% in 2009 and 2025 respectively when changing to acceleration traffic activity, as shown in **Figure 4.7**, consistent with the findings in Ritner et al. [31] and Papson, Hartley, and Kuo [32] that acceleration traffic activity dominates other traffic activities. Vehicle classes with high percentages by fuel types, age groups, and vehicle types included diesel vehicles; vehicle ages 8 and older; or heavy-duty vehicles (e.g. combination short- and long-haul trucks, buses, and refuse trucks).

For the average traffic speed influence, the default driving cycles in MOVES assumes that vehicles on a flat-road with low average traffic speeds spend most time on braking, idling, and low-moderate speed running modes, while vehicles on the same road with high average traffic speeds spend less time on braking and idling, but more time on high-moderate speed running modes. Previous study showed that high vehicle emissions are generally associated with

low speed running modes [33]. Thus, the emission rates for low average traffic speeds appeared to be higher than those for high average traffic speeds at the same road grade. When lowering average traffic speeds on each way of the hypothetical roadway from 35 mph to 25 mph, the average percentage changes in 24-hour traffic-related PM2.5 concentrations and corresponding attributable fractions were nearly 30% in 2009 and 35% in 2025. When increasing average traffic speeds from 35 mph to 45 mph, the average percentage changes were around -15% in 2009 and -20% in 2025, as shown in **Figure 4.8**. Compressed natural gas vehicles and gasoline vehicles; vehicle ages 14 and younger; or heavy-duty vehicles appeared to be more sensitive to altering average traffic speeds than diesel vehicles; vehicle ages 15 and older; or light-duty vehicles (e.g. passenger cars or trucks, and light commercial trucks) respectively.

For the road grade influence, the default driving cycles in MOVES assumes that vehicles on a uphill road (positive road grades) spend large time on low-moderate speed cruising-accelerating modes with high-moderate vehicle specific power, whereas vehicles on a downhill road (negative road grades) spend major time on braking, low-moderate speed coasting, and high speed cruising-accelerating modes with low vehicle specific power. An increase in vehicle specific power due to large positive road grade leads to higher vehicle emissions [34]. Thus, the emission rates uphill appeared to be larger than those downhill at the same average traffic speed.

When changing road grades on each way of the hypothetical roadway from 0% to ± 10% (both traffic ways were assigned the same road grade, but one with positive values and another with negative values), the average percentage changes in 24-hour traffic-related concentrations and corresponding attributable fractions were increased non-linearly with the road grade increases: up to around +175% in both 2009 and 2025 for the *uphill-roadside* receptors, and up to nearly +110% and +130% in 2009 and 2025 respectively for *downhill-roadside* receptors, as

shown in **Figure 4.9 and 4.10**. Changing road grades tended to be more influential to emissions from gasoline vehicles; vehicle ages 8 and older; or motorcycles and light-duty vehicles than compressed natural gas vehicles and diesel vehicles; vehicle ages 7 and younger; or heavy-duty vehicles respectively.

The differences in the average percentage changes between 2009 and 2025 were primarily resulted from the internal assumptions to project the emission rates in MOVES. For light-duty gasoline vehicles, MOVES assumes that the new vehicle (i.e., zero-mile level) PM2.5 emission rates are decreased exponentially with model years, as vehicles get cleaner engine fuel controls and after-treatment systems. These emission rates are projected to be increased exponentially with vehicle age, as an effect of deterioration, but remained unchanged after 20 years. For light-duty diesel vehicles, the emission rates for the model year 2004 and later are assumed to be the same as those for the light-duty gasoline vehicles, because the same certification standards would be applied to vehicles running on both fuels [35]. For heavy-duty diesel vehicles, MOVES assumes that the new vehicle emission rates are decreased according to the emission standards introductions. For the mode year 2007 and later, the emission rates are considerably reduced due to implementing diesel particulate filter standard. Additionally, the emission rates are projected to be increased with age as an effect of tampering and mal-maintenance, and leveled off after the end of useful life ages (i.e. 4–10 years). For heavy-duty gasoline vehicles, the emission rates are proportioned to those for the light-duty gasoline vehicles, which a factor of 1.40 used in the calculation [36]. For motorcycles and compressed natural gas vehicles, the emission rates were determined based on those for the light-duty passenger car, and the medium heavy-duty gasoline vehicles respectively [37, 38].

Figure 4.7 2009 and 2025 Average percentage changes in near-road traffic-related PM2.5 pollution and related health impacts when adjusting traffic activity on each way of the hypothetical roadway from cruise to queue and acceleration. The percentage of combination short-long haul truck and refuse truck for queue traffic activity did not present here. The MOVES default distributions of vehicle operating for these vehicle types did not include the time fractions of idling for Op-Mode 1, probably due to the model bug needed to be fixed in the next version of MOVES.

Figure 4.1 2009 and 2025 average percentage changes in near-road traffic-related PM2.5 pollution and related health impacts when altering the average traffic speed on each way of the hypothetical roadway from 35 mph to 25 and 45 mph

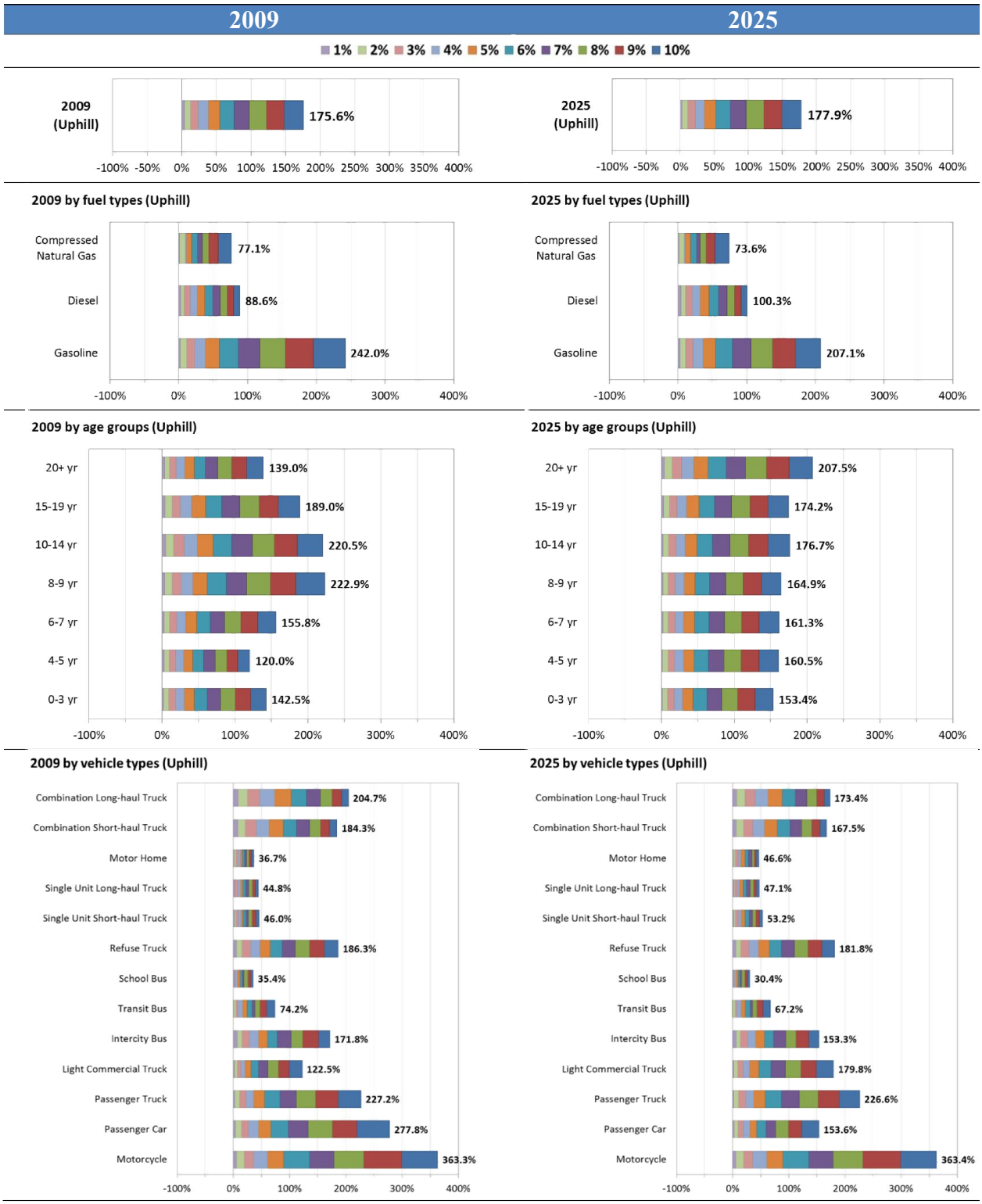

Figure 4.9 2009 and 2025 average percentage changes in near-road traffic-related PM2.5 pollution and related health impacts on *the uphill-roadside receptors* when changing road grade on each way of the hypothetical roadway from 0% to ± 10% (both traffic ways were assigned the same road grades, but one with positive values and another with negative values)

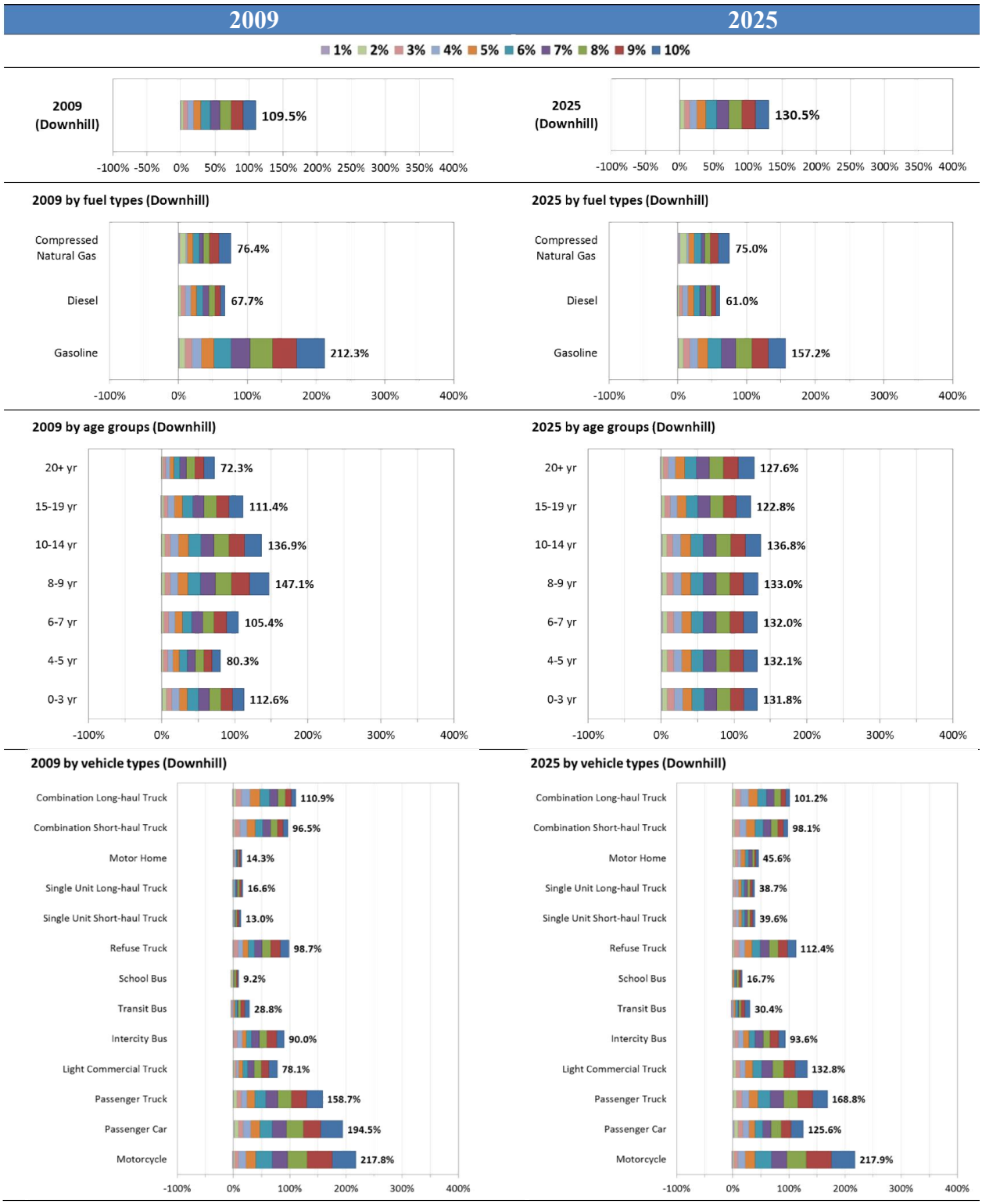

Figure 4.10 2009 and 2025 average percentage changes in near-road traffic-related PM2.5 pollution and related health impacts on *the downhill-roadside receptors* when changing road grade on each way of the hypothetical roadway from 0% to ±10% (both traffic ways were assigned the same road grades, but one with positive values and another with negative values)

The results illustrate that large road grade is most influential to near-road traffic-related PM2.5 pollution and related health impacts. When comparing the average percentage changes across the traffic parameter being analyzed, it reveals that changing the traffic activity from acceleration to cruise may help may help lessen near-road traffic-related PM2.5 pollution and related health impacts as similar level as reducing hourly average traffic volumes by 50% each way, or converting queue traffic activity to cruise plus increasing average traffic speed from 35 to 45 mph. Moreover, the results suggested that the uphill roadside could be more affected by traffic-related air pollution than the downhill roadside (although of course the pollution dispersion depending on local wind directions and speeds). A city planner may consider placing barriers along the uphill roadside to help protect pedestrians and residents from excess exposure to traffic-related air pollution. Baldauf et al. [39] found that a noise barrier near highway could reduce carbon monoxide and particle number concentrations behind the barrier by 15–50% under certain meteorological conditions, but the barrier could lead to higher on-road pollution as well. Hagler et al. [40] also noted that a roadside brick wall could lower ultra-fine particle concentrations behind the wall by 50%, and vegetative buffers effectiveness are variable depending on vegetation type, height, thickness, and leaf coverage.

Model Validation

Figure 4.11 and **Figure 4.12** show examples of comparisons of attributable fractions for cardiovascular mortality per million due to short-term exposure to traffic-related PM2.5 at the centroids of four census blocks located adjacent to the segment of Martin Luther King Jr Boulevard between the intersections with Estes Drive and Piney Mountain Road/ Municipal Drive from the simplified equations to those obtained from using a full MOVES-CAL3QHCR modeling approach described in Chart-asa, Sexton, and MacDonald Gibson [41]. The expected

traffic condition on the segment of Martin Luther King Jr Boulevard is generally similar to the base traffic condition, but with different hourly average traffic volumes, i.e. 1130 and 1744 veh/hr in 2009 and 2025 scenarios with Carolina North respectively, or -29% and +9% compared the hourly average traffic volume in the baseline traffic condition (i.e., 1600 veh/hr). According to the locations of census block centroids, the first three census blocks used the set of east-side equations and the fourth census block used the set of west-side equations. The distances from the census block centroids to the roadway edges are 118, 313, 2407, and 2753 feet for the first, second, third, and fourth census block respectively.

The orientation of the segment of Martin Luther King Jr Boulevard is 351 degree clockwise from north. As a result, the wind direction relative to this roadway will be the wind direction from due north-south plus 9 degrees. Thus, the estimates from the simplified equations were corrected for these different road orientations before making the comparisons. The correction factors were calculated based on the frequency distribution of wind direction in each season. The 360 degrees of wind direction were broken into 36 bins (each 10 degrees). The middle value of each bin (e.g. 5.5, 15.5, 25.5, and so on) was used in equation (8). The correction factors for each bin were weighted by the frequency within each bin, and then summed over to obtain the correction factors for each season: 0.94, 0.91, 0.89, and 0.93 for winter, spring, summer, and fall respectively.

At least with this comparison case, the simplified equations appeared to over-estimate the attributable fractions of cardiovascular mortality from the full modeling approach in both 2009 and 2025 with Carolina North scenarios. For the first two census blocks (ID 371350119013003 and 371350119013002), the ratios of the estimates from these two approaches (i.e., the ratios of the estimate produced by the full model to that from the simplified model) ranged from about

0.24–0.71 when excluding the percentage change due to different hourly average traffic volume, and about 0.27–0.85 when including this average percentage change. The adjustment for different hourly average traffic volume improved the agreements in 2009 scenarios, but decrease agreement between approaches in 2025 with Carolina North scenario. The best agreement (i.e., ratios is closest to one) occurred for the winter estimates. Possible explanation for the disagreements are that the simplified equations are derived from the estimates at short perpendicular distances from the middle of the edges of north-south corridor with the assumption of constant traffic condition over the analysis period, while the full modeling approach accounts for actual angles between receptors and the roadway as well as variability in traffic conditions throughout the analysis period. For the other two census blocks (which their centroids further from the roadway edges), the full modeling approach reported zero or nearly zero estimates due to the effects of the internal rounding process in CAL3QHCR, while the simplified equations provided positive estimates. Similar trends also occur for the other three health impacts.

Further validation on a site-specific basis is required to confirm whether this trend is consistent for other road segments and exposure locations or not. It is important to recognize that the model validation in this study uses a short road segment with traffic conditions similar to those along the hypothetical road used for deriving the simplified equations. For a longer roadway with variable traffic conditions, the traffic emissions from each of road segment may affect each exposure location of interest differently. The estimates from the simplified equations may under-estimate the air quality and health impacts at the exposure locations of interest, compared to those from the modeling approach, if the adjustments for traffic volume, activity, average speed, or road grade lead to lower traffic emissions than those from the most influential road segments for each of exposure locations of interest. Thus, it is critical to properly

incorporate variability in traffic conditions over the road segment of concern, particularly road grade and traffic activity, within the simplified equations.

As mentioned before, the parameters *A* and *B* for the reduced-form model in this study are estimated by fitting power-law curves to the estimates obtained from the integrated MOVES-CAL3QHCR modeling. Therefore, these two parameters are specific to the data used in the integrated modeling, and applying them to other sites with different road geometry (e.g. a curvy road with more traffic lanes), vehicle fleet composition, and meteorological conditions may mislead the estimations of near-road traffic-related PM2.5 pollution and related health impacts.

There are limitations to be noted about the concentration-response functions used for estimating the parameters *A* and *B* for attributable fractions of cardiovascular and respiratory mortality and unscheduled hospital admissions. These functions were developed using the ambient concentrations from central monitors as a surrogate for population exposures to PM2.5, which may imply that these functions are appropriate only for health impact assessments at coarse spatial resolution. Moreover, the concentration-response functions used in this study are specific to Atlanta, GA, and the southeast region, which may not sufficiently represent the population exposure to PM2.5, the composition of PM2.5 to which populations are exposed, and the adverse health events associated with PM2.5 in Chapel Hill, NC. However, developing location-specific concentration-response coefficients accounting for personal exposure at a finer spatial resolution, as demonstrated in Chang, Fuentes, and Frey [41], is beyond the scope of this study.

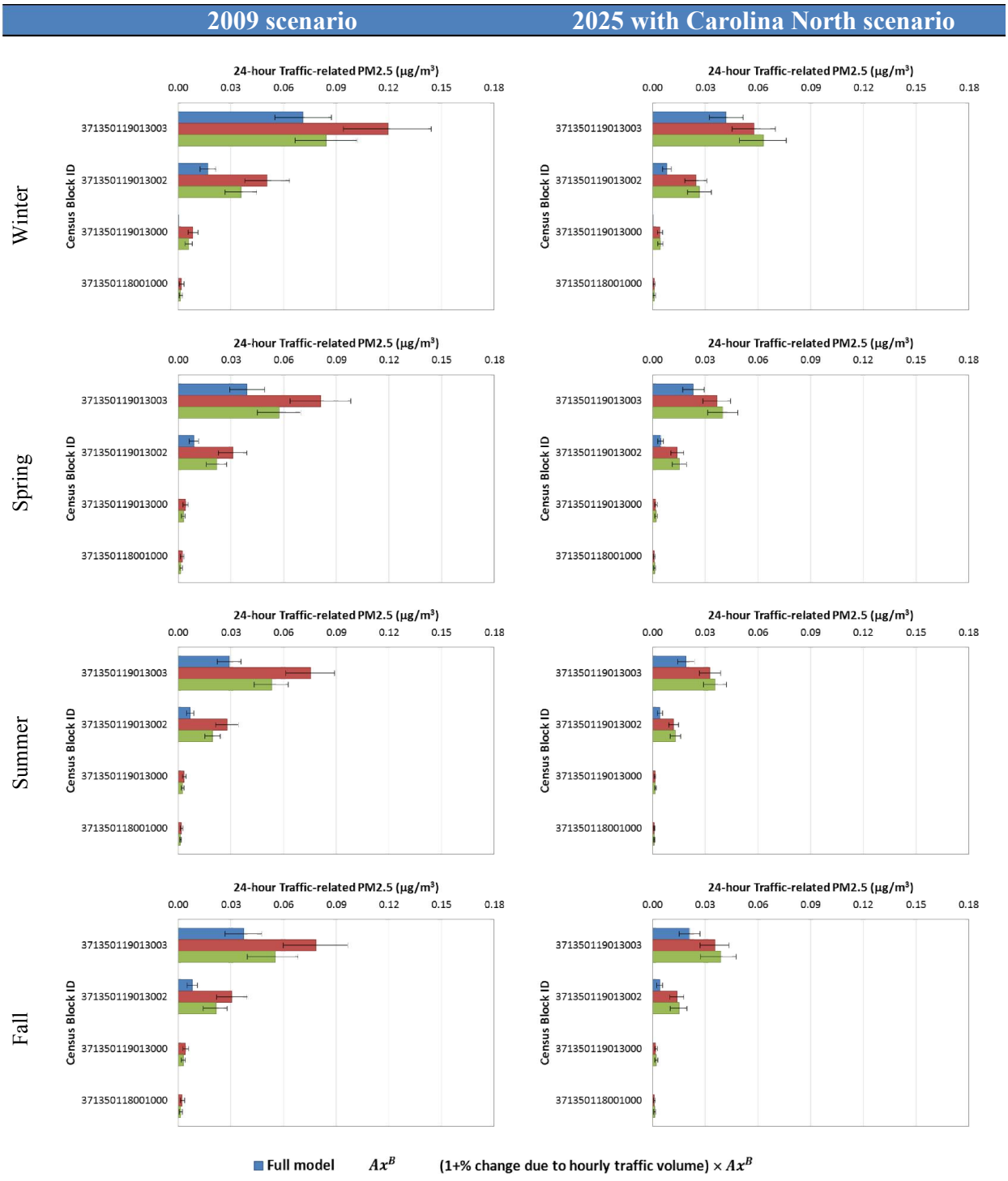

Figure 4.11 Comparisons between the 24-hour traffic-related PM2.5 concentrations (µg/m^3) from the simplified equations and the full MOVES-CAL3QHCR modeling in 2009 and 2025 with Carolina North scenarios. The percentage changes due to hourly average traffic volume are -29% and +9% compared to the baseline traffic volume (1600 veh/hr) for 2009 and 2025 with Carolina North scenarios respectively.

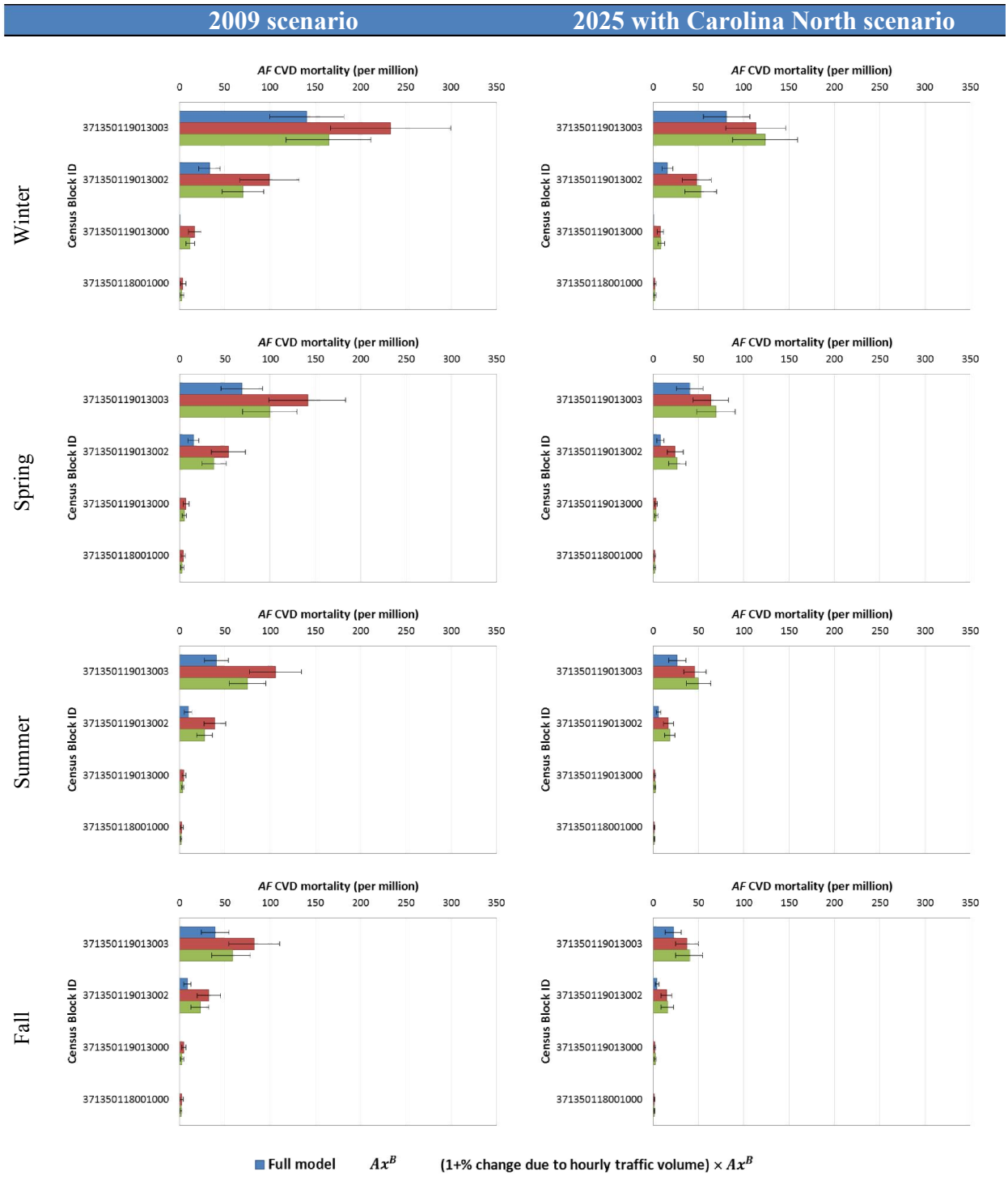

Figure 4.12 Comparisons between the attributable fractions (*AF*) of cardiovascular (CVD) mortality (per million) from the simplified equations and the full MOVES-CAL3QHCR modeling in 2009 and 2025 with Carolina North scenarios. The percentage changes due to hourly average traffic volume are -29% and +9% compared to the baseline traffic volume (1600 veh/hr) for 2009 and 2025 with Carolina North scenarios respectively.

Conclusions

The simplified framework demonstrated in this study has potential as a tool for use by HIA practitioners and others for preliminary evaluations of the air quality and health impacts of increased traffic brought by new urban developments. However, additional validation and calibration with either the full modeling approach or roadside measurements are needed. Future work may focus on validating and refining the framework to extend its capability and applicability. In addition, future work may provide guidelines on the best ways to incorporate variability in road grade and traffic activity within the simplified framework, since the air quality and health impact estimates are highly sensitive to these parameters.

REFERENCES

[1] A. Wernham, "Health Impact Assessments are Needed in Decision Making about Environmental and Land-Use Policy," *Health Aff. (Millwood).*, vol. 30, no. 5, pp. 947–56, 2011.

[2] National Research Council, *Improving Health in the United States: The Role of Health Impact Assessment*. Washington, DC: The National Academies Press, 2011.

[3] J. M. MacDonald, R. J. Stokes, D. a Cohen, A. Kofner, and G. K. Ridgeway, "The Effect of Light Rail Transit on Body Mass Index and Physical Activity," *Am. J. Prev. Med.*, vol. 39, no. 2, pp. 105–12, 2010.

[4] L. Singleton-baldrey, "The Impacts of Health Impact Assessment: A Review of 54 Health Impact Assessments, 2007-2012," University of North Carolina at Chapel Hill, 2012.

[5] R. Bhatia and E. Seto, "Quantitative Estimation in Health Impact Assessment: Opportunities and Challenges," *Environ. Impact Assess. Rev.*, vol. 31, no. 3, pp. 301–309, 2011.

[6] K. Zhang and S. Batterman, "Near-Road Air Pollutant Concentrations of CO and PM2.5: A Comparison of MOBILE6.2/CALINE4 and Generalized Additive Models," *Atmos. Environ.*, vol. 44, no. 14, pp. 1740–1748, 2010.

[7] S. a Batterman, K. Zhang, and R. Kononowech, "Prediction and analysis of near-road concentrations using a reduced-form emission/dispersion model.," *Environ. Health*, vol. 9, p. 29, 2010.

[8] I. Longley, G. Olivares, S. Harper, and K. Shrestha, "Tools for assessing exposure to land transport emissions. NZ Transport Agency research report 451," 2011.

[9] Sacramento Metropolitan Air Quality Management District, "Recommended Protocol for Evaluating the Location of Sensitive Land Uses Adjacent to Major Roadways," Sacramento, CA, 2011.

[10] K. Wark and C. F. Warner, *Air Pollution: Its Origin and Control*. New York, 1981.

[11] US Environmental Protection Agency, "Transportation conformity guidance for quantitative hot-spot analyses in PM 2.5 and PM 10 nonattainment and maintenance areas, EPA-420-B-10-040," Washington, DC, 2010.

[12] J. Koupal, M. Beardsley, D. Brzezinski, J. Warila, and W. Faler, "U.S. EPA's MOVES2010 vehicle emission model: overview and considerations for international application," in *the 18th International Symposium on Transport and Air Pollution*, 2010, pp. 1–7.

[13] S. Bai, D. Eisinger, and D. Niemeier, "MOVES vs EMFAC : a comparative assessment based on a Los Angeles county case study (Task Orders No. 9 and 53)," Davis, CA, 2008.

[14] P. A. Eckhoff and T. N. Braverman, "Addendum to the User's Guide to CAL3QHC Version 2.0 (CAL3QHCR User's Guide)," 1995.

[15] P. E. Benson, "A review of the development and application of the CALINE3 and 4 models," *Atmos. Environ. Part B. Urban Atmos.*, vol. 26, no. 3, pp. 379–390, 1992.

[16] Town of Chapel Hill, "Guidelines for Traffic Impact Analysis," Chapel Hill, NC, 2001.

[17] X. Liu and H. C. Frey, "Modeling of In-Vehicle Human Exposure to Ambient Fine Particulate Matter," *Atmos. Environ. (1994).*, vol. 45, no. 27, pp. 4745–4752, 2011.

[18] National Climatic Data Center, "Quality Controlled Local Climatological Data (QCLCD)," 2013.

[19] National Oceanic and Atmospheric Administration, "NOAA/ESRL Radiosonde Database," 2013.

[20] N.C. Division of Air Quality, "MOVES Input and Output Files: Hickory and Triad PM2.5 Redesignation Demonstration and Maintenance Plan," 2011.

[21] US Environmental Protection Agency, "Quantitative health risk assessment for particulate matter, EPA-452/R-10-005," Research Triangle Park, NC, 2010.

[22] Y. Li, J. MacDonald Gibson, P. Jat, G. Puggioni, M. Hasan, J. J. West, W. Vizuete, K. Sexton, and M. Serre, "Burden of disease attributed to anthropogenic air pollution in the United Arab Emirates: estimates based on observed air quality data.," *Sci. Total Environ.*, vol. 408, no. 23, pp. 5784–93, 2010.

[23] A. Zanobetti and J. Schwartz, "The effect of fine and coarse particulate air pollution on mortality: a national analysis.," *Environ. Health Perspect.*, vol. 117, no. 6, pp. 898–903, 2009.

[24] M. L. Bell, K. Ebisu, R. D. Peng, J. Walker, J. M. Samet, S. L. Zeger, and F. Dominici, "Seasonal and regional short-term effects of fine particles on hospital admissions in 202 US counties, 1999-2005," *Am. J. Epidemiol.*, vol. 168, no. 11, pp. 1301–10, 2008.

[25] Vanasse Hangen Brustlin Inc., "Transportation Impact Analysis for the Carolina North Development," Watertown, MA, 2009.

[26] D. Choi, M. Beardsley, D. Brzezinski, J. Koupal, and J. Warila, "MOVES Sensitivity Analysis: The Impacts of Temperature and Humidity on Emissions," in *The MOVES Workshop 2011*, 2011.

[27] H. C. Frey and S. R. Patil, "Identification and review of sensitivity analysis methods.," *Risk Anal.*, vol. 22, no. 3, pp. 553–78, 2002.

[28] C. Frey and J. Zheng, "Chapter 8 – Methods for Assessment of Uncertainty and Sensitivity in Inventories," in *Improving Emission Inventories for Effective Air Quality Management Across North America*, 2005.

[29] P. E. Benson, "CALINE3, A Versatile Dispersion Model for Predicting Air Pollutant Levels Near Highways and Arterial Streets," Sacramento, CA, 1979.

[30] J. B. Lindemann, "A Sensitivity Evaluation of EPA's CAL3QHC Dispersion Model for Carbon Monoxide Analysis at Urban Intersections," Oregon State University, 1994.

[31] M. Ritner, K. K. Westerlund, C. D. Cooper, and M. Claggett, "Accounting for Acceleration and Deceleration Emissions in Intersection Dispersion Modeling Using MOVES and CAL3QHC," *J. Air Waste Manage. Assoc.*, vol. 63, no. 6, pp. 724–736, 2013.

[32] A. Papson, S. Hartley, and K.-L. Kuo, "Analysis of Emissions at Congested and Uncongested Intersections with Motor Vehicle Emission Simulation 2010," *Transp. Res. Rec. J. Transp. Res. Board*, vol. 2270, no. -1, pp. 124–131, 2012.

[33] Texas Transportation Institute, "MOVES Sensitivity Study," College Station, Texas, 2011.

[34] K. Zhang and H. C. Frey, "Road grade estimation for on-road vehicle emissions modeling using light detection and ranging data.," *J. Air Waste Manag. Assoc.*, vol. 56, no. 6, pp. 777–88, 2006.

[35] US Environmental Protection Agency, "Development of Emission Rates for Light-Duty Vehicles in the Motor Vehicle Emissions Simulator (MOVES2010), EPA-420-R-11-011," Washington, DC, 2011.

[36] US Environmental Protection Agency, "Development of Emission Rates for Heavy-Duty Vehicles in the Motor Vehicle Emissions Simulator (MOVES2010), EPA-420-B-12-049," Washington, DC, 2012.

[37] A. Eilbert and A. Kahan, "Proposed Exhaust Emission Rates for Compressed Natural Gas Transit Buses in MOVES2013," in *MSTRS MOVES Review Work group*, 2012.

[38] US Environmental Protection Agency, "Use of Data from 'Development of Emission Rates for the MOVES Model,' Sierra Research, March 3, 2010. EPA-420-R-12-022," Washington, DC, 2012.

[39] R. Baldauf, E. Thoma, A. Khlystov, V. Isakov, G. Bowker, T. Long, and R. Snow, “Impacts of noise barriers on near-road air quality,” *Atmos. Environ.*, vol. 42, no. 32, pp. 7502–7507, 2008.

[40] G. S. W. Hagler, M.-Y. Lin, A. Khlystov, R. W. Baldauf, V. Isakov, J. Faircloth, and L. E. Jackson, “Field investigation of roadside vegetative and structural barrier impact on near-road ultrafine particle concentrations under a variety of wind conditions,” *Sci. Total Environ.*, vol. 419, pp. 7–15, 2012.

[41] C. Chart-asa, K. G. Sexton, and J. MacDonald Gibson, “Traffic Impacts on Fine Particulate Matter Air Pollution at the Urban Project Scale : A Quantitative Assessment,” *J. Environ. Prot. (Irvine,. Calif).*, vol. 4, 2013.

[42] H. H. Chang, M. Fuentes, and H. C. Frey, “Time series analysis of personal exposure to ambient air pollution and mortality using an exposure simulator.,” *J. Expo. Sci. Environ. Epidemiol.*, vol. 22, no. 5, pp. 483–8, 2012.

CHAPTER 5

CONCLUSIONS

This dissertation has expanded the evidence and tools available for quantitative health impact assessments (HIAs) of traffic-related PM2.5 at the urban project scale. The dissertation has advanced knowledge and methods in three ways: (1) by developing a new algorithm to incorporate hourly meteorological variability in the assessment of traffic impacts on near-roadway air pollution, (2) by illustrating the importance of including variability and uncertainty in HIAs, and (3) by developing a simplified modeling approach for quantitative HIAs.

Chapter 2 of this dissertation developed and empirically validated a new algorithm for including hourly meteorological variability in estimating local exposure to traffic-related PM2.5 pollution under alternative future traffic scenarios. This approach also accounts for the effects of variability in traffic activities, average traffic speed, and road grades. An empirical validation for a case study roadway corridor (Martin Luther King, Jr., Blvd., in Chapel Hill North Carolina) showed that the improved modeling approach predicted traffic-related PM2.5 pollution to within a factor of two of measured values. Hence, the improved approach satisfies the usual standard against which air quality predictive models are validated. The improved modeling approach should benefit HIA practitioners and others conducting quantitative assessment of the changes in local population exposure to traffic-related PM2.5 pollution. Applying the model to the traffic conditions on the case study corridor under present-day and potential future conditions for the year 2025 reveals that the uncertainty in model prediction error appears to have a greater effect on the prediction of local population exposure than the variability in hourly meteorological

conditions. Moreover, the key factor in protecting public health from the air quality and health impacts of traffic emissions is ensuring continued improvements in vehicle fuel economy and emissions standards. In fact, the model shows that air quality impacts of the case study roadway corridor will decrease in the year 2025, despite future predicted increases in traffic. These future emission reductions reflect the built-in assumptions of MOVES. Thus, the EPA should evaluate these assumptions periodically to validate the model predictions. Future work may apply the improved modeling approach to evaluate cumulative exposure to multiple traffic-related pollutants and/or in different micro-environments (e.g. sidewalk and in-vehicle).

Chapter 3 of the dissertation investigated the extent to which HIA estimates are affected by including variability in seasonal average traffic-related PM2.5 concentrations, seasonal concentration-response coefficients and health incidents, and population demographic characteristics at a fine spatial scale as well as uncertainty in air quality model accuracy and concentration-response coefficients. The results demonstrated that the deterministic approach of current HIAs may under-estimate health impacts of traffic emissions along the case study roadway corridor and therefore may lead to decisions that are not cost effective and/or sufficiently protective of public health. Future HIAs of the built environment and transportation projects should incorporate these influential variability and uncertainty sources in the analysis of air quality and health impacts.

Chapter 4 developed a simplified framework for quantifying the air quality and health impacts of traffic emissions, while incorporating variability and uncertainty sources, as a tool to assist HIA practitioners and others who may not have the resources to run full scale air quality dispersion models. The results demonstrated that the simplified framework tends to provide conservative estimates of health impacts compared to those from the full scale modeling

approach and could be used for a screening analysis for estimating an upper bound of potential impacts or determining whether a detailed analysis is necessary or not. Future work should focus on validating and refining the framework to extend its capability and further validate its predictive capacity.

Overall, this dissertation has demonstrated the importance of including variability and uncertainty in HIAs that assess air quality and health impacts of alternative development and transportation projects at the local scale. The case study demonstrated that the current deterministic approach could under-estimate risk. Furthermore, the dissertation has demonstrated that it may be possible to develop HIA modeling tools that enable HIA practitioners with limited time and resources to conduct quantitative HIAs that consider the impacts of variability in meteorology, traffic, and population characteristics along with uncertainty in the performance of air quality predictive models and the effects of air pollution on public health. Further development of a streamlined approach could result in HIAs having a larger influence on decision-making, because the output of such quantitative HIAs can be used to quantify health effects and associated costs, so that these impacts are weighed along with other kinds of economic impacts when deciding among alternative projects.

APPENDIX A
SUPPLEMENTAL MATERIALS FOR MOVES MODELING OF EMISSION RATES OF TRAFFIC-RELATED PM2.5

MOVES 2010b was used to estimate 8,316 of traffic-related PM2.5 emission rates (g/veh-mile) for defined traffic conditions as combinations of two emission years (i.e., 2009 and 2025), eleven traffic activities (i.e., cruise, acceleration, and queue with time fraction of idling from 0.1–0.9), three average traffic speeds (i.e., 25, 35, and 45 mph), twenty-one unit road grades (i.e., -10% to +10%), and six temperatures (i.e., 10, 30, 50, 70, 90, and 110 °F). The modeling accounted for emissions from thirteen vehicle types (i.e., motorcycle, passenger car, passenger truck, light commercial truck, intercity bus, transit bus, school bus, refuse truck, single unit short-haul truck, single unit long-haul truck, motor home, combination short-haul truck, and combination long-haul truck), and three fuel types (i.e., gasoline, diesel fuel, compressed natural gas). For each model run, all MOVES inputs were manually keyed into a MySQL database via MOVES graphical user interface, and corresponding outputs were programed to store in a separate database. The model run specifications (i.e., RunSpec) were saved into a file, and later called for batch processing. Examples of the RunSpec of MOVES run and the batch processing commands are shown below:

Example of a RunSpec of MOVES for estimating 2009 emission rates for cruise traffic activity, 35 mph average traffic speed, unit road grade -10% to +10%, and 70 °F

```
<runspec>
    <description><![CDATA[Estimating 2009 emission rates based on cruise traffic
activity, 35 mph average traffic speed, and unit road grade -10% to 10% under 70
degree Fahrenheit]]></description>
    <modelscale value="Rates"/>
    <modeldomain value="PROJECT"/>
    <geographicselections>
        <geographicselection type="COUNTY" key="37135" description="NORTH CAROLINA -
Orange County"/>
    </geographicselections>
```

```
    <timespan>
        <year key="2009"/>
        <month id="4"/>
        <day id="5"/>
        <beginhour id="9"/>
        <endhour id="9"/>
        <aggregateBy key="Hour"/>
    </timespan>
    <onroadvehicleselections>
        <onroadvehicleselection fueltypeid="3" fueltypedesc="Compressed Natural Gas
(CNG)" sourcetypeid="42" sourcetypename="Transit Bus"/>
        <onroadvehicleselection fueltypeid="2" fueltypedesc="Diesel Fuel"
sourcetypeid="62" sourcetypename="Combination Long-haul Truck"/>
        <onroadvehicleselection fueltypeid="2" fueltypedesc="Diesel Fuel"
sourcetypeid="61" sourcetypename="Combination Short-haul Truck"/>
        <onroadvehicleselection fueltypeid="2" fueltypedesc="Diesel Fuel"
sourcetypeid="41" sourcetypename="Intercity Bus"/>
        <onroadvehicleselection fueltypeid="2" fueltypedesc="Diesel Fuel"
sourcetypeid="32" sourcetypename="Light Commercial Truck"/>
        <onroadvehicleselection fueltypeid="2" fueltypedesc="Diesel Fuel"
sourcetypeid="54" sourcetypename="Motor Home"/>
        <onroadvehicleselection fueltypeid="2" fueltypedesc="Diesel Fuel"
sourcetypeid="21" sourcetypename="Passenger Car"/>
        <onroadvehicleselection fueltypeid="2" fueltypedesc="Diesel Fuel"
sourcetypeid="31" sourcetypename="Passenger Truck"/>
        <onroadvehicleselection fueltypeid="2" fueltypedesc="Diesel Fuel"
sourcetypeid="51" sourcetypename="Refuse Truck"/>
        <onroadvehicleselection fueltypeid="2" fueltypedesc="Diesel Fuel"
sourcetypeid="43" sourcetypename="School Bus"/>
        <onroadvehicleselection fueltypeid="2" fueltypedesc="Diesel Fuel"
sourcetypeid="53" sourcetypename="Single Unit Long-haul Truck"/>
        <onroadvehicleselection fueltypeid="2" fueltypedesc="Diesel Fuel"
sourcetypeid="52" sourcetypename="Single Unit Short-haul Truck"/>
        <onroadvehicleselection fueltypeid="2" fueltypedesc="Diesel Fuel"
sourcetypeid="42" sourcetypename="Transit Bus"/>
        <onroadvehicleselection fueltypeid="9" fueltypedesc="Electricity"
sourcetypeid="32" sourcetypename="Light Commercial Truck"/>
        <onroadvehicleselection fueltypeid="9" fueltypedesc="Electricity"
sourcetypeid="54" sourcetypename="Motor Home"/>
        <onroadvehicleselection fueltypeid="9" fueltypedesc="Electricity"
sourcetypeid="21" sourcetypename="Passenger Car"/>
        <onroadvehicleselection fueltypeid="9" fueltypedesc="Electricity"
sourcetypeid="31" sourcetypename="Passenger Truck"/>
        <onroadvehicleselection fueltypeid="9" fueltypedesc="Electricity"
sourcetypeid="51" sourcetypename="Refuse Truck"/>
        <onroadvehicleselection fueltypeid="9" fueltypedesc="Electricity"
sourcetypeid="43" sourcetypename="School Bus"/>
```

```
        <onroadvehicleselection fueltypeid="9" fueltypedesc="Electricity"
sourcetypeid="52" sourcetypename="Single Unit Short-haul Truck"/>

        <onroadvehicleselection fueltypeid="9" fueltypedesc="Electricity"
sourcetypeid="42" sourcetypename="Transit Bus"/>

        <onroadvehicleselection fueltypeid="1" fueltypedesc="Gasoline"
sourcetypeid="61" sourcetypename="Combination Short-haul Truck"/>

        <onroadvehicleselection fueltypeid="1" fueltypedesc="Gasoline"
sourcetypeid="32" sourcetypename="Light Commercial Truck"/>

        <onroadvehicleselection fueltypeid="1" fueltypedesc="Gasoline"
sourcetypeid="54" sourcetypename="Motor Home"/>

        <onroadvehicleselection fueltypeid="1" fueltypedesc="Gasoline"
sourcetypeid="11" sourcetypename="Motorcycle"/>

        <onroadvehicleselection fueltypeid="1" fueltypedesc="Gasoline"
sourcetypeid="21" sourcetypename="Passenger Car"/>

        <onroadvehicleselection fueltypeid="1" fueltypedesc="Gasoline"
sourcetypeid="31" sourcetypename="Passenger Truck"/>

        <onroadvehicleselection fueltypeid="1" fueltypedesc="Gasoline"
sourcetypeid="51" sourcetypename="Refuse Truck"/>

        <onroadvehicleselection fueltypeid="1" fueltypedesc="Gasoline"
sourcetypeid="43" sourcetypename="School Bus"/>

        <onroadvehicleselection fueltypeid="1" fueltypedesc="Gasoline"
sourcetypeid="53" sourcetypename="Single Unit Long-haul Truck"/>

        <onroadvehicleselection fueltypeid="1" fueltypedesc="Gasoline"
sourcetypeid="52" sourcetypename="Single Unit Short-haul Truck"/>

        <onroadvehicleselection fueltypeid="1" fueltypedesc="Gasoline"
sourcetypeid="42" sourcetypename="Transit Bus"/>

    </onroadvehicleselections>

    <offroadvehicleselections>

    </offroadvehicleselections>

    <offroadvehiclesccs>

    </offroadvehiclesccs>

    <roadtypes>

        <roadtype roadtypeid="1" roadtypename="Off-Network"/>

        <roadtype roadtypeid="5" roadtypename="Urban Unrestricted Access"/>

    </roadtypes>

    <pollutantprocessassociations>

        <pollutantprocessassociation pollutantkey="110" pollutantname="Primary Exhaust
PM2.5 - Total" processkey="1" processname="Running Exhaust"/>

        <pollutantprocessassociation pollutantkey="110" pollutantname="Primary Exhaust
PM2.5 - Total" processkey="2" processname="Start Exhaust"/>

        <pollutantprocessassociation pollutantkey="110" pollutantname="Primary Exhaust
PM2.5 - Total" processkey="15" processname="Crankcase Running Exhaust"/>

        <pollutantprocessassociation pollutantkey="110" pollutantname="Primary Exhaust
PM2.5 - Total" processkey="16" processname="Crankcase Start Exhaust"/>

        <pollutantprocessassociation pollutantkey="110" pollutantname="Primary Exhaust
PM2.5 - Total" processkey="17" processname="Crankcase Extended Idle Exhaust"/>

        <pollutantprocessassociation pollutantkey="110" pollutantname="Primary Exhaust
```

```
PM2.5 - Total" processkey="90" processname="Extended Idle Exhaust"/>
        <pollutantprocessassociation pollutantkey="116" pollutantname="Primary PM2.5 -
Brakewear Particulate" processkey="9" processname="Brakewear"/>
        <pollutantprocessassociation pollutantkey="112" pollutantname="Primary PM2.5 -
Elemental Carbon" processkey="1" processname="Running Exhaust"/>
        <pollutantprocessassociation pollutantkey="112" pollutantname="Primary PM2.5 -
Elemental Carbon" processkey="2" processname="Start Exhaust"/>
        <pollutantprocessassociation pollutantkey="112" pollutantname="Primary PM2.5 -
Elemental Carbon" processkey="15" processname="Crankcase Running Exhaust"/>
        <pollutantprocessassociation pollutantkey="112" pollutantname="Primary PM2.5 -
Elemental Carbon" processkey="16" processname="Crankcase Start Exhaust"/>
        <pollutantprocessassociation pollutantkey="112" pollutantname="Primary PM2.5 -
Elemental Carbon" processkey="17" processname="Crankcase Extended Idle Exhaust"/>
        <pollutantprocessassociation pollutantkey="112" pollutantname="Primary PM2.5 -
Elemental Carbon" processkey="90" processname="Extended Idle Exhaust"/>
        <pollutantprocessassociation pollutantkey="111" pollutantname="Primary PM2.5 -
Organic Carbon" processkey="1" processname="Running Exhaust"/>
        <pollutantprocessassociation pollutantkey="111" pollutantname="Primary PM2.5 -
Organic Carbon" processkey="2" processname="Start Exhaust"/>
        <pollutantprocessassociation pollutantkey="111" pollutantname="Primary PM2.5 -
Organic Carbon" processkey="15" processname="Crankcase Running Exhaust"/>
        <pollutantprocessassociation pollutantkey="111" pollutantname="Primary PM2.5 -
Organic Carbon" processkey="16" processname="Crankcase Start Exhaust"/>
        <pollutantprocessassociation pollutantkey="111" pollutantname="Primary PM2.5 -
Organic Carbon" processkey="17" processname="Crankcase Extended Idle Exhaust"/>
        <pollutantprocessassociation pollutantkey="111" pollutantname="Primary PM2.5 -
Organic Carbon" processkey="90" processname="Extended Idle Exhaust"/>
        <pollutantprocessassociation pollutantkey="115" pollutantname="Primary PM2.5 -
Sulfate Particulate" processkey="1" processname="Running Exhaust"/>
        <pollutantprocessassociation pollutantkey="115" pollutantname="Primary PM2.5 -
Sulfate Particulate" processkey="2" processname="Start Exhaust"/>
        <pollutantprocessassociation pollutantkey="115" pollutantname="Primary PM2.5 -
Sulfate Particulate" processkey="15" processname="Crankcase Running Exhaust"/>
        <pollutantprocessassociation pollutantkey="115" pollutantname="Primary PM2.5 -
Sulfate Particulate" processkey="16" processname="Crankcase Start Exhaust"/>
        <pollutantprocessassociation pollutantkey="115" pollutantname="Primary PM2.5 -
Sulfate Particulate" processkey="17" processname="Crankcase Extended Idle Exhaust"/>
        <pollutantprocessassociation pollutantkey="115" pollutantname="Primary PM2.5 -
Sulfate Particulate" processkey="90" processname="Extended Idle Exhaust"/>
        <pollutantprocessassociation pollutantkey="117" pollutantname="Primary PM2.5 -
Tirewear Particulate" processkey="10" processname="Tirewear"/>
        <pollutantprocessassociation pollutantkey="91" pollutantname="Total Energy
Consumption" processkey="1" processname="Running Exhaust"/>
        <pollutantprocessassociation pollutantkey="91" pollutantname="Total Energy
Consumption" processkey="2" processname="Start Exhaust"/>
        <pollutantprocessassociation pollutantkey="91" pollutantname="Total Energy
Consumption" processkey="90" processname="Extended Idle Exhaust"/>
    </pollutantprocessassociations>
```

```
    <databaseselections>
    </databaseselections>
    <internalcontrolstrategies>
<internalcontrolstrategy
classname="gov.epa.otaq.moves.master.implementation.ghg.internalcontrolstrategies.rate
ofprogress.RateOfProgressStrategy"><![CDATA[
useParameters   No


]]></internalcontrolstrategy>
    </internalcontrolstrategies>
    <inputdatabase servername="" databasename="" description=""/>
    <uncertaintyparameters uncertaintymodeenabled="false"
numberofrunspersimulation="0" numberofsimulations="0"/>
    <geographicoutputdetail description="LINK"/>
    <outputemissionsbreakdownselection>
        <modelyear selected="true"/>
        <fueltype selected="true"/>
        <emissionprocess selected="true"/>
        <onroadoffroad selected="true"/>
        <roadtype selected="true"/>
        <sourceusetype selected="true"/>
        <movesvehicletype selected="false"/>
        <onroadscc selected="false"/>
        <offroadscc selected="false"/>
        <estimateuncertainty selected="false" numberOfIterations="2"
keepSampledData="false" keepIterations="false"/>
        <sector selected="false"/>
        <engtechid selected="false"/>
        <hpclass selected="false"/>
    </outputemissionsbreakdownselection>
    <outputdatabase servername="" databasename="Cruise35_Y09T70RH90_out"
description=""/>
    <outputtimestep value="Hour"/>
    <outputvmtdata value="true"/>
    <outputsho value="false"/>
    <outputsh value="false"/>
    <outputshp value="false"/>
    <outputshidling value="false"/>
    <outputstarts value="false"/>
    <outputpopulation value="true"/>
    <scaleinputdatabase servername="localhost" databasename="Cruise35_Y09T70RH90_in"
description=""/>
```

```
    <pmsize value="0"/>
    <outputfactors>
        <timefactors selected="true" units="Hours"/>
        <distancefactors selected="true" units="Miles"/>
        <massfactors selected="true" units="Grams" energyunits="Joules"/>
    </outputfactors>
    <savedata>

        <class
name="gov.epa.otaq.moves.master.implementation.ghg.MesoscaleLookupOperatingModeDistrib
utionGenerator"/>
    </savedata>

    <donotexecute>

    </donotexecute>

    <generatordatabase shouldsave="true" servername=""
databasename="Cruise35_Y09T70RH90_in" description=""/>
        <donotperformfinalaggregation selected="false"/>
    <lookuptableflags scenarioid="Cruise35_Y09T70RH90" truncateoutput="false"
truncateactivity="false"/>
</runspec>
```

Example of batch processing command for MOVES

```
setenv.bat
java -Xmx300m gov.epa.otaq.moves.master.commandline.MOVESCommandLine -rl
"C:\link.batch.txt"
```

These codes are entered at MOVES folder in Command Prompt. The “link.batch.txt” contains a list of full addresses of the RunSpec files to be processed.

Once all MOVES runs were completed, the model outputs were manually exported from MySQL database as tables containing base emission rates per distance by vehicle types, vehicle ages, vehicle fuel types, pollutants and processes, and other related information for each traffic condition. Then, a total emission rate for each traffic condition were computed as a sum of the base emission-rates per distance for exhaust (pollutant ID 110), brake wear (pollutant ID 116), and tire wear (pollutant ID 117) weighted by matched source type hour fraction, age fraction,

and fuel type and engine technology fraction. Examples of MATLAB code for calculating composite emission rates from an exported table of MOVES outputs are shown below:

Example of MATLAB code for calculating 2009 total emission rates from an exported table of MOVES outputs based on cruise traffic activity, 35 mph average traffic speed, and unit road grade -10% to 10% under 70 °F

```
linkID=[1 2 3 4 5 6 7 8 9 10 11 12 13 14 15 16 17 18 19 20 21];
linkrate=ones(size(linkID,2),1);

xlsin='Cruise_35mph_Y09_T70_raw.csv';
[num,txt,raw]=xlsread(xlsin,1);
[m,n]=size(raw);
tmpX=raw(2:m,:);
pollutant1=tmpX([tmpX{:,3}]==110,:);
pollutant2=tmpX([tmpX{:,3}]==116,:);
pollutant3=tmpX([tmpX{:,3}]==117,:);
X=[pollutant1;pollutant2;pollutant3];
X(:,13)=num2cell(cell2mat(X(:,9)).*cell2mat(X(:,10)).*cell2mat(X(:,11)).*cell2mat(X(:,
12)));
idx=isnan(cell2mat(X(:,13)));
X(idx,13)=num2cell(0);

for lnk=1:size(linkID,2)
    linkrate(lnk,1)=sum(cell2mat(X([X{:,2}]==lnk,22)));
    lnk;
end

csvout='Cruise_35mph_Y09_T70_total.csv';
csvwrite(csvout,linkrate);
```

Example of MATLAB code for calculating 2009 total emission rates by vehicle fuel types from the exported table of MOVES outputs based on cruise traffic activity, 35 mph average traffic speed, and unit road grade -10% to 10% under 70 °F

```
fuelTypeID=[1 2 3];
linkrate=ones(21,3);

xlsin='Cruise_35mph_Y09_T70_raw.csv';
[num,txt,raw]=xlsread(xlsin,1);
```

```
[m,n]=size(raw);
tmpX=raw(2:m,:);
pollutant1=tmpX([tmpX{:,8}]==110,:);
pollutant2=tmpX([tmpX{:,8}]==116,:);
pollutant3=tmpX([tmpX{:,8}]==117,:);
tmpX=[pollutant1;pollutant2;pollutant3];

for i=1:size(fuelTypeID,2)
    X=tmpX([tmpX{:,12}]==fuelTypeID(i),:);

    for lnk=1:21
        linkrate(lnk,i)=sum(cell2mat(X([X{:,7}]==lnk,22)));
        lnk;
    end

    i;
end

csvout='Cruise_35mph_Y09_T70_byfuelType.csv';
csvwrite(csvout,linkrate);
```

Example of MATLAB code for calculating 2009 total emission rates by vehicle age groups from the exported table of MOVES outputs based on cruise traffic activity, 35 mph average traffic speed, and unit road grade -10% to 10% under 70 °F

```
modelYearID=[1979 1980 1981 1982 1983 1984 1985 1986 1987 1988 1989 1990 1991 1992
1993 1994 1995 1996 1997 1998 1999 2000 2001 2002 2003 2004 2005 2006 2007 2008 2009];
tmplinkrate=ones(21,30);
linkrate=ones(21,7);

xlsin='Cruise_35mph_Y09_T70_raw.csv';
[num,txt,raw]=xlsread(xlsin,1);
[m,n]=size(raw);
tmpX=raw(2:m,:);
pollutant1=tmpX([tmpX{:,8}]==110,:);
pollutant2=tmpX([tmpX{:,8}]==116,:);
pollutant3=tmpX([tmpX{:,8}]==117,:);
tmpX=[pollutant1;pollutant2;pollutant3];

for i=1:size(modelYearID,2)
```

```
    X=tmpX([tmpX{:,13}]==modelYearID(i),:);

    for lnk=1:21
        tmplinkrate(lnk,i)=sum(cell2mat(X([X{:,7}]==lnk,22)));
        lnk;
    end

    i;
end

linkrate(:,1)=tmplinkrate(:,1)+tmplinkrate(:,2)+tmplinkrate(:,3)+tmplinkrate(:,4)+tmpl
inkrate(:,5)+tmplinkrate(:,6)+tmplinkrate(:,7)+tmplinkrate(:,8)+tmplinkrate(:,9)+tmpli
nkrate(:,10)+tmplinkrate(:,11);
linkrate(:,2)=tmplinkrate(:,12)+tmplinkrate(:,13)+tmplinkrate(:,14)+tmplinkrate(:,15)+
tmplinkrate(:,16);
linkrate(:,3)=tmplinkrate(:,17)+tmplinkrate(:,18)+tmplinkrate(:,19)+tmplinkrate(:,20)+
tmplinkrate(:,21);
linkrate(:,4)=tmplinkrate(:,22)+tmplinkrate(:,23);
linkrate(:,5)=tmplinkrate(:,24)+tmplinkrate(:,25);
linkrate(:,6)=tmplinkrate(:,26)+tmplinkrate(:,27);
linkrate(:,7)=tmplinkrate(:,28)+tmplinkrate(:,29)+tmplinkrate(:,30)+tmplinkrate(:,31);

csvout='Cruise_35mph_Y09_T70_byageGroup.csv';
csvwrite(csvout,linkrate);
```

Example of MATLAB code for calculating total emission rates by vehicle types from the exported table of MOVES outputs based on cruise traffic activity, 35 mph average traffic speed, and unit road grade -10% to 10% under 70 °F

```
sourceID=[11 21 31 32 41 42 43 51 52 53 54 61 62];
linkrate=ones(21,13);

xlsin='Cruise_35mph_Y09_T70_raw.csv';
[num,txt,raw]=xlsread(xlsin,2);
[m,n]=size(raw);
tmpX=raw(2:m,:);
pollutant1=tmpX([tmpX{:,8}]==110,:);
pollutant2=tmpX([tmpX{:,8}]==116,:);
pollutant3=tmpX([tmpX{:,8}]==117,:);
tmpX=[pollutant1;pollutant2;pollutant3];

for i=1:size(sourceID,2)
```

```
    X=tmpX([tmpX{:,10}]==sourceID(i),:);

    for lnk=1:21
        linkrate(lnk,i)=sum(cell2mat(X([X{:,7}]==lnk,22)));
        lnk;
    end

    i;
end

csvout='Cruise_35mph_Y09_T70_bysourceID.csv';
csvwrite(csvout,linkrate);
```

Example of an exported table of MOVES outputs used in MATLAB code (as Cruise_35mph_Y09_T70_raw.csv)

yearID	linkID	pollutantID	processID	sourceTypeID	fuelTypeID	modelYearID	temperature	ratePerDistance	sourceTypeHourFraction	fuelEngFraction	ageFraction
2009	1	91	1	11	1	1979	70		0.0188	1	0
2009	1	91	1	21	1	1979	70	3535650	0.4885	0.968833708	0.000766183
2009	1	91	1	31	1	1979	70	4469720	0.3438	0.986080001	0.00203896
2009	1	91	1	32	1	1979	70	4422140	0.1149	0.958150008	0.00203896
2009	1	91	1	43	1	1979	70	4709860	0.0025	0.95401	0.00462916
2009	1	91	1	51	1	1979	70	3899680	0.0003	0.040000001	0.00214817
2009	1	91	1	52	1	1979	70	3943700	0.017	0.734499997	0.00936422
2009	1	91	1	53	1	1979	70	3953910	0.002	0.734499997	0.00059688
2009	1	91	1	54	1	1979	70	3989790	0.0039	0.850000001	0.00697201
2009	1	91	1	61	1	1979	70	3984080	0.0037	0.085362008	0.00488189
2009	1	91	1	11	1	1980	70		0.0188	1	0
2009	1	91	1	21	1	1980	70	3098940	0.4885	0.953329287	0.000722473
2009	1	91	1	31	1	1980	70	4542210	0.3438	0.987630001	0.00185744
2009	1	91	1	32	1	1980	70	4534000	0.1149	0.89311994	0.00185744
2009	1	91	1	43	1	1980	70	4707830	0.0025	0.94061	0.00395579

APPENDIX B
SUPPLEMENTAL MATERIALS FOR CAL3QHCR MODELING OF TRAFFIC-RELATED PM2.5 CONCENTRATIONS AT 160 CENCUS BLOCK CENTROIDS ANALYZED

CAL3QHCR dated 04244 was used to estimate seasonal average of population exposure concentrations as 24-hour traffic-related PM2.5 concentrations ($\mu g/m^3$) at each centroid of census blocks located within 500 meter from the study corridor in 2009 and 2025 with/without the Carolina North Development scenarios. The modeling included 1,200 of links and 160 census block centroids (i.e., receptors). Due to limitations in the maximum numbers of links and census block centroids allowed in one model run (i.e., 120 links and 60 receptors), the modeled links and census block centroids were divided into 10 and 3 sets respectively. CAL3QHCR was run for all combinations of these link and receptor sets using hourly meteorological profile of 2,100 days (including 525 days for winter, 560 days for spring, 532 days for summer, and 483 days for fall) that obtained from the EPA's Meteorological Processor for Regulatory Models using 2006–2012 surface and upper air data at the national weather stations in Chapel Hill and Greensboro respectively. Hourly emission rates for each link were determined by interpolating two MOVES emission rates nearest to hourly temperatures in each day. Surface roughness was fixed at 175 cm reflecting city land use – office. Settling and deposition velocity were assumed to be 0 m/s over the analysis period. The modeling assumed that the major pollution and health impacts will be from traffic emissions during 6 a.m. to 7 p.m., so the link-specific emission rates and traffic volumes during these hours were set to zero. A total number of CAL3QHCR runs in each development scenarios was $10 \times 3 \times 2{,}100 = 63{,}000$. The examples of MATLAB codes and associated data for generating input files (.INP), control files (.CTL), and the batch processing command files (.BAT) for CAL3QHCR are shown below:

Example of MATLAB code for generating the input files (.INP) for CAL3QHCR to model 24-hour traffic-related PM2.5 concentrations in 2009 scenario

```
for metset=2006:2012
    xlsmet=['MPRM',num2str(metset),'_24hr.xlsx'];
    [nummet,txtmet,rawmet]=xlsread(xlsmet,1);
    [mmet,nmet]=size(rawmet);

    for lnkset=1:10
        xlslnkam=['Link_2009_am_set',num2str(lnkset),'.xlsx'];
        xlslnkmd=['Link_2009_md_set',num2str(lnkset),'.xlsx'];
        xlslnkpm=['Link_2009_pm_set',num2str(lnkset),'.xlsx'];
        [numlnkam,txtlnkam,rawlnkam]=xlsread(xlslnkam,1);
        [mlnkam,nlnkam]=size(rawlnkam);
        [numlnkmd,txtlnkmd,rawlnkmd]=xlsread(xlslnkmd,1);
        [mlnkmd,nlnkmd]=size(rawlnkmd);
        [numlnkpm,txtlnkpm,rawlnkpm]=xlsread(xlslnkpm,1);
        [mlnkpm,nlnkpm]=size(rawlnkpm);

        for rcpset=1:3
            xlsrcp=['CensusBlockCentroids_set',num2str(rcpset),'.xlsx'];
            [numrcp,txtrcp,rawrcp]=xlsread(xlsrcp,1);
            [mrcp,nrcp]=size(rawrcp);
            rmet=2;

            for d=1:(mmet-1)/24
                fname=[num2str(rawmet{rmet,1}),'_2009_',num2str(lnkset),'_',num2str(rc
                pset)];
                fid=fopen([fname,'.INP'],'wt');
                JOB=['''',fname,''''];
                ATIM=60;
                Z0=175;
                VS=0;
                VD=0;
                NR=mrcp-1;
                SCAL=0.3048;
                IOPT=1;
                fprintf(fid,'%s,%d,%d,%1.4f,%1.4f,%d,%1.4f,%d\n',JOB,ATIM,Z0,VS,VD,NR,
                SCAL,IOPT);
```

```
STARTMO=rawmet{rmet,3};
STARTDY=rawmet{rmet,4};
STARTYR=rawmet{rmet,2};
ENDMO=rawmet{rmet,3};
ENDDY=rawmet{rmet,4};
ENDYR=rawmet{rmet,2};
fprintf(fid,'%d,%d,%d,%d,%d,%d\n',STARTMO,STARTDY,STARTYR,ENDMO,ENDDY,
ENDYR);

METSF=93785;
METSYR=rawmet{rmet,2};
METUA=13723;
METUYR=rawmet{rmet,2};
fprintf(fid,'%d,%d,%d,%d\n',METSF,METSYR,METUA,METUYR);

FLINK=1;
FAMB=0;
RU='''U''';
fprintf(fid,'%d,%d,%s\n',FLINK,FAMB,RU);

for rrcp=2:mrcp
    RCP=['''',rawrcp{rrcp,2},''''];
    XR=rawrcp{rrcp,3};
    YR=rawrcp{rrcp,4};
    ZR=rawrcp{rrcp,5};
    fprintf(fid,'%s,%5.1f,%5.1f,%1.1f\n',RCP,XR,YR,ZR);
    rrcp;
end

JTIER=2;
MODE='''P''';
fprintf(fid,'%d,%s\n',JTIER,MODE);

IPATRY1=1;
IPATRY2=1;
IPATRY3=1;
IPATRY4=1;
IPATRY5=1;
IPATRY6=1;
IPATRY7=1;
```

```
fprintf(fid,'%d,%d,%d,%d,%d,%d,%d\n',IPATRY1,IPATRY2,IPATRY3,IPATRY4,I
PATRY5,IPATRY6,IPATRY7);


RUN=['''',fname,''''];
NUMLNK=mlnkam-1;
fprintf(fid,'%s,%d\n',RUN,NUMLNK);


for rlnk=2:mlnkam
    COD=rlnk-1;
    IQ=1;
    fprintf(fid,'%d,%d\n',COD,IQ);


    LNK=['''',rawlnkam{rlnk,2},''''];
    TYP='''AG''';
    X1=rawlnkam{rlnk,3};
    Y1=rawlnkam{rlnk,4};
    X2=rawlnkam{rlnk,5};
    Y2=rawlnkam{rlnk,6};
    SH=rawlnkam{rlnk,7};
    WL=rawlnkam{rlnk,8};
    fprintf(fid,'%s,%s,%5.1f,%5.1f,%5.1f,%5.1f,%d,%d\n',LNK,TYP,X1,Y1,
    X2,Y2,SH,WL);


    rlnk;
end


for hr=1:6
    HE=hr;
    AMB=0;
    fprintf(fid,'%d,%d\n',HE,AMB);


    for rlnk=2:mlnkam,
        COD=rlnk-1;
        VPHL=0;
        EFL=0;
        fprintf(fid,'%d,%d,%1.4f\n',COD,VPHL,EFL);
        rlnk;
    end


    hr;
```

```
end

for hr=7:9
    HE=hr;
    AMB=0;
    fprintf(fid,'%d,%d\n',HE,AMB);

    for rlnk=2:mlnkam,
        COD=rlnk-1;
        VPHL=rawlnkam{rlnk,9};
        fahrenheit=(rawmet{hr+rmet-1,8}-273.15)*1.8000+32.00;
        if fahrenheit<=10
            EFL=rawlnkam{rlnk,10};
        elseif and(fahrenheit>10,fahrenheit<=30)
            EFL=rawlnkam{rlnk,10}+((fahrenheit-10)*(rawlnkam{rlnk,11}-
            rawlnkam{rlnk,10})/20);
        elseif and(fahrenheit>30,fahrenheit<=50)
            EFL=rawlnkam{rlnk,11}+((fahrenheit-30)*(rawlnkam{rlnk,12}-
            rawlnkam{rlnk,11})/20);
        elseif and(fahrenheit>50,fahrenheit<=70)
            EFL=rawlnkam{rlnk,12}+((fahrenheit-50)*(rawlnkam{rlnk,13}-
            rawlnkam{rlnk,12})/20);
        elseif and(fahrenheit>70,fahrenheit<=90)
            EFL=rawlnkam{rlnk,13}+((fahrenheit-70)*(rawlnkam{rlnk,14}-
            rawlnkam{rlnk,13})/20);
        elseif and(fahrenheit>90,fahrenheit<=110)
            EFL=rawlnkam{rlnk,14}+((fahrenheit-90)*(rawlnkam{rlnk,15}-
            rawlnkam{rlnk,14})/20);
        else fahrenheit>110
            EFL=rawlnkam{rlnk,15};
        end
        fprintf(fid,'%d,%d,%1.4f\n',COD,VPHL,EFL);
        rlnk;
    end

    hr;
end

for hr=10:16
    HE=hr;
    AMB=0;
```

```
    fprintf(fid,'%d,%d\n',HE,AMB);

    for rlnk=2:mlnkmd,
        COD=rlnk-1;
        VPHL=rawlnkmd{rlnk,9};
        fahrenheit=(rawmet{hr+rmet-1,8}-273.15)*1.8000+32.00;
        if fahrenheit<=10
            EFL=rawlnkmd{rlnk,10};
        elseif and(fahrenheit>10,fahrenheit<=30)
            EFL=rawlnkmd{rlnk,10}+((fahrenheit-10)*(rawlnkmd{rlnk,11}-
            rawlnkmd{rlnk,10})/20);
        elseif and(fahrenheit>30,fahrenheit<=50)
            EFL=rawlnkmd{rlnk,11}+((fahrenheit-30)*(rawlnkmd{rlnk,12}-
            rawlnkmd{rlnk,11})/20);
        elseif and(fahrenheit>50,fahrenheit<=70)
            EFL=rawlnkmd{rlnk,12}+((fahrenheit-50)*(rawlnkmd{rlnk,13}-
            rawlnkmd{rlnk,12})/20);
        elseif and(fahrenheit>70,fahrenheit<=90)
            EFL=rawlnkmd{rlnk,13}+((fahrenheit-70)*(rawlnkmd{rlnk,14}-
            rawlnkmd{rlnk,13})/20);
        elseif and(fahrenheit>90,fahrenheit<=110)
            EFL=rawlnkmd{rlnk,14}+((fahrenheit-90)*(rawlnkmd{rlnk,15}-
            rawlnkmd{rlnk,14})/20);
        else fahrenheit>110
            EFL=rawlnkmd{rlnk,15};
        end
        fprintf(fid,'%d,%d,%1.4f\n',COD,VPHL,EFL);
        rlnk;
    end

    hr;
end

for hr=17:19
    HE=hr;
    AMB=0;
    fprintf(fid,'%d,%d\n',HE,AMB);

    for rlnk=2:mlnkpm,
        COD=rlnk-1;
        VPHL=rawlnkpm{rlnk,9};
```

```
        fahrenheit=(rawmet{hr+rmet-1,8}-273.15)*1.8000+32.00;
        if fahrenheit<=10
            EFL=rawlnkpm{rlnk,10};
        elseif and(fahrenheit>10,fahrenheit<=30)
            EFL=rawlnkpm{rlnk,10}+((fahrenheit-10)*(rawlnkpm{rlnk,11}-
            rawlnkpm{rlnk,10})/20);
        elseif and(fahrenheit>30,fahrenheit<=50)
            EFL=rawlnkpm{rlnk,11}+((fahrenheit-30)*(rawlnkpm{rlnk,12}-
            rawlnkpm{rlnk,11})/20);
        elseif and(fahrenheit>50,fahrenheit<=70)
            EFL=rawlnkpm{rlnk,12}+((fahrenheit-50)*(rawlnkpm{rlnk,13}-
            rawlnkpm{rlnk,12})/20);
        elseif and(fahrenheit>70,fahrenheit<=90)
            EFL=rawlnkpm{rlnk,13}+((fahrenheit-70)*(rawlnkpm{rlnk,14}-
            rawlnkpm{rlnk,13})/20);
        elseif and(fahrenheit>90,fahrenheit<=110)
            EFL=rawlnkpm{rlnk,14}+((fahrenheit-90)*(rawlnkpm{rlnk,15}-
            rawlnkpm{rlnk,14})/20);
        else fahrenheit>110
            EFL=rawlnkpm{rlnk,15};
        end
        fprintf(fid,'%d,%d,%1.4f\n',COD,VPHL,EFL);
        rlnk;
    end
    hr;
end

for hr=20:24
    HE=hr;
    AMB=0;
    fprintf(fid,'%d,%d\n',HE,AMB);

    for rlnk=2:mlnkam,
        COD=rlnk-1;
        VPHL=0;
        EFL=0;
        fprintf(fid,'%d,%d,%1.4f\n',COD,VPHL,EFL);
        rlnk;
    end

    hr;
```

```
                end

                fclose(fid);
                rmet=rmet+24;
                d;
            end

            rcpset;
        end

        lnkset;
    end

    metset;
end
```

Example of MATLAB code for generating the control files (.CTL) for CAL3QHCR to model 24-hour traffic-related PM2.5 concentrations in 2009 scenario

```
for metset=2006:2012
    xlsmet=['MPRM',num2str(metset),'_24hr.xlsx'];
    [nummet,txtmet,rawmet]=xlsread(xlsmet,1);
    [mmet,nmet]=size(rawmet);

    for lnkset=1:10

        for rcpset=1:3
            rmet=2;

            for d=1:(mmet-1)/24
                fname=[num2str(rawmet{rmet,1}),'_2009_',num2str(lnkset),'_',num2str(rc
                pset)];
                CTL=[fname,'.CTL'];
                MSG=['temp','.MSG'];
                INP=[fname,'.INP'];
                MET=[num2str(rawmet{rmet,1}),'.MET'];
                ET1=['temp','.ET1'];
                ET2=['temp','.ET2'];
                OUT=[fname,'.OUT'];
                ILK=['temp','.ILK'];
```

```
                fid=fopen(CTL,'wt');
                fprintf(fid,'%s\n%s\n%s\n%s\n%s\n%s\n%s\n',MSG,INP,MET,ET1,ET2,OUT,ILK
                );
                fclose(fid);
                rmet=rmet+24;
                d;
            end

            rcpset;
        end

        lnkset;
    end

    metset;
end
```

Example of MATLAB code for generating the batch processing command files (.BAT) for CAL3QHCR to model 24-hour traffic-related PM2.5 concentrations in 2009 scenario

```
for metset=2006:2012
    fBAT=[num2str(metset),'_2009.BAT'];
    disp(fBAT);
    fid=fopen(fBAT,'wt');
    xlsmet=['MPRM',num2str(metset),'_24hr.xlsx'];
    [nummet,txtmet,rawmet]=xlsread(xlsmet,1);
    [mmet,nmet]=size(rawmet);

    for lnkset=1:10

        for rcpset=1:3
            rmet=2;

            for d=1:(mmet-1)/24
                fCTL=[num2str(rawmet{rmet,1}),'_2009_',num2str(lnkset),'_',num2str(rcp
                set),'.CTL'];
                fprintf(fid,'%s %s %s\n','copy',fCTL,'cal3r.ctl');
                fprintf(fid,'%s\n','CAL3QHCR');
                rmet=rmet+24;
                d;
            end
```

```
            rcpset;

        end
        lnkset;

    end
    fclose(fid);

    metset;
end
```

Example of meteorological data used in MATLAB code (as MPRM2006_24hr.xlsx)

Date	Year	Month	Day	Hour	Wind Dir	Wind Spd	Temp	Stability	Urban Mixh	Rural Mixh
20060101	6	1	1	1	131	2.5722	281.5	6	649	34
20060101	6	1	1	2	108	2.0578	280.9	6	679.6	34
20060101	6	1	1	3	104	1.5433	277.6	7	710.2	34
20060101	6	1	1	4	103	0	275.9	7	740.8	34
20060101	6	1	1	5	133	2.0578	276.5	6	771.5	34
20060101	6	1	1	6	142	2.5722	277	6	802.1	34
20060101	6	1	1	7	35	1.5433	274.3	7	832.7	34
20060101	6	1	1	8	33	0	274.8	6	76.6	108.1
20060101	6	1	1	9	47	1.5433	278.2	5	238.4	264.6
20060101	6	1	1	10	51	0	282	4	400.1	421.1
20060101	6	1	1	11	54	0	285.4	3	561.8	577.6
20060101	6	1	1	12	46	0	286.5	2	723.5	734
20060101	6	1	1	13	53	0	288.2	2	885.3	890.5
20060101	6	1	1	14	49	0	287.6	2	1047	1047
20060101	6	1	1	15	92	1.5433	287.6	2	1047	1047

Example of link data used in MATLAB code (as Link_2009_am_set1.xlsx)

No	LinkDscrpt	X_Start	Y_Start	X_End	Y_End	SourceHeight	LinkWidth	TrafficVol	EFL_10F	EFL_30F	EFL_50F	EFL_70F	EFL_90F	EFL_110F
1	Intrsctn01_NBA	174.0849	14546.81624	143.74595	14654.47219	0	32	461	0.083687	0.059958	0.047396	0.040747	0.040308	0.040308
2	Intrsctn01_NBA	143.74595	14654.47219	113.3444	14760.65366	0	32	461	0.083687	0.059958	0.047396	0.040747	0.040308	0.040308
3	Intrsctn01_NBD	-64.71086	15476.77876	-79.40944	15534.16873	0	32	233	0.083687	0.059958	0.047396	0.040747	0.040308	0.040308
4	Intrsctn01_NBD	-0.55209	15224.77967	-11.57779	15268.39958	0	32	233	0.083687	0.059958	0.047396	0.040747	0.040308	0.040308
5	Intrsctn01_NBD	-11.57779	15268.39958	-64.71086	15476.77876	0	32	233	0.074263	0.05434	0.043792	0.03821	0.037842	0.037842
6	Intrsctn01_NBR	40.77023	15104.80657	32.71372	15137.83826	0	32	251	0.056939	0.040398	0.031641	0.027007	0.026699	0.026699
7	Intrsctn01_NBR	48.80071	15071.76854	40.77023	15104.80657	0	32	251	0.055874	0.03968	0.031107	0.026569	0.026268	0.026268
8	Intrsctn01_NBR	92.61173	14891.5265	48.80071	15071.76854	0	32	251	0.055874	0.03968	0.031107	0.026569	0.026268	0.026268
9	Intrsctn01_NBR	113.3444	14760.65366	92.61173	14891.5265	0	32	251	0.055874	0.03968	0.031107	0.026569	0.026268	0.026268
10	Intrsctn01_NBT	113.3444	14760.65366	102.2489	14805.48242	0	32	210	0.055874	0.03968	0.031107	0.026569	0.026268	0.026268
11	Intrsctn01_NBT	20.56095	15135.52345	-0.55209	15224.77967	0	32	210	0.083687	0.059958	0.047396	0.040747	0.040308	0.040308
12	Intrsctn01_NBT	28.72974	15102.51935	20.56095	15135.52345	0	32	210	0.05907	0.041835	0.032711	0.027882	0.027562	0.027562
13	Intrsctn01_NBT	36.89854	15069.51524	28.72974	15102.51935	0	32	210	0.05907	0.041835	0.032711	0.027882	0.027562	0.027562
14	Intrsctn01_NBT	45.06733	15036.51114	36.89854	15069.51524	0	32	210	0.055874	0.03968	0.031107	0.026569	0.026268	0.026268
15	Intrsctn01_NBT	53.23613	15003.50704	45.06733	15036.51114	0	32	210	0.055874	0.03968	0.031107	0.026569	0.026268	0.026268

Example of receptor data used in MATLAB code (CensusBlockCentroids_set1.xlsx)

No	Receptor	X	Y	Z
1	block114001002	3776.2	-2551.7	4.9
2	block122011010	3089.6	-14795.5	4.9
3	block118001000	-823.3	2675.3	4.9
4	block122011029	2158.4	-14432.6	4.9
5	block119011037	3136.0	6184.2	4.9
6	block118001006	1081.7	3853.5	4.9
7	block113001016	1518.0	-6690.0	4.9
8	block113001000	2754.0	-2755.1	4.9
9	block113001010	1268.5	-5956.3	4.9
10	block118002016	2304.4	-2627.5	4.9
11	block117001013	2330.0	-9481.1	4.9
12	block117002003	1066.5	-10018.7	4.9
13	block117002010	1880.6	-10715.6	4.9
14	block116012002	4034.7	-8212.4	4.9
15	block117001015	2460.5	-10377.8	4.9

Once all CAL3QHCR runs for each development scenarios were completed, the 24-hour traffic-related PM2.5 concentrations at each census block centroid in each day were extracted from the model output files into a spreadsheet. The estimated concentrations at the same census block centroid were summed to obtain the population exposure to traffic-related PM2.5 at that census block. The example of MATLAB code and associated data for this process is shown below:

Example of MATLAB code for extracting and summing the 24-hour traffic-related PM2.5 concentrations at census block centroids from the CAL3QHCR output files in 2009 scenario

```
for metset=2006:2012
    xlsmet=['MPRM',num2str(metset),'_24hr.xlsx'];
    [nummet,txtmet,rawmet]=xlsread(xlsmet,1);
    [mmet,nmet]=size(rawmet);
    indx=1:24:mmet-1;
    metDate=rawmet(indx+1,1);

    cd('C:\CAL3QHCR_24hr_2009\');

    rcpset=1;
    xlsrcp=['CensusBlockCentroids_set',num2str(rcpset),'.xlsx'];
    [numrcp,txtrcp,rawrcp]=xlsread(xlsrcp,1);
    [mrcp,nrcp]=size(rawrcp);
    rcpName1=rawrcp(2:mrcp,2)';
```

```
PM1=cell((mmet-1)/24,mrcp-1);

cd(['C:\CAL3QHCR_24hr_2009\',num2str(metset)]);

for lnkset=1:10
    rmet=2;

    for d=1:(mmet-1)/24
        fname=[num2str(rawmet{rmet,1}),'_2009_',num2str(lnkset),'_',num2str(rcpset
        ),'.OUT'];
        fid=fopen(fname);
        nlines=1;
        while feof(fid)==0
            tline{nlines}=fgetl(fid);
            nlines=nlines+1;
        end
        fclose(fid);

        i=1;

        startline=498;
        endline=498;
        for rout=startline:endline
            str=tline{rout};
            scn=textscan(str,'%d%.2f%s%s%s%s%s');
            if isempty(PM1{d,i})==1
                PM1{d,i}=scn{2};
            else PM1{d,i}=PM1{d,i}+scn{2};
            end
            i=i+1;
            rout;
        end

        startline=512;
        endline=552;
        for rout=startline:endline
            str=tline{rout};
            scn=textscan(str,'%d%f%s%s%d');
            if isempty(PM1{d,i})==1
```

```
                PM1{d,i}=scn{2};
            else PM1{d,i}=PM1{d,i}+scn{2};
            end
            i=i+1;
            rout;
        end

        startline=566;
        endline=583;
        for rout=startline:endline
            str=tline{rout};
            scn=textscan(str,'%d%f%s%s%d');
            if isempty(PM1{d,i})==1
                PM1{d,i}=scn{2};
            else PM1{d,i}=PM1{d,i}+scn{2};
            end
            i=i+1;
            rout;
        end

        rmet=rmet+24;
        d;
    end

    lnkset;
end

cd('C:\CAL3QHCR_24hr_2009\');

rcpset=2;
xlsrcp=['CensusBlockCentroids_set',num2str(rcpset),'.xlsx'];
[numrcp,txtrcp,rawrcp]=xlsread(xlsrcp,1);
[mrcp,nrcp]=size(rawrcp);
rcpName2=rawrcp(2:mrcp,2)';

PM2=cell((mmet-1)/24,mrcp-1);

cd(['C:\CAL3QHCR_24hr_2009\',num2str(metset)]);

for lnkset=1:10
```

```
rmet=2;


for d=1:(mmet-1)/24
    fname=[num2str(rawmet{rmet,1}),'_',scenario,'_',num2str(lnkset),'_',num2st
    r(rcpset),'.OUT'];
    disp(fname);
    fid=fopen(fname);
    nlines=1;
    while feof(fid)==0
        tline{nlines}=fgetl(fid);
        nlines=nlines+1;
    end
    fclose(fid);


    i=1;


    startline=498;
    endline=498;
    for rout=startline:endline
        str=tline{rout};
        scn=textscan(str,'%d%.2f%s%s%s%s%s');
        if isempty(PM2{d,i})==1
            PM2{d,i}=scn{2};
        else PM2{d,i}=PM2{d,i}+scn{2};
        end
        i=i+1;
        rout;
    end


    startline=512;
    endline=552;
    for rout=startline:endline
        str=tline{rout};
        scn=textscan(str,'%d%f%s%s%d');
        if isempty(PM2{d,i})==1
            PM2{d,i}=scn{2};
        else PM2{d,i}=PM2{d,i}+scn{2};
        end
        i=i+1;
        rout;
```

```
        end

        startline=566;
        endline=583;
        for rout=startline:endline
            str=tline{rout};
            scn=textscan(str,'%d%f%s%s%d');
            if isempty(PM2{d,i})==1
                PM2{d,i}=scn{2};
            else PM2{d,i}=PM2{d,i}+scn{2};
            end
            i=i+1;
            rout;
        end

        rmet=rmet+24;
        d;
    end

    lnkset;
end

cd('C:\CAL3QHCR_24hr_2009\');

rcpset=3;
xlsrcp=['CensusBlockCentroids_set',num2str(rcpset),'.xlsx'];
[numrcp,txtrcp,rawrcp]=xlsread(xlsrcp,1);
[mrcp,nrcp]=size(rawrcp);
rcpName3=rawrcp(2:mrcp,2)';

PM3=cell((mmet-1)/24,mrcp-1);

cd(['C:\CAL3QHCR_24hr_2009\',num2str(metset)]);

for lnkset=1:10
    rmet=2;

    for d=1:(mmet-1)/24
        fname=[num2str(rawmet{rmet,1}),'_',scenario,'_',num2str(lnkset),'_',num2st
        r(rcpset),'.OUT'];
```

```
    disp(fname);
    fid=fopen(fname);
    nlines=1;
    while feof(fid)==0
        tline{nlines}=fgetl(fid);
        nlines=nlines+1;
    end
    fclose(fid);

    i=1;

    startline=459;
    endline=468;
    for rout=startline:endline
        str=tline{rout};
        scn=textscan(str,'%d%.2f%s%s%s%s%s');
        if isempty(PM3{d,i})==1
            PM3{d,i}=scn{2};
        else PM3{d,i}=PM3{d,i}+scn{2};
        end
        i=i+1;
        rout;
    end

    startline=482;
    endline=521;
    for rout=startline:endline
        str=tline{rout};
        scn=textscan(str,'%d%f%s%s%d');
        if isempty(PM3{d,i})==1
            PM3{d,i}=scn{2};
        else PM3{d,i}=PM3{d,i}+scn{2};
        end
        i=i+1;
        rout;
    end

    rmet=rmet+24;
    d;
end
```

```
    lnkset;
end

cd('C:\CAL3QHCR_24hr_2009\');
rcpName=[rcpName1,rcpName2,rcpName3];
PM=[PM1,PM2,PM3];
metMonth=zeros(size(metDate,1));

for j=1:size(metDate,1)
    tmpmetdate=num2str(metDate{j,1});
    metMonth(j,1)=str2num(tmpmetdate(5:6));
    j;
end

winterDate=[metDate(metMonth==1,:);metDate(metMonth==2,:);metDate(metMonth==12,:)]
;
springDate=[metDate(metMonth==3,:);metDate(metMonth==4,:);metDate(metMonth==5,:)];
summerDate=[metDate(metMonth==6,:);metDate(metMonth==7,:);metDate(metMonth==8,:)];
fallDate=[metDate(metMonth==9,:);metDate(metMonth==10,:);metDate(metMonth==11,:)];

winterPM=[PM(metMonth==1,:);PM(metMonth==2,:);PM(metMonth==12,:)];
springPM=[PM(metMonth==3,:);PM(metMonth==4,:);PM(metMonth==5,:)];
summerPM=[PM(metMonth==6,:);PM(metMonth==7,:);PM(metMonth==8,:)];
fallPM=[PM(metMonth==9,:);PM(metMonth==10,:);PM(metMonth==11,:)];

xlsout=['Centroids_2009PM_',num2str(metset),'.xlsx'];
xlswrite(xlsout,[['Date';winterDate],[rcpName;winterPM]],'Winter');
xlswrite(xlsout,[['Date';springDate],[rcpName;springPM]],'Spring');
xlswrite(xlsout,[['Date';summerDate],[rcpName;summerPM]],'Summer');
xlswrite(xlsout,[['Date';fallDate],[rcpName;fallPM]],'Fall');

excelFileName = xlsout;
excelFilePath = pwd;
sheetName = 'Sheet';
objExcel = actxserver('Excel.Application');
objExcel.Workbooks.Open(fullfile(excelFilePath, excelFileName));
try
    objExcel.ActiveWorkbook.Worksheets.Item([sheetName '1']).Delete;
    objExcel.ActiveWorkbook.Worksheets.Item([sheetName '2']).Delete;
```

```
        objExcel.ActiveWorkbook.Worksheets.Item([sheetName '3']).Delete;
    catch
        ;
    end

    objExcel.ActiveWorkbook.Save;
    objExcel.ActiveWorkbook.Close;
    objExcel.Quit;
    objExcel.delete;

    metset;
end
```

Example of CAL3QHCR output file used in MATLAB code (as 20060101_2009_1_1.OUT)

```
506          THE HIGHEST   1 - DAY AVERAGE CONCENTRATIONS
507                    IN MICROGRAMS/M**3
508          EXCLUDING AMBIENT BACKGROUND CONCENTRATIONS.
509
510             Receptor        Maximum   Ending
511              Number          Conc    Day Hr   Calm
512                   2          0.00   (  1, 0)  C    0
513                   3          0.00   (  1, 0)  C    0
514                   4          0.00   (  1, 0)  C    0
515                   5          0.00   (  1, 0)  C    0
516                   6          0.00   (  1, 0)  C    0
517                   7          0.00   (  1, 0)  C    0
518                   8          0.00   (  1, 0)  C    0
519                   9          0.00   (  1, 0)  C    0
520                  10          0.00   (  1, 0)  C    0
521                  11          0.00   (  1, 0)  C    0
522                  12          0.00   (  1, 0)  C    0
523                  13          0.00   (  1, 0)  C    0
524                  14          0.04   (  1,24)  C   16
525                  15          0.00   (  1, 0)  C    0
```

The left column represents the line number in the CAL3QHCR output

Seasonal average of 24-hour traffic-related PM2.5 concentrations at each census block centroid was used to represent the population exposure concentration in that census block, and its variability was characterized using a bootstrap technique. For each season, the 24-hour traffic-related PM2.5 concentrations at each census block centroid were resampled with replacement for 91 days, and then computed a mean value of these 91 samples as the seasonal average of 24-hour traffic-related PM2.5 concentrations. This step was repeated for 1,999 times, in order to obtain 2,000 mean values that served as a basis for deriving the distribution parameters (i.e., mean and

standard deviation) used to represent the variability in the seasonal average of 24-hour traffic-related PM2.5 concentrations at each census block. The example of MATLAB code and associated data for this process is shown below:

Example of MATLAB code for characterizing the variability in the seasonal average of 24-hour traffic-related PM2.5 concentrations at 160 census block centroids in 2009 scenario, using the bootstrap technique

```
iteration=2000;
m=160;
season=[{'Winter'} {'Spring'} {'Summer'} {'Fall'}];

for sheet=1:size(season,2)
    sampleMu=cell(iteration,1);
    estimateMu=cell(m,1);
    estimateSd=cell(m,1);

    xlsin='Centroid_2009PM_2006-2012.xlsx';
    [numPM,txtPM,rawPM]=xlsread(xlsin,sheet);
    [mPM,nPM]=size(rawPM);
    PM=rawPM(2:mPM,2:nPM);

    for rcp=1:size(PM,2)

        for j=1:iteration
            sampleIndx=datasample(1:size(PM,1),91,'Replace',true);
            samplePM=PM(sampleIndx,rcp);
            sampleMu{j,1}=mean(cell2mat(samplePM));
            j;
        end

        estimateMu{rcp,1}=mean(cell2mat(sampleMu));
        estimateSd{rcp,1}=std(cell2mat(sampleMu));
        rcp;
    end

    csvwrite(['muPM_',season{sheet},'.csv'],estimateMu);
    csvwrite(['sdPM_',season{sheet},'.csv'],estimateSd);
```

```
    sheet;
end
```

Example of 24-hour traffic-related PM2.5 concentration data at 160 census block centroids used in MATLAB code (as Centroid_2009PM_2006-2012.xlsx)

Date	371350114001002	371350122011010	371350118001000	371350122011029	371350119011037	371350118001006	371350113001016	371350113001000
20060101	0	0	0	0.09	0	0	0	0
20060102	0.01	0	0	0.01	0	0.04	0.02	0.16
20060103	0.02	0	0	0.05	0	0	0	0
20060104	0	0	0	0	0	0.02	0.02	0.09
20060105	0.03	0.01	0	0.09	0	0	0	0.01
20060106	0.02	0	0	0.08	0	0	0	0
20060107	0.01	0	0	0.01	0	0	0	0.03
20060108	0	0	0	0	0	0	0	0.07
20060109	0	0	0	0	0	0	0	0.06
20060110	0	0	0	0	0	0	0	0.04
20060111	0	0	0	0	0	0.03	0.01	0.14
20060112	0	0	0	0.03	0	0	0	0.03
20060115	0.08	0	0	0.23	0	0	0	0
20060116	0	0	0	0	0	0.01	0.02	0.11
20060117	0	0	0	0	0	0	0	0.04

15-digit in the header column represents a 2010 census block ID.

APPENDIX C
SUPPLEMENTAL MATERIALS FOR CAL3QHCR MODELING OF TRAFFIC-RELATED PM2.5 CONCENTRATIONS AT PERPENDICULAR DISTANCES FROM THE MIDDLE OF THE EDGES OF HYPOTHETICAL ROADWAY

CAL3QHCR dated 04244 was used to estimate hourly "unit" traffic-related PM2.5 concentrations at 16 perpendicular distances from the middle of the edges of hypothetical roadway based on the emission rate of 1.0 g/veh-mile, and the traffic volume of 10,000 veh/hr. The hypothetical roadway was represented by 2 links. Each link contribution to the hourly "unit" traffic-related PM2.5 concentration at each distance was estimated based on the hourly meteorological profile for 13-hour period during 6 a.m. to 7 p.m. of 2,100 days, including 525 days for winter, 560 days for spring, 532 days for summer, and 483 days for fall, obtained from the EPA's Meteorological Processor for Regulatory Models, using 2006–2012 surface and upper air data at the national weather stations in Chapel Hill and Greensboro respectively. Surface roughness was fixed at 175 cm reflecting city land use – office. Settling and deposition velocity were assumed to be 0 m/s over the analysis period. A total number of CAL3QHCR runs was 2,100 × 13 = 27,300. The examples of MATLAB codes and associated data for generating input files (.INP), control files (.CTL), and the batch processing command files (.BAT) for CAL3QHCR are shown below:

Example of MATLAB code for generating the input files (.INP) for CAL3QHCR to model the hourly "unit" traffic-related PM2.5 concentration

```
for metset=2006:2012
    xlsmet=['MPRM',num2str(metset),'_6am-7pm.xlsx'];
    [nummet,txtmet,rawmet]=xlsread(xlsmet,1);
    [mmet,nmet]=size(rawmet);

    xlslnk='LinkObj3.xlsx';
    [numlnk,txtlnk,rawlnk]=xlsread(xlslnk,1);
    [mlnk,nlnk]=size(rawlnk);
```

```
xlsrcp='ReceptorObj3.xlsx';
[numrcp,txtrcp,rawrcp]=xlsread(xlsrcp,3);
[mrcp,nrcp]=size(rawrcp);

for rmet=2:mmet
    fname=[num2str(rawmet{rmet,1}),'_hr',num2str(rawmet{rmet,5})];
    fid=fopen([fname,'.INP'],'wt');
    JOB=['''',fname,''''];
    ATIM=60;
    Z0=175;
    VS=0;
    VD=0;
    NR=mrcp-1;
    SCAL=0.3048;
    IOPT=1;
    fprintf(fid,'%s,%d,%d,%1.4f,%1.4f,%d,%1.4f,%d\n',JOB,ATIM,Z0,VS,VD,NR,SCAL,IOP
    T);

    STARTMO=rawmet{rmet,3};
    STARTDY=rawmet{rmet,4};
    STARTYR=rawmet{rmet,2};
    ENDMO=rawmet{rmet,3};
    ENDDY=rawmet{rmet,4};
    ENDYR=rawmet{rmet,2};
    fprintf(fid,'%d,%d,%d,%d,%d,%d\n',STARTMO,STARTDY,STARTYR,ENDMO,ENDDY,ENDYR);

    METSF=93785;
    METSYR=rawmet{rmet,2};
    METUA=13723;
    METUYR=rawmet{rmet,2};
    fprintf(fid,'%d,%d,%d,%d\n',METSF,METSYR,METUA,METUYR);

    FLINK=1;
    FAMB=0;
    RU='''U''';
    fprintf(fid,'%d,%d,%s\n',FLINK,FAMB,RU);

    for rrcp=2:mrcp
        RCP=['''',rawrcp{rrcp,2},''''];
```

```
    XR=rawrcp{rrcp,3};
    YR=rawrcp{rrcp,4};
    ZR=rawrcp{rrcp,5};
    fprintf(fid,'%s,%5.1f,%5.1f,%1.1f\n',RCP,XR,YR,ZR);
    rrcp;
end

JTIER=2;
MODE='''P''';
fprintf(fid,'%d,%s\n',JTIER,MODE);

IPATRY1=1;
IPATRY2=1;
IPATRY3=1;
IPATRY4=1;
IPATRY5=1;
IPATRY6=1;
IPATRY7=1;
fprintf(fid,'%d,%d,%d,%d,%d,%d,%d\n',IPATRY1,IPATRY2,IPATRY3,IPATRY4,IPATRY5,I
PATRY6,IPATRY7);

RUN=['''',fname,''''];
NUMLNK=mlnk-1;
fprintf(fid,'%s,%d\n',RUN,NUMLNK);

for rlnk=2:mlnk
    COD=rlnk-1;
    IQ=1;
    fprintf(fid,'%d,%d\n',COD,IQ);

    LNK=['''',rawlnk{rlnk,2},''''];
    TYP='''AG''';
    X1=rawlnk{rlnk,3};
    Y1=rawlnk{rlnk,4};
    X2=rawlnk{rlnk,5};
    Y2=rawlnk{rlnk,6};
    SH=rawlnk{rlnk,7};
    WL=rawlnk{rlnk,8};
    fprintf(fid,'%s,%s,%5.1f,%5.1f,%5.1f,%5.1f,%d,%d\n',LNK,TYP,X1,Y1,X2,Y2,SH
    ,WL);
```

```
            rlnk;
        end

        for hr=1:24
            HE=hr;
            AMB=0;
            fprintf(fid,'%d,%d\n',HE,AMB);

            for rlnk=2:mlnk,
                COD=rlnk-1;
                VPHL=rawlnk{rlnk,9};
                EFL=rawlnk{rlnk,10};
                fprintf(fid,'%d,%d,%1.4f\n',COD,VPHL,EFL);
                rlnk;
            end

            hr;
        end

        fclose(fid);
        rmet;
    end

    metset;
end
```

Example of MATLAB code for generating the control files (.CTL) for CAL3QHCR to model the hourly "unit" traffic-related PM2.5 concentration

```
for metset=2006:2012
    xlsmet=['MPRM',num2str(metset),'_6am-7pm.xlsx'];
    [nummet,txtmet,rawmet]=xlsread(xlsmet,1);
    [mmet,nmet]=size(rawmet);

    for rmet=2:mmet
        fname=[num2str(rawmet{rmet,1}),'_hr',num2str(rawmet{rmet,5})];
        CTL=[fname,'.CTL'];
        MSG=['temp','.MSG'];
        INP=[fname,'.INP'];
        MET=[num2str(rawmet{rmet,1}),'_hr',num2str(rawmet{rmet,5}),'.MET'];
```

```
        ET1=['temp','.ET1'];
        ET2=['temp','.ET2'];
        OUT=[fname,'.OUT'];
        ILK=['temp','.ILK'];
        fid=fopen(CTL,'wt');
        fprintf(fid,'%s\n%s\n%s\n%s\n%s\n%s\n%s\n',MSG,INP,MET,ET1,ET2,OUT,ILK);

        fclose(fid);
        rmet;
    end

    metset;
end
```

Example of MATLAB code for generating the batch processing command files (.BAT) for CAL3QHCR to model the hourly "unit" traffic-related PM2.5 concentration

```
for metset=2006:2012
    fBAT=[num2str(metset),'_1hr.BAT'];
    fid=fopen(fBAT,'wt');
    xlsmet=['MPRM',num2str(metset),'_6am-7pm.xlsx'];
    [nummet,txtmet,rawmet]=xlsread(xlsmet,1);
    [mmet,nmet]=size(rawmet);

    for rmet=2:mmet
        fCTL=[num2str(rawmet{rmet,1}),'_hr',num2str(rawmet{rmet,5}),'.CTL'];
        fprintf(fid,'%s %s %s\n','copy',fCTL,'cal3r.ctl');
        fprintf(fid,'%s\n','CAL3QHCR');
        rmet;
    end

    fclose(fid);
    metset;
end
```

Example of meteorological data used in MATLAB code (as MPRM2006_6am-7pm.xlsx)

Date	Year	Month	Day	Hour	Wind Dir	Wind Spd	Temp	Stability	Urban Mixh	Rural Mixh
20060101	6	1	1	7	35	1.5433	274.3	7	832.7	34
20060101	6	1	1	8	33	0	274.8	6	76.6	108.1
20060101	6	1	1	9	47	1.5433	278.2	5	238.4	264.6
20060101	6	1	1	10	51	0	282	4	400.1	421.1
20060101	6	1	1	11	54	0	285.4	3	561.8	577.6
20060101	6	1	1	12	46	0	286.5	2	723.5	734
20060101	6	1	1	13	53	0	288.2	2	885.3	890.5
20060101	6	1	1	14	49	0	287.6	2	1047	1047
20060101	6	1	1	15	92	1.5433	287.6	2	1047	1047
20060101	6	1	1	16	94	0	288.2	3	1047	1047
20060101	6	1	1	17	91	0	284.3	3	1047	1047
20060101	6	1	1	18	87	0	280.4	4	1033.4	1033.4
20060101	6	1	1	19	94	0	279.8	5	1017.8	840
20060102	6	1	2	7	289	1.5433	280.4	4	830.4	830.4
20060102	6	1	2	8	286	0	281.5	4	814.8	814.8

Example of link data used in MATLAB code (as LinkObj3.xlsx)

No	LinkDscrpt	X_Start	Y_Start	X_End	Y_End	SourceHeight	LinkWidth	TrafficVol	EFL
1	SouthBound	2129.57	1933.27	2129.57	1441.14	0	44	10000	1.0
2	NorthBound	2163.48	1933.27	2163.48	1441.14	0	44	10000	1.0

Example of receptor data used in MATLAB code (as ReceptorObj3.xlsx)

No	Receptor	X	Y	Z
1	West-side-10ft	2107.1	1687.2	4.9
2	West-side-25ft	2092.1	1687.2	4.9
3	West-side-50ft	2067.1	1687.2	4.9
4	West-side-100ft	2017.1	1687.2	4.9
5	West-side-200ft	1917.1	1687.2	4.9
6	West-side-300ft	1817.1	1687.2	4.9
7	West-side-400ft	1717.1	1687.2	4.9
8	West-side-500ft	1617.1	1687.2	4.9
9	East-side-10ft	2185.7	1687.2	4.9
10	East-side-25ft	2200.7	1687.2	4.9
11	East-side-50ft	2225.7	1687.2	4.9
12	East-side-100ft	2275.7	1687.2	4.9
13	East-side-200ft	2375.7	1687.2	4.9
14	East-side-300ft	2475.7	1687.2	4.9
15	East-side-400ft	2575.7	1687.2	4.9
16	East-side-500ft	2675.7	1687.2	4.9

Once all CAL3QHCR runs were completed, link contributions to the hourly "unit" traffic-related PM2.5 concentration at each distance were extracted from the model output files into a spreadsheet. These hourly "unit" concentrations at each distance were then scaled down by the hourly emission rates and traffic volumes reflecting the traffic condition of interest, and averaged to obtain 24-hour concentrations. It should be noted that hourly emission rates for each link were determined by interpolating two MOVES emission rates nearest to hourly temperatures in each day, and CAL3QHCR's average divisors for the 24-hour concentration are equal to

24–the number of hours of consecutive calm winds. The examples of MATLAB codes and associated data for this process are shown below:

Example of MATLAB code for extracting the hourly "unit" traffic-related PM2.5 concentrations from the CAL3QHCR output files into a spreadsheet

```
for metset=2006:2012;
    cd('C:\CAL3QHCR_1hr\');

    xlsmet=['MPRM',num2str(metset),'_6am-7pm.xlsx'];
    [nummet,txtmet,rawmet]=xlsread(xlsmet,1);
    [mmet,nmet]=size(rawmet);

    xlslnk='LinkObj3.xlsx';
    [numlnk,txtlnk,rawlnk]=xlsread(xlslnk,1);
    [mlnk,nlnk]=size(rawlnk);

    xlsrcp='ReceptorObj3.xlsx';
    [numrcp,txtrcp,rawrcp]=xlsread(xlsrcp,2);
    [mrcp,nrcp]=size(rawrcp);

    lnkhead=rawlnk(2:mlnk,2)';

    cd(['C:\CAL3QHCR_1hr\',num2str(metset)]);

    PM=cell(mmet-1,mlnk-1,mrcp-1);

    for rmet=2:mmet;
        fname=[num2str(rawmet{rmet,1}),'_hr',num2str(rawmet{rmet,5}),'.OUT'];
        disp(fname);
        fid=fopen(fname);
        nlines=1;
        while feof(fid)==0
            tline{nlines}=fgetl(fid);
            nlines=nlines+1;
        end
        fclose(fid);
```

```
    rcp=1;
    startline=247;
    endline=262;
    for rout=startline:endline
        str=tline{rout};
        scn=textscan(str,'%16d%8.2f%1s%7s%7.2f%8.2f%8.2f%8.2f');
        PM{rmet-1,1,rcp}=scn{7};
        PM{rmet-1,2,rcp}=scn{8};
        rcp=rcp+1;
        rout;
    end

    rmet;
end

cd('C:\CAL3QHCR_1hr\');
for rcp=1:mrcp-1
    xlsout=['PM_rcp',num2str(rcp),'_MPRM',num2str(metset),'_Obj3.xlsx'];
    sheet=rawrcp{rcp+1,2};
    sheet(isspace(sheet))=[];
    xlswrite(xlsout,[rawmet,[lnkhead;PM(:,:,rcp)]],sheet);

    excelFileName = xlsout;
    excelFilePath = pwd;
    sheetName = 'Sheet';
    objExcel = actxserver('Excel.Application');
    objExcel.Workbooks.Open(fullfile(excelFilePath, excelFileName));
    try
        objExcel.ActiveWorkbook.Worksheets.Item([sheetName '1']).Delete;
        objExcel.ActiveWorkbook.Worksheets.Item([sheetName '2']).Delete;
        objExcel.ActiveWorkbook.Worksheets.Item([sheetName '3']).Delete;
    catch
    end
    objExcel.ActiveWorkbook.Save;
    objExcel.ActiveWorkbook.Close;
    objExcel.Quit;
    objExcel.delete;
    rcp;
end
```

```
    metset;
end
```

Example of MATLAB code for scaling the hourly "unit" traffic-related PM2.5 concentrations, and averaging to obtain the 24-hour traffic-related concentrations corresponding to the traffic condition of interest

```
i=27301;
j=13;
k=16;

xlsAvg='CAL3QHCR_AvgDivisor.xlsx';
[numAvg,txtAvg,rawAvg]=xlsread(xlsAvg,1);
[mAvg,nAvg]=size(rawAvg);

PM=cell(i,j,k);

for rcp=1:k
    cd('C:\CAL3QHCR_1hr\');
    tmpPM=cell(1,j);

    for metset=2006:2012
        xlsPM=['PM_rcp',num2str(rcp),'_MPRM',num2str(metset),'_Obj3.xlsx'];
        [numPM,txtPM,rawPM]=xlsread(xlsPM,1);
        [mPM,nPM]=size(rawPM);
        tmpPM=[tmpPM;rawPM(2:mPM,:)];
        metset;
    end

    tmpPM(1,:)=[];
    tmpPM(cellfun(@isnan,tmpPM))={0};
    tmpPM=[rawPM(1,:);tmpPM];
    [mPM,nPM]=size(tmpPM);
    PM(:,:,rcp)=tmpPM;
    rcp;
end

xlsEFL='TrafficEmissionRates_2009.xlsx';
[numEFL,txtEFL,rawEFL]=xlsread(xlsEFL,1);
[mEFL,nEFL]=size(rawEFL);
```

```
rowEFL=[33 96 411];

for spd=1:size(rowEFL,2)
    nameEFL=rawEFL{rowEFL(spd),1};
    nameEFL(isspace(nameEFL))=[];
    Fahrenheit=((cell2mat(PM(2:mPM,8,1))-273.15).*1.8000)+32.00;
    [mFahrenheit,nFahrenheit]=size(Fahrenheit);
    EFL=cell2mat(cell(mFahrenheit,1));

    for j=1:mFahrenheit
        if Fahrenheit(j,1)<=10
            EFL(j,1)=rawEFL{rowEFL(spd),2};
        elseif and(Fahrenheit(j,1)>10,Fahrenheit(j,1)<=30)
            EFL(j,1)=rawEFL{rowEFL(spd),2}+((Fahrenheit(j,1)-
            10)*(rawEFL{rowEFL(spd),3}-rawEFL{rowEFL(spd),2})/20);
        elseif and(Fahrenheit(j,1)>30,Fahrenheit(j,1)<=50)
            EFL(j,1)=rawEFL{rowEFL(spd),3}+((Fahrenheit(j,1)-
            30)*(rawEFL{rowEFL(spd),4}-rawEFL{rowEFL(spd),3})/20);
        elseif and(Fahrenheit(j,1)>50,Fahrenheit(j,1)<=70)
            EFL(j,1)=rawEFL{rowEFL(spd),4}+((Fahrenheit(j,1)-
            50)*(rawEFL{rowEFL(spd),5}-rawEFL{rowEFL(spd),4})/20);
        elseif and(Fahrenheit(j,1)>70,Fahrenheit(j,1)<=90)
            EFL(j,1)=rawEFL{rowEFL(spd),5}+((Fahrenheit(j,1)-
            70)*(rawEFL{rowEFL(spd),6}-rawEFL{rowEFL(spd),5})/20);
        elseif and(Fahrenheit(j,1)>90,Fahrenheit(j,1)<=110)
            EFL(j,1)=rawEFL{rowEFL(spd),6}+((Fahrenheit(j,1)-
            90)*(rawEFL{rowEFL(spd),7}-rawEFL{rowEFL(spd),6})/20);
        else Fahrenheit(j,1)>110
            EFL(j,1)=rawEFL{rowEFL(spd),7};
        end

        j;
    end

    traffic=1600;

    for trf=1:size(traffic,2)
        VPHL=ones(mFahrenheit,1)*traffic(trf);
        avgPM=cell(mAvg-1,k);

        for rcp=1:k
```

```
    lnkPM1=cell2mat(PM(2:mPM,12,rcp)).*(EFL.*VPHL/10000);
    lnkPM2=cell2mat(PM(2:mPM,13,rcp)).*(EFL.*VPHL/10000);
    hrPM=lnkPM1+lnkPM2;

    r=1;
    for d=2:mAvg
        avgPM(d-1,rcp)=num2cell(sum(hrPM(r:r+12,1))/rawAvg{d,7});
        r=r+13;
        d;
    end

    rcp;
end

monthAvg=cell2mat(rawAvg(2:mAvg,3));
avgPM=[rawAvg(2:mAvg,1),avgPM];

avgWinter=[avgPM(monthAvg==1,:);avgPM(monthAvg==2,:);avgPM(monthAvg==12,:)];

avgSpring=[avgPM(monthAvg==3,:);avgPM(monthAvg==4,:);avgPM(monthAvg==5,:)];

avgSummer=[avgPM(monthAvg==6,:);avgPM(monthAvg==7,:);avgPM(monthAvg==8,:)];

avgFall=[avgPM(monthAvg==9,:);avgPM(monthAvg==10,:);avgPM(monthAvg==11,:)];

xlsrcp='ReceptorObj3.xlsx';
[numrcp,txtrcp,rawrcp]=xlsread(xlsrcp,2);
[mrcp,nrcp]=size(rawrcp);

xlsout=['PM09_VHPL',num2str(traffic(trf)),'_',nameEFL,'.xlsx'];
xlswrite(xlsout,[['Date',rawrcp(2:mrcp,2)'];avgWinter],'Winter');
xlswrite(xlsout,[['Date',rawrcp(2:mrcp,2)'];avgSpring],'Spring');
xlswrite(xlsout,[['Date',rawrcp(2:mrcp,2)'];avgSummer],'Summer');
xlswrite(xlsout,[['Date',rawrcp(2:mrcp,2)'];avgFall],'Fall');

excelFileName = xlsout;
excelFilePath = pwd;
sheetName = 'Sheet';
objExcel = actxserver('Excel.Application');
objExcel.Workbooks.Open(fullfile(excelFilePath, excelFileName));
try
```

```
            objExcel.ActiveWorkbook.Worksheets.Item([sheetName '1']).Delete;
            objExcel.ActiveWorkbook.Worksheets.Item([sheetName '2']).Delete;
            objExcel.ActiveWorkbook.Worksheets.Item([sheetName '3']).Delete;
        catch
        end
        objExcel.ActiveWorkbook.Save;
        objExcel.ActiveWorkbook.Close;
        objExcel.Quit;
        objExcel.delete;

        trf;
    end

    spd;
end
```

Example of hourly "unit" traffic-related PM2.5 concentration data used in MATLAB code (as PM_rcp1_MPRM2006_Obj3.xlsx)

Date	Year	Month	Day	Hour	Wind Dir	Wind Spd	Temp	Stability	Urban Mixh	Rural Mixh	SouthBound	NorthBound
20060108	6	1	8	7	35	0	270.9	7	849.5	122	0	0
20060108	6	1	8	8	31	0	270.9	6	53.5	166.7	0	0
20060108	6	1	8	9	30	0	274.3	5	168.3	262.6	0	0
20060108	6	1	8	10	30	0	277	4	283	358.5	0	0
20060108	6	1	8	11	29	0	280.4	3	397.8	454.4	0	0
20060108	6	1	8	12	177	2.0578	282.6	3	512.5	550.2	194.1	44.2
20060108	6	1	8	13	309	3.0866	283.2	3	627.3	646.1	150.9	84.8
20060108	6	1	8	14	334	2.5722	284.3	3	742	742	200	90.9
20060108	6	1	8	15	182	2.0578	285.4	3	742	742	215.3	55.9
20060108	6	1	8	16	179	2.0578	286.5	4	742	742	238.2	35.5
20060108	6	1	8	17	348	2.0578	285.4	4	742	742	320	95.2
20060108	6	1	8	18	180	1.5433	283.7	5	734.6	698.1	319.8	50.5
20060108	6	1	8	19	183	2.0578	283.2	6	725.1	641.7	275.1	52.2

Example of PM2.5 emission rates for specific traffic condition us\ed in MATLAB code (as TrafficEmissionRates_2009.xlsx)

Traffic_Condition	EFL_10F	EFL_30F	EFL_50F	EFL_70F	EFL_90F	EFL_110F
Accel, 35mph, 0% grade	0.1377	0.0957	0.0734	0.0616	0.0608	0.0608
Cruise, 35mph, 0% grade	0.0824	0.0578	0.0448	0.0379	0.0374	0.0374
Queue with 50% idle time, 35mph, 0% grade	0.0906	0.0637	0.0494	0.0418	0.0413	0.0413

Seasonal average of 24-hour traffic-related PM2.5 concentrations at each distance from the edges of hypothetical roadway, and its variability was characterized using the same process as shown in **Appendix B**.

APPENDIX D
SUPPLEMENTAL MATERIALS FOR MODELING OF HEALTH BURDENS ATTRIBUTABLE TO SHORT-TERM EXPOSURE TO TRAFFIC-RELATED PM2.5 AT 160 CENCUS BLOCK CENTROIDS ANALYZED

Four health burdens attributable to short-term exposure to traffic-related PM2.5 (Δy), including cardiovascular and respiratory mortality (all ages) and unscheduled hospital admissions (age 65 and over), in each census blocks were quantified as a product of seasonal baselines incidents for given adverse health outcomes (y^0) and seasonal averages of fraction of given adverse health incidents attributable to exposure to traffic-related PM2.5 (AF). The seasonal baselines incidents were estimated as a sum of product of seasonal incidence variation factors; baseline incidence rates by age group, gender, and race; and census block populations by age group, gender, and race. The seasonal averages of attributable fractions were calculated as $AF = 1 - e^{-\beta(xUF)}$, where β is the seasonal concentration coefficient for given adverse health outcomes, x is the seasonal averages of population exposures to traffic-related PM2.5 in each census block from the integrated MOVES-CAL3QHCR modeling, and UF is the uncertainty factor of the integrated MOVES-CAL3QHCR modeling. To account for variability and uncertainty in the health burden estimates, β was represented by zero-truncated normal distributions with means and standard deviations as shown in **Table X**, x was represented by zero-truncated normal distributions with means and standard deviations derived using the bootstrap technique with a set of seasonal 24-hour traffic-related PM2.5 concentrations from CAL3QHCR modeling, and UF was represented by a triangular distribution with lower limit = 0.5, upper limit = 2.0, and mode =1.0, reflecting the expected factor-of-two uncertainty in the model predictions. The quantifications were performed for 2,000 iterations using random values from the given distributions of β, x, and UF, in order to derive means and standard deviations of

Δy in each census block. The examples of MATLAB codes and associated data for this process are shown below:

Example of MATLAB code for quantifying cardiovascular mortality (all ages) attributable to short-term exposure to traffic-related PM2.5 at 160 census block centroids in 2009 scenario

```
iteration=2000;
m=160;
l=12;

CRfunction='seasonal_CVD_Death';
season=[{'Winter'} {'Spring'} {'Summer'} {'Fall'}];

variation=[0.251770766 0.305859627 0.199613651 0.242755956];

betaMu=[0.00135 0.00076 0.00062 -0.00018];
betaSd=[0.00167091836734694 0.00178061224489796 0.0014515306122449
0.0014030612244898];

tridist=makedist('Triangular','a',0.5,'b',1.0,'c',2.0);

xlsRate='DetailedMortalityRates_2010_Orange.xlsx';
[numRate,txtRate,rawRate]=xlsread(xlsRate,1);
[mRate,nRate]=size(rawRate);

RateWM=cell(m,l);
RateWF=cell(m,l);
RateBM=cell(m,l);
RateBF=cell(m,l);
RateOM=cell(m,l);
RateOF=cell(m,l);

for j=1:m

    RateWM(j,:)=rawRate(2,2:nRate-1);
    RateWF(j,:)=rawRate(3,2:nRate-1);
    RateBM(j,:)=rawRate(4,2:nRate-1);
    RateBF(j,:)=rawRate(5,2:nRate-1);
    RateOM(j,:)=rawRate(6,2:nRate-1);
    RateOF(j,:)=rawRate(7,2:nRate-1);

    j;
end

xlsWM='CensusBlock_White_Male.xlsx';
[numWM,txtWM,rawWM]=xlsread(xlsWM,1);
[mWM,nWM]=size(rawWM);

xlsWF='CensusBlock_White_Female.xlsx';
[numWF,txtWF,rawWF]=xlsread(xlsWF,1);
```

```
[mWF,nWF]=size(rawWF);

xlsBM='CensusBlock_Black_Male.xlsx';
[numBM,txtBM,rawBM]=xlsread(xlsBM,1);
[mBM,nBM]=size(rawBM);

xlsBF='CensusBlock_Black_Female.xlsx';
[numBF,txtBF,rawBF]=xlsread(xlsBF,1);
[mBF,nBF]=size(rawBF);

xlsOM='CensusBlock_Other_Male.xlsx';
[numOM,txtOM,rawOM]=xlsread(xlsOM,1);
[mOM,nOM]=size(rawOM);

xlsOF='CensusBlock_Other_Female.xlsx';
[numOF,txtOF,rawOF]=xlsread(xlsOF,1);
[mOF,nOF]=size(rawOF);

WM=rawWM(2:mWM,3:14);
WF=rawWF(2:mWF,3:14);
BM=rawBM(2:mBM,3:14);
BF=rawBF(2:mBF,3:14);
OM=rawOM(2:mOM,3:14);
OF=rawOF(2:mOF,3:14);

for s=1:size(season,2)

    betaNormal=makedist('Normal','mu',betaMu(s),'sigma',betaSd(s));
    betaTruncated=truncate(betaNormal,0,inf);

    xlsPM=['mu-sdPM_',season{s},'2009.xlsx'];
    [numPM,txtPM,rawPM]=xlsread(xlsPM,1);
    [mPM,nPM]=size(rawPM);

    muPM=rawPM(2:mPM,2);
    sdPM=rawPM(2:mPM,3);

    for rcp=1:size(muPM,1)

        pmNormal=makedist('Normal','mu',muPM{rcp,1},'sigma',sdPM{rcp,1});
        pmTruncated=truncate(pmNormal,0,inf);

        sampleBeta=random(betaTruncated,iteration,1);
        samplePM=random(pmTruncated,iteration,1);
        sampleUF=random(tridist,iteration,1);

        sampleAF=1-exp(-1*sampleBeta.*samplePM.*sampleUF);


Y0=variation(s)*((cell2mat(RateWM(rcp,:)).*cell2mat(WM(rcp,:)))+(cell2mat(Rat
eWF(rcp,:)).*cell2mat(WF(rcp,:)))...

+(cell2mat(RateBM(rcp,:)).*cell2mat(BM(rcp,:)))+(cell2mat(RateBF(rcp,:)).*cel
l2mat(BF(rcp,:)))...
```

```
+(cell2mat(RateOM(rcp,:)).*cell2mat(OM(rcp,:)))+(cell2mat(RateOF(rcp,:)).*cel
l2mat(OF(rcp,:))));

        if isnan(mean(sampleAF))==1
            mudeltaY(rcp,1)=0;
            sddeltaY(rcp,1)=0;
        else
            deltaY=sum(Y0)*sampleAF*10^6;
            mudeltaY(rcp,1)=mean(deltaY);
            sddeltaY(rcp,1)=std(deltaY);
        end

        rcp;
    end

    csvwrite(['mu_',CRfunction,'_',season{s},'.csv'],mudeltaY);
    csvwrite(['sd_',CRfunction,'_',season{s},'.csv'],sddeltaY);

    s;
end
```

Example of cardiovascular mortality rates by age group, gender, and race used in MATLAB code (as DetailedMortalityRates_2010_Orange.xlsx)

Race & Sex	Age 0-4	Age 5-9	Age 10-14	Age 15-19	Age 20-24	Age 25-34	Age 35-44	Age 45-54	Age 55-64	Age 65-74	Age 75-84	Age 85+
W M	0	0	0	0	0	0	0.0002	0.0003	0.0018	0.0034	0.0165	0.0525
W F	0	0	0	0	0	0	0	0.0001	0.0009	0.0024	0.0077	0.0303
B M	0	0	0	0	0	0	0	0.0027	0.0024	0.0072	0.0172	0.0263
B F	0	0	0	0	0	0	0.0009	0.0015	0.0010	0	0.0206	0.0230
O M	0	0	0	0	0	0	0	0	0.0026	0	0	0.1250
O F	0	0	0	0	0	0	0	0	0	0	0	0

Example of census block population by age group used in MATLAB code (as CensusBlock_White_Male.xlsx)

BLOCKID10	All Age	Age 0-4	Age 5-9	Age 10-14	Age 15-19	Age 20-24	Age 25-34	Age 35-44	Age 45-54	Age 55-64	Age 65-74	Age 75-84	Age 85+
371350114001002	79	0	1	0	1	52	14	3	3	1	1	3	0
371350122011010	4	0	0	0	1	0	1	0	0	2	0	0	0
371350118001000	276	13	5	3	8	146	33	18	24	16	8	1	1
371350122011029	0	0	0	0	0	0	0	0	0	0	0	0	0
371350119011037	20	0	1	3	2	0	0	1	5	4	0	4	0
371350118001006	8	0	1	1	2	0	1	1	1	0	1	0	0
371350113001016	12	0	0	0	0	8	0	2	0	1	1	0	0
371350113001000	3	0	0	0	0	3	0	0	0	0	0	0	0
371350113001010	51	0	0	0	1	37	11	1	1	0	0	0	0
371350118002016	12	5	0	0	0	0	0	3	2	1	1	0	0
371350117001013	51	3	2	0	0	22	13	5	1	3	2	0	0
371350117002003	10	0	0	0	0	3	0	1	1	2	1	0	2
371350117002010	32	1	2	3	0	4	3	4	2	9	4	0	0
371350116012002	0	0	0	0	0	0	0	0	0	0	0	0	0
371350117001015	14	0	0	0	3	6	3	0	1	0	1	0	0

Example of mean and standard deviation data for seasonal averages of population exposures to traffic-related PM2.5 in each census block used in MATLAB code (as mu-sdPM_winter2009.xlsx)

BLOCKID10	mu_Winter	sd_Winter
371350114001002	0.01078	0.00185
371350122011010	0.00038	0.00020
371350118001000	0.00000	0.00000
371350122011029	0.03292	0.00460
371350119011037	0.00004	0.00006
371350118001006	0.00393	0.00108
371350113001016	0.00342	0.00085
371350113001000	0.04724	0.00660
371350113001010	0.00138	0.00053
371350118002016	0.00724	0.00173
371350117001013	0	0
371350117002003	0.00006	0.00008
371350117002010	0.00229	0.00062
371350116012002	0.00008	0.00009
371350117001015	0.00695	0.00168

APPENDIX E
DISTRIBUTION OF THE CENTROID DISTANCES FROM THE EDGES OF STUDY CORRIDOR AMONG 160 CENSUS BLOCKS ANALYZED

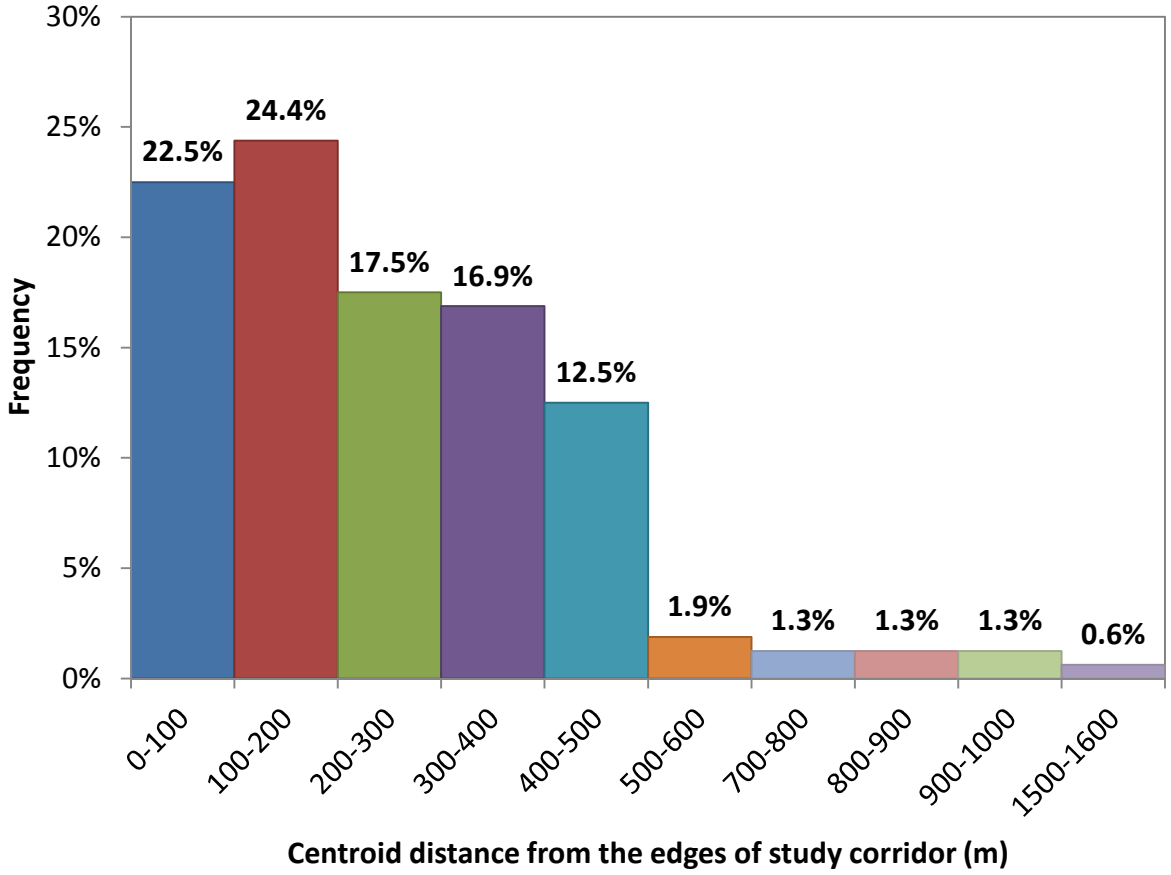

APPENDIX F
POPULATION DEMOGRAPHIC CHARACTERISTICS WITHIN 160 CENSUS BLOCKS ANALYZED

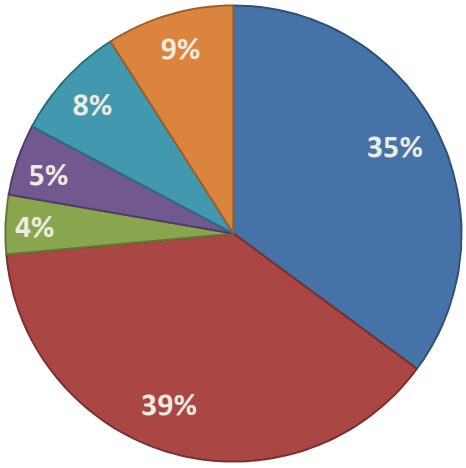

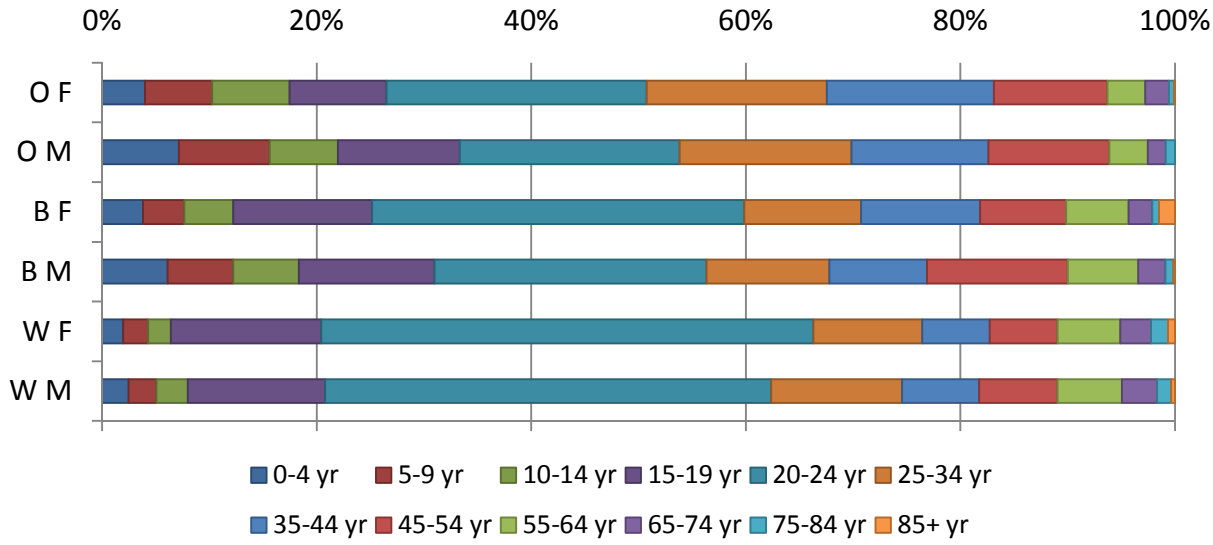

W M = white male; W M = white female; B M = black or African America male; B F = black or African America male; O M = other races male; and O F = other races female

APPENDIX G
CUMULATIVE DISTRIBUTION OF PREDICTED SEASONAL AVERAGE OF 24-HOUR TRAFFIC-RELATED PM2.5 CONCENTRATION WITHIN 160 CENSUS BLOCKS ANALYZED

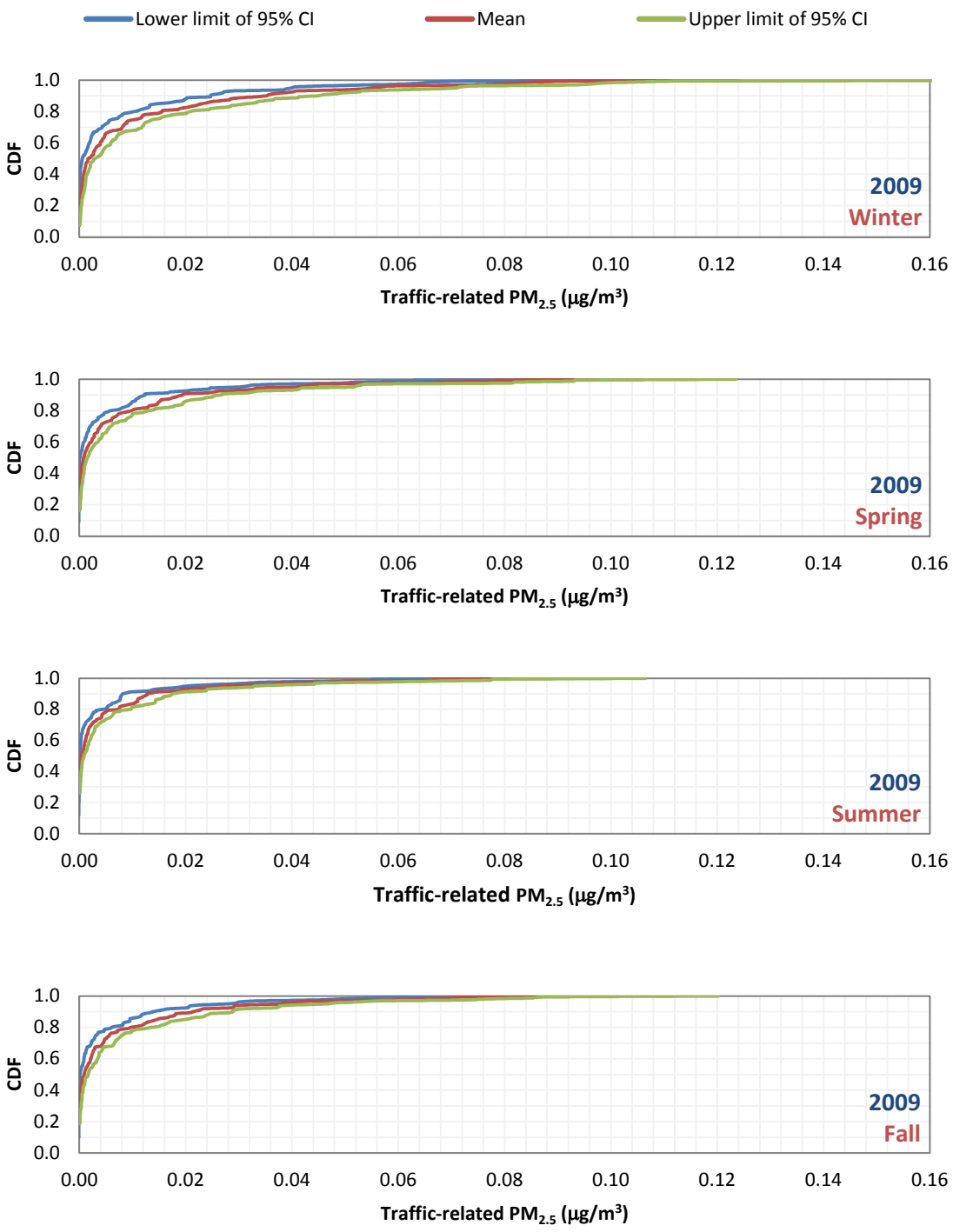

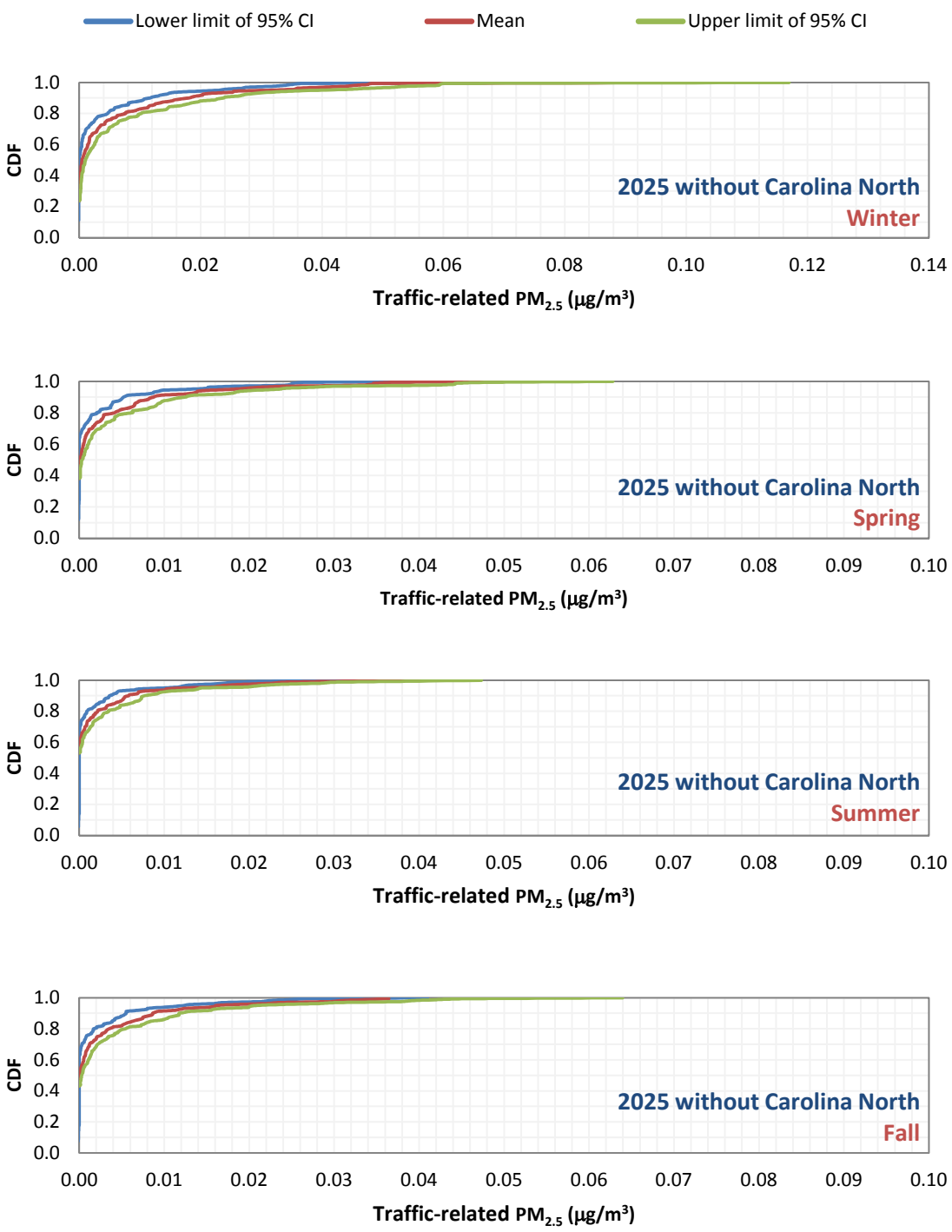
Lower limit of 95% CI
Mean
Upper limit of 95% CI
CDF
1.0
0.8
0.6
0.4
0.2
0.0
0.00
0.02
0.04
0.06
0.08
0.10
0.12
0.14
Traffic-related PM2.5 (µg/m3)
2025 without Carolina North
Winter
CDF
1.0
0.8
0.6
0.4
0.2
0.0
0.00
0.01
0.02
0.03
0.04
0.05
0.06
0.07
0.08
0.09
0.10
Traffic-related PM2.5 (µg/m3)
2025 without Carolina North
Spring
CDF
1.0
0.8
0.6
0.4
0.2
0.0
0.00
0.01
0.02
0.03
0.04
0.05
0.06
0.07
0.08
0.09
0.10
Traffic-related PM2.5 (µg/m3)
2025 without Carolina North
Summer
CDF
1.0
0.8
0.6
0.4
0.2
0.0
0.00
0.01
0.02
0.03
0.04
0.05
0.06
0.07
0.08
0.09
0.10
Traffic-related PM2.5 (µg/m3)
2025 without Carolina North
Fall

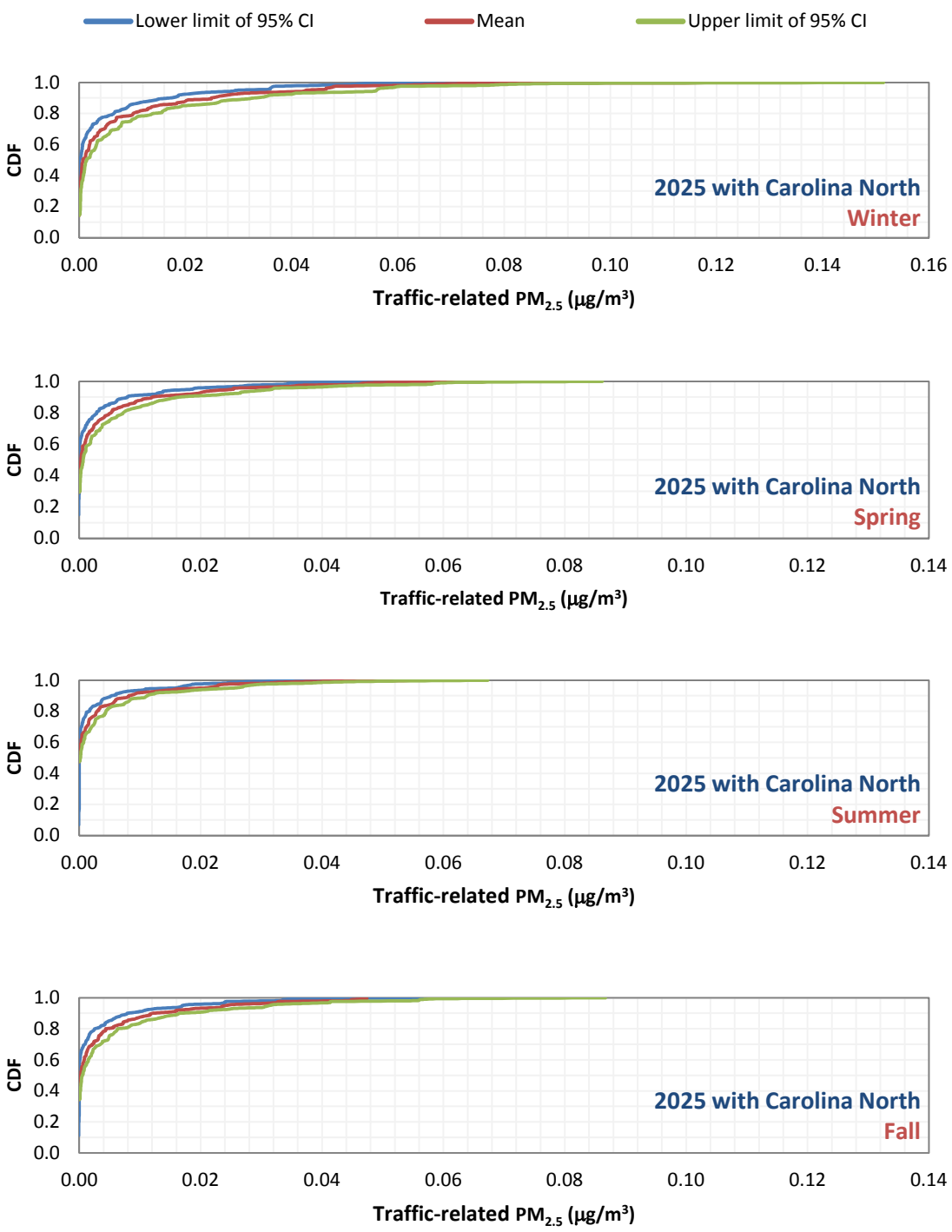
Lower limit of 95% CI
Mean
Upper limit of 95% CI
CDF
1.0
0.8
0.6
0.4
0.2
0.0
0.00
0.02
0.04
0.06
0.08
0.10
0.12
0.14
0.16
Traffic-related PM2.5 (µg/m3)
2025 with Carolina North
Winter
2025 with Carolina North
Spring
2025 with Carolina North
Summer
2025 with Carolina North
Fall

APPENDIX H
CUMULATIVE DISTRIBUTION OF PREDICTED SEASONAL AVERAGE OF CARDIOVASCULAR MORTALITY ATTRIBUTABLE TO SHORT-TERM EXPOSURE TO TRAFFIC-RELATED PM2.5 WITHIN 160 CENSUS BLOCKS ANALYZED

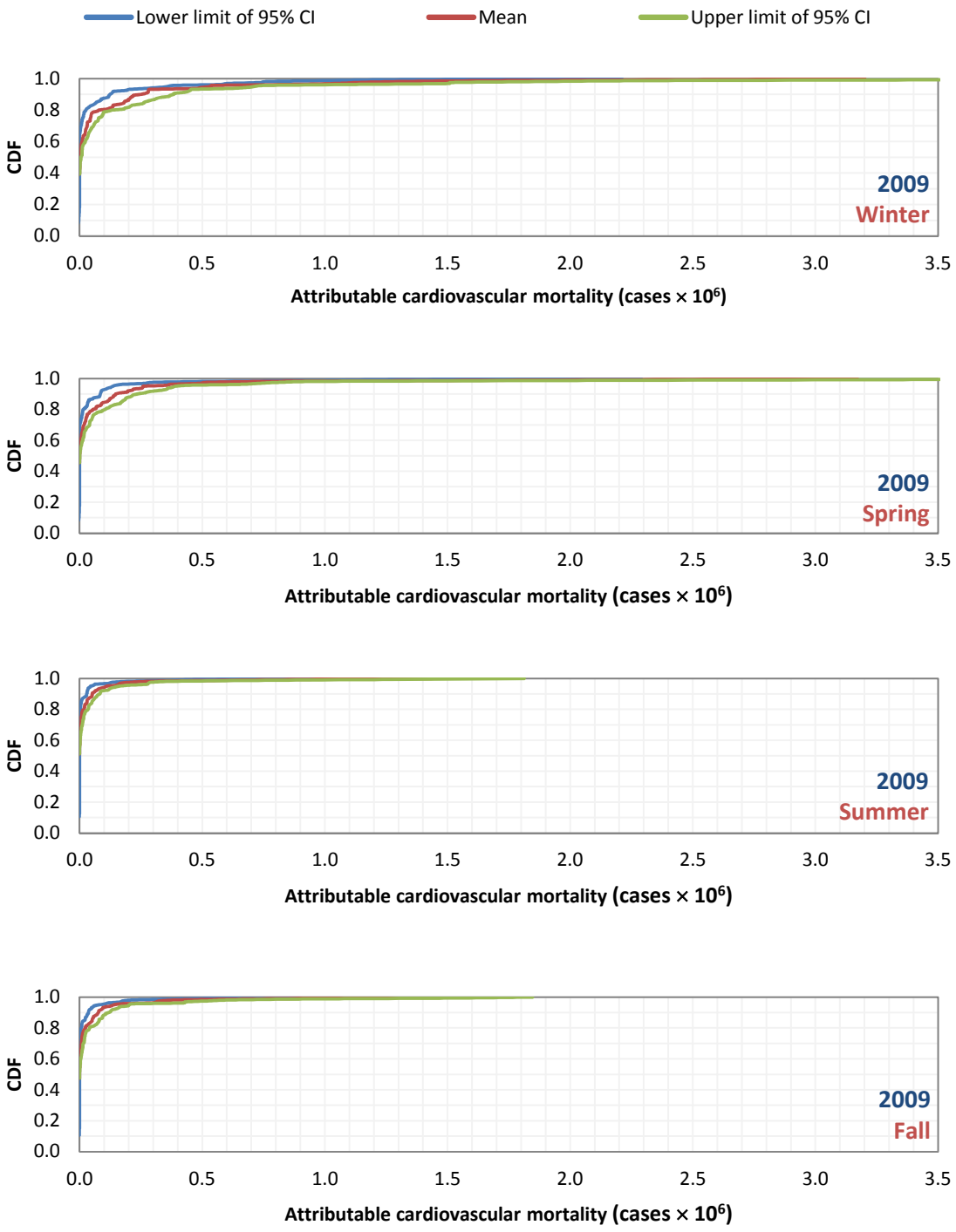

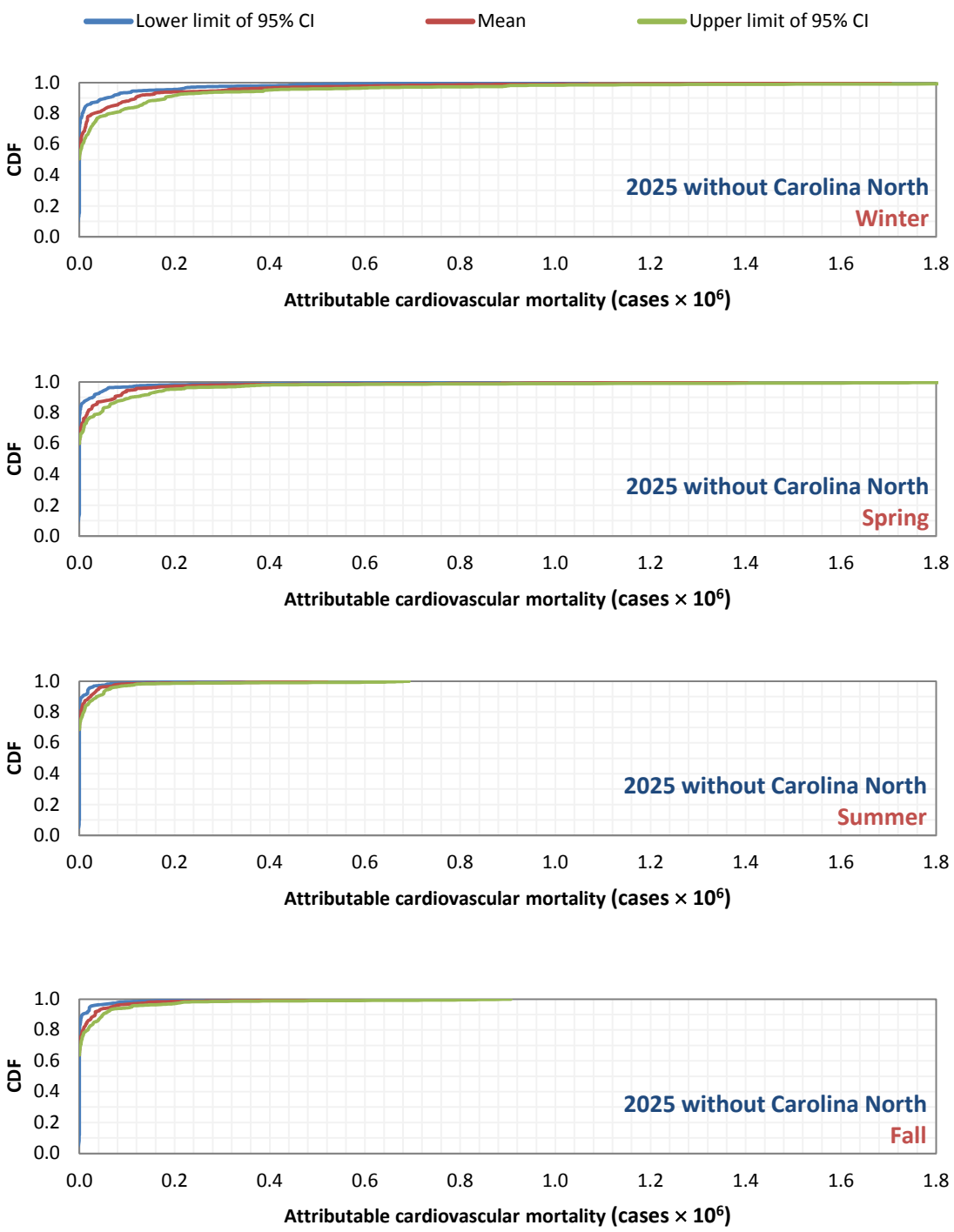
Lower limit of 95% CI
Mean
Upper limit of 95% CI
CDF
1.0
0.8
0.6
0.4
0.2
0.0
0.0
0.2
0.4
0.6
0.8
1.0
1.2
1.4
1.6
1.8
Attributable cardiovascular mortality (cases × 10⁶)
2025 without Carolina North
Winter
2025 without Carolina North
Spring
2025 without Carolina North
Summer
2025 without Carolina North
Fall

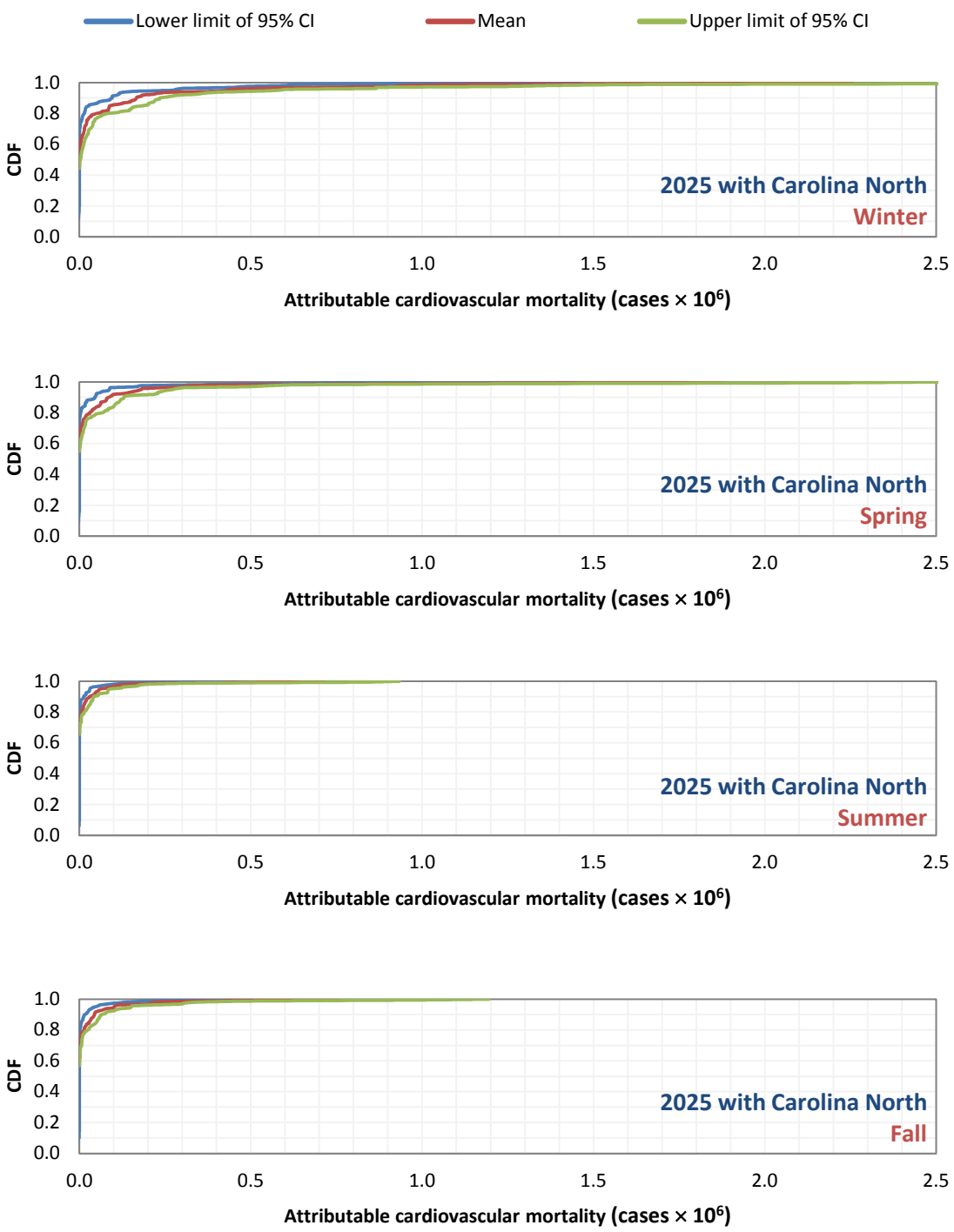
Lower limit of 95% CI
Mean
Upper limit of 95% CI
CDF
1.0
0.8
0.6
0.4
0.2
0.0
0.0
0.5
1.0
1.5
2.0
2.5
Attributable cardiovascular mortality (cases × 10^6)
2025 with Carolina North
Winter
2025 with Carolina North
Spring
2025 with Carolina North
Summer
2025 with Carolina North
Fall

APPENDIX I
CUMULATIVE DISTRIBUTION OF PREDICTED SEASONAL AVERAGE OF RESPIRATORY MORTALITY ATTRIBUTABLE TO SHORT-TERM EXPOSURE TO TRAFFIC-RELATED PM2.5 WITHIN 160 CENSUS BLOCKS ANALYZED

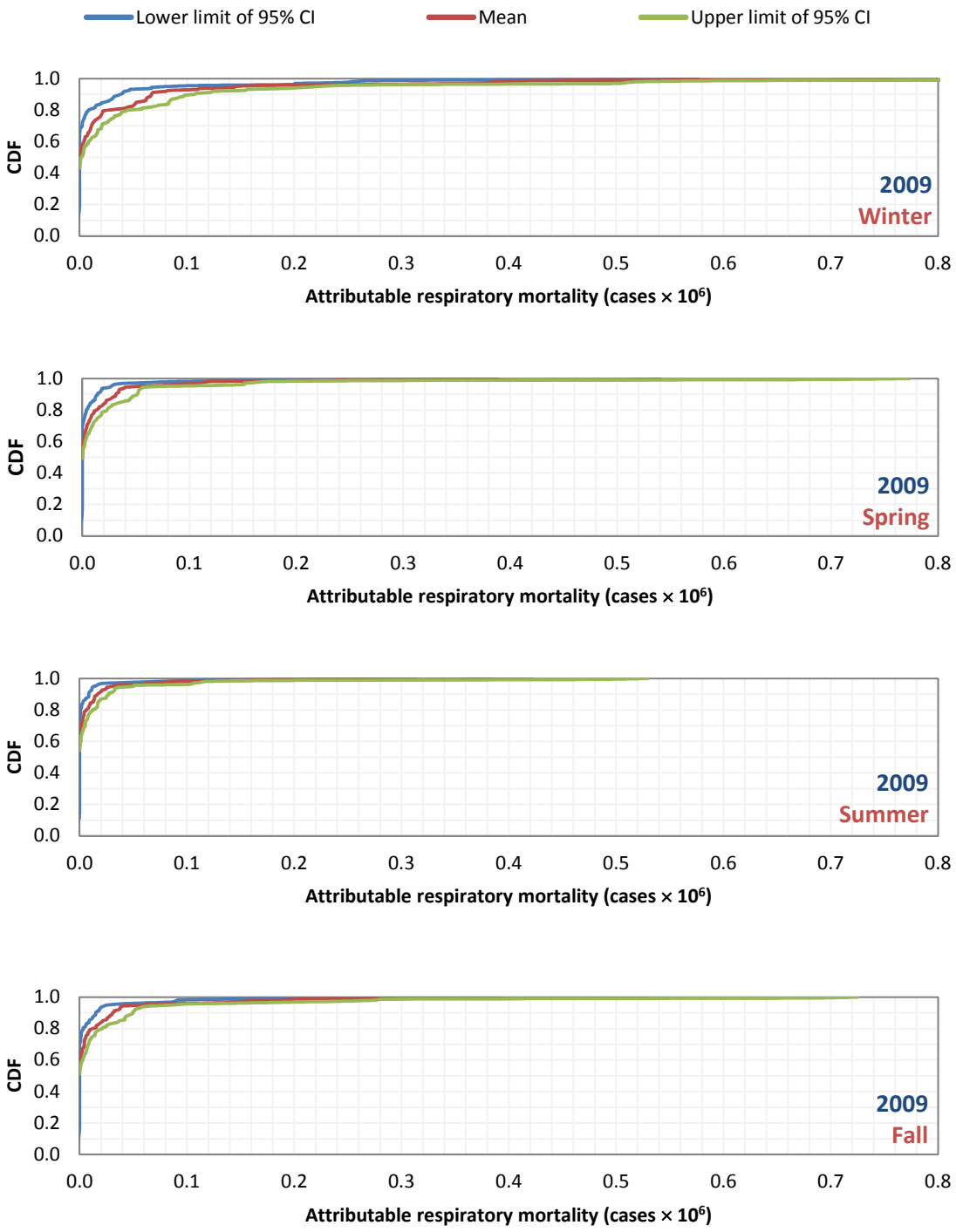

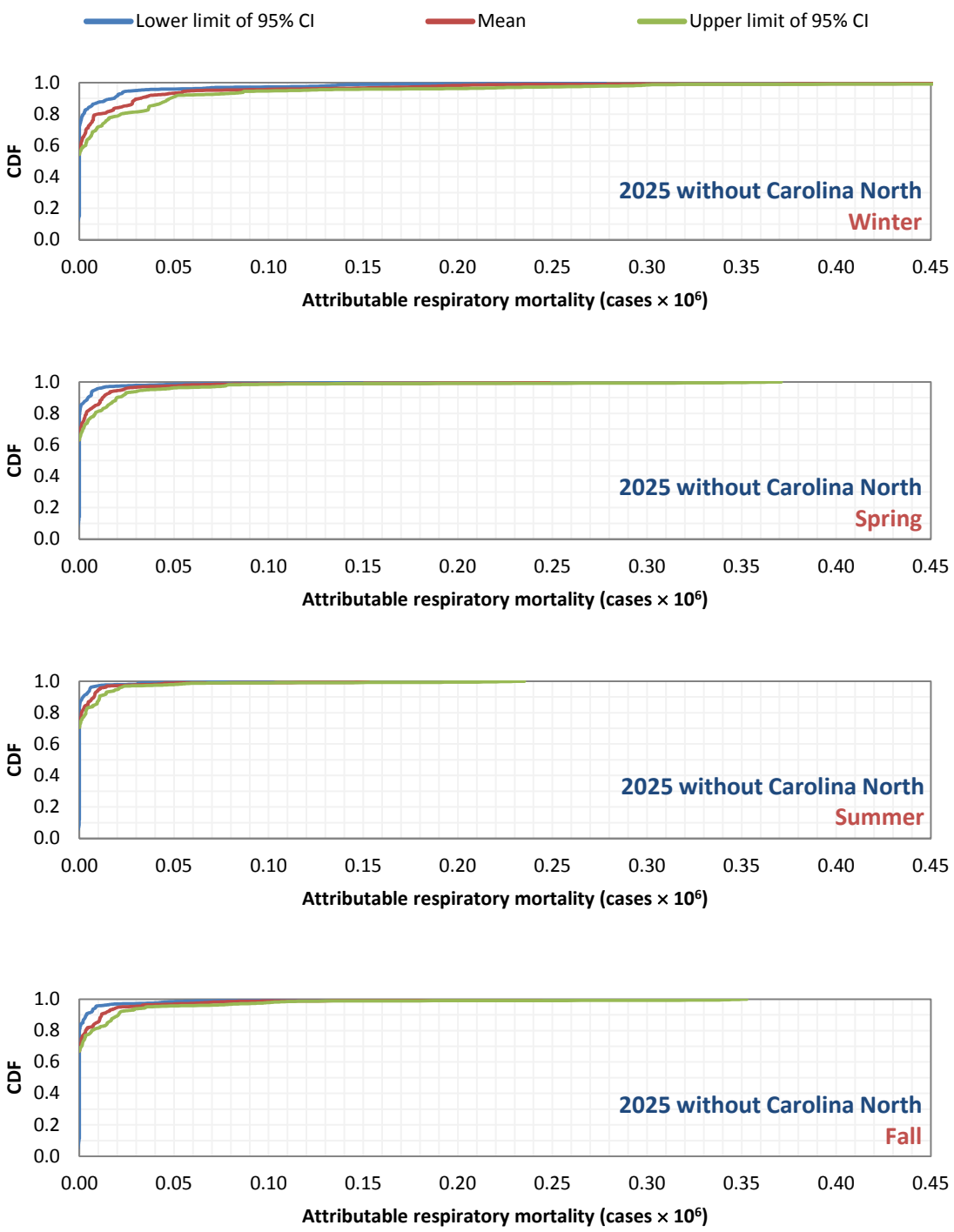
Lower limit of 95% CI
Mean
Upper limit of 95% CI
CDF
1.0
0.8
0.6
0.4
0.2
0.0
0.00
0.05
0.10
0.15
0.20
0.25
0.30
0.35
0.40
0.45
Attributable respiratory mortality (cases × 10⁶)
2025 without Carolina North
Winter
2025 without Carolina North
Spring
2025 without Carolina North
Summer
2025 without Carolina North
Fall

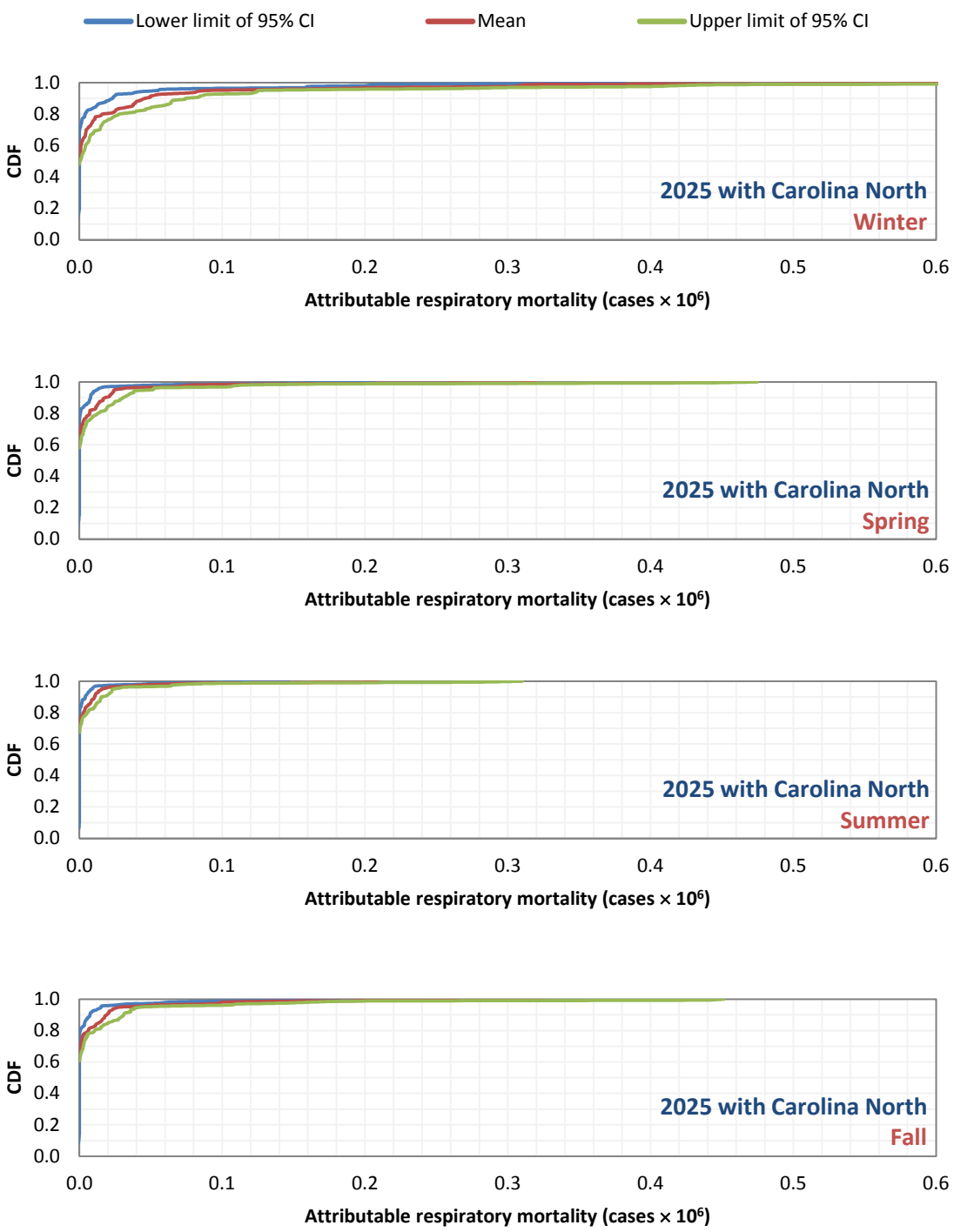
Lower limit of 95% CI
Mean
Upper limit of 95% CI
CDF
1.0
0.8
0.6
0.4
0.2
0.0
0.0
0.1
0.2
0.3
0.4
0.5
0.6
Attributable respiratory mortality (cases × 10⁶)
2025 with Carolina North
Winter
2025 with Carolina North
Spring
2025 with Carolina North
Summer
2025 with Carolina North
Fall

APPENDIX J
CUMULATIVE DISTRIBUTION OF PREDICTED SEASONAL AVERAGE OF CARDIOVASCULAR HOSPITAL ADMISSIONS (UNSCHEDULED) ATTRIBUTABLE TO SHORT-TERM EXPOSURE TO TRAFFIC-RELATED PM2.5 WITHIN 160 CENSUS BLOCKS ANALYZED

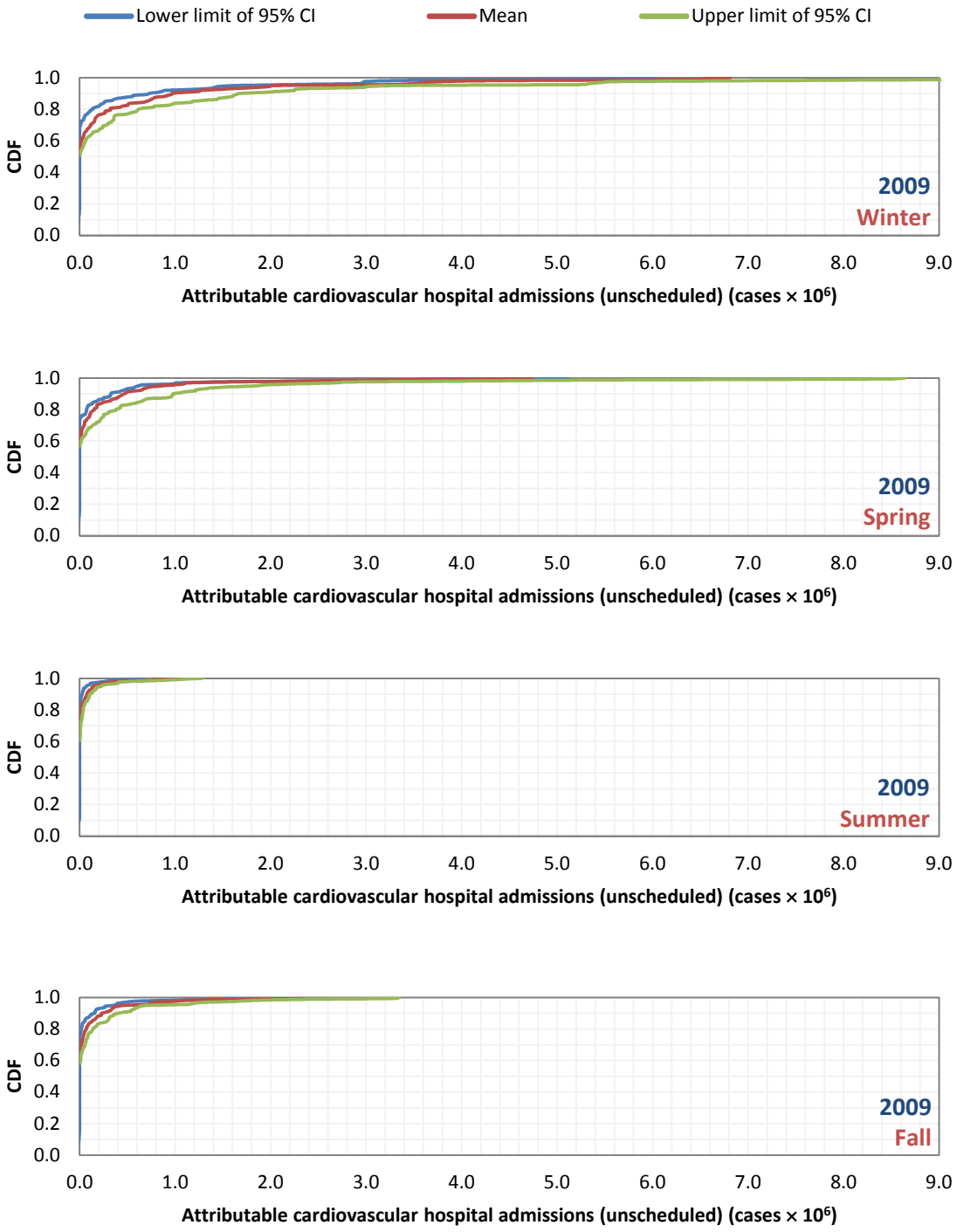

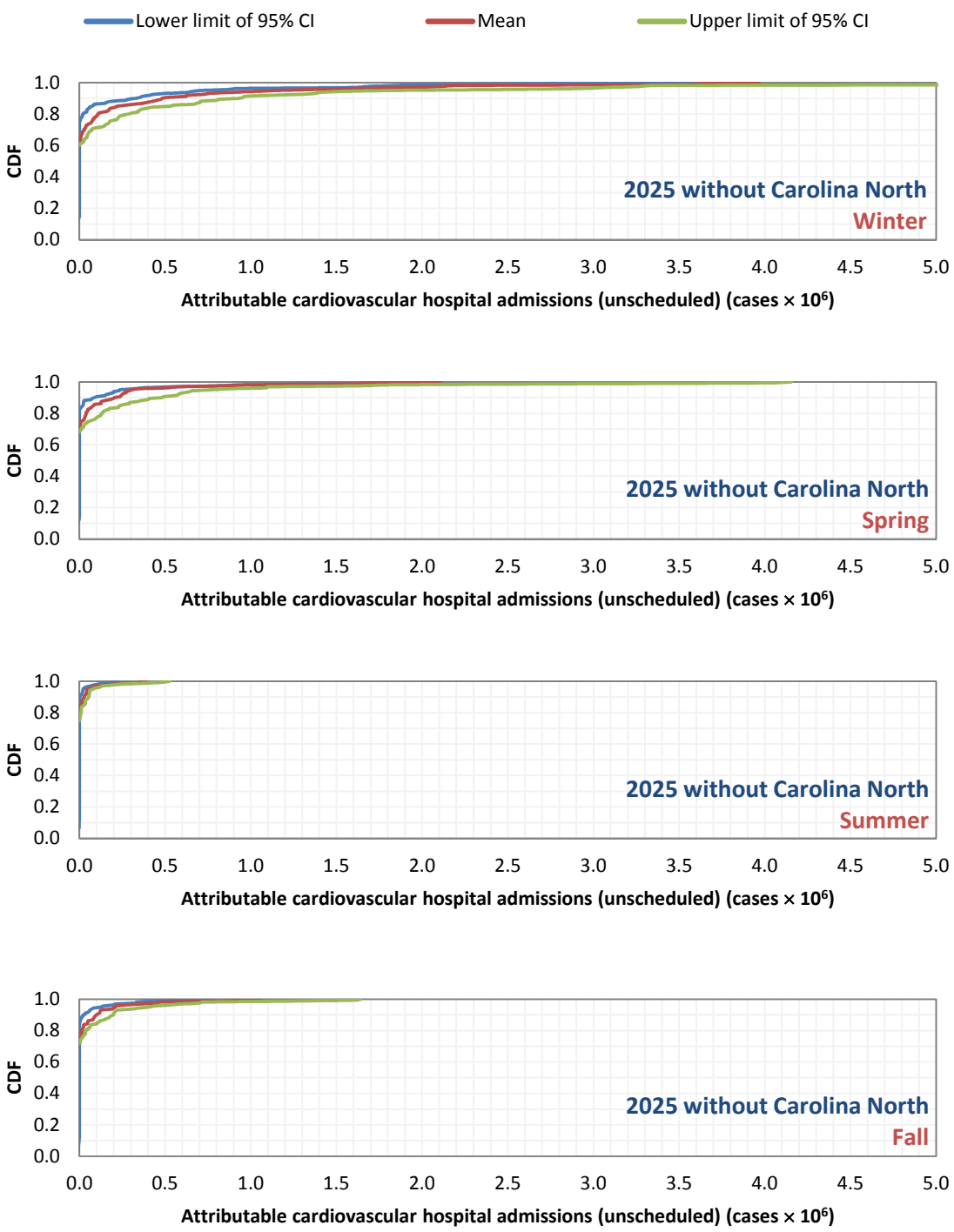
Lower limit of 95% CI
Mean
Upper limit of 95% CI
CDF
1.0
0.8
0.6
0.4
0.2
0.0
0.0
0.5
1.0
1.5
2.0
2.5
3.0
3.5
4.0
4.5
5.0
2025 without Carolina North
Winter
Attributable cardiovascular hospital admissions (unscheduled) (cases × 10⁶)
2025 without Carolina North
Spring
Attributable cardiovascular hospital admissions (unscheduled) (cases × 10⁶)
2025 without Carolina North
Summer
Attributable cardiovascular hospital admissions (unscheduled) (cases × 10⁶)
2025 without Carolina North
Fall
Attributable cardiovascular hospital admissions (unscheduled) (cases × 10⁶)

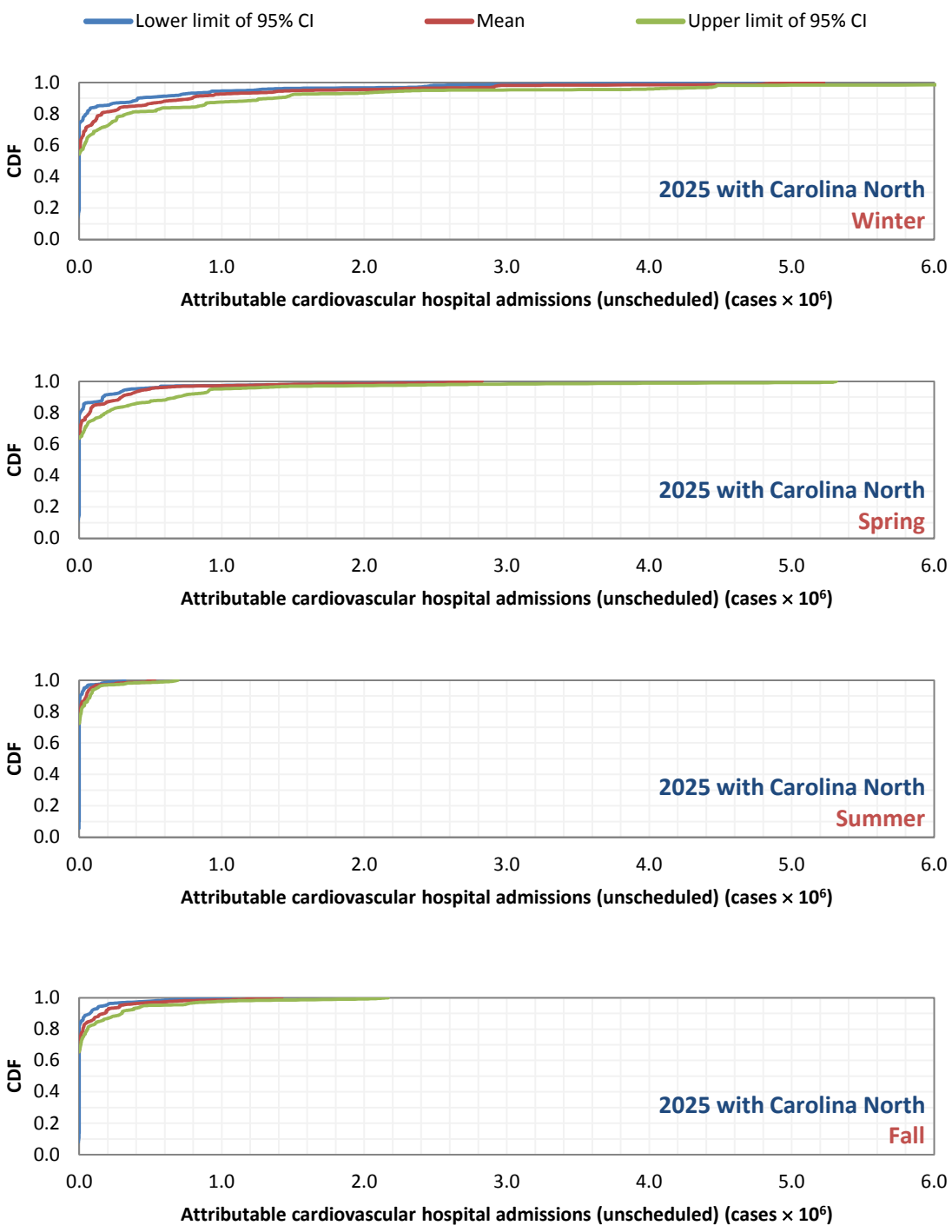
Lower limit of 95% CI
Mean
Upper limit of 95% CI
CDF
1.0
0.8
0.6
0.4
0.2
0.0
0.0
1.0
2.0
3.0
4.0
5.0
6.0
2025 with Carolina North
Winter
Attributable cardiovascular hospital admissions (unscheduled) (cases × 10⁶)
2025 with Carolina North
Spring
2025 with Carolina North
Summer
2025 with Carolina North
Fall

APPENDIX K
CUMULATIVE DISTRIBUTION OF PREDICTED SEASONAL AVERAGE OF RESPIRATORY HOSPITAL ADMISSIONS (UNSCHEDULED) ATTRIBUTABLE TO SHORT-TERM EXPOSURE TO TRAFFIC-RELATED PM2.5 WITHIN 160 CENSUS BLOCKS ANALYZED

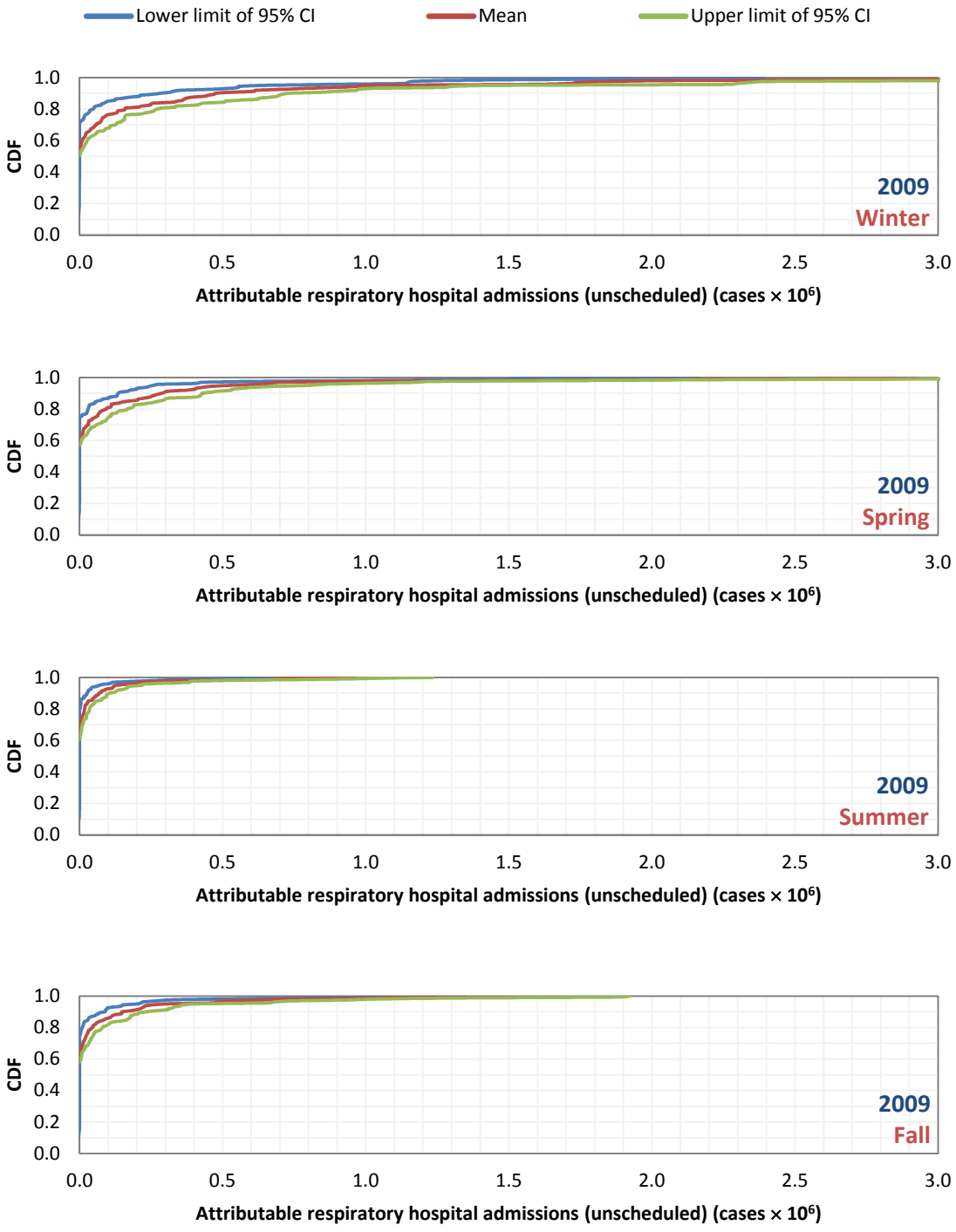

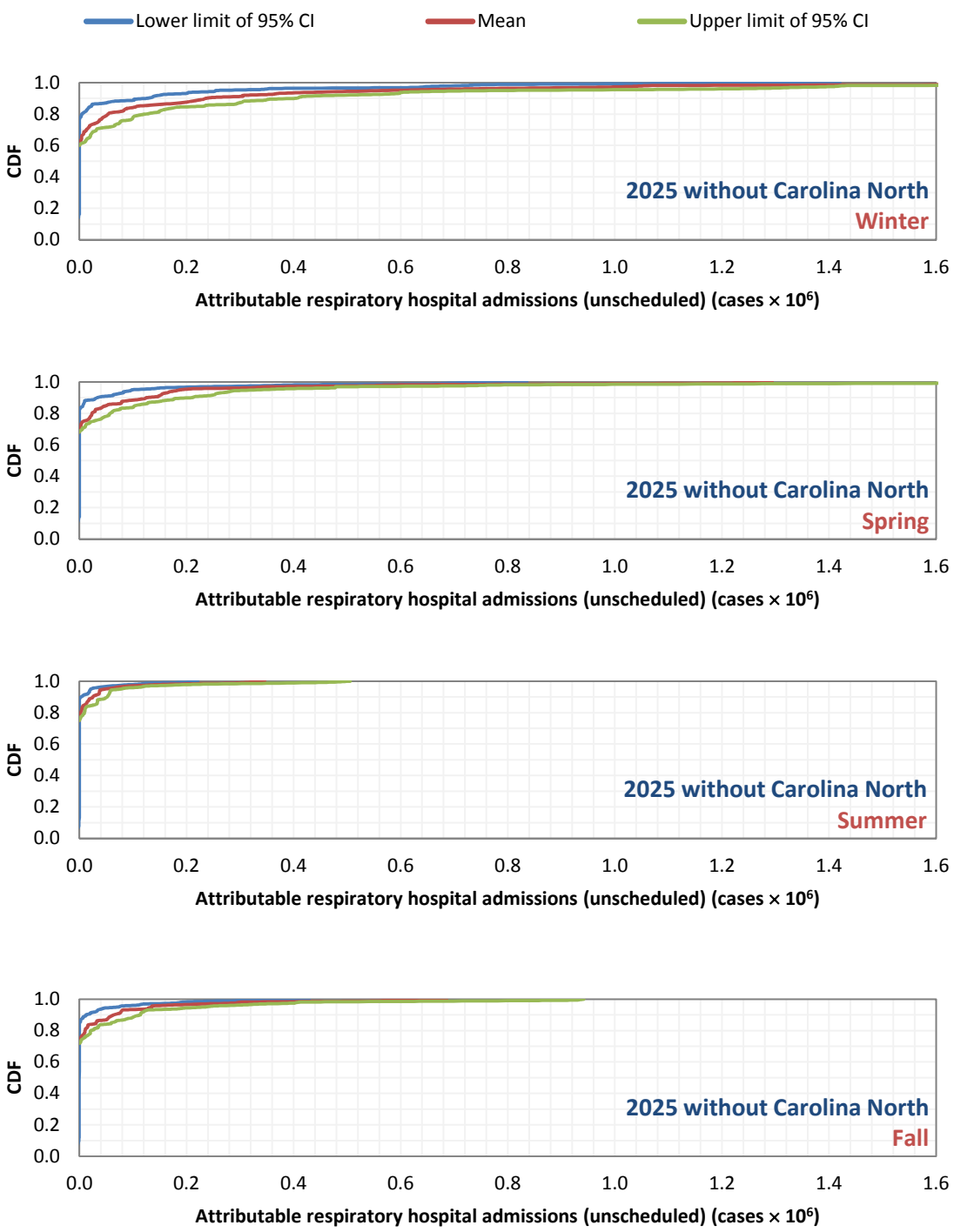
Lower limit of 95% CI
Mean
Upper limit of 95% CI
CDF
1.0
0.8
0.6
0.4
0.2
0.0
0.0
0.2
0.4
0.6
0.8
1.0
1.2
1.4
1.6
2025 without Carolina North
Winter
Attributable respiratory hospital admissions (unscheduled) (cases × 10⁶)
2025 without Carolina North
Spring
2025 without Carolina North
Summer
2025 without Carolina North
Fall

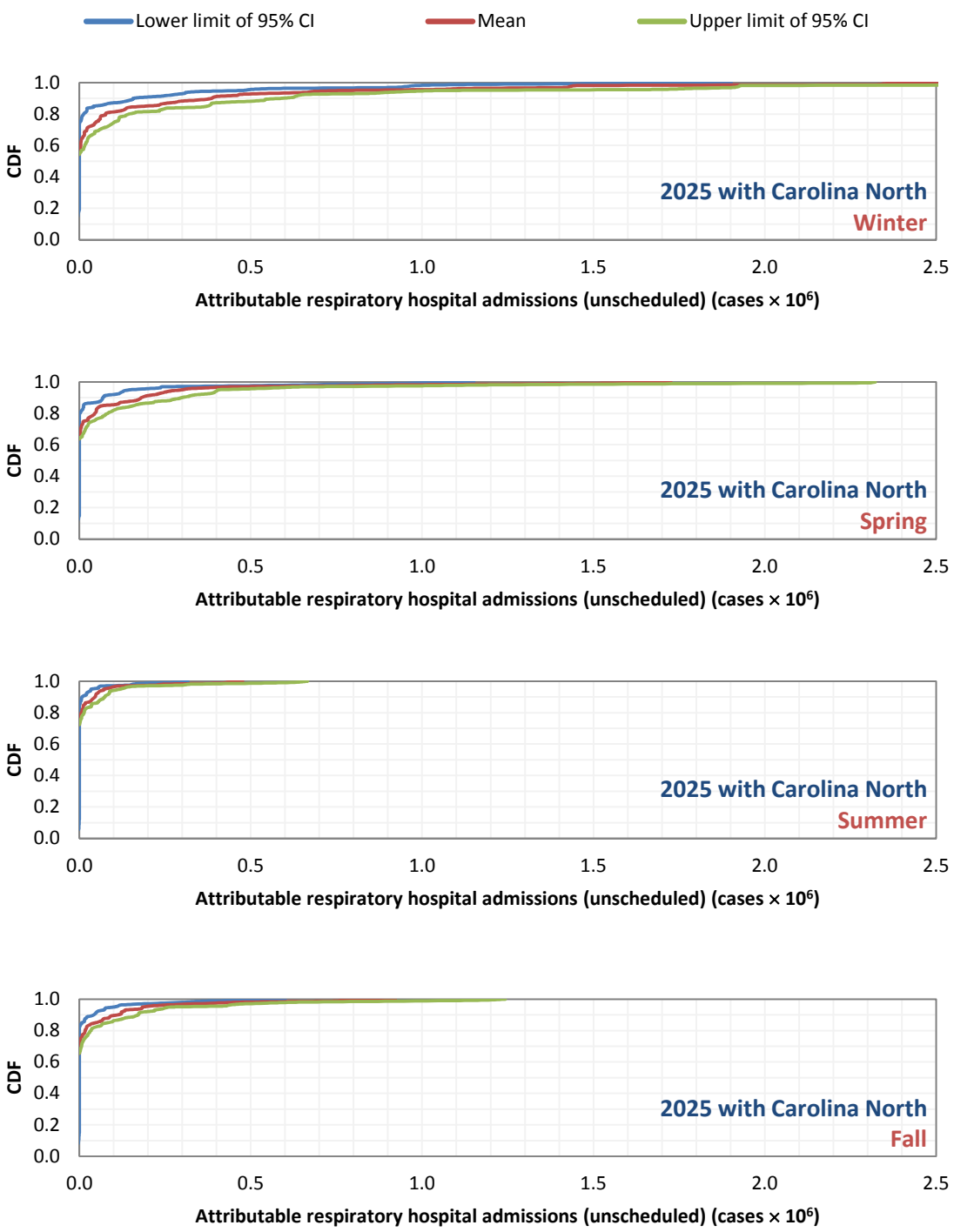
Lower limit of 95% CI
Mean
Upper limit of 95% CI
CDF
1.0
0.8
0.6
0.4
0.2
0.0
0.0
0.5
1.0
1.5
2.0
2.5
Attributable respiratory hospital admissions (unscheduled) (cases × 10⁶)
2025 with Carolina North
Winter
2025 with Carolina North
Spring
2025 with Carolina North
Summer
2025 with Carolina North
Fall